Physiological and Molecular changes of Photosynthetic Apparatus under Drought Stress in *Pisum sativum* L. (pea)

Thesis submitted for the degree of

Doctor of Philosophy in Plant Sciences

Submitted by

Jayendra Pandey

(Reg. No. 17LPPH05)

Under Supervision of

Prof. S. Rajagopal

हैदराबाद विश्वविद्यालय

University of Hyderabad

प्रतिष्ठित संस्थान

INSTITUTION OF EMINENCE

राष्ट्रीय अपेक्षाएँ, वैश्विक मानक

National Needs, Global Standards

Department Of Plant Sciences

School Of Life Sciences

University Of Hyderabad

Telangana 500046

June 2023

Department of Plant Sciences
School of Life Sciences
University of Hyderabad
500046

CERTIFICATE

This is to certify that **Mr JAYENDRA PANDEY** has carried out the research work embodied in the present thesis under the supervision and guidance of Professor S. Rajagopal for a full period prescribed under the Ph.D. ordinances of this University. We recommend her thesis entitled **"Physiological and Molecular changes of Photosynthetic Apparatus Under Drought Stress in *Pisum sativum* L. (pea)"** for submission for the degree of Doctor of Philosophy of the University.

Jayendra Pandey

Date: 23-06-2023

Jayendra Pandey

Enrolment Number: 17LPPH05

Prof. Subramanyam Rajagopal

(Supervisor)

Prof. S. RAJAGOPAL
Dept. of Plant Sciences
School of Life Sciences
University of Hyderabad
Hyderabad-500 046.

Department of Plant Sciences
School of Life Sciences
University of Hyderabad
500046

DECLARATION

This is to declare that the work embodied in this thesis entitled **"Physiological and Molecular Changes of Photosynthetic Apparatus under Drought Stress in *Pisum Sativum* L. (pea)"** has been carried out by me under the supervision of Prof. S. Rajagopal, Department of Plant Sciences, School of Life Sciences. The work presented in this thesis is a bonafide research work and has not been submitted for any degree or diploma in any other University or Institute. A report on plagiarism statistics from the University Librarian is enclosed.

Jayendra Pandey

Jayendra Pandey

Date: 23-06-2023

Prof. Subramanyam Rajagopal

(Supervisor)

Prof. S. RAJAGOPAL
Dept. of Plant Sciences
School of Life Sciences
University of Hyderabad
Hyderabad-500 046.

Department of Plant Sciences
School of Life Sciences
University of Hyderabad
500046

CERTIFICATE

This is to certify that this thesis entitled **"Physiological and Molecular Changes of Photosynthetic Apparatus under Drought stress in *Pisum sativum* L. (pea)"** is a record of Bonafide work done by Mr. Jayendra Pandey, a research scholar for Ph.D. programme under the Department of Plant Sciences, School of Life Sciences, University of Hyderabad under my guidance and supervision. This thesis is free from plagiarism and has not been submitted in part or in full to this or any other University or institution for the award of any degree or diploma.

Parts of the thesis have been:

A. Published in the following publications:

1. The Plant Journal (2023) 113:60-74.

2. Plant Physiology and Biochemistry 185 (2022) 144-154.

B. Presented in the following conferences:

1. Poster presentation in "8th International conference on "Photosynthesis and hydrogen energy research for sustainability 2017" at University of Hyderabad, Hyderabad, India from October 30th - November 3rd, 2017.
2. Oral presentation in International Conference on "Physiological and Molecular Mechanisms of Abiotic Stress Tolerance in Plants" October 26th-28th 2022 organized by the Department of Botany, University of Calicut, Kerala.

Further, the student has passed the following courses towards the fulfilment of the coursework requirement for Ph.D.

S.No.	Course code	Name	Credits	Pass/Fail
1	PL801	Research Methodology and Analytical Techniques	4	Pass
2	PL802	Research ethics, Biosafety, Data analysis and Biostatistics	4	Pass
3	PL803	Scientific Writing and Research Proposal	4	Pass

28/6/2023

Supervisor

Prof. S. RAJAGOPAL
Dept. of Plant Sciences
School of Life Sciences
University of Hyderabad
Hyderabad-500 046.

29/6/2023

Head

अध्यक्ष / HEAD
वनस्पति विज्ञान विभाग / Dept. of Plant Sciences
जैविक विज्ञान संकाय / School of Life Sciences
हैदराबाद विश्वविद्यालय / University of Hyderabad
हैदराबाद / Hyderabad-500 046, भारत / INDIA

29/6/23

Dean

संकाय अध्यक्ष / Dean
जीव विज्ञान संकाय / School of Life Science
हैदराबाद विश्वविद्यालय / University of Hyderab
हैदराबाद / Hyderabad-500 046.

Department of Plant Sciences
School of Life Sciences
University of Hyderabad
500046

Plagiarism Free Certificate

This is to certify that the similarity index of this thesis as checked by the Library of University of Hyderabad is 33 %. Out of this 24 % similarity has been found to be identified from the candidate's own publication which forms the major part of the thesis. The details of student's publication are as follows:

1. **Reversible changes in structure and function of photosynthetic apparatus of pea (Pisum sativum) leaves under drought stress (Chapter 3).**
2. **Temperature-induced reversible changes in photosynthesis efficiency and organization of thylakoid membranes from pea (Pisum sativum).**
3. **High light induced changes in thylakoid supercomplexes organization from cyclic electron transport mutants of *Chlamydomonas reinhardtii*.**

About 9 % similarity was identified from external sources in the present thesis which is according to prescribed regulations of the University. All the publications related to this thesis have been appended at the end of the thesis. Hence, the present thesis considered to be plagiarism free.

23/6/2023

Prof. S. Rajagopal

(Supervisor)

Prof. S. RAJAGOPAL
Dept. of Plant Sciences
School of Life Sciences
University of Hyderabad
Hyderabad-500 046.

Dedicated to my parents

ACKNOWLEDGEMENTS

I express my immense gratitude to my supervisor ***Prof. S. Rajagopal,*** *for giving me an opportunity to work in his lab. Words can't express my gratefulness for his constant support and guidance during my tenure of doctoral research. I would like to thank him for building my courage, his inputs to improve my work. I am inspired by his dedication to the scientific field. I am fortunate and privileged to have him as my supervisor.*

I thank my doctoral committee members ***Prof. A.S. Raghavendra and Prof. G. Padmaja*** *for their valuable suggestions and guidance throughout my research.*

I extend my sincere gratitude to Head of the Department of Plant Sciences, ***Prof. S. Rajagopal****, and former Heads,* ***Prof. G. Padmaja*** *and* ***Prof Ch. Venkata Ramana*** *providing the necessary department facilities for my research work.*

I am thankful to Dean ***Prof. N Siva Kumar*** *and former Deans* ***Prof. S. Dayananda, Prof. KVA Ramaiah, Prof. P. Reddanna*** *for extending the facilities in School of Life Sciences.*

I sincerely thank ***Prof. Yuchiro Takahashi****,* ***Dr. Shin-Ichiro Ozawa, Dr. Hiroshi Khudawa, Miyuki Ishihara san****, for scientific discussion Japan-Asian Youth Exchange Program in Science (SAKURA Exchange Program) for my visit to Okayama University, Japan conducted by JSTA in 2018.*

I am also thankful ***Prof. Jian-Ren Shen****,* ***Toshiharu Shikanai****,* ***Kentaro Ifuku*** *for scientific discussion during my visit in Japan.*

I would like to thank ***Prof. Nathan Nelson*** *and* ***Prof. Gyozo Garab*** *for helpful discussions during their visit to our laboratory. I thank* ***Dr. Jagadish Gupta Kapuganti****, National Institute of Plant Genome Research, New Delhi for metabolomic analysis experiment and his student Ms. Pooja for helping in analysis.*

I am extremely thankful to Faculty members, Department of Plant Sciences and School of Life Sciences for their support and suggestions. Sincere thanks to the non-teaching and technical staff of the School of Life Sciences. I thank the School of Life Science instrument facility and Plant Sciences instrument facility. I also thank Dashrath and Monica for helping in the confocal microscopy, circular dichroism, ultracentrifugation facility, Proteomics facility, GC-MS facility and other office staff.

*I am especially grateful to **Prof. A.S. Raghavendra** for allowing me to work and use his lab facilities and for measuring ROS, antioxidant activity parameters and **Dr. Deepak Saini** for helping in analysis.*

*I especially thank **Dr. Suresh Marriboina** for helping me in the analysis of proteomics data.*

I am thankful to all seniors and colleagues Dr. Elsin, Dr. Sai, Dr. Shreya, Dr. Manjunath, Dr. Nageshrao, Dr. Venkateswara, Dr. Divya, Kunal, Dr. Ranay, Dr. Nisha, Yusuf, Jyothi Ranjan, Pavitra, Jerome, Praveena, Narendra, Sailaja, Vijay, Shriya, Namrata, Ganesh and Prashant for their support and maintaining a cheerful environment in the lab.

*I thank faculty members of the school of life sciences for their support and encouragement. Sincere thanks to the non-teaching and technical staff of the School of Life Sciences. I thank the school of Life Science instrument facility and plant sciences instrument facility. I also thank **Dashrath** for helping me in the confocal microscopy and ultracentrifugation facility and other office staff.*

*I am thankful to BBL, Indo-Israel (ISF), IoE for my fellowship and all funding agencies **DBT-Builder, UGC-SAP, DST-FIST, IoE, DBT, SERB, UGC-ISF, JST, CSIR and DST** supporting departmental facilities helping in completion of my research work.*

"It's not what we have in life, but who we have in our life that matters." I have been fortunate to meet wonderful people in my life whom I can call my people. They have helped me to believe in myself, gave me courage and support. They have given me my best and happy time of my life. I am grateful to all my friends- Janish, Ramana, Harish Dubey, Mahati, Bharat, Shashi, Dr. Easwar who have supported me and were pillars of support.

Words can't express my gratitude to my sister (Dr.Madhavi, Dr. Ranjana) and elder brother (Deependra). Thank you for being my pillar of support and believing in me when I couldn't believe in myself. Thank you for helping me to have faith in myself and impart the courage to pursue my dreams.

I am indebted to my parents for believing in me and helping me achieve my dreams. I am so grateful to my father for always listening to my worries and being my biggest supporter. I am who I am because of you Amma and Papa. I am thankful to my family-

grandparents, aunts, uncles and cousins for their support. I finally thank God almighty for all the blessings.

TABLE CONTENTS

List of Figures and Tables

Figures

Figure 6.6 Comparison of differentially expressed gene level transcript KEGG pathway (a) Pathways in Condition A (b) Pathways in Condition B.

Figure 6.7 GO analysis of DEGs between control (a) Gene ontology distribution of condition A (Biological process) (b) Cellular process and (c) Molecular process.

Figure 6.8 GO analysis of DEGs between drought (a) Gene ontology distribution of condition B Biological process (b) Cellular process (c) Molecular process.

Figure 6.9 Identification of transcription factors (a) Condition A Upregulated transcription factors (b) Condition B Upregulated transcription factors.

Figure 6.10 (a) Characterization of the proteome of *P.sativum* plant based on significance (b) downregulated proteins in *P.sativum* under drought stress (c) upregulated proteins in *P.sativum* under drought stress based on their functionality.

Figure 6.11 Hierarchical cluster heat maps of down and up regulated proteins and protein-protein correlations in leaf of *P.sativum* at drought stress in PSI-LHCI proteins.

Figure 6.12 Hierarchical cluster heat maps of down and up regulated proteins and protein-protein correlations in leaf of *P.sativum* at drought stress in PSII-LHCII proteins.

Figure 6.13 Hierarchical cluster heat maps of down and up regulated proteins and protein-protein correlations in leaf of *P.sativum* at drought stress in ROS proteins.

Figure 6.14 Hierarchical cluster heat maps of down and up regulated proteins and protein-protein correlations in leaf of *P.sativum* at drought stress in ABC_ATP transporter proteins.

Figure 6.15 Hierarchical cluster heat maps of down and up regulated proteins and protein-protein correlations in leaf of *P.sativum* at drought stress in carotenoids transporter proteins.

Figure 6.16 Hierarchical cluster heat maps of down and up regulated proteins and protein-protein correlations in leaf of *P.sativum* at drought stress in GTP binding proteins.

Figure 6.17 Hierarchical cluster heat maps of down and up regulated proteins and protein-protein correlations in leaf of *P.sativum* at drought stress in heat shock proteins.

Figure 6.18 Hierarchical cluster heat maps of down and up regulated proteins and protein-protein correlations in leaf of *P.sativum* at drought stress in Kinase proteins.

Figure 6.19 Hierarchical cluster heat maps of down and up regulated proteins and protein-protein correlations in leaf of *P.sativum* at drought stress in ATP_binding proteins.

Figure 6.20 Photosynthetic proteins obtained from iTRAQ analysis from drought stress leaf tissues from PSI, PSII and stress marker proteins.

Figure 6.21 iTRAQ proteins quantification obtained from leaf tissues of *P.sativum*. Most of the proteins are upregulated in drought stress (TP, TRX, dnaJ, PER, RDX).

Figure 6.22 Correlation network analysis to illustrate relationships among the ABC_ATP binding proteins with control and drought treated leaf tissues of *P.sativum*.

Tables

List of Abbreviations

$^1O_2$	Singlet oxygen
^{3}Chl*	Triplet chlorophyll
77 K	77-degree Kelvin = -196 degree Celsius
ABA	Abscisic acid
ABS/CSm	Absorption flux per excited CS
Asat	Light saturated net photosynthetic rate
ATG	Autophagy-related protein
ATP	Adenosine tri phosphate
ATP	Adenosine triphosphate
BNPAGE	Blue-native polyacrylamide gel electrophoresis
BSA	Bovine serum albumin
CBLP	Guanidine nucleotide-binding protein beta subunit-like
CD	Circular Dichroism
CET	Cyclic electron transfer around PSI
CET	Cyclic electron transport
Chl	Chlorophyll
CO_2	Carbon dioxide
Cyto	Cytochrome
DAB	Diaminobenzidine
DDM	n-dodecyl β-D maltoside
DGDG	Digalactosyldiacylglycerol
DIo/CSm	Dissipated energy flux per excited CS
DIo/RC	Dissipated energy flux per RC
DW	Dry weight
E	Transpiration rate
ETC	Electron transfer chain between PSII and PSI
ETo/CSm	Electron transport flux per excited CS
FAME	Fatty acid methyl esters
Fd	Ferrodoxin
Fm	Maximum fluorescence in the dark-adapted
Fo	Minimum fluorescence value after the onset of actinic illumination at 50µs
Fp=Fm	Maximum fluorescence intensity under saturating illumination at P-step
Fru	Fructose
Fv	Variable chlorophyll fluorescence
Fv/Fm	Maximum quantum efficiency of PSII
FW	Fresh weight
GA3	Gibberellin
GC	Gas chromatography
Glu	Glutamate
Gluc	Glucose
gs	Stomatal conductance
H_2O_2	Hydrogen per oxide
HPLC	High performance liquid chromatography
IPCC	Intergovernmental Panel on Climate Change

kDa	**Kilo daltons**
KEGG	**Kyoto Encyclopedia Genes and Genome**
LC/MS	**Liquid chromatography/mass spectrometry**
LET	**Linear electron transport**
LHCI	**Light harvesting complex I**
LHCII	**Light harvesting complex II**
LMC	**Leaf moisture content**
LRWC	**Leaf relative water content**
MGDG	**Monogalactosyldiacylglycerol**
MSTFA	**N-methyl-N-(trimethylsilyl) trifluoroacetamide**
NADPH	**Nictotinamide adenine dinucleotide phosphate**
NBT	**Nitroblue tetrazolium**
NPQ	**Non-photochemical quenching**
O_2	**Oxygen**
OEC	**Oxygen Evolving Complex**
OEC	**Oxygen evolving complexes**
P680, P680*	**Reaction centre Chl of PSII and its excited singlet state**
PDB	**Protein data bank**
PGR5	**Proton gradient regulation 5**
PI(ABS)	**Performance index on absorption basis**
Pro	**Proline**
PSI	**Photosystem I complex**
PSII	**Photosystem II complex**
PUFA	**Polyunsaturated fatty acids**
Q_A and Q_B	**Primary and secondary plastoquinone electron acceptor of PSII**
Rb	**Ribitol**
RC	**Reaction centre**
RC/CSm	**Density of active reaction centers per cross-section (CS)**
ROS	**Reactive oxygen species**
ROS	**Reactive oxygen species**
RT-PCR	**Real time polymerase chain reaction**
SDGUC	**Sucrose density gradient ultracentrifugation**
SDS-PAGE	**Sodium dodecyl sulphate-polyacrylamide gel electrophoresis**
SFA	**Saturated fatty acid**
SQDG	**Sulfoquinovosyldiacylglycerol**
Suc	**Sucrose**
TAG	**triacylglycerol**
TCA	**Tri-carboxylic acid**
TEM	**Transmission electron microscopy**
TLC	**Thin layer chromatography**
TMS	**Trimethyl silane**
TPS	**Trehalose 6 phosphate synthase**
TW	**Turgid weight**
UPLC	**Ultra performance liquid chromatography**

Chapter 1

Introduction and Review of Literature

1.1 Photosynthesis

Photosynthesis in organisms like higher plants and cyanobacteria that convert inorganic raw materials into organic compounds is Earth's most important photochemical activity. The net primary productivity in this process is estimated to be between 85-120 Gt carbon per year, producing all the food and energy we consume. To meet the demands of the exponentially expanding population and numerous scientific and technical disciplines, it is crucial to comprehend photosynthesis's theoretical and practical elements. Oxygenic photosynthetic organisms use light energy from the sun to transform CO_2 and H_2O into energy-dense carbohydrates during photosynthesis.

Oxygenic photosynthesis involves the evolution of molecular oxygen (O_2) as a by-product, through the absorption of solar radiation in the photosynthetically active radiation (PAR) range (400–700 nm). Through a sequence of protein complexes enmeshed in thylakoid membranes, electrons from H_2O, the initial electron donor, are transferred during this process (Figure 1.1). In the end, the electron transfer converts $NADP^+$ to NADPH. Additionally, the thylakoid membranes maintain a proton gradient employed by ATP synthase to convert ADP and Pi into ATP. The light reactions are the name given to this process of converting solar energy in ATP and NADPH (Bolton, 1977; Alados et al., 1996).

Solar energy is responsible for powering the photosystem (PS) II, enabling the movement of electrons along the electron transport chain (ETC) to convert NADP+ into NADPH during oxygenic photosynthesis. Various protein complexes, including PSII, cytochrome (Cyt) b6/f, and PSI, as well as electron carrier molecules like plastocyanin (PC) and plastoquinone (PQ), facilitate the transport of electrons within the chain. The transfer of electrons generates a proton motive that fuels the ATP complex in thylakoid.

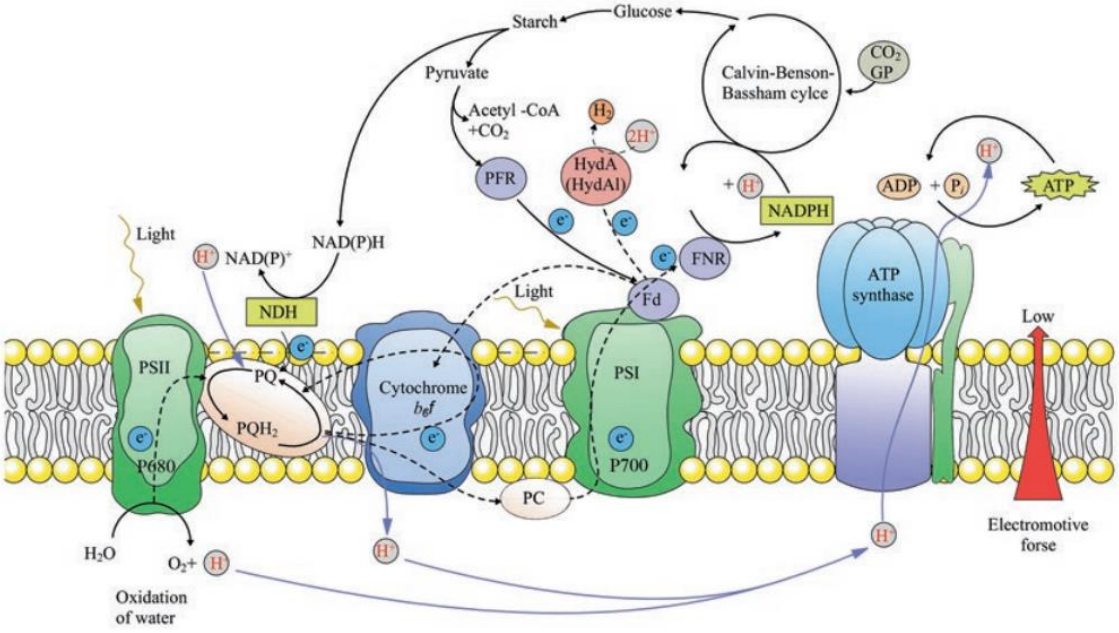

Figure 1.1 *Schematic representation of the photosynthetic electron transfer chain*

The CBB cycle, catalyzed by soluble proteins such as Ribulose-1,5-Bisphosphate Carboxylase/oxygenase (RuBisCO), plays a crucial role. Oxygenic photosynthesis is performed by both prokaryotic cells like cyanobacteria and prochlorophytes and eukaryotic cells. Eukaryotic cells initially acquired photosynthesis through an essential endosymbiosis event with a prokaryotic cell, which evolved into a chloroplast (Falkowski and Raven, 1997; Griffiths, 2006).

1.2 Light harvesting and energy transfer

The pigment molecules that surround PSII, absorb light as the first stage of oxygenic photosynthesis (Figure 1.2) (Blankenship, 2014). The excitation of the absorbed light energy then transfers it through various pigment molecules to a pair of P680 chlorophyll molecules in the reaction centre of PSII (Vredenberg and Duysens, 1963).

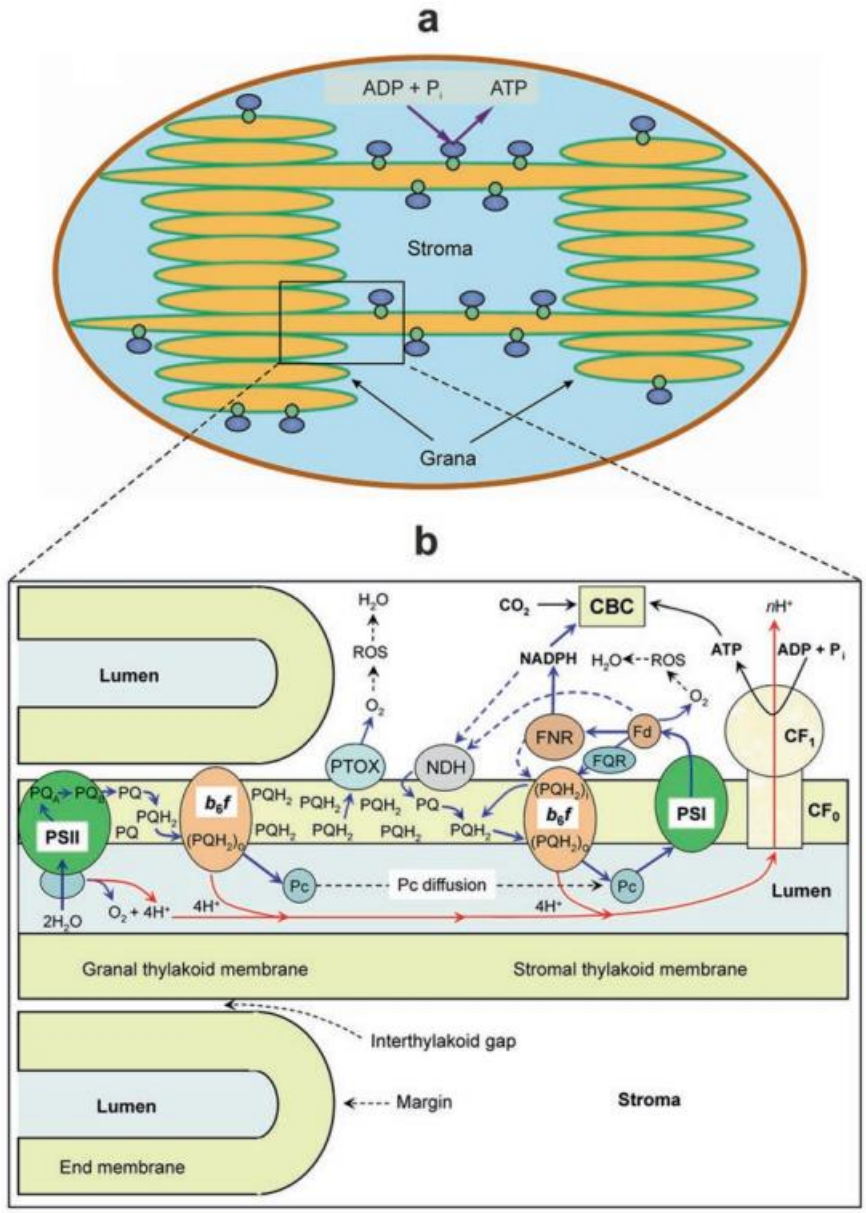

Figure 1.2 *A sketch of a chloroplast and a scheme of photosynthetic electron transport chain. When the chlorophyll molecules are excited; an electron is moved from them to a modified chlorophyll molecule called pheophytin (Adapted from Blankenship, 2014).*

In PSII, the initial redox reaction involves the oxidation of the P680 pigment, resulting in the formation of $P680^{+}$ and the reduction of pheophytin. Following this, the electron is swiftly transferred to a quinone called QB, which is tightly bound to the D2 subunit of the PSII core protein. This rapid transfer, occurring within 10 µs, prevents the electrons from reverting back to the specific special pair and being dissipated as heat.

To complete the electron transfer to QB, two high-energy electrons are required, leading to the reduction of QB to QH2. This process involves the uptake of protons from the chloroplast stroma. The resulting reduced quinone, also known as plastoquinol, moves across the thylakoid membrane and reaches the Cyt b6/f complex.

Concurrently, on the luminal side of PSII, the oxygen-evolving complex (OEC) facilitates the photooxidation of H_2O, which restores the electrons lost during the initial redox reaction. The electrons derived from the OEC are then passed on to the oxidized $P680^+$ through a tyrosine side chain located on the D1 subunit, which is bound to the TyZ subunit of PSII. Early studies by Hill (1937) and subsequent research by Nelson and Yocum (2006) have provided insights into this electron transfer process. The water splitting process can be summarized as follows:

$$2H_2O + 2A \longrightarrow 2AH_2 + O_2$$

During photosynthesis, light energy undergoes a conversion into chemical energy. At the PSII, the oxygen-evolving complex (OEC) contains a manganese-calcium oxide cluster at its core, resembling a cubane structure. This cluster stores reducing power until four manganese atoms have been reduced, initiating the water-splitting process (Umena et al., 2011). Positioned on the luminal side of the membrane, the OEC supplies electrons to PSII while also maintaining a proton gradient across the thylakoid membrane. The reduced membrane-plastoquinones then transfer from PSII to the Cyt b6/f complex, which plays a crucial role in providing two-thirds of the protons necessary for ATP production (Hasan et al., 2013). Within the Fe-S protein, an iron-sulfur center facilitates electron movement towards Cyt f and subsequently to plastocyanin, a mobile electron transporter (Green and Parson, 2003).

In addition to ferredoxin, cyclic electron transport originating from PSI contributes significantly to maintaining a balanced ratio of NADPH and ATP. Through the iron-sulfur center, a pair of electrons is transferred to plastocyanin, while two protons are acquired from the stromal to regenerate plastoquinone. Ultimately, four protons are transferred from the stroma to the luminal of the thylakoid membranes (Ferreira et al., 2004), ensuring the overall functionality of the photosynthetic process.

Cyclic electron transport, as described by Barber et al. (1997), enables the movement of electrons in PSI via ferredoxin. During non-cyclic electron transport, the cytochrome b6f complex or NADPH receives the electrons absorbed by PSI from PSII (Figure 1.2). Intermediate redox carriers, including antenna chlorophylls, phylloquinone, and iron-sulfur proteins, alongside the reaction center P700, facilitate this process. Similar to PSII, PSI is a transmembrane protein complex. Initially, an electron is transferred to a chlorophyll molecule (A0), then to phylloquinone (A1), and subsequently passed through three iron-sulfur centers (4Fe-4S), namely Fx, FA, and FB, upon excitation of the reaction center pigments P700. The chain's electron carrier (Fx) reduces ferredoxin. Additionally, an electron from plastocyanin oxidizes P700+ to regenerate P700 (Figure 1.2). The Z-scheme represents the flow of electrons in the oxygenic photosynthesis transfer chain, accompanied by an increase in the redox potential of electrons upon activation at both PSII and PSI (Senge et al., 2014).

1.3 The thylakoid membrane's photosynthetic apparatus

The photosynthetic apparatus necessary for transforming light energy into chemical energy in the form of ATP and NADPH are found in the thylakoid membrane. Two substantial protein complexes called PSI and PSII, which are encased in the thylakoid membrane, make up the photosynthetic apparatus. These complexes include different

pigments that participate in the absorption of light energy, including carotenoids, phycobilins, and chlorophylls. Once the light has been caught, it is used to reduce $NADP^+$ to NADPH in PSI and oxidise water molecules in PSII, which releases oxygen. The thylakoid membrane also includes a number of electron transport chains that shuttle electrons between photosystems and produce a proton motive that powers ATP synthase's synthesis of the energy molecule (Nelson et al., 2020).

1.3.1 Structure and function of PSII-LHCII complex

PSII is a multimeric protein-pigment supramolecular complex found in the thylakoid membranes of plants and cyanobacteria (Barber, 2003). By splitting H_2O into electrons and protons using light energy, PSII produces O_2 as a by-product. According to recent studies, higher plants have a PSII-LHCII structure of the $C_2S_2M_2$-type (Umena et al., 2011). Several number of light-harvesting complex II (LHCII) are connected to the core of PSII, which is in charge of photosynthesis within plant cells (Su et al., 2017). The PSII super-complex, also known as $C_2S_2M_2$, which has a dimeric core and two LHCIIs that are firmly bound and two that are only moderately bound, is the predominant PSII form in plants that have been accustomed to low light levels. Cryo-electron microscopy was recently used by Su et al. (2017) to describe the structures of two types of $C_2S_2M_2$ from *P. sativum*, which are stacked and unstacked. These structures had resolutions of 2.7 and 3.2 Å, respectively. Both weakly and moderately bound LHCII particularly combines with the peripheral antenna complex CP24 and CP29 heterodimer in both types of $C_2S_2M_2$ to form a pigment network that promotes energy transfer into the core and light harvesting at the periphery. The moderately bound LHCII and CP24, among other peripheral antennas with high mobility, provide insight into the functional control of plant PSII (Su et al., 2017).

As per the findings of Rutherford and Faller (2003), the PSII core consists of two proteins, PsbA and PsbB, arranged in a heterodimeric structure and housing the reaction center P680 (Figure 1.3). When light is absorbed, P680 undergoes excitation, and the resulting chlorophyll transfers an electron to the pheophytin (Phe). Subsequently, Phe transfers the electron to the primary acceptor QA, located in proximity to the D2 subunit. From there, the electron moves from QA to the secondary electron acceptor plastoquinone, QB, situated on the D1 subunit (Debus et al., 1988).

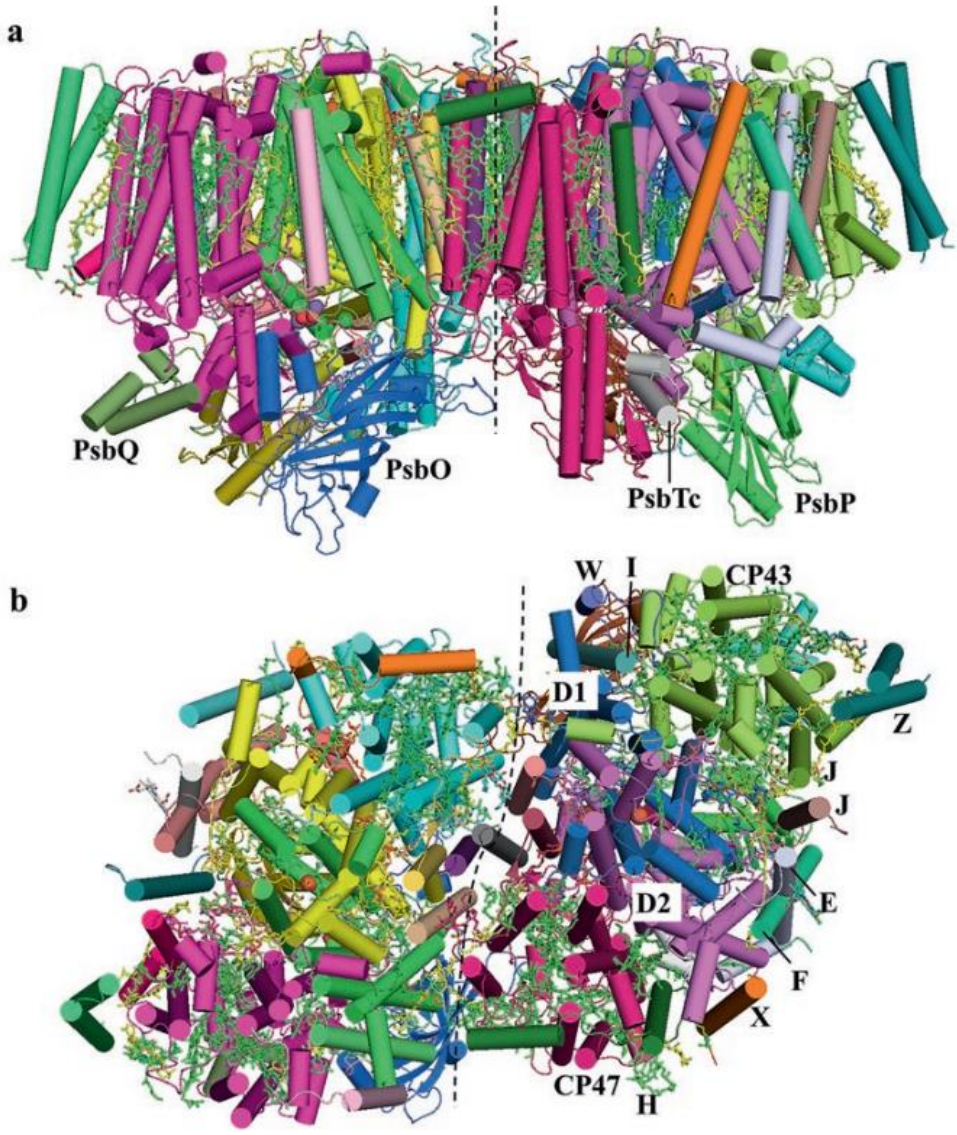

Figure 1.3 *Structure of higher plant PSII (adapted from Wei et al., 2016) (a) view perpendicular to the membrane plane (b) view from the stromal side of the membrane plane.*

PSII, an intricate protein complex residing in the thylakoid membrane of photosynthetic organisms, plays a vital role in the process of photosynthesis. Within PSII, an iron molecule (Fe^{2+}) positioned between the QA and QB sites acts as a mediator for electron transfer. The oxidized form of $P680^{+}$, a reaction center pigment, is reduced with the assistance of a cluster known as the oxygen-evolving complex (OEC), which facilitates water photolysis (Styring et al., 2012). Two antenna proteins, CP43 and CP47, combine to form an intrinsic antenna, with CP43 binding to the manganese center of OEC complex. The function of the peripheral antenna is to capture light energy and transfer it to the chlorophyll molecules in the reaction center, thereby regulating photosynthesis through a photo-protective mechanism (Schmid, 2008).

The light-harvesting complex, consisting of six distinct protein subunits from the light-harvesting multigene family, works in tandem with Chl *a*/*b* and xanthophyll pigments in various ratios. Each PSII-LHCII monomer contains at least 99 cofactors, including Chl, carotenoids, pheophytins, β-carotene, plastoquinone, heme, bicarbonate, lipid, the OEC (Mn_4CaO_5) cluster (with two Cl ions), one non-heme Fe^{2+}, and two putative Ca^{2+} ions (Shen et al., 2019). Two additional extrinsic proteins, PsbP (23 kDa) and PsbQ (17 kDa), are present in plants and algae, influencing the water-splitting reaction and maintaining optimal levels of Ca^{2+} and Cl^{-} ions in the cell (Debus, 1992).

The majority of PSII-related proteins, including intrinsic subunits like D1 and D2 of the reaction center, CP43 and CP47 of the reaction center core, and low-molecular-mass subunits like Cyt b559 (composed of PsbE and PsbF), are located in the thylakoid membrane of *P. sativum* (Wei et al., 2016). On the luminal side of the membrane, other extrinsic subunits associate with PSII, including OEC proteins and

PsbTn. The auxiliary antennas of the PSII core are encoded by six Lhcb genes (Jansson et al., 1999). These Lhcb apoproteins, along with pigments, contribute to the major component of the light-harvesting complex, known as LHCII, which consists of homo- and heterotrimers of Lhcb1, Lhcb2, and Lhcb3 (Jackowski et al., 2001; Caffari et al., 2004). Additionally, P. sativum possesses three monomeric minor LHCII species: CP29 (Lhcb4), CP26 (Lhcb5), and CP24 (Lhcb6) (Figure 1.3).

1.3.2 Cytochrome b6/f complex

Higher plants, green algae, and cyanobacteria have thylakoid membranes containing the Cyt b6/f complex, which functions as a plastoquinol-plastocyanin reductase thereby making it easier for electrons to go from plastoquinone to plastocyanin (Berg et al., 2007). Connecting PSII to PSI and creating a transmembrane proton gradient for ATP generation is essential for oxygenic photosynthesis (Tikhonov et al., 2014). A c-type cytochrome Cyt f, an iron group-containing Cyt b6/f, a Rieske iron-sulfur protein with a 2Fe-2S cluster, and subunit IV are among the 4 large subunits of the complex. The other four small subunits are PetG, PetL, PetM, and PetN. The complex is made up of two different monomers, each of which contains eight subunits (Whitelegge et al., 2002). The Cyt b6/f complex has a total molecular weight of 217 kDa (Whitelegge et al., 2002). Crystal structures of the complex have been found in spinach leaves, *C. reinahrdtii*, *M. laminosus*, and *Nostoc sp.* PCC 7120 (Stroebel et al., 2003; Yamashita et al., 2007; Baniulis et al., 2009; Malone et al., 2019) (Figure 1.4). By decreasing soluble plastocyanin or Cyt c6, the Cyt b6/f complex enhances electron transport between the PSII and PSI reaction centres (Smith et al., 2004). Heme-heme electron transport is given direction by lipids in the complex's intermembrane gap (Hasan & Cramer, 2014).

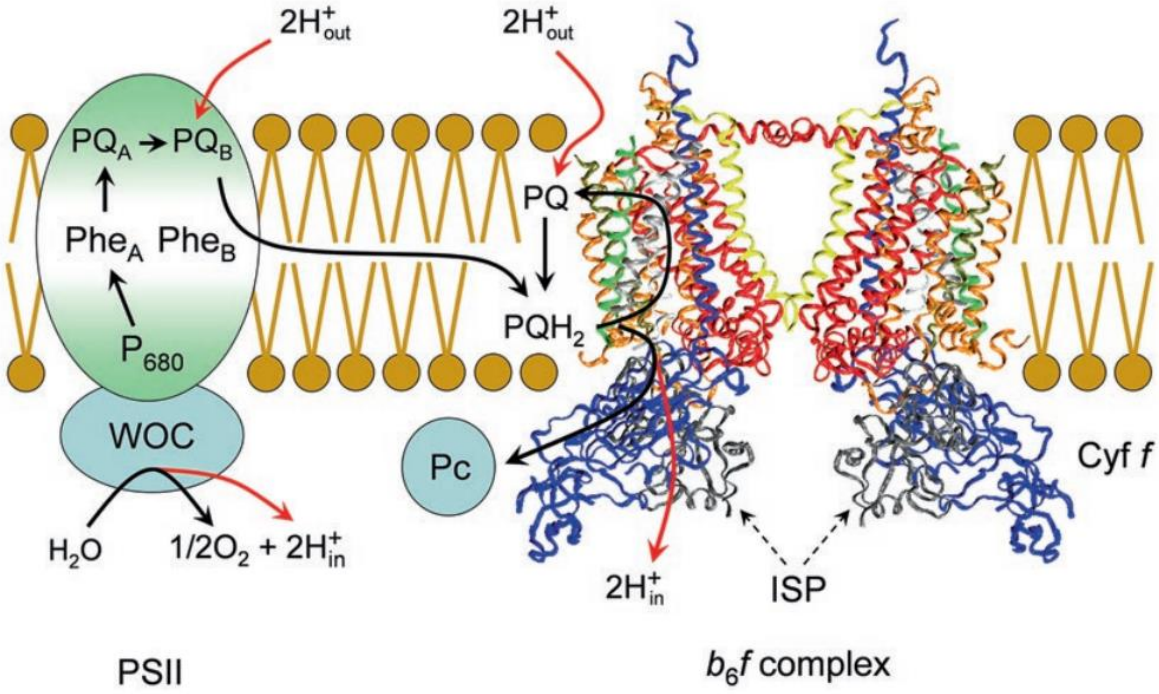

Figure 1.4 *A general view of the dimeric ensemble of the Cyt b6f complex from Chlamydomonas reinhardtii (PDB entry 1Q90, Stroebel et al. 2003) and its interaction with plastoquinol (PQH2). The figure was produced using Accelrys DV visualizer software package (http://www.accelrys.com).*

1.3.3 Structure and function of PSI-LHCI complex

The thylakoid membrane is home to PSI, a crucial multi-subunit protein complex essential for oxygenic photosynthesis. It is crucial for converting light energy into chemical energy and is also known as plastocyanin-ferredoxin oxidoreductase (Jolley et al., 2005; Amunts et al., 2007). At a resolution of 2.5 Å, the crystal structure of PSI from the thermophilic cyanobacterium *Synechococcus elongatus* has been established. The PSI complex comprises 127 cofactors, 12 protein subunits, 96 chlorophylls, 2 phylloquinones, three Fe_4S_4 clusters, 22 carotenoids, 4 lipids, Ca^{2+}, and 201 water molecules (Jordan et al., 2001). PSI, a trimeric protein complex found in cyanobacteria, consists of 36 protein subunits and 381 non-covalently bound cofactors. The crystal structure of PSI from higher plants, such as the pea (*P. sativum*), has been resolved at a

resolution of 2.6 Å. In higher plants, the PSI complex is composed of 16 subunits, along with approximately 2350 ligands, 35 lipids, and around 210 water molecules (Mazor et al., 2017) (Figure 1.5c). Within PSI and its associated LHCI, there are a total of 3 Fe-S clusters, 2 phylloquinones, and 235 chlorophyll molecules (Ben-Shem et al., 2003). The PSI complex's core subunits PsaA and PsaB interact with P700, A0, A1, and Fx. The Fx center, a 4Fe-4S cluster, is bound by four cysteines, two from PsaA and two from PsaB and PsaC, PsaO, PsaH, and PsaE. This creates a docking site for ferredoxin on the stromal side, while PsaN forms a docking site for plastocyanin on the luminal side (Fromme et al., 2001). Each PSI monomer contains twelve iron atoms (Jordan et al., 2001).

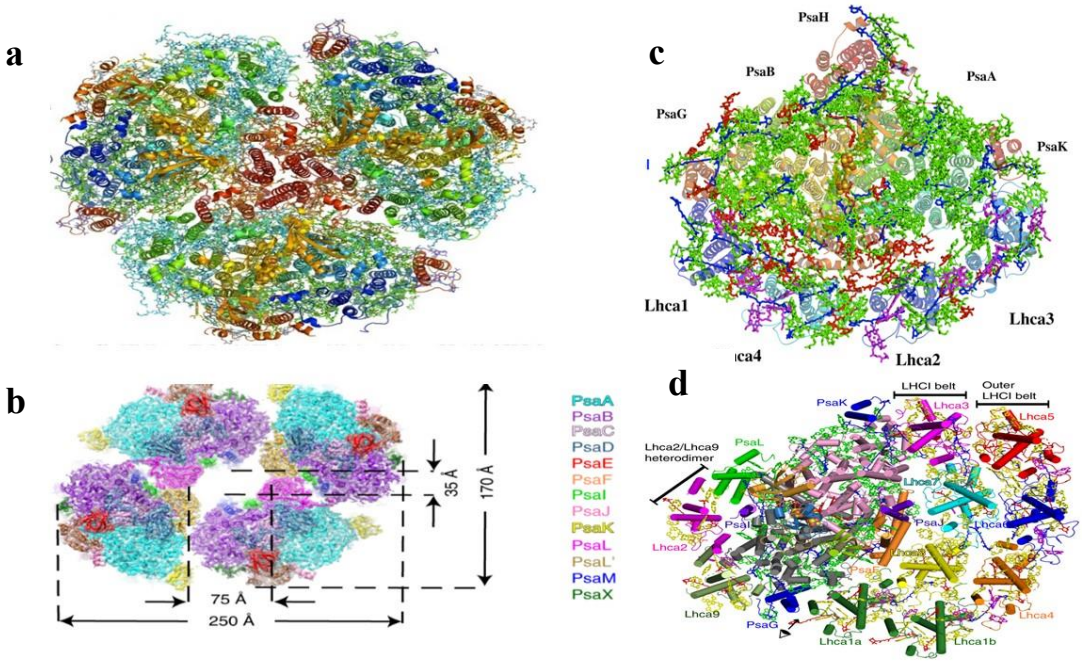

Figure 1.5 *Structures of PSI-LHCI complexes from Cyanobacteria to higher plants. (a) Trimeric form of PSI cyanobacteria. (b) Recent crystal tetrameric structure of PSI from Cyanobacteria. (c) PSI-LHCI supercomplex from the higher plant, Pea and PDB 5L8R, with Chl a in green, Chl b in magenta, carotenoids in blue, and lipids in red colour. (d) PSI-LHCI structure from C.reinhardtii showing two layers of LHC belts around core proteins (Figures were adapted from Nelson, 2006; Caspy and Nelson, 2018; Zheng et al., 2019; Qin et al., 2019).*

Despite showing a variety in its composition, the PSI light-harvesting complex is conserved throughout many photosynthetic species. The PSI complex in cyanobacteria and land plants consists of a trimer, where each monomer distributes the absorbed light energy for maximal effectiveness (Kubota-Kawai et al., 2018) (Figure 1.5). In contrast, it has been reported that the PSI complex from the filamentous cyanobacterium *Anabaena* sp. PCC7120 exists as a tetrameric and dimeric form rather than a trimeric complex (Watanabe et al., 2011). According to a recent study, cyanobacteria generate tetrameric PSI in light environments with elevated concentrations of PSI-bound carotenoids such as myxoxanthophyll and canthaxanthin and echinenone (Li et al., 2019). At a resolution of 2.3 Å, the crystal structure of the tetrameric PSI from the cyanobacterium *Anabaena* sp. PCC 7120 has been determined (Watanabe et al., 2011).

Four PSI monomers are produced when the PSI monomers are organized into a dimer through two different contacts (Zheng et al., 2019). In *C. reinhardtii*, PSI promotes the reduction of ferredoxin and oxidation of plastocyanin or cytochrome c6, which ultimately results in the production of NADPH via Fd-NADP-oxidoreductase (FNR). PSI is engaged in cyclic electron transfer reactions in addition to linear electron transfer reactions (Nelson and Junge, 2015). The reducing substances ATP and NADPH that are generated are used to fix CO_2 or acetate into starch. Figure 1.5 depicts the structure of the PSI-LHCI complex, which is found in cyanobacteria and higher plants. The tetrameric PSI structure in Cyanobacteria under strong light circumstances has been recently discovered (Zheng et al., 2019). The LHCI is bound in the PSI core antenna and takes the shape of a crescent just outside PsaF/PsaJ of the core complex (Yadavalli et al., 2011) used 3D model analysis to describe the structural makeup of PSI-LHCI and its physiological function in *C. reinhardtii*. Recently, (Ozawa et al., 2018) has shown

that mass spectrometry, immunodetection, and chemical cross-linking may be used to identify the cross-linked products and determine the entire configuration of the 10 LHCI subunits in the green algal PSI-LHCI supercomplex. Further, (Mazor et al., 2017), have deconvulated the PSI-LHCI crystal structure from *P.sativum*, where they have found 16 subunits, 45 transmembrane helices, 235 prosthetic group, 140 chlorophyll a, 16 chlorophyll b, 27 β-carotene, 7 lutein, 2 xanthophyll, 1 zeaxanthin, 23 monogalactosyl, 8 digalactosyl, 6 phosphatidyl glycerol, 2 quinones and 3 Fe-S clusters Figure 1.5c.

1.4 ROS and antioxidant enzyme

Plants experience an increase in reactive oxygen species (ROS) in response to both biotic and abiotic stresses. These molecules have a significant role on crucial processes such as photosynthesis, respiration Apel and Hirt (2004); (Mittler et al., 2017) suggest that ROS, which are by-products of aerobic metabolism, play a role in plant cell signaling. Scavengers of ROS, including antioxidants and antioxidant enzymes such as APX, CAT, and SOD, are known to mitigate their effects (Lee et al., 2007). Substances like ascorbate (ASC), glutathione (GSH), and tocopherols have been found effective in reducing ROS levels (Szarka et al., 2012). ROS are primarily produced in peroxisomes, the plasma membrane, mitochondria, and chloroplasts (Mansoor et al., 2022). The family of ROS includes singlet oxygen ($^1O_2$), superoxide (O_2), hydrogen peroxide (H_2O_2), and hydroxyl radicals (OH^-). When chlorophyll is excited by light, it can generate singlet oxygen, leading to damage in various biological components such as PSI and PSII, proteins, pigments, and nucleic acids (Sies, 1993). Singlet oxygen, with a half-life of approximately 3 seconds, has the potential to cause cellular harm (Oliveira et al., 2009).

Hydrogen peroxide (H_2O_2) is generated as a byproduct of normal metabolism through processes such as photorespiration, mitochondrial electron transport, and Mehler reactions in chloroplasts. Both biotic and abiotic stresses can further increase H_2O_2 production through pathways like plasma membrane-localized NADPH oxidase and peroxisomal glycolate oxidase. At low concentrations, H_2O_2 can act as a signaling molecule, influencing photosynthesis. Its relatively long half-life allows it to cross membranes and exert oxidative effects at locations distant from its source, unlike superoxide (Neill et al., 2002; Noctor et al., 2002).

During the electron transport chain, both thylakoids and mitochondria produce superoxide radicals, which can then be converted into other reactive oxygen species (ROS) like H_2O_2 and hydroxyl radicals. The hydroxyl radical (•OH), considered one of the most harmful ROS, is formed when iron (Fe^{2+}, Fe^{3+}) catalyzes the reaction between H_2O_2 and O_2 at neutral pH. Hydroxyl radicals can cause damage to proteins and membranes. Unlike other ROS, hydroxyl radicals cannot be effectively eliminated through enzymatic mechanisms. Excessive production of hydroxyl radicals can lead to cell death (Pinto et al., 2003) (Figure 1.6).

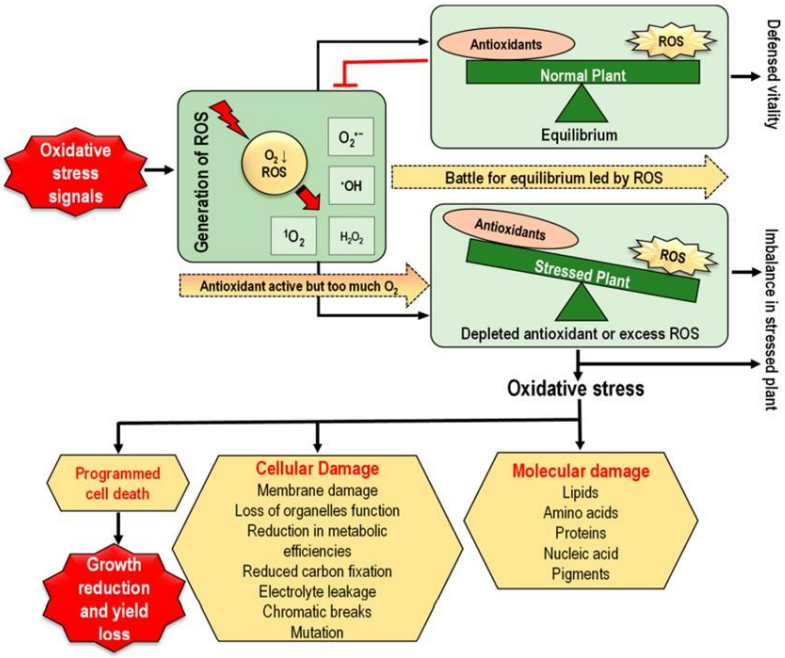

Figure 1.6 *Oxidative stress in plants and its consequences (ROS, reactive oxygen species; $^1O_2$, singlet oxygen; $O_2^{\bullet-}$, superoxide anion; H_2O_2, hydrogen peroxide; $^{\bullet}OH$, hydroxyl radical, adapted from Hasanuzzaman et al., 2020.*

1.5 Antioxidant defense machinery

The antioxidant defense mechanism is one part of the defense against reactive oxygen species (ROS) that result in damage from stress. Both enzymatic and non-enzymatic components make up this apparatus.

1.5.1 Non-enzymatic components

Ascorbate, glutathione, proline, tocopherol, carotenoids, and flavonoids are a few examples of non-enzymatic substances that can act as antioxidants and are often strengthened by a variety of abiotic stimuli, according to (Hasanuzzaman et al., 2019). As a cofactor and a factor in the production of tocopherol, ascorbate is an essential substrate for scavenging H_2O_2. Ascorbate has also been demonstrated to increase a plant's resistance to abiotic stress by strengthening its nutritional and water status, capacity for antioxidants, and overall photosynthetic efficiency.

Proline serves multiple functions in plants, acting as a strong osmoprotectant, a signaling molecule, and an important component of proteins and free amino acids in primary metabolism (Singh et al., 2015). Its unique ability to accumulate without causing harm to cellular structures makes it crucial for various physiological responses of plants to different stimuli. Additionally, proline plays a significant role as an antioxidant defense molecule, protein stabilizer, metal chelator, and scavenger of reactive oxygen species (ROS), contributing to plant defense mechanisms (Dar et al., 2016; Adejumo et al., 2021).

1.5.2 Antioxidant enzyme components

Superoxide dismutase (SOD), a potent antioxidant belonging to the metalloenzyme family, is present in all aerobic organisms. SOD enzymes play a crucial role in catalyzing the conversion of O_2 into H_2O_2 and O_2. Within plant cells, there are three distinct isoforms of SOD: Fe-SOD, Cu/Zn-SOD, and Mn-SOD, each located in different compartments (Mittler, 2002; Pilon et al., 2011) (Figure 1.7).

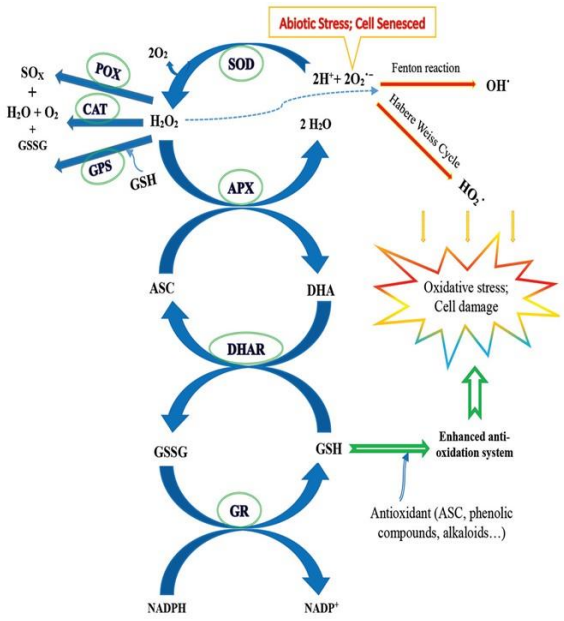

Figure 1.7 *Schematic demonstration of antioxidant defense mechanism in plants (Adapted from Xu et al., 2015).*

The capacity of the enzyme catalase (CAT) to convert H_2O_2 into O_2 and H_2O is widely recognized (Halliwell and Gutteridge, 2015; Mhamdi et al., 2012). Catalase exists in multiple isoforms, including CAT1, CAT2, and CAT3. CAT3 is predominantly found in vascular tissues, while CAT2 is primarily present in leaves (Frugoli et al., 1996; Mhamdi et al., 2010) (Figure 1.7).

1.6 Drought, a major effector of crop

It is anticipated that the frequency of drought events will increase throughout the world, with severe effects particularly in Mediterranean and subtropical climates, as a result of significant changes in global air temperature and precipitation patterns being brought on by the burning of fossil fuels, deforestation, and industrialization (Martorell et al., 2014). Since 1970s, earth has been experiencing severe drought effects and this keeps on increasing each year (Dai et al., 2004). Western and peninsular India are home to the majority of drought-prone areas in the country, including the desert, semi-arid, and sub-humid regions, encompassing around 54 percent of the national territory highly susceptible to drought stress (Figure 1.8). Drought is characterized by prolonged periods (days-weeks-months) of below-average rainfall. Climate change is expected to contribute to more frequent and severe drought in the future (IPCC 2013), exacerbating on various sectors such as water supply, agriculture, and health. Drought, as a significant abiotic stressor, significantly hampers plant growth and development, resulting in reduced productivity and alterations in the plant species (Chaves et al., 2009).

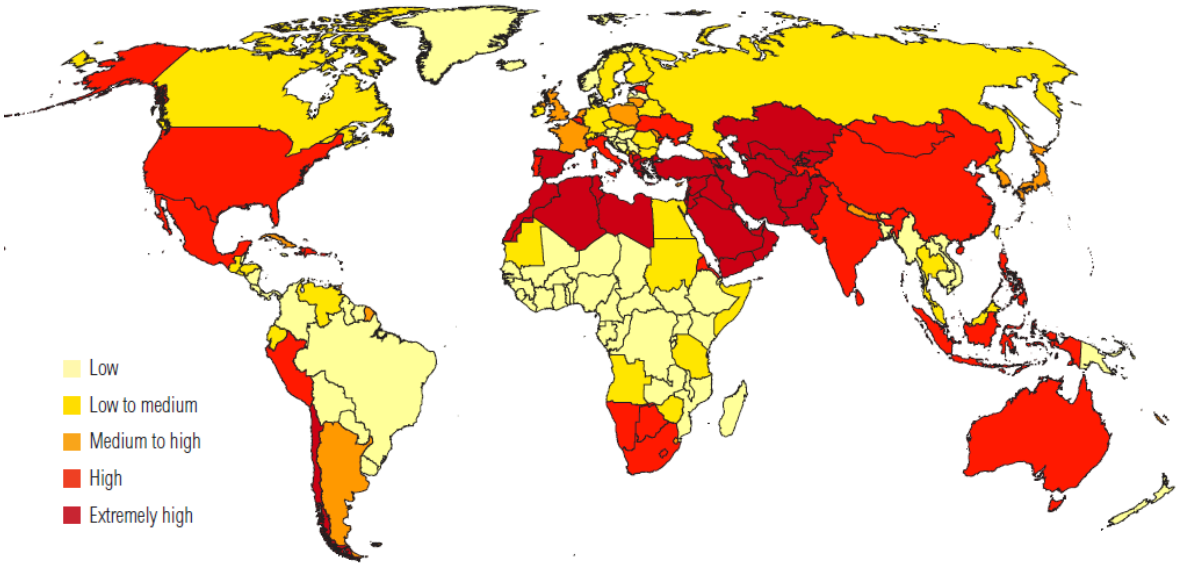

Figure 1.8 *At present, 54% of agricultural lands in India are facing high to extremely high-water stress, and it is expected to increase by 2040.*

We are presently seeing an increase in global hunger, with distressing crop yields, rising prices, and escalating food insecurity for large proportions of the world's population. Our current food system is dysfunctional regarding its impacts on both people and the planet—and change is urgently needed. Subsistence farmers play a major role in the conversion of degraded lands into productive farms, enabling the world to produce nutritious food in a more sustainable manner. Environmental stresses greatly affect plant productivity—with stress from temperature, salinity, and drought being among the worst scourges of agriculture. Water deficits occur during drought as well as during cold conditions, causing turgor stress at the cellular level. The altered osmotic potential across the plasma membrane is likely to trigger the stress response at the molecular level, resulting in an oxidative burst under drought stress conditions. Oxidative species are initially generated from the acceptor side of PS I.

Environmental stresses trigger a wide variety of plant responses, ranging from altered gene expression and cellular metabolism to changes in growth rates and crop

yields. All plants experience such environmental stress during their lifetime. More commonly, drought, salinity, low and high temperatures, flood, pollutants, and radiation are the important stress factors limiting the productivity of crops. The prevailing conditions in the natural environment rarely support a maximum growth rate; thus, the ability to deal with stress is a fundamental aspect of plant growth. In highly stressful environments, natural selection leads to the evolution of tolerant plants that show conservative resource usage and slow growth. Such plants often have long-lived leaves that are physically tough and high in toxic or unpalatable defensive compounds, thus decreasing the loss of resources to herbivores. In contrast, most high-yielding agricultural species are mesophilic in nature—unable to tolerate extreme stress throughout their entire lifetime but equipped with sophisticated defense mechanisms to cope with daily environmental stress conditions (Foyer et al., 2000; Zhu et al., 2002; Asharaf and Harris, 2013).

Plants have developed numerous physiological and biochemical strategies to cope with adverse conditions. In response to dehydration stresses, plants perceive and transduce stress signals through signaling components, leading to the activation of stress-related genes and the synthesis of diverse functional proteins, ultimately prompting a variety of physiological and metabolic responses (Zhu 2002). Well-characterized proteins in plant cell protection from dehydration stress damage include molecular chaperons, osmotic adjustment proteins, ion channels, transporters, and antioxidation or detoxification proteins. These functional proteins' expressions are primarily regulated by specific transcription factors (Reddy et al., 2004). SNAC1-overexpressing rice plants show significantly enhanced drought resistance and salinity tolerance, suggesting the promise of this gene for genetic improvement of stress tolerance in rice (Hu et al 2006). Increased ZmPLC1 expression increases maize's

ability to withstand drought. According to (Wang et al., 2018) the genetically modified plants outperform conventional maize in terms of decreased lipid membrane peroxidation, osmotic adjustment, photosynthetic rates, reduced ion leakage, grain production relative water content and osmotic adjustment.

ROS have the capacity to be produced as a result of environmental stresses, which can result in oxidative damage. Increased membrane permeability, lipid peroxidation, enzyme dysfunction, and decreased photosynthetic rates are the symptoms of this damage. In extreme circumstances, the cell may die as a result of these impacts. Studies by (Shiu and Lee 2005, Subramanyam et al., 2005, Ashraf and Harris 2013), and others have shown that the acceptor side of PS I is typically where ROS production occurs. Oxidative stress is a key component of the overall stress response in marine organisms subjected to environmental stressors, such as thermal stress brought on by climate change. Like many other species, macroalgae and agricultural plants engage their antioxidant defence mechanisms to deal with oxidative circumstances. This entails raising the production of low molecular weight molecules and ROS-scavenging enzymes such superoxide dismutase, ascorbate peroxidase, and catalase (e.g., tocopherols, carotenoids, and ascorbic acid). These adaptive reactions have been shown in studies by (Aguilera et al., 2002; Rijstenbil 2003; Shiu and Lee 2005). The antioxidative capacity of a cell, which is an important aspect of its overall stress tolerance, determines its potential to survive oxidative damage brought on by ROS (Collen and Davison 1999). Drought is among the most important kinds of abiotic stress affecting plants. One inevitable consequence of drought stress is enhanced ROS production in chloroplasts (Moran et al., 1994; Ashraf and Harris 2013; Pandolfi et al., 2012; Shahid et al 2012). Intracellular ROS concentration is tightly controlled by a versatile and cooperative antioxidant system. However, in cases of prolonged drought

stress, ROS production will overwhelm the antioxidant system's scavenging action, resulting in extensive cellular damage and death. The chloroplast is a major cellular site responsible for ROS production (Foyer et al., 1994), and its protein complexes are the immediate subjects to ROS-inflicted damage. During photosynthesis, energy from sunlight is captured and transferred to two light-harvesting complexes (PSI and PSII) located in the chloroplast thylakoid membranes. On the PSI side, electron transport components (e.g., Fe-S centers and reduced thioredoxin) can be auto-oxidized, resulting in O_2 reduction (the Mehler reaction) and the formation of superoxide and H_2O_2 (Mehler et al., 1951). Approximately 10% of photosynthetic electrons are estimated to flow to the Mehler reaction (Foyer and Noctor 2000). This electron "leakage" to O_2 with corresponding ROS generation is favorable to the electron transport chain since it poises electron carriers to act more efficiently (Noctor and Foyer 1998). As the primary producer of superoxide, PSI likely utilizes sophisticated protective mechanisms.

1.6.1 Drought responses in higher plants

Depending on variables, including the degree and length of the stress, the genotype of the plant within the same species, and its developmental stage, different plants respond to drought in very different ways (Farooq et al., 2009). Plants constantly try to modify their development and physiology in an effort to adapt to the severity of the drought and survive. For plants to become tolerant of drought, they must retain this plasticity when there is a water shortage. Plants typically slow down the growth of their shoots and, to a lesser extent, their roots in reaction to drought. This is because in times of water scarcity, plants with an improved root-to-shoot ratio are typically more tolerant to drought. The primary physiological indication of a water deficit is the partial or total closure of stomata, which leads to a decreased transpiration rate and a decreased CO_2 intake for photosynthesis (Figure 1.9).

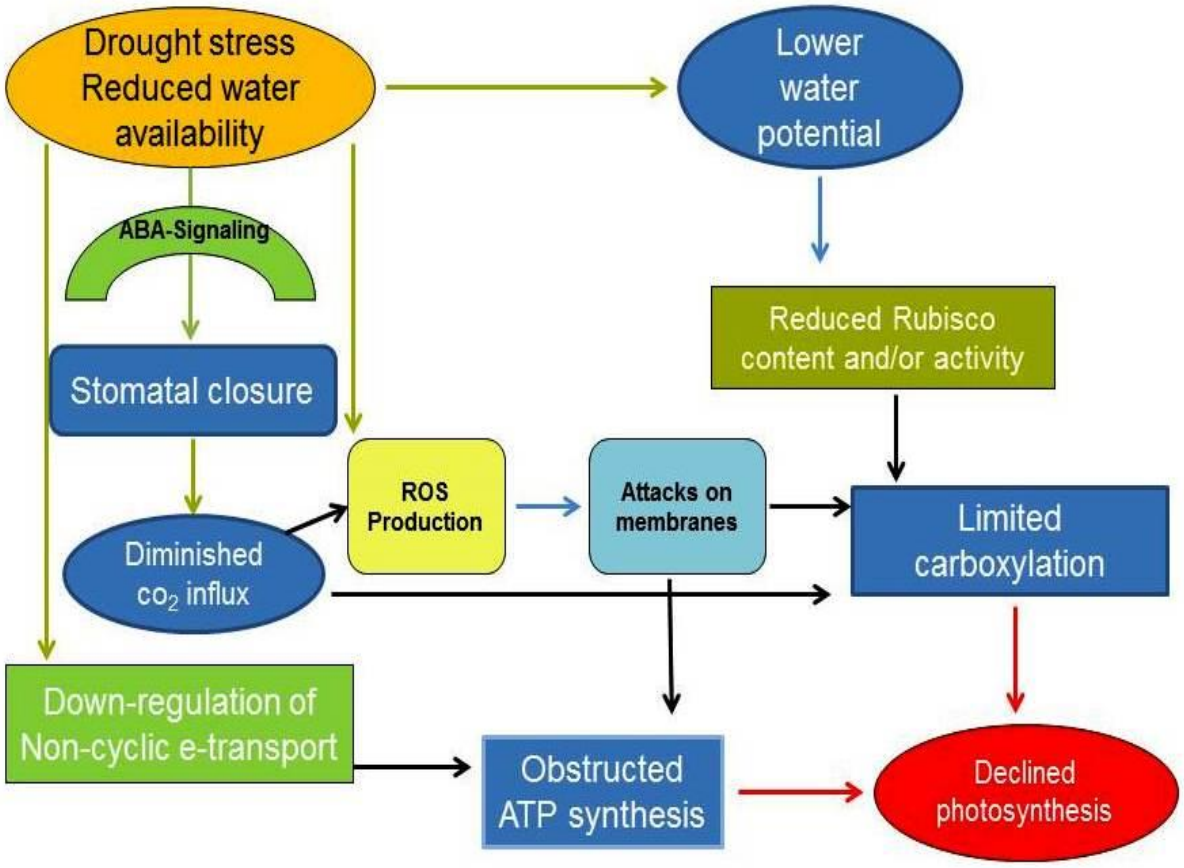

Figure 1.9 *Possible mechanisms in plants under drought stress.*

In times of low water availability, stomatal closure, which lowers transpiration rates, is thought to be a key adaptive mechanism for reducing water loss. However, when CO_2 uptake is limited, leaf carbon fixation also decreases. Drought stress prevents cell proliferation and growth, which lowers whole-plant carbon fixation. The ability to redirect photosynthesis and energy toward the synthesis of defensive chemicals. Also, maintaining root growth for continuous water uptake, or else for shoot growth during times of water deprivation, is another adaptive characteristic that helps plants survive. Drought stress can still cause stunted growth and development, wilting, desiccation, and ultimately the death of the plant, even though some species have the advantageous ability to accumulate stem reserves that allows them to maintain growth even during severe drought stress (Blum et al., 1994). Depending on the plant's species, growth

stage, the severity and length of the drought, as well as other interrelated environmental factors, the way that plants react to drought stress can vary greatly.

1.7 Physiological response under drought

Plants exhibit various physiological responses to drought, including reduced stomatal conductance, decreased photosynthesis, inhibited shoot growth, and lower yields. These responses are triggered by signals indicating the presence of drought stress, which are initially detected by the roots and then transmitted to other parts of the plant through inter-organ communication involving calcium ion (Ca^{2+}) waves, reactive oxygen species (ROS) signals, and electrical currents (Kuromori et al., 2022). The initial response of the plant to maintain leaf water potential is the closure of stomata (Laxa et al., 2019). This closure is caused by an imbalance of potassium (K^+), chloride (Cl^-), and hydrogen ions (H^+) in guard cells, leading to decreased turgor pressure and subsequent stomatal closure (Mukarram et al., 2021). Reduced transpiration rates and decreased leaf water potential contribute to a decrease in the relative leaf water content (RWC), which is another physiological adaptation to drought stress.

On the other hand, decreased transpiration and stomatal conductance result in improved water use efficiency (WUE). Unfortunately, limited stomatal conductance and reduced CO_2 uptake ultimately restrict photosynthesis, which reduces the synthesis of carbohydrates (Wahab et al., 2022). Additionally, reducing photosynthesis and drought can impact photosystems and chlorophyll pigments (Hu et al., 2018). Reduced photosynthesis next results in different photoassimilates distribution between sink organs and roots, which limits shoot growth and lower yields (Farooq et al., 2009) (Figure 1.10).

1.8 Biochemical response under drought

Drought-induced oxidative damage in plants leads to the production of reactive oxygen species (ROS), which can cause harm to proteins, lipids, and nucleic acids. ROS encompass superoxides, hydroxyl radicals, peroxides, singlet oxygen, and alpha oxygen. However, plants employ various defense mechanisms, including antioxidant enzymes, osmoprotectants, solutes, and other strategies to counteract ROS toxicity (Figure 1.10). To regulate ROS levels, osmoprotectants such as sugar alcohols, amino acids (e.g., proline and glycine betaine), and secondary metabolites are generated through these defense mechanisms. Antioxidants, which can be enzymatic or non-enzymatic, play a role in reducing ROS toxicity. Key enzymatic antioxidants include catalase, superoxide dismutase, glutathione peroxidase, glutathione reductase, and peroxidase. Non-enzymatic antioxidants encompass glutathione, ascorbic acid, carotenoids, and phenols, with drought inducing an increase in phenolic content in tomato plants (Mukarram et al., 2021).

Amino acids, such as proline, accumulate in response to drought due to factors like reduced protein synthesis, increased protein breakdown, or enhanced biosynthesis (Yadav et al., 2019; Huang and Jander, 2017). Proline also functions as a ROS scavenger and helps regulate cellular redox status (Wahab et al., 2022). Sugars, particularly trehalose, fructans, and soluble sugars, act as osmotic agents and osmoprotectants. Trehalose, specifically, serves as an energy and carbon source, aiding in the stabilization of proteins and membranes under stress conditions (Mukarram et al., 2021). Phytohormones play a crucial role in detecting and mitigating drought stress. Abscisic acid (ABA) is recognized as the primary chemical messenger involved in drought stress response. ABA-dependent or ABA-independent signaling pathways can trigger specific responses to drought stress. The ABA signal pathway involves ABA receptors of the

PYR/PYL/RCAR type, group A 2C protein phosphatase (PP2C), and SnRK2 proteins. When ABA accumulates and binds to ABA-induced genes' ABRE elements, such as bZip TFs (like EMP1), ABA receptors of the PYR/PYL/RCAR type are activated, leading to PP2C inactivation and subsequent release of SnRK2. Brassinosteroids, on the other hand, modulate osmoprotectant molecules and hydrotropic responses in roots independently of ABA, thereby mitigating the impact of drought stress. These phytohormones also regulate the expression of stress-responsive genes to alleviate the effects of drought stress.

1.9 Molecular responses in drought

Drought triggers the activation of drought-responsive genes, which are responsible for the production of proteins involved in signaling and transcriptional control. These proteins include protein kinases, phosphatases, transcription factors, late embryogenesis abundant proteins (LEAs), osmotin, aquaporins, and sugar transporters. They play essential roles in protecting cellular membranes, regulating water and ion transport, and facilitating various physiological responses to drought (Fang and Xiong, 2015; Kaur and Asthir, 2017) (Figure 1.10). Drought-responsive genes can be classified into two groups based on their dependence on the hormone ABA for activation: ABA-dependent and ABA-independent (Kaur and Asthir, 2017). Genes associated with the ABA-mediated response, such as ABI 1 and 3, exhibit differential regulation during drought conditions. ABI 1 is upregulated, while ABI 3 is downregulated. ABI 3 plays a role in the recovery from drought stress (Pinheiro and Chaves, 2011). The interplay between biochemical and physiological processes, along with the expression of drought responsive genes, enables plants to cope with drought stress and mount appropriate

responses.

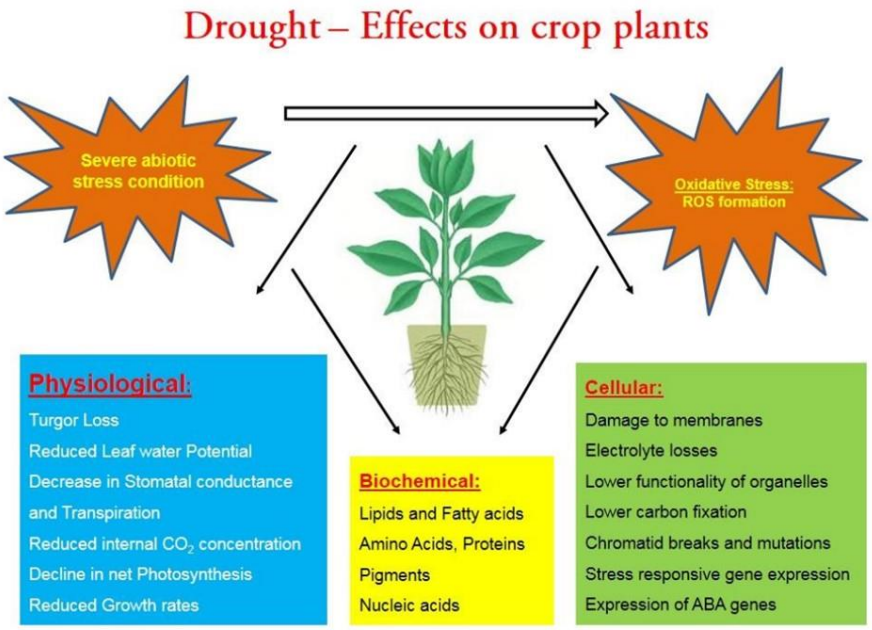

Figure 1.10 *Schematic representation of abiotic stress responses in plants. Severe abiotic stress leads to oxidative damage which eventually affects cellular, molecular and physiological components of plant metabolism (Reddy et al., 2004).*

1.10 Polar Lipids Role in the Thylakoid Membrane

The formation of a double-layered surface in all living cells relies on membrane lipids (Alberts et al., 2014). This non-polar bilayer serves a crucial function in preventing ion diffusion across the membrane, which generates a proton motive force essential for photochemical activities (Sacksteder and Kramer, 2000). Additionally, the membrane houses various proteins, receptors, and ionic pores that regulate the transport of molecules, thereby controlling metabolic processes (Alberts et al., 2014). These membrane lipids are highly conserved from cyanobacteria to higher plants, and they play a vital role in maintaining membrane integrity and ensuring the proper functioning of the photosynthetic apparatus (Figure 1.12) (Kobayashi et al., 2016). The three layers of the chloroplast, which perform photochemical and electron transport reactions, are

the outer and inner membranes, as well as the thylakoid intermembrane gap (Alberts et al., 2014). As per reports, four distinct lipid classes make up the majority of the chloroplast thylakoid membranes in plants and cyanobacteria (Boudière et al., 2014).

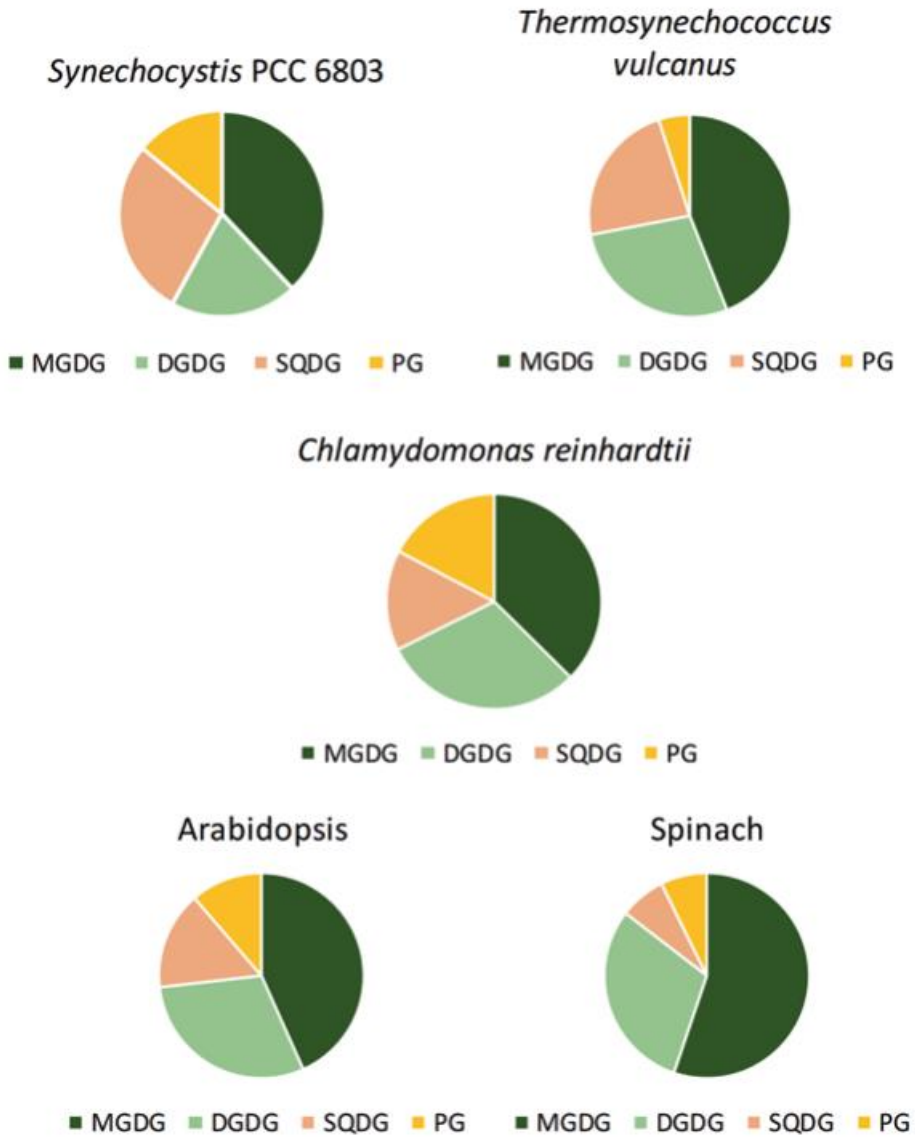

Figure 1.11 *Composition of lipids in thylakoid membranes from the cyanobacteria Synechocystis sp. PCC 6803 and Thermosynechococcus vulcanus, the green algae Chlamydomonas reinhardtii, and the higher plants Arabidopsis thaliana and spinach. The Data presented from cyanobacteria were obtained from Sakurai et al., 2006; spinach (Dorne et al., 1990); Chlamydomonas (Nguyen et al., 2013); and Arabidopsis (Alfonso et al., 2021).*

The most prevalent galactolipid in thylakoid membranes is monogalactosyldiacylglycerol (MGDG), followed by digalactosyldiacylglycerol (DGDG) and a sulphur containing lipid, sulfoquinovosyldiacylglycerol (SQDG). The phosphatidylglycerol (PG), is least prevalent (Dorne et al., 1990). Together, MGDG and DGDG account for roughly 75% of the uncharged lipids in thylakoid membranes, with MGDG making up about 50% and DGDG around 25% (Dorne et al., 1990). These two galactolipids are necessary for chloroplast photosynthesis to work properly (Kobayashi et al., 2007). Thylakoid membranes likewise include SQDG and PG, with PG being the only phospholipid detected in cyanobacteria and phosphatidylinositol (PI) being a minor component (Wada and Murata, 1998; Kobayashi, 2016) (Figure 1.12).

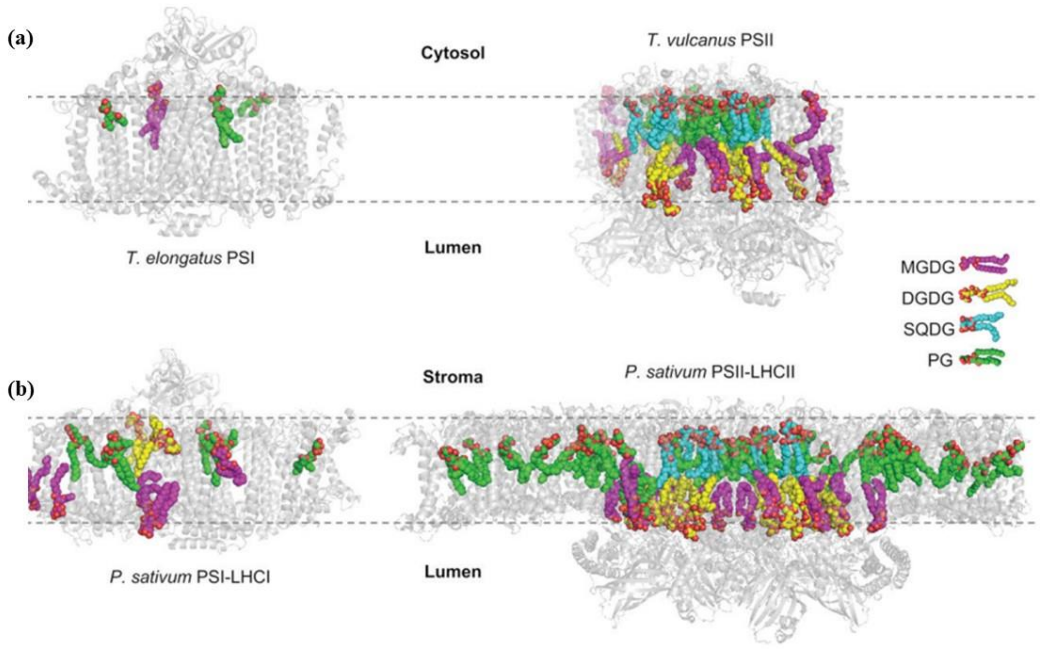

Figure 1.12 *Asymmetrical distribution of lipid molecules towards the stromal/cytosolic and lumenal sides in photosystems. (a) PSI (1JB0, Jordan et al., 2001) from Thermosynechococcus elongatus and PSII (4UB8, Suga et al., 2015) from Thermosynechococcus vulcanus (b) PSI–LHCI (7DKZ, Wang et al., 2021) and PSII–LHCII (5XNL, Su et al., 2017) from P. sativum. Side views along the membrane plane are shown for each complex. Lipid molecules are shown as colored spheres, with oxygen atoms in red. Protein backbones are shown as silver semi-transparent cartoons, and pigments and other cofactors are omitted for clarity. Broken lines represent the cytosolic/stromal and luminal surfaces of thylakoid membranes.*

Suga et al. (2019) found 15 lipids in the PSI-LHCI complex of *C. reinhardtii,* that were divided into three types: PG, DGDG, and MGDG. Four lipids, including PG846 related to PsaA, PG847 linked to PsaA, DGDG850 linked to PsaB, and PG851 linked to PsaB, are found in the PSI core and are dispersed in a pseudo-C2 symmetrical configuration (Suga et al., 2019) (Figure 1.13). The membranes of the chloroplast envelope are where galactolipids are made. In tobacco and Arabidopsis, MGD1, the enzyme that creates the majority of MGDG, is located near the chloroplast's inner membrane (Awai et al., 2001). The MGD1-1 knockout mutant in Arabidopsis exhibits a progressive breakdown of galactolipids, a 40% reduction in MGDG, and severe loss of thylakoid membranes (Kobayashi et al., 2007). According to Wu et al., (2013) and Fujii et al., (2014), partial MGDG lipid deficit in Arabidopsis, Tobacco, and Maize resulted in a decrease in the number of thylakoid membranes and changed morphology. Due to its capacity to facilitate the solubilization of violaxanthin and its ability to bind violaxanthin de-epoxidase to the thylakoid membrane, MGDG also plays a significant role in photoprotective nonphotochemical quenching (Jhans et al., 2009). However, the loss of PSII activity and the development of immature photosynthetic supercomplexes are brought on by the almost complete lack of MGDG (95%) (Kobayashi et al., 2013).

Research has shown that MGDG is essential for PSII dimerization and LHCII oligomerization, and it also improves the energy coupling between the LHCII and PSII core proteins (Schaller et al., 2011; Kansy et al., 2014). Two DGDG synthase complexes, DGD1 and DGD2, are found in the outer chloroplast envelope (Froehlich et al., 2001; Kelly et al., 2003). While DGD2 is active when phosphate is limited to provide the intermediate of lipids for cell survival, DGD1 synthesizes the majority of

DGDG. Similar outcomes were seen in the Tobacco MGD1 mutant, which displayed a bottleneck in electron transport as well as decreased levels of the Cyt b6f protein complex (Wu et al., 2013). The most crucial galactolipid for the healthy maturation and upkeep of thylakoid membranes is DGDG. Abnormal bends in the leaf chloroplast thylakoid membranes were seen in the DGDG mutant of *A. thaliana*. DGDG participates in the trimerization of LHCII and is necessary for the appropriate maintenance of PSII structure and function, particularly on the donor side (Steffen et al., 2005; Hölzl et al., 2009). The thylakoid membrane's development is similarly impacted by the loss of PG and SQDG in plants (Figure 1.13). The breakdown of PG in thylakoid membranes in spinach and pea plants impairs the electron transport pathway in PSII without impacting PSI activity (Droppa et al., 1995).

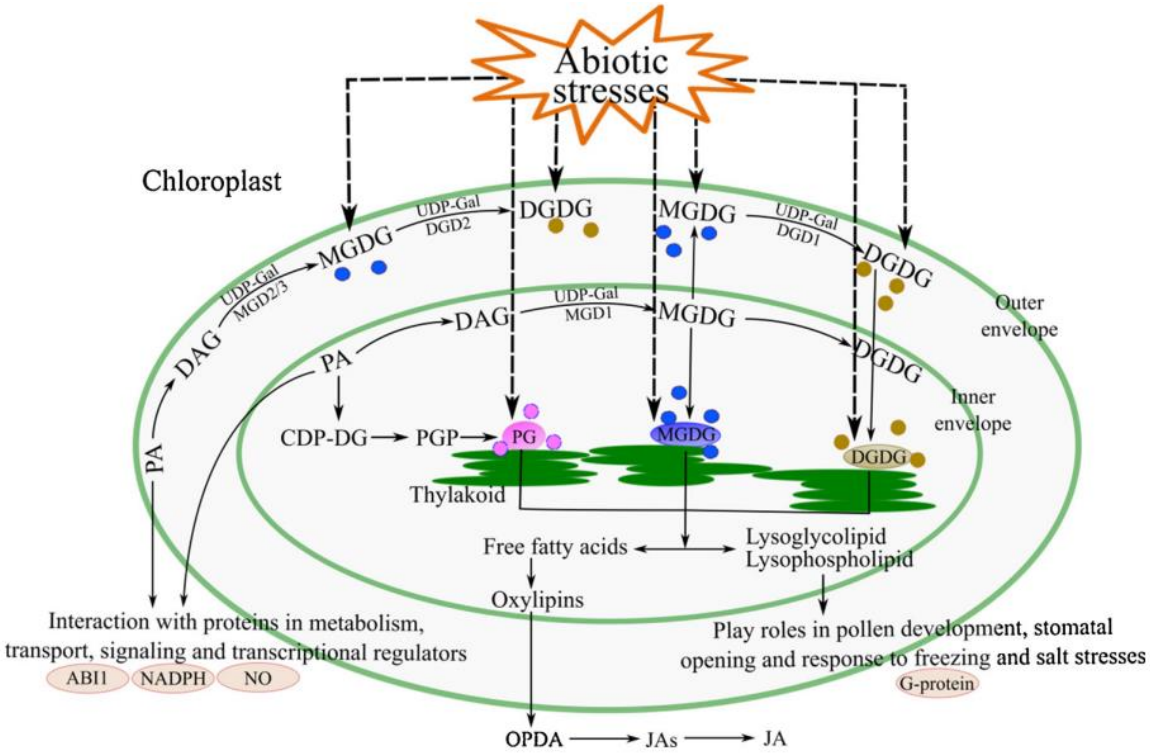

Figure 1.13 *A schematic diagram of the effect of abiotic stresses on membrane lipid remodeling in photosynthetic organisms and lipid-related signaling pathways in plants. Abiotic stresses caused perturbations in several primary membrane lipids, including MGDG, DGDG and PG (This figure was adapted from Liu et al., 2019).*

Loss of SQDG (sulfoquinovosyldiacylglycerol) leads to reduced grana stacking and significant curling in thylakoid membranes (Yu and Benning, 2003). Galactolipids (MGDGD and DGDG) and acidic lipids (PG and SQDG) are essential for maintaining thylakoid membrane integrity, stabilizing PSII dimer, facilitating proper PSI function, supporting the LHCII complex, and ensuring the activity of the oxygen-evolving complex (Yu and Benning, 2003). Furthermore, phosphatidylinositol (PI), phosphatidylethanolamine (PE), and diacylglyceryl-N, N, N-trimethylhomoserine (DGTS) play critical roles in cellular metabolism (Moellering et al., 2009).

Lipids are over-accumulated under environmental stress such as temperature, nutrient deficiency, salinity stress, and light stress. Under nitrogen-deficient conditions, for example, *C. reinhardtii* enhanced lipid synthesis by 93 %, while *Acutodesmus dimorphus* generated 75 % neutral lipids (Chokshi et al., 2017). Similarly, iron deficiency leads to enhanced lipid accumulation in *C. reinhardtii* (Devadasu et al., 2021). It's feasible that nitrogen deficiency stimulates lipid production in microalgae by altering other metabolic pathways (Srinuanpan et al., 2018). In *Phaeodactylum tricornutum*, *Nannochloropsis oceanica,* and *Chlorella protothecoides*, strong light intensity was utilised to stimulate the formation of neutral lipids (Krzeminska et al., 2015; Huete-Ortega et al., 2018). Under extreme salinity stress, lipid accumulation increased significantly in *Chlorella vulgaris* and *Dunaliella sp*. by 21.1 and 70 %, respectively (Takagi et al., 2006).

Lipids play a crucial role as the primary means of energy storage and as a key component of plasma membranes, which act as the boundary between cells and the external environment. Several types of lipids, such as phosphoinositide, phosphatidic acid, sphingolipids, oxylipins, and free fatty acids, also function as building blocks for the production of signaling molecules. Plant growth is known to be influenced by abiotic

stresses like drought and temperature fluctuations. Furthermore, these abiotic stresses can trigger specific lipid-dependent signaling pathways that regulate the activation of stress-responsive genes and aid in plant adaptation to stressful conditions. While numerous studies have focused on lipid production and the mechanisms of abiotic stress response, there is limited information available on the specific roles of plant lipids under abiotic stress.

The climate and food crises and the need to preserve biodiversity have generated significant scientific interest in screening and isolating microalgae and plants from harsh and extreme environments – including drought, salinity, deserts, hot springs and snow. The target plants of the proposed research are *P.sativum* that exhibit remarkable resilience to abiotic stimuli: drought, high light and extreme temperature emphasis on stress effects on lipids metabolism. Most of the green algae *Lobosphaera*, *Coestrella* sps and Chlamydomonas sps. that exhibit remarkable resilience to abiotic stimuli: freezing (*L. incisa*), high light, temperature, and desiccation (*Coestrella* sps). These organisms present unique examples of resilient green microalgae capable of revival from freezing and desiccation. These algae are also particularly interested in producing nutritionally important polyunsaturated fatty acids and carotenoids and are suitable for biotechnological applications. These microalgae are an effective photosynthetic source of food and feed ingredients and can be used in various applications, such as human, fish feed, and healthy supplements. We intend to gain deeper insights into the molecular mechanisms of these *P.sativum* extreme tolerance to specific stresses (particularly drought). To this aim, we wish to identify the metabolic and genetic control program that enables these unique traits.

1.11 Transcriptome analysis during drought stress

A potent tool for comprehending the molecular processes in determining the plant responses to abiotic stressors, through the study of the full set of RNA molecules in a cell/organism is known as transcriptomics. In recent years, it has been heavily used to examine the variations in gene expression in crop plants under drought stress conditions (Singh et al., 2017). This research has shown that, drought stress downregulates the genes involved in photosynthesis, reducing growth and photosynthesis. Additionally, the stress brought on by dryness results in the triggering of ROS, which can harm plant cells through oxidation. *P. sativum* increases the expression of antioxidant genes like superoxide dismutase (SOD), catalase (CAT), and peroxidase (POD) to avert this harm (Gill et al., 2010). The regulatory networks, signalling pathways, and molecular mechanisms underlying *P.sativum* drought stress response have all benefited from the analysis of transcriptome data.

Transcriptome research has been transformed by the application of RNA sequencing (RNA-seq), which offers a potent tool for examining the molecular components and functional characteristics of RNA in various organisms (Meyer et al., 2012). Stress-induced transcriptome investigations have uncovered major pathways that were previously unknown. With the recent development of sequencing technologies like Roche/454, AB SOLiD, and Illumina, non-model organisms without reference genome sequences can now be sequenced and annotated (Fan et al., 2015) with the help of *de novo* analysis. Despite these developments, the characterization of the entire transcriptome information in the pea plants, including the patterns of gene expression of the photosynthetic genes and lipid biosynthesis enzymes under drought, is still lacking. The change of lipids under drought stress has been addressed in Chapter 5.

Global transcriptome investigation on crop plants under drought stress, (Gao et al., 2021), demonstrated orderly modifications in biological functions, such as photosynthesis, protein turnover, and carbon fixation. Despite this, it is still unclear how the redox homeostasis mechanism in chloroplasts is regulated in response to drought stress. According to earlier research, PS I create both superoxide (O_2^-) and hydrogen peroxide (H_2O_2) as signalling molecules, but PS II solely produces O_2. As a result, transcriptional and post-translational acclimation mechanisms can be started by chloroplasts as an environmental sensor (Foyer et al., 2000). Our knowledge of drought-induced processes will also be aided by our growing understanding of the metabolome and transcriptome.

1.12 Metabolites function during drought stress

Abiotic stresses in plants lead to the accumulation of reactive oxygen species (ROS), which can have detrimental effects on their metabolic processes due to their immobility. In plants, ROS serve as important signaling molecules that regulate cell growth and function. However, excessive production of ROS can result in oxidative stress, causing cellular damage and activating metabolic pathways that lead to cell death (Mittler et al., 2017; Waszczak et al., 2018). To counteract oxidative stress, plants have developed sophisticated metabolic systems for detoxifying ROS. These systems include scavenging mechanisms that prevent ROS accumulation and provide necessary metabolites when ROS production is excessive. Antioxidants and compatible solutes are among the anti-stress substances that mitigate the toxicity of ROS. While certain metabolic responses are common to different types of stress, others are specific to individual stress conditions (Apel and Hirt, 2004).

1.13 Sugar: Exploring the Diverse Roles and Derivatives in Biological Systems

Under stress conditions, certain sugars such as glucose, sucrose, fructose, and raffinose have been observed to increase in plants. Raffinose, for example, is known for its ability to protect plant cells from oxidative damage (Nishizawa et al., 2008). On the other hand, sucrose is the primary sugar transported within plants. In Arabidopsis, exposure to H_2O_2 led to a rapid accumulation of sucrose and fructose and an increase in glucose levels (Morelli et al., 2003).

1.14 TCA cycle intermediate metabolites

The levels of intermediate metabolites in the tricarboxylic acid cycle (TCA cycle) are highly dynamic and serve as substrates for various biosynthetic pathways. These levels reflect the balance between metabolite generation and consumption. Research has shown that respiratory stimulation leads to an increase in TCA cycle metabolite levels. Conversely, oxidative stress typically decreases the pool of TCA cycle metabolites (Dastogeer et al., 2017). In such situations, manipulating TCA cycle enzyme activity becomes crucial for altering the metabolic profile. Oxidative stress inhibits several TCA cycle enzymes, including aconitase, 2-oxoglutarate-dehydrogenase, and pyruvate-dehydrogenase (Dastogeer et al., 2017).

1.15 Amino acids

Oxidative stress has a significant impact on the amino acid composition in plants, particularly affecting their role as substrates for secondary metabolite formation (Chen et al., 2015). Under stress conditions, various amino acids such as glutamine, proline, gamma-aminobutyric acid (GABA), and others are synthesized and can serve as suitable osmolytes or precursors for secondary metabolites. Conversely, low-abundance amino acids are not synthesized but can accumulate due to rapid protein degradation (Hildebrandt, 2018; Ishikawa et al., 2010; Lehmann et al., 2009).

1.16 *Pisum sativum* (Pea), our model plant for the studies

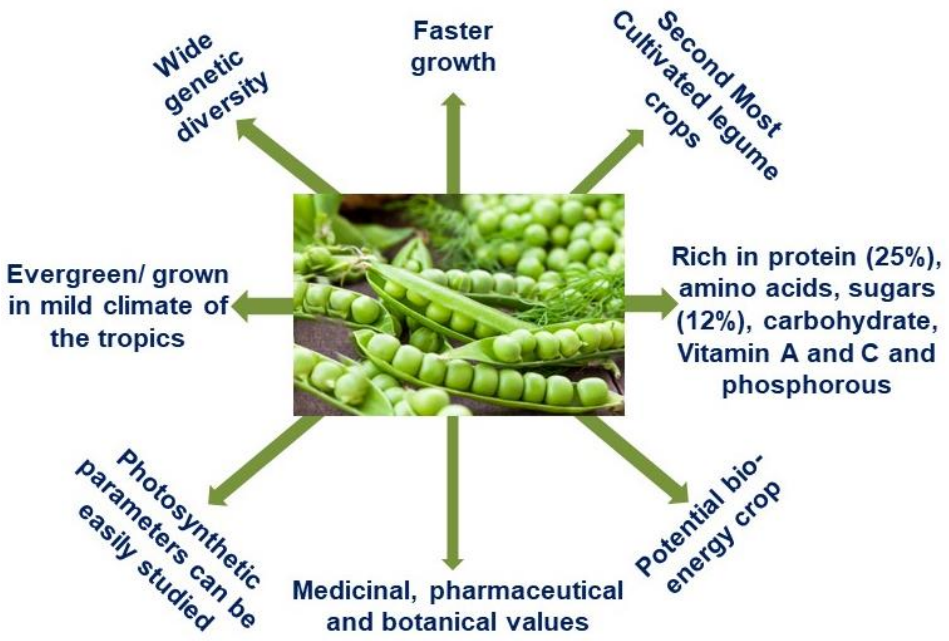

Figure 1.14 *A descriptive model and economic importance of P.sativum.*

I have selected *Pisum sativum* var. Arkel, commonly known as pea, which is an annual herb belonging to the Fabaceae family. Pea is the second most cultivated legume crop worldwide and is renowned for its high protein content, ranging from 22% to 24% in its seeds. Our proposed study aims to improve our understating of the molecular mechanisms of revival after drought in *P.sativum*, with regards to physiological, biochemical, and multiomics aspects. Our analyses will encompass protein, transcriptome, metabolome, functional validation, and molecular engineering approaches. The results are expected to facilitate our understanding of the molecular mechanisms of environmental stresses particularly drought and possibly to accelerate genetic improvement. The findings should help to understand better how environmental stresses like droughts are perceived at the molecular level. They may also hasten genetic advancement for economically significant or more tolerant plants through molecular breeding techniques.

Due to its year-round cultivation, pea crops are exposed to various stresses, particularly drought. Therefore, I have chosen pea as the focus of my study to investigate the photosynthetic parameters related to the organization of protein supercomplexes in thylakoids. This research includes comprehensive data on physiological parameters, photosynthetic efficiency, disruption of photosynthetic complexes, and the recovery process following rewatering. Additionally, my aim to uncover the role of lipids and osmoprotectants in the organization of photosynthetic complexes. However, the molecular mechanisms underlying the leaf tissue transcriptome, proteome, and metabolome in response to drought conditions in peas have not been fully established. Consequently, this research aims to address three fundamental questions that lie at the core of the study.

1. To improve our understanding of thylakoid organization under water stress?
2. To understand the recovery process after the drought stress?
3. To decipher stress tolerance proteins and genes, which play important roles during drought stress?

   Based on these questions, I have framed the following objectives for our studies.

Figure 1.15 *P. sativum seedlings (left panel) and 14th day grown plants (right panel).*

Objectives

- **Investigation of drought effects on physiology, photosynthetic performance, redox status and its reversible changes in structure and function of photosynthetic apparatus of pea leaves**
- **Macromolecular structural changes of supercomplexes of thylakoids in drought stress**
- **Decipher the role of lipids and osmo-protectants in organization of photosynthetic complexes**
- **Investigation of the drought-induced changes in transcriptome, proteome, and metabolomes from leaf tissues**

Chapter 2

Materials and Methods

2.1 Plant material, growth conditions, and drought treatment

Pea seeds (*Pisum sativum* L., cv Arkel) were obtained from Durga Seeds (Chandigarh, India). Seeds were washed with running water for ~2 h before surface sterilization with 0.2% sodium hypochlorite for 15 min. Further, the seeds were washed thoroughly with sterile distilled water and kept on moist blotting paper in a plastic container for imbibition. The seeds were allowed for germination at 22 °C for three days in the dark. Germinated seeds were transferred to a 1.5 L plastic tray filled with soil and farmyard manure (3:1). The seedlings were allowed to grow in a growth chamber under the following conditions: 14 h light/10 h dark cycle under cool-white, fluorescent light at photosynthetic photon flux density (PPFD) of 90 – 120 μmol photons m^{-2} s^{-1}.

Drought stress was imposed on 14 days old seedlings by withholding water for eight days, whereas control plants were maintained under well-watered conditions (Chen et al., 2016). For this study, we selected five-time points after imposition of drought stress at day 0 (D0), day 2 (D2), day 4 (D4), day 6 (D6), day 8 (D8), and seven days after rewatering. The growth and physiological measurements were taken at D0, D2, D4, D6, and D8 and then re-watered for the next seven days (DR) for stress recovery. The experiments were carried out in a laboratory growth chamber. There were six tubs, each with about 30–35 plants, which act as biological replicates. The experiment lasted for four weeks. Water was supplied to all six tubs over the first two weeks. Six tubs were separated into two sets at the end of the second week the 14^{th} day (Figure 2.2). There are two control tubs and four drought treatment tubs. Water was provided to control plants but not to drought plants during the third week (15^{th}–21^{st} days). Leaf samples were obtained from control and drought-treated plants at the end of the third week (the 21^{st} day). Water was given to four tubs of drought-treated plants from the beginning to the end of the fourth week (22^{nd}–28^{th} day) to allow them to

recover from drought stress. Leaf samples from drought-recovered plants were obtained at the end of the fourth week.

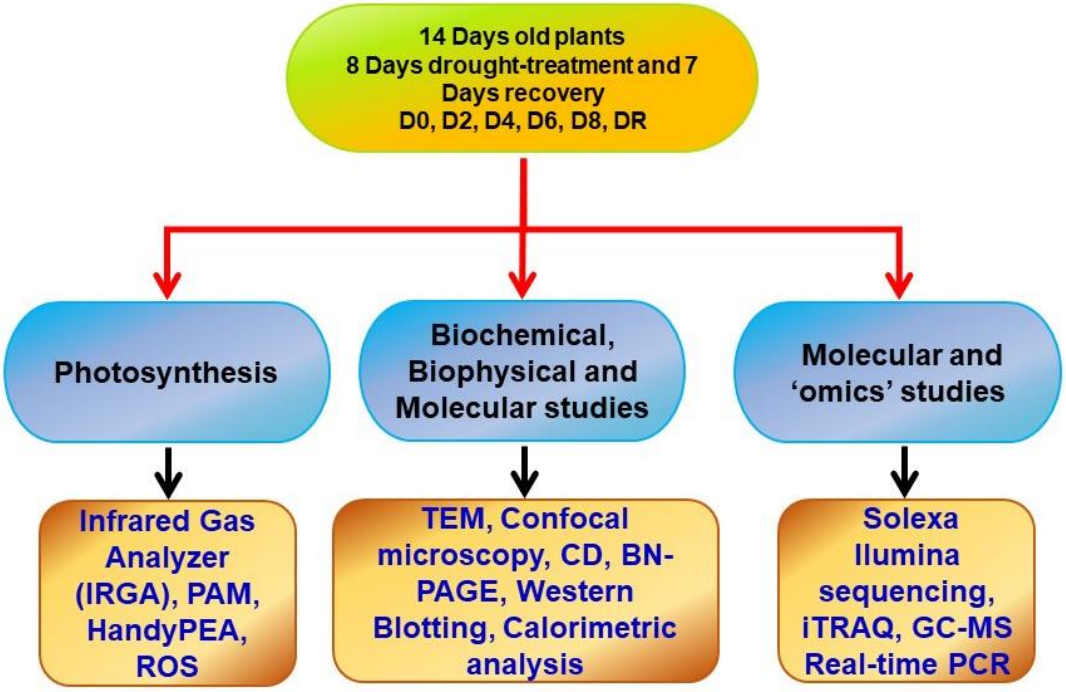

Figure 2.1 *Experimental layout and lists of methods involved for the drought studies in P. sativum.*

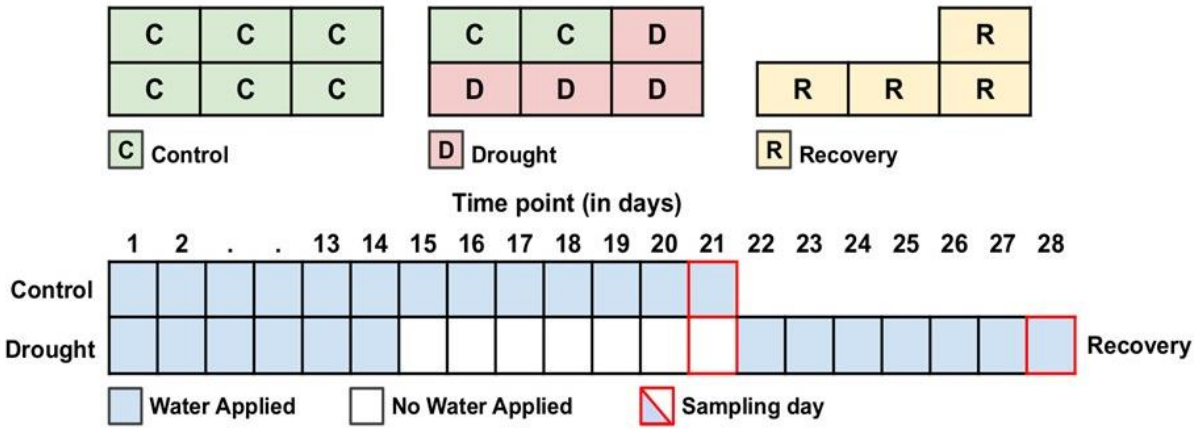

Figure 2.2 *Schematic diagram of experimental design, watering, and sampling plan. The upper picture in the diagram represents three treatments, i.e., control, drought, and recovery. Each block in the upper picture in the diagram represents one tub containing pea plants. The bottom picture in the diagram represents the watering and sampling plan. Each block in the bottom picture in the diagram represents water applied (blue boxes) or not applied (white boxes) and sampling (red outlined boxes) on a given day.*

2.2 Leaf relative water status

With some modifications, the leaf relative water content of control and drought-treated plants was measured according to Marriboina et al., (2020). Fully mature leaves were kept in a plastic tray containing double-distilled water in the dark for 24 h at 4 °C. After hydration, the leaf samples were weighed for the turgid weight (tw) after blotting the leaf surfaces to make them dry. The dry leaf weight (dw) was recorded after oven-dried samples at 60 °C for 72 h. The percentage of leaf relative water content (LRWC) was determined using the following formula: [(fw-dw)/ (tw-dw)] X 100.

2.3 Plant growth and biomass yield

The evaluation of plant biomass encompassed the assessment of control, drought, and recovery conditions. The objective was to measure various parameters such as plant height (both shoot and root) and the leaf area of the plants prior to harvesting. To determine plant height, measuring scales were employed to measure from the root to the top of the canopy. The plant shoots were coppiced above ground level, and subsequently, the different components (leaves, branches, and stems) were separated and promptly weighed in the field to obtain the total fresh biomass of the leaves.

2.4 Leaf gas exchange parameters

Leaf gas exchange measurements were performed using a portable infra-red gas analyzer (IRGA, LI-6400/LI-6400XT, LI-COR Inc., Lincoln, NE, USA), according to (Marriboina et al., 2017). Photosynthetic parameters such as light-saturated net photosynthetic rate (*Pn*), stomatal conductance (g_s), intercellular CO_2 concentration (C_i), and transpiration rate (*E*) were recorded. Further, leaf instant WUE was calculated as *Pn/E*.

2.5 Quantification of chlorophyll

The spectrophotometric measurement of total chlorophyll in isolated thylakoids was conducted following extraction with 80% (v/v) acetone (MERK). To initiate the process, 10 µl of isolated thylakoids were mixed with 990 µl of acetone and vortexed. The mixture was then placed in the dark at -20 ºC for a duration of 20 minutes. Subsequently, the samples were centrifuged at 10,000 x g for 10 min. The total chlorophyll content was determined based on the absorbance readings at 645 nm (A645) and 663 nm (A663) using a spectrophotometer from PerkinElmer, USA, following the methodology described by (Porra et al., 1989). The total chlorophyll (chlorophyll *a* + chlorophyll *b*: Chl a+b) concentration (µg/mL) was calculated as follows:

Chlorophyll *a* (mg/mL) = 12.7 x A663) – (2.69 x A645) x dilution factor.

Chlorophyll *b* (mg/mL) = (22.9 x A645) – (4.68 x A663) x dilution factor.

Total Chlorophyll (Chl *a* + *b*) (mg/mL) = (8.02 × A663) + (20.12 × A645) x dilution factor.

2.6 Reactive oxygen species (hydrogen peroxide and superoxide) quantification

ROS (H_2O_2/superoxide) quantification was done as described earlier with modifications (Bapatla et al., 2021). Freshly harvested leaves were taken in a petri dish containing DAB (1 mg mL^{-1} (pH 3.8)) and NBT (1 mg mL^{-1}) solution and incubated in the dark for 12 h. To visualize ROS, leaf pigments were removed by soaking in a mixture of ethanol: lactic acid: glycerol in the ratio of 3:1:1 (v/v/v) and then washed with methanol. The cleared leaves were preserved and photographed. H_2O_2 was visualized as a reddish-brown color, and superoxide radicals were detected as blue formazan. For quantification of hydrogen peroxide and superoxide, DAB and NBT stained leaves were powdered in liquid N_2 and homogenized in 0.2 M $HClO_4$ and 2 M KOH-DMSO (1/1.6) (*v/v)* solution.

The homogenate was subjected to centrifugation at 10,000 x g for 10 min at 4 ^{o}C. The absorbance of the supernatant was measured at 450 nm for H_2O_2 and 630 nm for superoxide and quantified by using a standard curve plotted with known concentrations of H_2O_2 in 0.2 M $HClO_4$-DAB with a known amount of NBT in KOH-DMSO.

2.7 Antioxidant enzyme assays

Leaves (approx. 100 mg fresh weight) were collected and ground to powder in liquid nitrogen. The powdered samples were homogenized in 50 mM phosphate buffer pH 7.0 containing 1 mM phenyl methane sulfonyl fluoride (PMSF). The homogenate was centrifuged at 10,000 $_{x}$ g for 10 min, and the supernatant was used to determine CAT and APX activity.

Catalase: Catalase (CAT) activity was measured spectrophotometrically by consumption of H_2O_2 at 240 nm, according to Patterson et al. (1984). For calculating H_2O_2 consumption, the known extinction coefficient (Ɛ) 43.6 mM^{-1} cm^{-1} was used.

Ascorbate peroxidase: Ascorbate peroxidase (APX) activity was measured spectrophotometrically as a decrease in absorbance at 290 nm, as described previously (Nakano and Asada 1981). The amount of AsA oxidized at 290 nm was calculated from the extinction coefficient (Ɛ) 2.8 mM^{-1} cm^{-1}.

Superoxide dismutase: SOD activity was measured by NBT reduction monitored at 560 nm (Bapatla et al., 2021). Approximately 100 mg of leaves were collected, powdered in liquid nitrogen, and homogenized in 50 mM phosphate buffer (pH 7.8).

2.8 Chl *a* fluorescence and OJIP parameters

Chl fluorescence measurements were performed using a portable Handy PEA (Plant Efficiency Analyzer-2126) fluorometer (Hansatech Instruments Ltd., Kings Lynn

Norfolk, UK) on fully expanded 2nd and 3rd leaves. Chl *a* fluorescence measurement was taken as described previously (Stirbet and Govindjee, 2011). Chl *a* fluorescence is a non-invasive tool to measure the photosynthetic efficiency of a plant. It has proven to help different aspects of photosynthesis in a wide range of plant species under other environmental stress conditions (Chen et al., 2016; Kalaji et al., 2016). Chl *a* fluorescence induction curves were measured after 14 days of growth (control) and successive day of drought treatment (D0, D2, D4, D6 and D8) using Handy-PEA (Plant Efficiency Analyser, Hansatech Instrument, King's Lynn, UK) after 30 min of dark incubation. All readings were taken after appropriate treatment. The control and drought samples were excited by an array of three light diodes with a peak value at 650 nm and photon flux density of 3000 μmol photon m^{-2} s^{-1}. The emitted fluorescence was detected by PIN-photodiode. The maximum quantum yield of PSII was calculated as Fv/Fm, where Fv = Fm – Fo. The fluorescence kinetics was measured from 10 μs to 1 s. Different OJ, JI, and IP curves were normalized as relative variable fluorescence; Fo (initial fluorescence) as O (20 μs), L (150 μs), K (300 μs), J (2 ms), and I (30 ms) and maximum fluorescence as P (300 ms) (Stirbet and Govindjee, 2011). The differences among relative variable fluorescence curves between untreated (control), and drought were calculated. The energy pipeline model has also been generated by calculating the OJIP test parameters using Biolyzer software (HP 25, Ver 2.0) to see the changes in the photosynthetic apparatus.

Table. 1 *Selected JIP parameters and their descriptions.*

Formulae	**Description of the individual JIP-test parameter**
F_O F_L F_K	Minimum fluorescence value after the onset of actinic illumination at 50 µs Fluorescence value at 150 µs Fluorescence value at 300 µs
F_J	Fluorescence value at 2 ms
F_I	Fluorescence value at 30 ms
$F_P=F_M$	Maximum fluorescence intensity under saturating illumination at P-step
F_V	Variable chlorophyll-a fluorescence
K_N	Non-photochemical de-excitation rate constant
K_P	Photochemical de-excitation rate constant
$\varphi_{Po} = TR_O/ABS = F_V/F_M = [1-(F_O/F_M)]$	Changes in the functional activity of PSII (according to Sipka et al., 2021)
$\psi_o = ET_O/TR_O = (1 - V_J)$	Possibility that a trapped exciton moves an electron into the electron transport chain beyond Q_A
$\varphi_{Eo} = ET_O/ABS = [1- (F_O/F_M)]$ ψ_o	Quantum efficiency of electron transport (at t = 0)
$DI_O/RC = (ABS/RC) – (TR_O/RC)$	Dissipated energy flux per RC
$RC/CS_m = \psi_o (V_J/M_O) (ABS/CS_m)$	Density of active reaction centers per cross-section (CS)
$ABS/CS_m = F_M$	Absorption flux per excited CS
$TR_O/CS_m = \varphi_{Po} (ABS/CS_m)$	Trapped energy flux per excited CS
$ET_O/CS_m = \varphi_{Eo} (ABS/CS_m)$	Electron transport flux per excited CS
$DI_O/CS_m = (ABS/CS_m)-(TRO/CS_m)$	Dissipated energy flux per excited CS
$PI_{(ABS)} = (RC/ABS) (\varphi_{Po} / (1-\varphi_{Po})) \times (\psi_o / (1-\psi_o))$	Performance index on absorption basis
$PI_{(csm)} = (RC/CSm) (\varphi_{Po} / (1-\varphi_{Po})) \times (\psi_o /(1-\psi_o))$	Performance index on cross-section basis

2.9 Determination of PSII and PSI photochemical efficiencies

The photochemical activity of PSII was monitored using a Dual-PAM 100 (Walz, Germany). Fully expanded 2nd and 3rd leaves were dark-adapted for 30 min before experimentation. Chl fluorescence measurements were performed according to Klughammer and Schreiber (1994). The *Fv*/*Fm* parameter (Table 1) was determined as *(Fm - Fo)*/*Fm* (Schreiber et al., 1986; Kramer et al., 2004). The Y(II) parameter was calculated as (*Fm′ - Ft*)/*Fm′*. The non-regulated energy dissipation of PSII, Y(NO), was calculated as *Ft*/*Fm* (Table 2). Further, the regulatory photo-protective energy dissipation of PSII, Y(NPQ), was calculated as (*Fm′ - Ft*/*Fm)*/*Ft*. The non-photochemical quenching of PSII, NPQ, was calculated according to Demmig-Adams et al., (1990); and photochemical quenching parameters were calculated according to the puddle and lake model, respectively, qP (Schreiber et al., 1986) and qL (Kramer et al., 2004) (Table 2).

Further, the PSI efficiency was assessed using a Dual-PAM 100 (Walz, Germany) (Schreiber et al., 2008). The photochemical energy conversion in PSI, Y(I), was determined as (*Pm′ - P*)/*Pm,* P*m*, represents the maximal change of the P700 signal, and the acceptor side limitation of PSI, Y(NA), as (*Pm - Pm′*)/*Pm,* and the donor side limitation of PSI, Y(ND) as *P*/*Pm*, respectively (Klughammer and Schreiber, 1994). Three energy fractions of PSI were defined: Y(I) + Y(NA) + Y(ND).

Table. 2 *Description of PSI and PSII parameters obtained from PAM instrument.*

PSII components	
ETR(II)	Electron transport rate of PSII
Y(II)	Quantum yield of PSII
NPQ	Non-photochemical quenching coefficient
Y(NPQ)	Quantum yield of NPQ-regulated energy dissipation of PSII
Y(NO)	Quantum yield of nonregulated energy dissipation of PSII
qP	The coefficient of photochemical quenching
qL	The coefficient of photochemical quenching-Actual extent of open PSII reaction centers
PSI components	
Pm	Maximal P700 change
ETR(I)	Electron transport rate of PSI
Y(I)	Quantum yield of PSI
Y(ND)	The Donor side limitation of PSI
Y(NA)	The Acceptor side limitation of PSI

2.10 Transmission electron microscopy

Leaves of control, drought, and recovery-treated plants were excised using a biopsy punch, fixed with fixation solution containing 2.5% (v/v) glutaraldehyde and 2% (w/v) paraformaldehyde in 0.05 M sodium cacodylate buffer (pH 6.9) for 3 h at 27 °C and sample were kept for overnight at 4 °C. The sample processing and sectioning were performed according to Koskela et al. (2018). The sections were examined with a Hitachi H-7650 TEM (Hitachi High-Technologies Europe) operating at 100 kV and fitted with an AMT XR41-M digital camera. Repeat distances were measured from control, drought, and recovery-treated plants in triplicates (three biological repetitions). The repeats distance were calculated as average heights per granum membrane layer or the stacking repeat of the thylakoid membrane. Repeat distance is the sum calculated from half of the one-lumen distance to the next one or half of the stromal gap distance to the consecutive one. The repeat distance is calculated by the sum of the stromal gap

and the lumen plus membrane, according to Li et al. (2020). The image processing was done using ImageJ software.

2.11 Isolation of thylakoid membrane

The thylakoid membrane was isolated, according to Mazor et al. (2015). Freshly harvested leaves of control and drought-treated plants were weighed about 10 g and ground with a blender for 30 s in 50 mL of ice-cold buffer containing 0.3 M sucrose, 15 mM NaCl, 30 mM Tricine-NaOH (pH 8.0), 1 mM PMSF, 15 μM leupeptin, and 1 μM pepstatin A (Sigma, USA) under dark condition. The further procedure was followed as described earlier by Mazor et al. (2015).

2.12 Circular dichroism spectroscopy

The circular dichroism (CD) spectra were recorded using a JASCO-1500 spectropolarimeter (Japan), as described previously (Devadasu et al., 2021). The measurements were taken in the visible region (400 - 750 nm), and the three biological replicates were used for scanning the CD spectra at a scan speed of 100 nm min^{-1}. The CD measurements were recorded under the following conditions: bandwidth at 4 nm, data pitch at 1 nm, and an optical path length of 1 cm (Toth et al., 2016). Three scans were accumulated with continuous scan mode. Equal chlorophyll (20 μg mL^{-1}) was maintained for all the samples, and the thylakoids were suspended in 20 mM Tricine-NaOH (pH 8.0) buffer containing 0.4 M sucrose, 10 mM $MgCl_2$, and 5 mM $CaCl_2$. The baseline was corrected with the same buffer.

2.13 Low-temperature fluorescence emission spectra measurements

A Perkin Elmer LS55 fluorescence spectrophotometer (U.K.) was used to detect the fluorescence spectra (77 K) (Murakami et al., 2001). To guarantee uniformity, a (10 μg/mL) equal Chl content was kept constant during each experiment. The emission

range was chosen between 650 and 750 nm, while the excitation wavelength employed was 436 nm. The emission and excitation slits' widths were both fixed to 5 nm (Murakami et al., 2001).

2.14 Separation of supercomplexes from Blue native PAGE (BN-PAGE)

The blue native gel electrophoresis is a versatile system for observing the intact organization of thylakoid photosynthetic supercomplexes. An acrylamide gradient of 4-12% (w/v) was suitable for protein complexes, and 3% (w/v) in the stacking gel was used. The isolated thylakoids were prepared using 1% w/v *n*-Dodecyl β-D-maltoside (Sigma, USA) and the protease inhibitor 1 mM PMSF, 15 µM leupeptin, and 1 µM pepstatin A (Schagger and Vonjagow et al., 1991). The samples were run on gradient gel at 4 °C along with standard protein markers (GE Healthcare, UK) with increasing voltage 35, 55, 75, 120, 150, 200, and 250 V as described earlier in our laboratory to solubilize thylakoid membranes without disturbing the native form of proteins and the complexes (Madireddi et al., 2014).

2.15 Protein Extraction

P. sativum leaf was collected and macerated with liquid nitrogen in an amount of around 100 mg. The macerated leaf sample was added to a freshly made buffer that contained 0.1 M Tris pH 6.8, 0.1 M DTT, and 4 % SDS. The mixture was then vortexed twice for a total of two cycles of 30 sec each. The sample was then heated for 10 min at 75 °C. The sample was centrifuged at 1800 x g for 10 min after chilling, and the supernatant collected was put into a 1.5 mL eppendorf tube. The Bradford method was used to measure the amount of total protein in the supernatant. A 12 % Bis-tris gel with equal amount of protein (4 µg) in each wells was employed to separate different polypeptides.

2.16 Protein identification by Immunoblots

About 4 µg of total extract protein was loaded on 15% Bis-Tris gel and was transferred onto nitrocellulose membrane (0.45 µm) for 1 h using a trans-blot system (Bio-Rad, USA) according to the manufacturer's instruction. Further, the nitrocellulose membrane was incubated with primary antibodies (PSI, PSII, LHCI, and LHCII) raised in rabbits. The antibody dilutions were as follows: for PSII-LHCII complex, PsbA (1:10000), PsbB (1:5000), CP43 (1:3000), CP47(1:2000), PSBS (1:10000), (Cyt)b_6f (1:5000), PsbO (1:5000), PsbP (1:5000), Histone 3 (1:5000), Lhcb1 (1:2000), Lhcb2 (1:5000), Lhcb3 (1:2000), Lhcb4 (1:7000), Lhcb5 (1:1000), Lhcb6 (1:5000), Dehydrin (1:1000) and Aquaporins (1:1000). For PSI-LHCI complex, PsaA, PsaB, PsaC, PsaD, PsaE, PsaF, PsaG PsaH, PsaL, Ferredoxin (1:1000), Lhca1 (1:5000), Lhca2 (1:5000), Lhca3 (1:5000) Lhca4 (1:5000) and antioxidants enzymes Catalase (1:1000), Mn-SOD (1:5000), APX (1:2000), Cu-ZnSOD (1:1500), PDAT1 (1:250), DGAT1 (1:1000) and ATG8 (1:2000) procured from (Agrisera, Sweden). The secondary antibodies (anti-rabbit IgG (1:20000)) conjugated with horseradish peroxidase (Agrisera, Sweden) was used. The images were developed by incubating with chemiluminescence (ECL) dye (Bio-Rad, USA). Images were captured using a CCD imager (Bio-Rad Touch Imaging Chemi-Doc System, USA), and band intensities were quantified using ImageJ software. The Histone3 (1:5000) and various dilutions (in %) was used as a loading control.

2.17 Green gel electrophoresis

The fresh thylakoids were solubilized in 20 mM MES-NaOH (pH 6.6) buffer containing 100 mM sucrose, 15 mM NaCl, and 0.22 percent LDS in accordance with the method of (Maroc et al., 1987). Mild-denaturing polyacrylamide gel electrophoresis was analysed with 4 % stacking and 8-17 percent for gradient resolving gel (Garstka et al., 2005).

2.18 Observation of disassembled proteins by fluorescence and confocal microscopy

Some of the core and LHCs induced were denatured and disassembled by drought stress observed using fluorescence microscopy (Nikon TE200, Japan) and confocal microscopy (TCS-SP-2-Leica, Heidelberg, Germany). The disassembled proteins were imaged using an excitation range of 530 to 550 nm and an emission range of 590 to 750 nm. The fluorescence images were taken at 40-fold magnification using a digital camera. The unsolubilized pellet was diluted in 10 mM Tricine buffer, pH 7.8, containing 0.003% DM, and chlorophyll concentration was 2 mg mL^{-1}. The further procedure was followed as described earlier (Tang et al., 2007)

2.19 Determination of protein abundance in the insoluble fraction

To determine the disassembled proteins in the pellet, freshly harvested control, and drought-treated pea leaves were macerated, and the isolated thylakoid membranes were dissolved in 1% n-Dodecyl β-D-maltoside (β-DM). The reaction mixture was incubated in the dark for 10 min and centrifuged at 10,000 × g for 10 min at 4 °C (Devadasu et al., 2021). We maintained the final Chl concentration of 0.8 mg mL^{-1} Chl in both control and drought-treated leaves. The flow-through was discarded, and the pellet was dissolved in a solubilization buffer containing 2% β-mercaptoethanol. We took 10 µL of protein from both control and drought-treated loaded onto the gel. After running the electrophoresis, the gel was transferred to a nitrocellulose membrane using a semi-dry transfer blot. We have immunoblotted the PSI (PsaA, PsaB, and PsaF), PSII (D1, D2, CP43, and CP47), and LHCII (Lhcb2, Lhcb5, and Lhcb6) proteins to see the protein abundancy in the pellet.

2.20 Separation of supercomplexes from sucrose density gradient

Discontinuous sucrose density gradient (SDG) was prepared by the sequential layering of 1.3 M, 1.0 M, 0.7 M, 0.4 M, and 0.1 M sucrose (from bottom to top). Solubilized thylakoid membranes were separated in an SDG centrifugation. Thylakoid membranes corresponding to 0.8 mg/mL of chlorophyll were resuspended in (0.4 M sucrose and 20 mM Tricine-NaOH, pH 8.0) buffer and solubilized in 1% n-dodecyl β-D-maltoside (β-DM) at 4 °C in the dark for 10 min and centrifuged at 12,000 rpm for 5 min at 4 °C and obtained the solubilized thylakoid membrane in the supernatant. The solubilized thylakoid membrane was loaded on top of the prepared sucrose density gradients and centrifuged at 180,000 ×g for 17 h using Rotor SW41Ti (Beckman) at 4 °C.

2.21 Measurement of absorption and circular dichroism spectra

Absorption spectroscopy of the SDG fractions obtained from SDG (F1, F2, F3 and F4) of control, drought and recovery was recorded with UV–Visible Perkin Elmer spectrophotometer lambda 35 (USA). Samples were suspended in 0.1 M sucrose and 10 mM Tricine, pH 8.0. The measurement was taken in the visible region of 400–800 nm with a path length of 1 cm. Measurement was done from the fractions obtained from the SDG on an equal chlorophyll basis. The circular dichroism (CD) spectra of SDG fractions were recorded using a JASCO-1500 spectropolarimeter (Japan), as mentioned previously. Equal chlorophyll (20 μg mL^{-1}) was maintained for all the samples, and the thylakoids were suspended in 20 mM Tricine-NaOH (pH 8.0) buffer containing 0.4 M sucrose, 10 mM $MgCl_2$, and 5 mM $CaCl_2$.

2.22 RNA extraction and cDNA synthesis

The samples (leaf) were used for total RNA extraction using the Spectrum Plant Total RNA isolation kit from Sigma (USA), following the manufacturer's protocol. A total of

1 µg of RNA was utilized for cDNA synthesis, which was performed using the Reverse Aid First Strand cDNA Synthesis Kit from Takara (Japan). The cDNA synthesis process involved priming at 65 ℃ and reverse transcription for 1 hour at 42 ℃ in a 20 µl reaction mixture. The concentration of RNA was determined at 260 nm using a Nanodrop1000 spectrophotometer from Thermo Fisher (U.S).

2.23 Quantitative real-time PCR

Using quantitative real-time qRT-PCR in an Eppendorf thermal cycler, the mRNA expression levels of genes involved in antioxidants, photosynthesis, and stress indicators (Tables 3 and Table 4) were evaluated. The PCR reactions employed the the SYBR FAST qPCR Universal Master Mix (2X) from KAPA Biosystems (USA) was used for the PCR reactions. First-strand cDNA in a volume of 1 µL was utilised as the template in each reaction, which had a 10 µL overall reaction volume. A denaturation step at 95 ℃ for 2 min was followed by 40 cycles of denaturation at 95 ℃ for 20 sec and annealing/extension at the particular melting temperature (Tm) for 20 sec as part of the amplification programme. The $2^{-\Delta\Delta Ct}$ technique was used to calculate the relative expression levels (Livak and Schmittgen, 2001).

Table. 3 *List of primers used for antioxidants and stress markers gene transcripts.*

Genes	Forward Primer	Reverse Primer
HSP	ACTGCCTCCAGAACTTTCCA	TGAGAAACACGAACCATCCA
DHN1	CTGCTCCATCCGTATTGGTT	GGTGTGGGTGGTTATGGAAC
DHN2	GTTCCATAACCACCCACACC	ATGGAAACCCAATGAACCAA
DHN3	ACCACCCACACCACCTGTAT	ATGGAAACCCAGTGAACCAA
CAT	CGAGGTATGACCAGGTTCGT	AGGGCATCAATCCATCTCTG
APX	GGATCCTATGGGAAAATCATACCCA ACTG	CTCGAGTCTTAGGCTTCAGCAAATCC AAG
GR	TTTTGCGAACACTGCTTTTG	AGCCTGAGGTGAAGACCAGA
Cu/ZnSOD	GAACAATGGTGAAGGCTGTG	GTGACCACCTTTCCCAAGAT
FeSOD	GCACCACAGAGCTTATGTAG	GGAGTGGATGATGATGGTTC
MnSOD	GGAGCAAGTTTGGTTCCATT	AAGGTTATTCGGCCAGATTG
P5CS	GCAAGCTGCAGGGTAATC	AGGAAAGGAAGCCCGAAG
P5CR	GCCGCTCCTAACTAAGGACA	ACCACTGCCACTTAGACCAG
Actin2	AATGGTGAAGGCTGGATTTG	AGCAAGATCCAAACGAAGGA
CAT4	AAGGCTGGGAAAGCGGTGTA	AGACCATGCGACCAACAGGCT
GmPOD	CTACTCCAGTTCTTGTCCAA	CGTCTTAGCGTCTCTTCTT
PmH^+-ATPase1	GTAGGGATGTTGGGTGATCCGA	ACTTCCTGGTAGGCTGCTGCA
$PpPmH^+$-ATPase4/like	GAGGAAGACCACCAGATTGGC	AGCATCACCCTCCAGAAGACG
$PpPmH^+$-ATPase4.1	TGCTGCTGCTGCTCTTATGG	AGAATGTGTGGACACCGGTTG
$PpPmH^+$-ATPase4.1 like	AGGGATAGCCGATGGTGTGA	CACACCGGTCGCAATCACAA
$PpVH^+$-ATPase subunit b	CTGATGCTCTTCGTGAGGTATC	CAACCGAGATAGTGATGGAAGG
PpVH+-ATPase subunit e	AGTTGAAGCCGACAAGAAGAA	ACATCGCAACAAGACAGAAGA
SOS1	GCTTGGAGGACTTCTGAGTGCT	CTGAACCCTCCTGAGCAGTGAA
Gm SOS3	GCAGCATTCACATTCAGT	AATTCAGCCTCCATTGGT

Table. 4 *List of primers used for the expression of photosynthesis regulatory gene transcripts.*

Genes	Forward Primer	Reverse Primer
PSBS	TTATGAAGCTGAGCCTCTCCTC	GAAAGCAAATCCCAGTTGAGCC
D1	CTATGCACGGTTCCTTGGTAAC	CATAGTGCTGATACCTAACGCG
D2	CATTCTCCGGTCCAATTGCTG	GCCATGAATAGCGCATAGTAGG
CP43	CCAACTTCACCCTTAGTCCAAG	TAGACCATACTAGTGCACGCC
CP47	GGGTTACAGGTGTAGTTTTGGG	GTCAAGGTAGATTGTCCCACAC
PsbO	GACTCATTCTCCTTCAAGCCAG	TCTCCTCGAATTTCACACTCCC
Lhcb1	GGTGAGTCTCCATCCTACTTGA	CCACCCTCGCTAAAGATTTGAG
Lhcb2	AAGGACTAGACCCACTTTACCC	CAGGGTCAGCAACATGGTCATA
Lhcb3	ATGGAAGATGGGCTATGCTAGG	CTTCGACGAGTCCCATTAGAAC
PsaA	GATACATGTACTTGATGCCCCG	GGCGAGCATCTGGAATAACTAG
PsaB	CTTATGTCCACGCCCCAATCTA	CTGCCATTCTAACACTTCTCGG
Lhca1	CGCTTCTCTCTTCTTCCAAGTC	GTATCTCTCAAGGTTCGCTGGA
Lhca2	CTTGGGTGGTAAGAAACTGAGG	GTTCCATTTTAGACTGTCCGGG
Lhca3	GTGACTACGGATTTGACCCTCT	CCCAGTAGTTGTATGTTCCTGC
PIP2-1	CATTGGGAGGTTGTGCTATTGG	AGCCCGTCCAGTTACAGTTATG
PetA	TATTACTCTTGCTTCCGTCGGG	CGTCTTTCGCCCCAGATTAAAG
PetB	CAGTTCATCGATGGTCAGCAAG	TTACAGGAATAGCGTCGGGTAC
PetC	GAATGGCTCAAGACTCATGCAC	CAGGTCCTCTCACAACTCTTCC
PSBP	AAGAGAGAGAGTTCCCTGGTCA	CACTGGTGCTGAGCTCTCTAAG
FED1	CCAATGGCTTTCTCGGTTTG	GATCAACTTCACCGCCAACAAC

.

2.24 Pigment content determination by HPLC analysis

The isolated thylakoids and the *P. sativum* leaves were collected, macerated with liquid nitrogen, and lyophilized at -108 °C. In order to extract the pigments from the leaf tissues pigments, equal weights of leaf tissues were employed (1:1). After centrifuging, the supernatant was collected and dried using N_2 gas. The dried pigments were reconstituted using 50 µL of a 1:1 methanol and acetone solution, and the resulting mixture was then injected into an HPLC system for carotenoid analysis. SDG fractions were created using a 1:1 combination of acetone and methanol. The materials were extracted, centrifuged for 15 min at 12,000 rpm, and the supernatant was then filtered through a 0.25 µm filter before HPLC analysis. A C-18 column (250 X 4.6 mm, 5 m; Phenomenex) was used in an HPLC system (Shimadzu). The mobile phase was a 45 min isocratic gradient of Methanol: Acetonitrile: Acetone (70:20:10, v/v/v). By comparing each compound's retention time and peak area to standards, carotenoids were located and quantified. Utilizing a UV-Vis detector, pigments were found at 455 nm.

2.25 Total proline content analysis

The approach outlined by (Bates et al., 1973) was used to estimate the proline content. Leaf samples were crushed in liquid nitrogen with sulfosalicylic acid at a concentration of 4% (w/v). After that, extracted material underwent a 10 min centrifugation at 15200 g. Sulfosalicylic acid, glacial acetic acid, and acid ninhydrin were added to an aliquot of the clear extract, and the combination was then incubated at 96 °C for an hour. By placing the tubes on ice, the reaction was stopped. The mixture was then given 3 mL of toluene, stirred for 45 sec, and allowed to phase separate for 5 min. Using toluene as a standard, the absorbance of the toluene layer was calculated at 520 nm. Analyzing the absorbance measurements against a standard curve allowed us to calculate the proline content.

2.26 Leaf biochemical analysis

The approach was used to examine the reducing sugars, free sugars, starch, and total carbohydrate in the leaf samples. First, the leaf samples were dried. The dried samples were then homogenised in hot, 80% ethanol. The resultant mixture was centrifuged, and the soluble sugars were calculated using the DNS (3,5-dinitrosalicylic acid) technique from the supernatant. After centrifugation, the flow through was collected, diluted in 6 mL of water, and then extracted with 7.5 mL of 52 % perchloric acid. The flow through was obtained following a second round of centrifugation and used to estimate starch using Hedge and Hofreiter's anthrone technique (1962). In accordance with the procedure described by (Giannoccaro et al., 2006), 120-130 mg of the leaf was homogenised in 1.5 mL of MilliQ water and vortexed for 20 min to extract the free sugars. After that, the sample was centrifuged at ambient temperature for 10 min at 13,000 rpm. 700 mL of 95 % acetonitrile was added to 500 mL of the supernatant and stirred for 30 min at room temperature in a rotor spin. After a second centrifugation of the mixture, the supernatant was removed. After the supernatant was evaporated at 95 °C in a dry bath, the left-over material was dissolved in 1 mL of MilliQ water.

2.27 Lipids extraction

With a few minor modifications, the procedure outlined by Bligh and Dyer (1959) was used to extract total lipids from the leaf tissues. 20 mg of dried leaf tissues were obtained, and they were then reconstituted in 1.2 mL of a chloroform/methanol (2:1, v/v) solution. 100 mL of a 0.9 % KCl solution was added to the mixture in order to extract neutral lipids. The same quantity of dried tissue was collected and resuspended in a 2:1 mixture of chloroform and methanol for the extraction of polar lipids. Following the addition of 100 mL of 1 M KH_2PO_4, the mixture was vortexed. Phase separation was made possible by centrifuging the sample mixture at 3,000 x g for 5 min at room

temperature. The lipids were carefully removed from the lower chloroform phase. This procedure was done three times, using the residual upper fractions for further lipid extraction. The lower phase was gathered, pooled, and evaporated using purging of N_2 gas. In order to conduct further investigation, the produced lipids were then dissolved in 25 µL of chloroform and kept at -80 °C.

2.28 Triacylglycerol analysis by thin-layer chromatography

25 µL of the lipid extract were spotted onto a TLC plate to determine the amount of lipid present (TLC Silica gel, Merck). 20 µg of glyceryl trioleate (Sigma) was also used as a triglyceride (TAG) standard. Hexane, ether, and acetic acid were used as the solvent system for chromatography (70:30:1, v/v/v). The TLC plates were created and then dried by air. The plates were exposed to iodine vapour at 45 °C for 10 min in order to see the separated TAGs. Gray semi-quantitative analysis with ImageJ (ver1.45, NIH) was used to quantify the amount of TAG in each sample. Using a 2D TLC, polar lipids were separated. The TLC plates were run in the first dimension using a solvent solution of chloroform, methanol, and water (40:20:2, v/v/v). The plates were created in the second dimension using a mixture of glacial acetic acid, methanol, chloroform, and water (35:7:6:1, v/v/v). The solvent was evaporated from the plates after development by heating them to 95 °C. By treating the plates with 7% phosphomolybdic acid (Sigma) in 90% ethanol, the lipids were made visible. In order to guarantee the correctness and dependability of the findings, three duplicates were carried out using three different samples.

2.29 Fatty acid methyl esters analysis for the total lipids

The lyophilized leaf tissues (25 mg) was dissolved in 1,000 µL of formic acid (FA)-free acetonitrile (ACN) and vortexed for 1 hour at 1000 rpm at room temperature (RT). 100 µL of the supernatant was collected following centrifugation at 13,000 rpm for 10 min

at 4 °C, and the pellet was speed vacuum dried. The dried pellet was mixed with 10 mL of the normal internal mixture and 90 mL of ACN 0.1 percent FA (v/v) to dissolve it. The samples were then dried using a speed vacuum at 40 °C after being vortexing for 30 min at 1000 rpm at RT. The dried pellets were derivatized in n-Butanol at 60 °C for 20 min, and then they were dried once more under a speed vacuum for 15 min at 60 °C. After being dissolved in 200 µL of ACN 0.2 % FA, the pellets were vortexed for 10 min at 1000 rpm before being centrifuged. An LC-MS/MS apparatus was used to transport the supernatant to HPLC sample vials. Based on the internal standards' area under the curve (AUC), concentrations were estimated.

Analyte	**Internal Standard (IS)**	**Precursor [amu]; [M+H]**	**Product [amu]**
C14:0	$^{2}H_3$ C14	428.2	85.1
C14:1	$^{2}H_3$ C14	426.2	85.1
C14:2	$^{2}H_3$ C14	424.2	85.1
C14:3	$^{2}H_3$ C14	444.2	85.1
C16:0	$^{2}H_3$ C16	456.3	85.1
C16:1	$^{2}H_3$ C16	454.3	85.1
C16:2	$^{2}H_3$ C16	470.3	85.1
C16:3	$^{2}H_3$ C16	472.3	85.1
C18:0	$^{2}H_3$ C18	484.3	85.1
C18:1	$^{2}H_3$ C18	482.3	85.1
C18:2	$^{2}H_3$ C18	489.3	85.1
C18:3	$^{2}H_3$ C18	498.3	85.1
C18:4	$^{2}H_3$ C18	500.3	85.1

Table. 5 *For molecular mass quantifications from fragmentations ions from each fatty acid.*

Time in min	**Flow rate**	**% B**
0.35	0.1ml/min	100
0.36	0.5ml/min	100
0.75	0.5ml/min	100
0.76	0.1ml/min	100
1.0	STOP	

Table.6 *Gradient conditions for sample measurements for all the conditions.*

2.30 RNA extraction, creation of libraries, and transcriptome sequencing

Using Trizol reagent, total RNA was extracted from the frozen leaf samples (Invitrogen, Carlsbad, CA, USA). For each leaf tissue, three separate biological replicates were carried out. Utilizing the Bioanalyzer 2100 equipment and the RNA Nano 6000 Assay Kit, the quality and integrity of the extracted RNA were assessed (Agilent Technologies, CA, USA). 1 µg of RNA per sample was used as the input material for sample preparation. The NEBNext Ultra RNA Library Prep Kit for Illumina (NEB, Ipswich, MA, USA) was used to prepare the sequencing libraries. Index codes were integrated to assign sequences to each unique sample.

2.31 Data filtering, *de novo* assembly, and functional annotation

Custom Perl scripts were used to perform the first processing of the raw RNA-Seq data in FASTQ format. By eliminating adapter-containing sequences, poly N sequences, and low-quality reads, this phase attempted to provide clean reads. Key indicators including Q20 and Q30 scores, as well as GC content, were simultaneously computed for the clean data. The clean reads were then put together using Trinity (http://trinityrnaseq.github.io) into contigs, transcripts, and unigenes. After that, Hisat2 was used to match the assembled clean reads to the reference genome sequence (version 2.1.0). For additional examination and annotation based on the reference genome, only reads with a perfect match or one mismatch were taken into consideration. Several databases were used to annotate gene function, including Swiss-Prot (a manually annotated and reviewed protein sequence database), KO (KEGG Ortholog database), Nr (NCBI non-redundant protein sequences), Nt (NCBI non-redundant nucleotide sequences), and Pfam (Protein Family) (Gene Ontology).

2.32 Quantification of gene expression levels and differential expression analysis

To get clean reads, a preprocessing step was applied to the raw FASTQ RNA-Seq data. This required eliminating adapter-containing, poly-N sequence-containing, and low-quality reads. The percentage of bases with a quality score greater than or equal to 20 and 30, respectively, was also determined during this stage, as were the Q20 and Q30 scores. The clean data's GC content was also identified. After that, the assembled data was processed using the Trinity software (http://trinityrnaseq.github.io). Clean readings were compiled into contigs, which are overlapping pieces of the original transcripts, during the assembly process. These contigs were then combined to create larger transcripts, which were then further assembled into a set of non-redundant unigenes. Overall, the raw RNA-Seq data may be converted into a set of assembled contigs, transcripts, and unigenes utilising this pipeline of read preprocessing and assembly using Trinity. These generated contigs, transcripts, and unigenes can then be further examined for downstream applications with the following assemblers, i.e., Jellyfish for extract and count k-mers from the raw reads, Incworm for assemblies initial contigs by "greedily" extending sequences with most abundant K-mers, Chrysalis for clusters overlapping Inchworm contigs, builds de Bruijin graphs for each cluster, partitions reads between clusters, Butterfly resolves alternatively spliced and paralogous transcripts independently for each cluster (in parallel).

Steps:

1. Merge: Concatenating the read files into single file per direction and indicated as left and forward files (/1 and /2 for forward and Reverse reads).

2. I run the Trinity with default parameters, including left and right merged reads constructed in the previous step.

3. Assessing assembly quality was performed using TrinityStats.pl Perl program and generated alignment summary statistics for the constructed library.

4. align_and_estimate_abundance.pl was used for replicate wise to estimate abundance with est_method RSEM, aln_method bowtie2 with default parameters.

5. Generated matrix for gene level as well as isoform level using abundance_estimates_to_ matrix.pl program.

6. Differentially expressed analysis was performed for gene-level transcript IDs using run_DE_analysis.pl program.

7. I derive the list of significantly up-regulated and -down-regulated transcript IDs using analyze_diff_expr.pl program with a threshold as a 2-fold change.

2.33 GO and KEGG enrichment analysis of DEGs Gene Ontology (GO)

We used Trinotate, a comprehensive annotation suite for functional annotation of our *de novo* assembled transcriptomes from non-model organisms. Trinotate with different well-referenced methods for functional annotation, including homology search to known sequence data (BLAST+/SwissProt), protein domain identification (HMMER/PFAM), protein signal peptide and transmembrane domain prediction (signalP/tmHMM) and leveraging various annotation databases (eggNOG/GO/Kegg databases). All functional annotation data derived from the analysis of transcripts is integrated into SQLite database, which allows fast, efficient searching for terms with specific qualities related to a desired scientific hypothesis or a means to create a whole annotation report for a transcriptome.

2.34 Protein preparation for iTRAQ analysis

Place 2 mL of dry powder in a 2 mL tube. Keep on ice for the entire extraction protocol. Add 1 ml lysis buffer (lysis buffer: 7 mol/L Urea, 2 mol/L Thiourea, 4% CHAPS, 40 mmol/L Tris-HCl, pH 8.5, 1 mM PMSF, 2 mmol/L EDTA). Place the sample in the homogenizer and transfer all particles to the homogenizer. Homogenize each sample 3 times homogenizer cycle by moving up and down the tube (press down and twist each cycle to get all particles homogenized). Pour samples into a new 1.5 mL tube and carry out 3 X 25 seconds burst of sonication (30 sec in between) on ice. Samples are then placed on ice and every 15 min vortex for 30 sec (repeat 4 times). Spin the tubes at max speed (15,000 rpm) for 5 min. Transfer 0.5 ml of the cleared supernatant to a new 2 mL snap cap tube. To each tube add 300 µL of 100% TCA (final 15%), add 1200 µL of cold acetone containing 0.2% DTT samples were mixed and placed at -20 °C. Next day spin at max centrifuge for 20 min and then discard the supernatant and should have a white-greenish pellet. Wash the pellet with 0.5 mL of 100% acetone with 0.2% DTT twice by centrifuging for 3 min each time and discarding the wash. Last, wash with 0.5 mL of cold 80% acetone. Discard the liquid as much as possible and allow the pellet to dry.

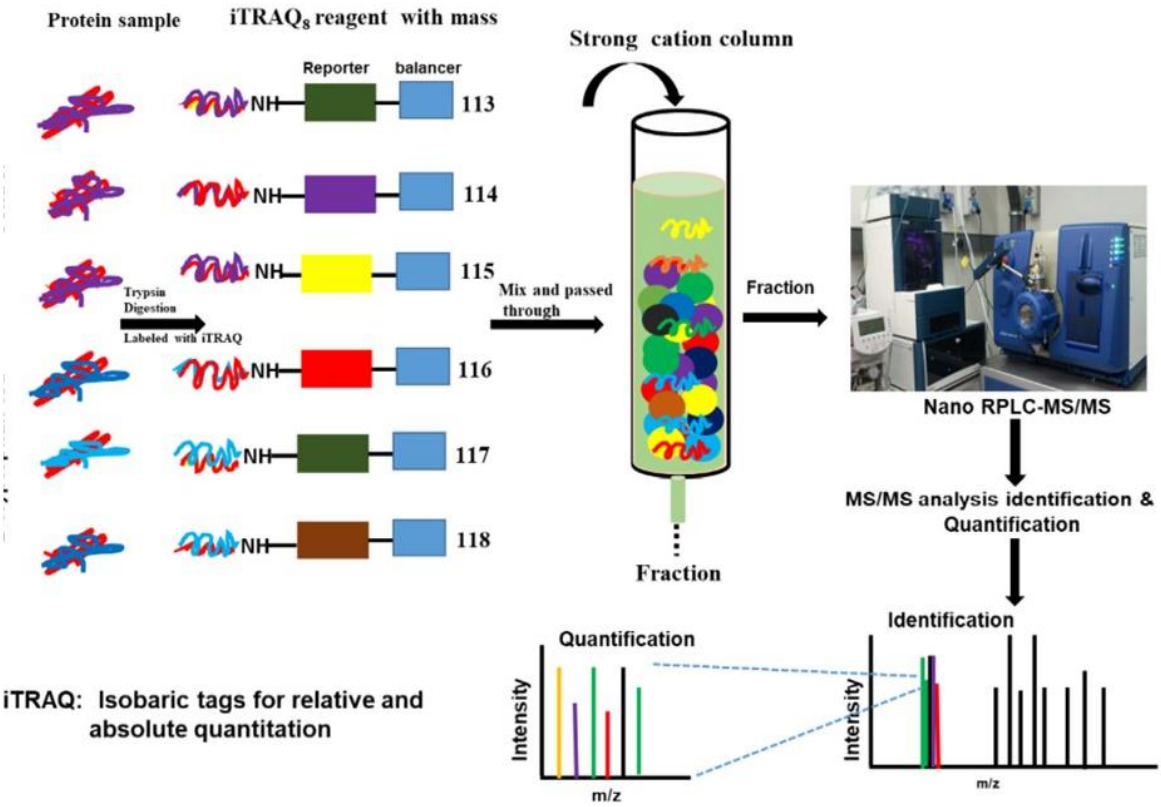

Figure 2.3 *Flowchart representing the iTRAQ based proteomic analysis used for this study.*

2.35 Protein digestion

200 µL of the sample were combined with 6 M Guanidine HCl to start the protein manufacturing process. The mixture was then boiled for 10 min, cooled at room temperature for 5 min, and then added back to the sample. Three times were completed in this cycle of boiling and cooling. Afterward, the proteins were precipitated by adding methanol until it reached a final concentration of 90%, vortexing, and centrifuging for 10 min at maximum speed (14,000 rpm) in a tabletop microfuge. By carefully inverting the tube onto an absorbent surface and tapping to drain any leftover liquid, the soluble portion was extracted. The final pellet was redissolved in 200 µL of 8 M urea that had been made with 100 mM Tris pH 8. After that, TCEP was added at a final concentration of 10 mM, and 40 mM of chloroacetamide solution was added. Five minutes were spent

vortexing the mixture. Three portions of 50 mM Tris pH 8.0 were diluted with the sample to bring the urea content down to 2 M. Trypsin was added in a 1:50 ratio with water for enzymatic digestion, and the mixture was incubated at 37 °C for 12 hours. The resulting mixture was thoroughly mixed after being acidified with TFA to a final concentration of 0.5 percent TFA. C18-StageTips (Thermo Scientific) were used to desalt the sample in accordance with the manufacturer's instructions. After resuspending the peptides in TMT buffer, the sample's peptide concentration was lastly determined using the BCA test.

2.36 TMT labeling

Tags from TMT 10 kit (ThermoFisher Sceintific #90309) were used to label the samples. The labeling protocol as described by the manufacturer. The tag references of our samples: Control CI (TMT10-128C), CII(TMT10-129N), CIII(TMT10-129C) and Treated TI(TMT10-130N), TII (TMT 10-130C), TIII (TMT 10-131).

2.37 High pH fractionation

Pierce™ High pH Reversed-Phase Peptide Fractionation Kit (Catalog number: 84868) was used. Fractionation protocol as described by the manufacturer kit to generate 8 unique peptide fractions for further LC-MS-MS analysis.

2.38 LC-MS/MS

Each fraction was subjected to examination utilising tandem mass spectroscopy (LC-MS/MS) using nano-spray ionisation UPLC. Thermo's Orbitrap fusion Lumos hybrid mass spectrometer and Thermo Dionex UltiMateTM 3000 RSLC nano System, a nanoscale reversed-phase UPLC system, were both used in the nano-spray ionisation research. A 25-centimetre, 75-micron ID glass capillary with 1.7 m C18 (130) BEHTM beads was part of the UPLC system (Waters corporation). Using a linear gradient of

ACN (Acetonitrile) ranging from 5 %to 80 %, at a flow rate of 375 µLmin^{-1} for 90 min, peptides were extracted from the C18 column into the mass spectrometer. Buffer A (98 percent H_2O_2 percent ACN, and 0.1 percent formic acid) and Buffer B were used to construct the ACN gradient (100 percent ACN, 0.1 percent formic acid). The following mass spectrometer settings were used: With quadrupole isolation, a resolution setting of 60,000, a spray voltage of 2200 V, an ion transfer tube temperature of 290 °C, an AGC target of 400,000, and a maximum injection period of 50 ms, an MS1 survey scan was performed utilising the orbitrap detector in the mass range of 400-1500 m/z. The next step involved data-dependent scans that selected ions with minimum intensities of 50,000 and targeted the strongest ions with charge states of +2 to +5, with a 5-second exclusion time. The initial configuration of the quadrupole isolation window was 0.8 m/z (mass-to-charge ratio). The next collision event used a collision energy of 38% and occurred in the high-energy collision cell (HCD). In the orbitrap detector, fragment masses were examined using an automated scan with the first scan starting at m/z=100 and a resolution of 30,000. The maximum injection time was 54 ms, and the AGC target was set to 30,000. Using Peaks Studio 8.5, proteins were identified and quantified (Bioinformatics solutions Inc.). Filtered proteins were those that met standards such a false discovery rate of less than 1%, a minimum of two distinct peptides, and an unused protscore > 2 (99 % confidence level). For FC analysis, proteins that met these requirements were taken into consideration. Proteins with iTRAQ FC ratios below 0.8 ($\log_2$FC < -0.26) were considered to be down-regulated, and those with ratios above 1.2 ($\log_2$FC > 0.26) were considered to be up-regulated (with $p \leq 0.05$ in at least two out of four expression ratios). The KEGG (www.genome.jp/kegg/) database was used to classify differentially expressed proteins (DEP) according to their functions. These experiments were carried out at UC-Davis in San Diego, California, in the United States.

2.39 Metabolite profiling through GC–MS

The leaf sample was lyophilized, weighed, and then extracted according to a modified version of the procedure outlined by (Schauer et al., 2005). In particular, 30 mg of lyophilized leaves were extracted using 480 µL of pure methanol. As an internal reference, 20 µL of a 0.2 mg mL^{-1} ribitol solution were also added. The resulting mixture was then heated at 70 °C for 15 min after being forcefully stirred for 2 min. Then 250 µL of chloroform was added and well mixed, after which an equivalent volume of water was added and mixed. At room temperature (around 25 °C), the mixture was centrifuged at 2200 x g for 10 min. A speed vacuum rotator was used to collect and dry the upper aqueous phase at 35 °C. The dried fraction was redissolved in 40 µL of a methoxamine hydrochloride in pyridine solution containing 20 mg mL^{-1}, and it was then incubated at 37 °C for 90 min. The mixture was then mixed with 60 µL of MSTFA (N-methyl-N-trimethylsilyl trifluoroacetamide), and the incubation was carried out at 37 °C for an additional 30 min. After completing this derivatization process, a 2 µL sample volume was analysed using GC-MS. Shimadzu GC-MS-QP2010TM equipment linked to an autosampler-auto-injector was used for the analysis (AOC-20si). The analysis used helium as the carrier gas and a Rtx-5® capillary column from Restek Corporation in the United States. A preliminary isothermal heating at 80 °C for 2 min was followed by a ramp rate of 5 °C min^{-1} up to 250 °C, a 2 min pause, and a final ramp of 10 °C min^{-1} with a 24 min hold in the GC temperature programme. The NIST14s and WILEY8 spectrum libraries were used to identify derivatized metabolites, and chromatogram integration and mass spectra analysis were carried out using the GC-MS solution software (Shimadzu®).

Based on real standards that were GC-MS examined, the presence of glucose, sucrose, and fructose was established. For the purposes of data analysis, metabolites

that underwent various TMS group derivatizations were regarded as unique metabolites. Following the (Lisec et al., 2006) described approach, the peak regions for metabolites with numerous peaks were added once the spectral data were verified. The peak area of ribitol, the internal standard (IS), was used to standardise the peak areas of each component in each GC-MS run. The peak areas of each component were normalised by dividing them by the peak area of the ribitol internal standard. This normalisation method enables more precise comparisons of peak regions between various components by accounting for changes in sample size or instrument response.

For the calculation of fold-change for metabolites below the detection limit, a normalised value of 0.001 was employed. By dividing the normalised peak area of the treatment sample by the normalised peak area of the control sample, the fold change was computed, and its logarithmic (log10) value was found.

2.40 Statistical analysis

All physiological and biochemical results are the average of at least three independent experiments done on different days. The results were analyzed by ANOVA. Each data point averages three replicates, and error bars are represented as ±SE. Asterisks indicated the level of significance of the drought effect compared to the respective control as * ($p<0.05$), ** ($p<0.01$), and *** ($p<0.001$), respectively. Various software was used such as Sigmaplot 11.0 and Origin Graphing Analysis. Using the R programming language, Pearson correlation analysis was performed on the RT-PCR genes and metabolites. Calculating the correlation coefficients between gene and metabolite pairs was a part of the investigation. The correlation coefficients ranged from -1 to 1, with low values denoting no association and high values denoting either a positive or negative correlation (Figure 6).

S.NO	Pearson correlation coefficient	The significance level of correlation
1.	**> 0.5**	**Strong positive correlation**
2.	**0-0.5**	**Moderate positive correlation**
3.	**0**	**No correlation**
4.	**0- (-0.5)**	**Moderate negative correlation**
5.	**< -0.5**	**Strong negative correlation**

Table.6 *Pearson correlation coefficient and their correlation significance levels.*

Chapter 3

Investigation of drought effects on physiology, photosynthetic performance, redox status and its reversible changes in structure and function of photosynthetic apparatus of pea leaves

3.1 INTRODUCTION

Drought stress is a significant environmental constraint that hampers crop yield, particularly in arid and semi-arid regions. There is an urgent need to develop varieties that can grow under limited water conditions without compromising yields. In this direction, it is crucial to understand the physiological, molecular, and photosynthetic responses of crop species under drought. Upon exposure to drought stress, plants displayed various morphological symptoms such as wilting, desiccation of leaves, chlorosis, leaf curling, burning of leaf edges, and necrosis (Seleiman et al., 2021). Parallelly, the stomatal conductance decreased to reduce the water evaporation through leaves (Li et al., 2017). Low stomatal conductance decreases intercellular CO_2, minimizing the supply for photosynthesis (Kelly et al., 2016). As a result, plants water use efficiency (WUE) decreased. Similarly, the leaf relative water content (RWC), an indicator of stress intensity, was also lowered.

The drought-induced imbalance between light capture and its utilization leads to the accumulation of reactive oxygen species (ROS) in the chloroplast and, subsequently, the disorganization of thylakoid membranes (Das and Roychoudhury, 2014). To combat ROS, plants utilize several antioxidant enzymes, such as ascorbate peroxidase (APX), catalase (CAT), and superoxide dismutase (SOD) during drought stress (Thakur and Anand, 2021). The net photosynthetic rate, chlorophyll (Chl) fluorescence, and antioxidant activities were significantly altered under water deficit conditions (Iqbal et al., 2019). The fast Chl *a* fluorescence is an efficient parameter to monitor the photosystem (PS)II and PSI photochemistry (Sánchez-Reinoso et al., 2019; Sipka et al., 2021). However, drought stress can limit the availability of water molecules for the photolysis of water, affecting the efficiency of the PSII oxygen-evolving complex (OEC), particularly D1 activity of PSII (Sasi et al., 2018).

The present study has three aims. The first is to improve our understanding of thylakoid organization under water stress. The second is to assess the use of Chl fluorescence to monitor the drought tolerance of pea. The third is to understand the recovery process after the drought stress. *Pisum sativum* var. Arkel (pea) is an annual herb belonging to the Fabaceae family and the second most cultivated legume crop globally. The seeds are well known for their high protein content, up to 22-24%. Since the pea crop is grown throughout the year, it is exposed to various stresses, particularly drought. Therefore, pea has chosen to study the photosynthetic parameters in relation to the protein supercomplex organization in thylakoids. I present detailed data on the physiological parameters, photosynthetic efficiency, disorganization of photosynthetic complexes, and recovery process in response to rewatering.

3.2 Results

3.2.1 Drought-induced changes in morphology, pigments, photosynthetic parameters, and redox status

Upon imposition of drought stress, pea plants appeared normal until D2. However, plants started displaying leaf curling and wilting responses after 4 days. The leaves were desiccated after 8 days of drought stress (Figure 3.1). In order to see how drought stress affects the morphology of the plants, shoot length, root length, leaf area, and total plant length are measured. Shoot length and Leaf area are found to be significantly decreased in drought-treated plants, while in recovery plants, shoot length has increased, but the increase in leaf area is not significant in recovery plants. Root length is found to be significantly increased in drought-treated plants compared to control plants. Total plant length change was not significant between control and recovery plants (Figure 3.2).

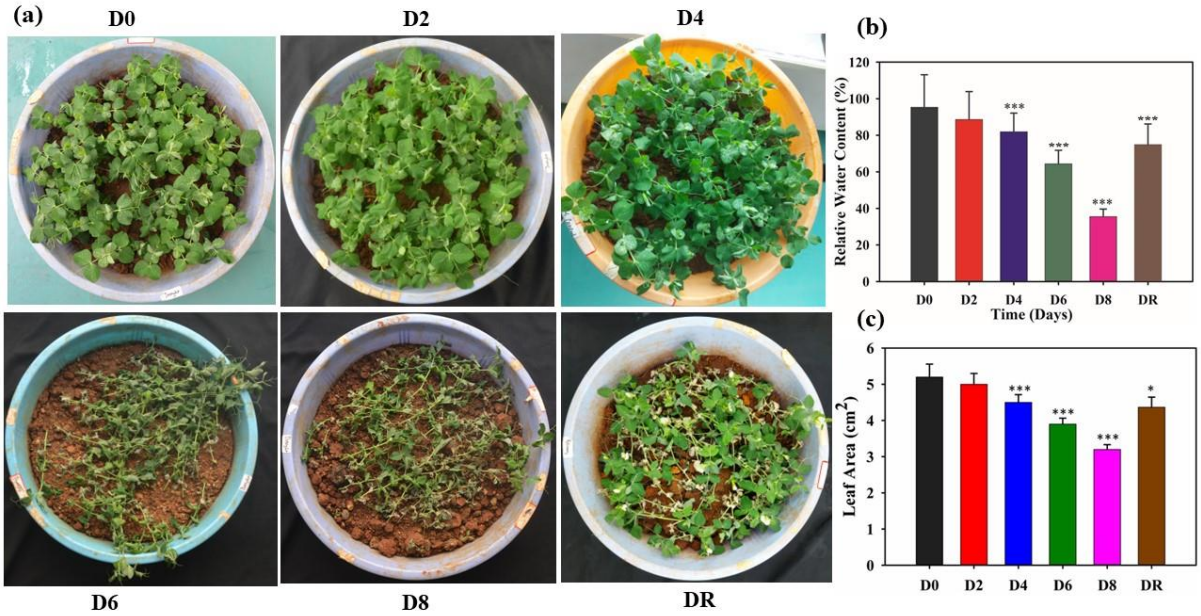

Figure 3.1 *Drought induces changes in physiological and morphological characteristics of pea leaves. (a) Symptoms and relative water content (b) in Pisum plant under drought stress for 0/ 2/ 4/ 6/ 8 days and recovery after rewatering on the 22nd day for seven days (c) Leaf Area of the control and treated plants. The data points are the averages of three replicates, and the error bars represent ±SE. One-way ANOVA (Bonferroni t-test) was performed to measure the P-values ns (not significant). Asterisks indicate the level of significance of the drought effect compared to the respective control * (p<0.05), ** (p<0.01) and *** (p<0.001), respectively.*

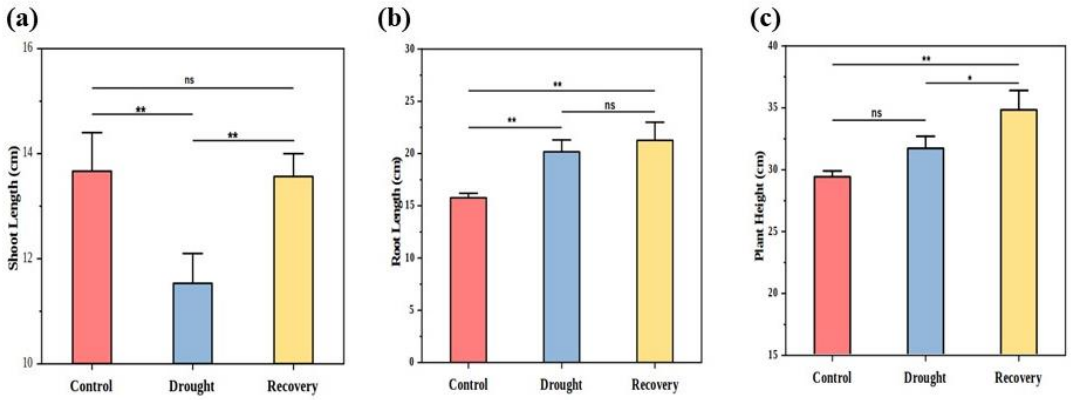

Figure 3.2 *shows a) Shoot length, b) Root length, c) Total plant length in control, drought, and recovery plants. The error bars represent the standard deviation (n= 3). The data points are the averages of three replicates, and the error bars represent ±SE. One-way ANOVA (Bonferroni t-test) was performed to measure the P-values ns (not significant). Asterisks indicate the level of significance of the drought effect compared to the respective control * (p<0.05), ** (p<0.01) and *** (p<0.001), respectively.*

The leaf RWC did not change till D2, while a significant decrease was observed at D4, D6, and D8, respectively, compared to the control. The total chlorophyll content was similar to the control values till D2, whereas a decrease was observed from D4 to D8. During recovery after 7 days of rewatering, the chlorophyll content recovered to the level of control (Figure 3.3a). In contrast, carotenoid content increased significantly from D4 to D8, whereas in recovery, it reached almost the control level (Figure 3.3b). Also, the infra-red gas exchange parameters, such as net photosynthetic rate (*Pn*) and stomatal conductance (g_s), were decreased progressively in drought-stress plants from D4 to D8 (Figure 3.4). At the same time, *E* and WUEi (ratio of *Pn/E*) were slightly decreased at D2, whereas a concomitant decrease was observed from D4 to D8 (Figure 3.4c, d). The Ci values were progressively reduced with drought stress from D2 to D8 (Figure 3.4e). A linear correlation was observed between *Pn* and g_s ($R^2 = 0.941$) as well as *E* and g_s ($R^2 = 0.978$) in drought-treated leaves of pea.

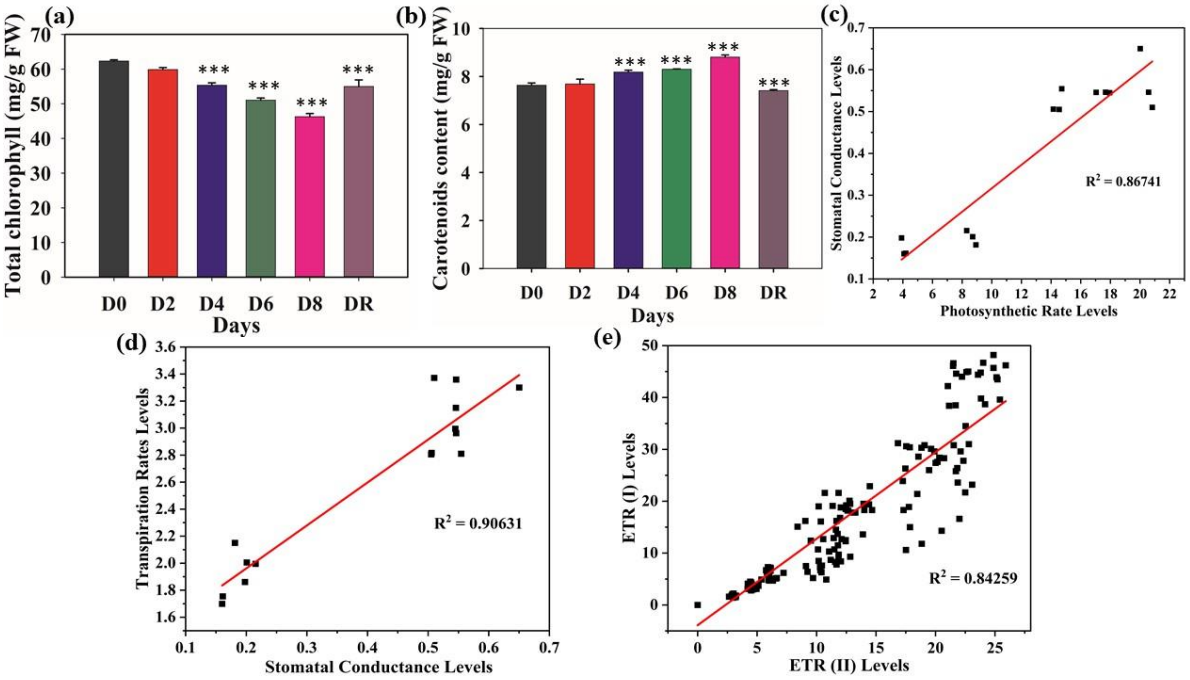

Figure 3.3 *Measurements of different physiological parameters of control and drought-stressed pea plants. All the parameters were collected from 0/ 2/ 4/ 6/ 8 days and recovered after rewatering on the 22nd day for seven days. (a) Total chlorophyll content from control and drought treated and recovered leaf (b) carotenoids content. (c-e) Relationship between stomatal conductance (gs) and photosynthetic rates (P_N), transpiration rate (E) with stomatal conductance (gs) and electron transport rate (ETR I) and (ETR II). (c) Regression analysis between stomatal conductance and photosynthetic rates (R^2=0.8674). (d) Regression analysis between transpiration rate and stomatal conductance (R^2=0.9063). (e) Regression analysis between ETR (I) and ETR (II) (R^2=0.8425). The data point we took is the average of three replicates, and the error bars represent ±SE. One-way ANOVA (Bonferroni t-test) was performed to measure the P-values; ns (not significant). Asterisks indicate the level of significance of the drought effect compared to the respective control * (p<0.05), ** (p<0.01) and *** (p<0.001), respectively.*

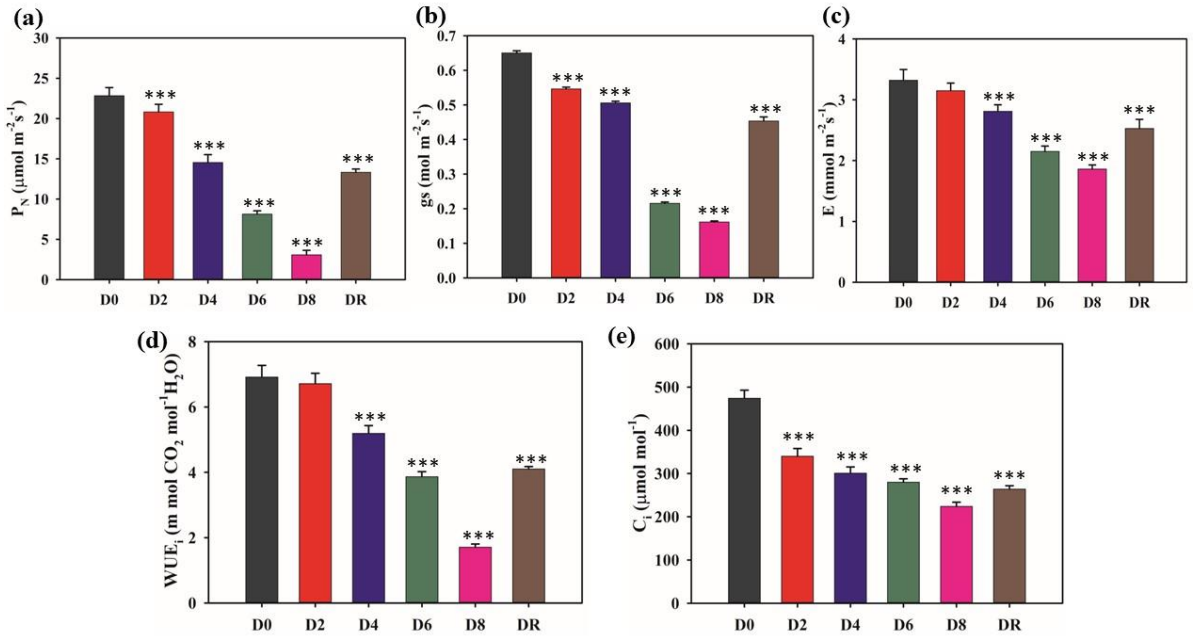

Figure 3.4 *Changes of photosynthetic leaf gas exchange parameters of Pisum sativum under progressive drought stress conditions. (a) Net CO_2 assimilation rate (P_N); (b) stomatal conductance (gs); (c) transpiration rate (E); (d) instantaneous water uses efficiency (WUE); (e) sub-stomatal CO_2 concentration (C_i) under drought stress for 0/ 2/ 4/ 6/ 8 days and recovery after rewatering on the 22nd day for seven days. The data point we took is the average of three replicates, and the error bars represent ±SE. One-way ANOVA (Bonferroni t-test) was performed to measure the P-values ns (not significant). Asterisks indicate the level of significance of the drought effect compared to the respective control * ($p<0.05$), ** ($p<0.01$), and *** ($p<0.001$), respectively.*

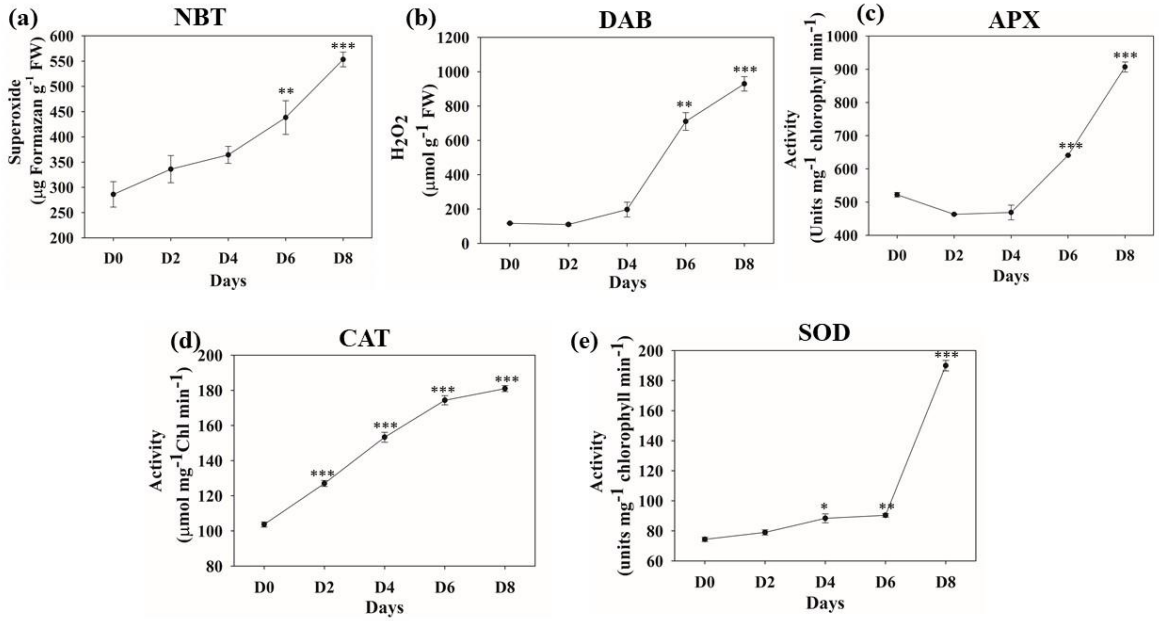

Figure 3.5 *Evaluation of ROS in Pisum sativum after control and drought stress by NBT, DAB, and antioxidants enzymes such as SOD, APX and Catalase. (a) quantification of superoxide radicals as represented at different days by using NBT staining from the stained leaves; and (b) represented via the quantification of H_2O_2 on different days using DAB staining from the stained leaves; (c-e) shows the activity of antioxidant enzymes APX, CAT and SOD compared to control with progressive drought stress condition (for 0/ 2/ 4/ 6/ 8 days) measured in leaves of a pea seedling. The data point we took is the average of three replicates, and the error bars represent ±SE. One-way ANOVA (Bonferroni t-test) was performed to measure the P-values ns (not significant). Asterisks indicate the level of significance of the drought effect compared to the respective control * ($p<0.05$), ** ($p<0.01$), and *** ($p<0.001$), respectively.*

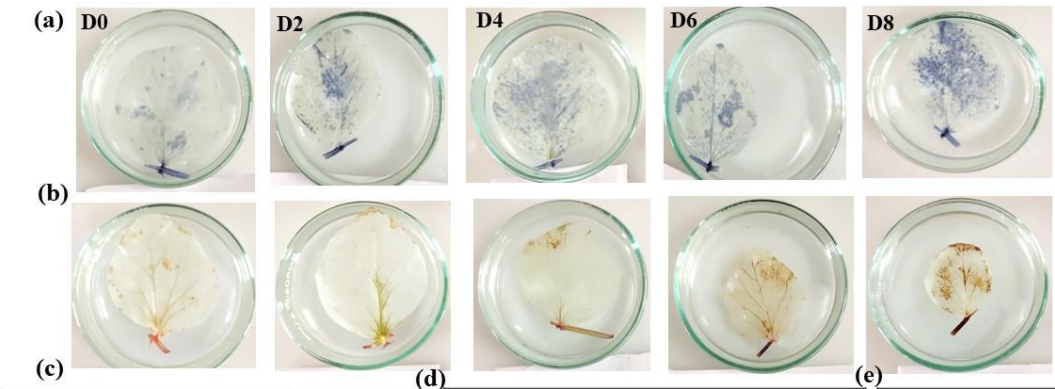

Superoxide (µg Formazan g^{-1} FW)	
D0	286 (100 %)
D2	336 (117 %)
D4	364 (127 %)
D6	438 (153 %)
D8	550 (192 %)

H_2O_2 (µmol g^{-1} FW)	
D0	117 (100 %)
D2	110 (94 %)
D4	197 (169 %)
D6	710 (609 %)
D8	929 (796 %)

APX activity (µmol mg^{-1} Chl min^{-1})	
D0	517 (100 %)
D2	463 (90 %)
D4	469 (91 %)
D6	640 (124 %)
D8	907 (175 %)

(f)

CAT activity (µmol mg^{-1} Chl min^{-1})	
D0	107 (100 %)
D2	129 (121 %)
D4	150 (141 %)
D6	176 (165 %)
D8	181 (170 %)

(g)

SOD activity (unit mg^{-1} Chl min^{-1})	
D0	75 (100 %)
D2	79 (106 %)
D4	89 (119 %)
D6	91 (121 %)
D8	190 (255 %)

Figure 3.6 *Evaluation of ROS in Pisum sativum after control and drought stress by NBT, DAB, and antioxidants enzymes such as SOD, APX and Catalase. (a) Visualization of superoxide (O^{2-}) at different days from (D0 to D8) using NBT staining. (b) Visualization of hydrogen peroxide (H_2O_2) at different days using DAB staining (c) and percentage change at different days by using NBT is staining from the stained leaves. (d) Quantification of H_2O_2 on different days using DAB staining in the form of percentages from the stained leaves. The activity of antioxidant enzymes APX, CAT and SOD are based on percentage changes in figure (e-g) compared to control with progressive drought stress condition measured in pea leaves. The data point we took is the average of three replicates, the error bars represent ±SE.*

During the drought treatment, the superoxide accumulation indicated by formazan formation increased progressively (Figure 3.5). The formazan content significantly increased by 117%, 127%, 153%, and 198% in the drought-treated plant at D2, 4, 6, and 8, respectively (Figure 3.6). Similarly, the H_2O_2 accumulation in control leaves and drought-treated plants was assessed using the DAB staining method (Kwon et al., 2013). A brown precipitate formation increased progressively with the drought treatment. H_2O_2 content was significantly increased by 94%, 169%, 609%, and 796% in the drought-treated plant at D2, 4, 6, and 8, respectively (Figure 3.6). Notably, no marked changes were observed in the H_2O_2 level on day 2 in drought-treated plants.

APX activity remained unaffected among the antioxidative enzymes at D2 and 4, while it significantly increased by 124% and 175% at D6 and 8, respectively (Figure 3.6). Additionally, the CAT activity was increased by 121%, 141%, 165%, and 170% on days 2, 4, 6, and 8 (Figure 3.5d and Figure 3.6f). Similarly, the SOD activity remained unchanged at D2. At the same time, it was significantly enhanced by 119%, 121%, and 255% at D4, 6, and 8, respectively (Figure 3.5e and Figure 3.6g), followed by a linear correlation observed between APX and H_2O_2, catalase, and H_2O_2, APX, and superoxide, catalase, and superoxide, SOD and superoxide, SOD and H_2O_2, respectively (Figure 3.6). A maximum correlation was observed between APX and H_2O_2 (R^2=0.8349), catalase and H_2O_2 (R^2=0.7501), APX and superoxide (R^2=0.7491), catalase and superoxide levels (R^2=0.73412), SOD and superoxide (R^2=0.7332), SOD and H_2O_2 (R^2=0.65988), in drought treated leaves, respectively (Figure 3.7). Interestingly the contents of antioxidant enzyme proteins (catalase, Mn-SOD, APX, and Cu-ZnSOD) increased under severe drought stress (Figure 3.8). Therefore, all the anti-oxidative enzyme activities progressively increased with the duration of drought exposure.

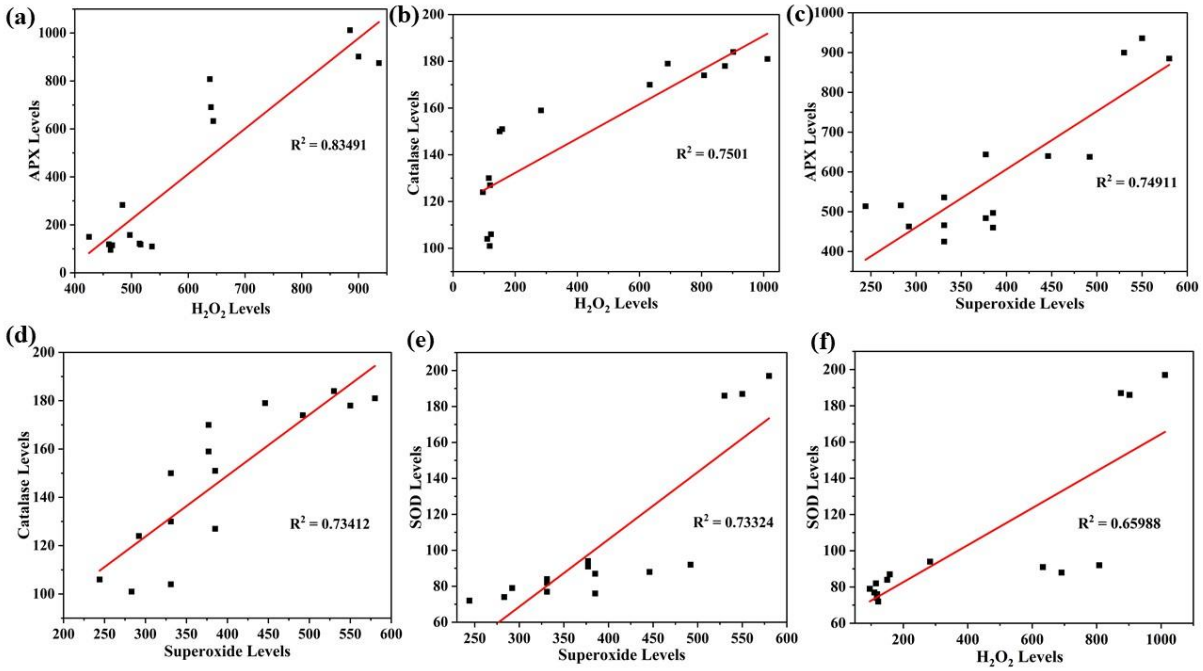

Figure 3.7 *Relationship between APX and H_2O_2 levels, catalase and H_2O_2, APX and superoxide levels, catalase and superoxide levels, SOD and superoxide levels, SOD and H_2O_2 levels during the period of drought stress. Regression analyses between (a) APX and H_2O_2 levels (R^2=0.8349); (b) catalase and H_2O_2 levels (R^2=0.7501); (c) APX and superoxide levels (R^2=0.7491); (d) catalase and superoxide levels (R^2=0.734); (e) SOD and superoxide levels (R^2=0.733); and (f) SOD and H_2O_2 levels (R^2=0.659). The data point we took is the average of three replicates, the error bars represent ±SE.*

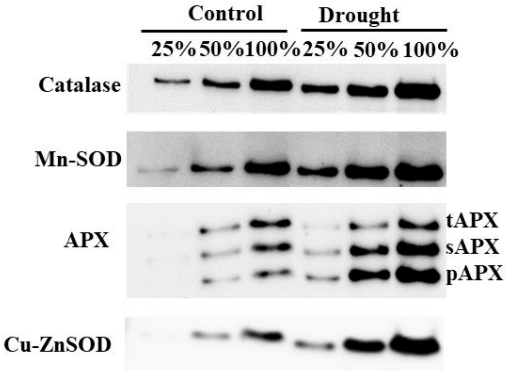

Figure 3.8 *Immunoblot analysis of antioxidants enzymes was performed from leaves of Pisum sativum (Catalase, Mn-SOD, APX isoforms (tAPX-thylakoid ascorbate peroxidase, sAPX-stromal ascorbate peroxidase, pAPX- peroxisomal ascorbate peroxidase, Cu-ZnSOD) from control and drought condition. Polypeptides were loaded with equal protein concentration, and the dilution was made from control and drought. The different dilutions (25%, 50%, and 100%) were used for easy comparison.*

3.2.2 Changes in Chl *a* fluorescence kinetics reflecting the PSI and PSII efficiency

A reduction was observed in the OJIP curve pattern from D2 to D8 (Figure 3.9a). However, drought-treated plants exhibited a similar OJIP curve pattern at D4 and D6. The curve patterns of both O-I phases shifted slightly from D2 to D6, whereas at D8, the curve pattern of both phases differed significantly with respect to their controls. Conversely, the I-P phase significantly reduced in drought treatment from D2 to D8. In contrast, Fv/Fm showed no change at D2, 4, and 6. Concomitant decreases were observed at D8 in drought-stressed plants (Figure 3.9b). The normalized relative variable fluorescence between O to J phase (50 μs to 2 ms) is represented as V_{OJ} (Figure 3.9c). At D2 drought-treated plants, a negative K-band value was recorded between 0 μs and 50 μs, indicating that all the reaction centers are the active and efficient transfer of electrons around PSII due to minimal drought effect.

Conversely, a positive K-band with a maximum peak was recorded between 50 μs and 1 ms. It was due to the lack of electron transfer from the OEC to the Q_A site of the PSII complex in drought-treated plants at D4, 6, and 8, respectively. The normalized relative variable fluorescence between O to K phase (50 μs to 300 μs) is expressed as V_{OK} (Figure 3.9c, d). Similarly, electron transfer from Q_A to Q_B site and organization of PSII is denoted with the L band (Devadasu et al., 2021). Our results showed a negative bell-shaped L-band with a maximum peak at 125 μs was observed in drought-treated plants at D2, which indicates that there is an efficient transfer of electrons between Q_A to Q_B site of PSII, whereas the positive bell-shaped L-band values recorded at 175 μs in drought treated plants at D4. Notably, the positive bell-shaped L-band values were recorded at around 100 and 125 μs. Furthermore, the recovery plants displayed almost similar photosynthetic activity (JIP parameters) as control when the drought-induced plants were watered for 7 days (Figure 3.9a).

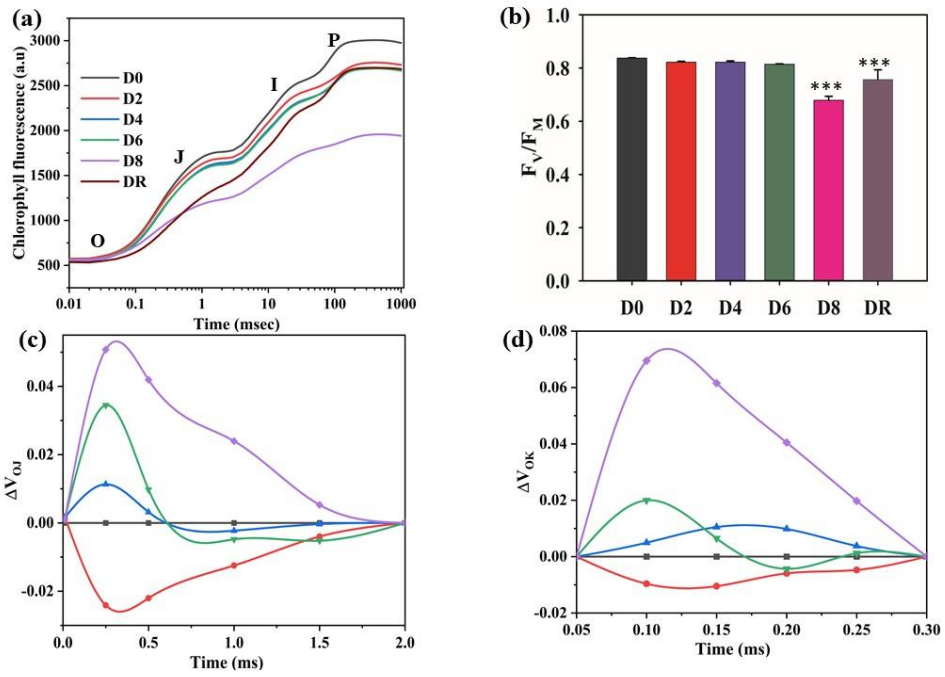

Figure 3.9 *The OJIP Chl a fluorescence transient of Pisum sativum under control, drought, and recovery stress conditions. (a) Raw Chl a fluorescence transient exhibiting fluorescence intensity (F_t), was recorded between 0.1 ms to 1000 ms time; (b) Fv/Fm; (c) kinetic difference of V_{OJ} [D_{VOJ} = (F_t - F_O)/ (F_K - F_O)] showing K-band; (d) kinetic difference of V_{OK} [D_{VOK} = (F_t - F_O)/ (F_K - F_O)] showing L-band at 0.15 ms. The curves in black represent the control D0, in red color D2, purple color D4, green color D6, and D8 plants and brown color recovery, respectively. All the parameters are deduced from the OJIP-test analysis conducted on fully expanded 2nd-3rd leaves of a pea seedling. The data point we took is the average of three replicates, and the error bars represent ±SE. One-way ANOVA (Bonferroni t-test) was performed to measure the P-values ns (not significant). Asterisks indicate the level of significance of the drought effect compared to the respective control * ($p<0.05$), ** ($p<0.01$), and *** ($p<0.001$), respectively.*

The changes of phenomenological fluxes in control and drought-treated plants were represented as the energy pipeline leaf model (Figure 3.10). As drought stress progresses the closed reaction centres in PSII were increased from D2 to D8 in drought-treated plants. Both TRo/CSo and ETo/CSo were significantly decreased, while ABS/CSo showed no change with respect to that of controls from D2 to D8 in drought-treated pea plants. Interestingly, the DIo/CSo values were increased significantly at D6 and D8 in drought-treated plants (Figure 3.10).

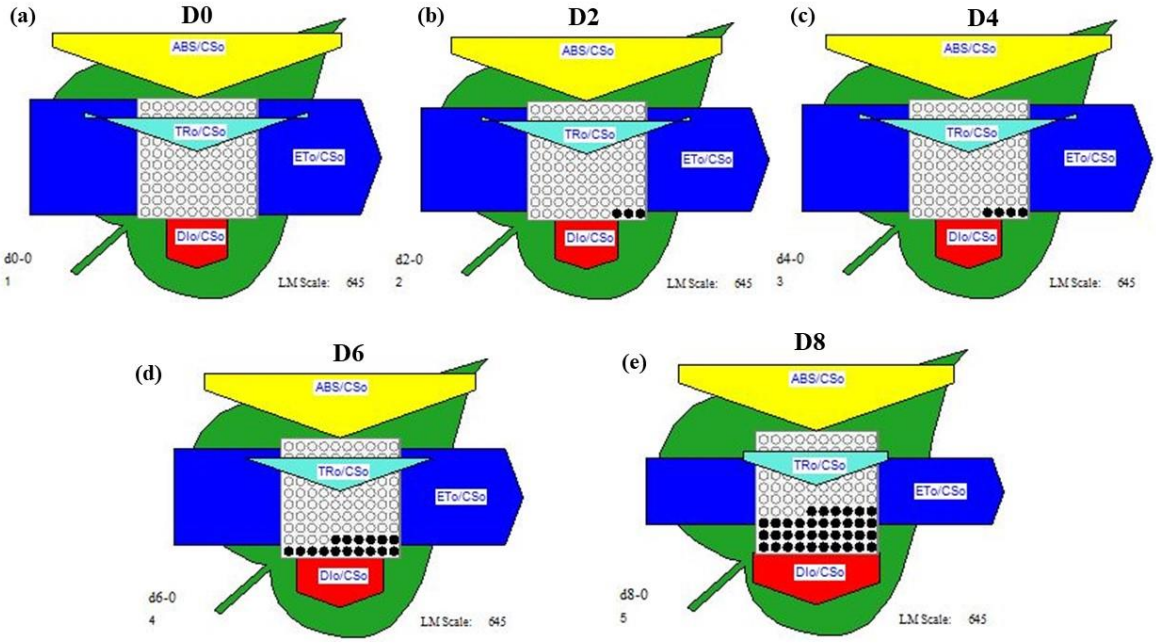

Figure 3.10 *Leaf model of Photosystem II efficiency of control and drought-grown plants (a-e). The model indicates higher open reaction centers and electron transport rates in successive drought stress as compared with control. All the parameters are deduced from the OJIP-test analysis on fully expanded upper canopy leaves during 9:00-10:00 h.*

PSII fluorescence parameters were measured with increasing photosynthetic active radiation (PAR) from 0 to 800 µmol photons m^{-2} s^{-1} (Figure 3.11a-d and Figure 3.12a-d). The patterns of Y(II), Y(NO), ETR(II), qP and qL responsive curves decreased progressively with the treatment time. Conversely, the magnitude of Y(NPQ), NPQ, and qN curves increased. Thus, NPQ is raised by drought conditions, indicating that luminal pH is acidified.

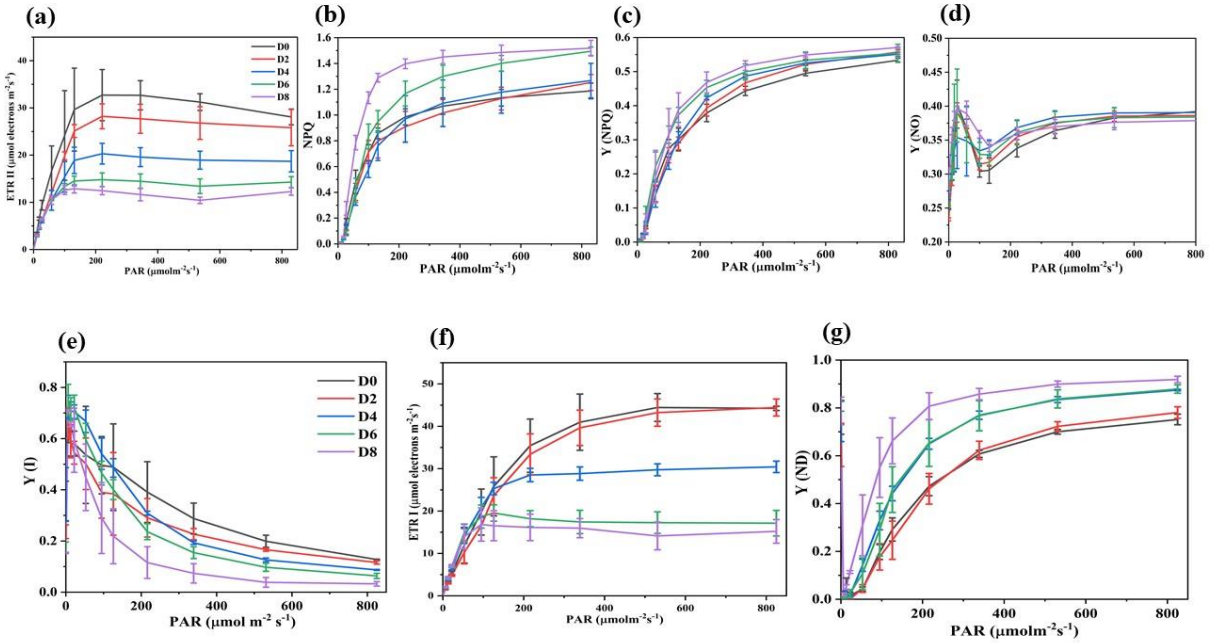

Figure 3.11 *Effect of drought stress on steady-state photosynthetic parameters. The light intensity dependence of the chlorophyll fluorescence parameter of PSII is represented from (a-d). As represented, PSI (e-g) was determined in control and progressive drought stress conditions for 0/ 2/ 4/ 6/ 8 days. Photosynthetic parameters of PSII are (a) ETR (II), (b) NPQ, (c) Y(NPQ), (d) Y(NO) and PSI in terms of (e) Y(I), (f) ETR(I) and (g) Y(ND). The data point we took is the average of three replicates, and the error bars represent ±SE.*

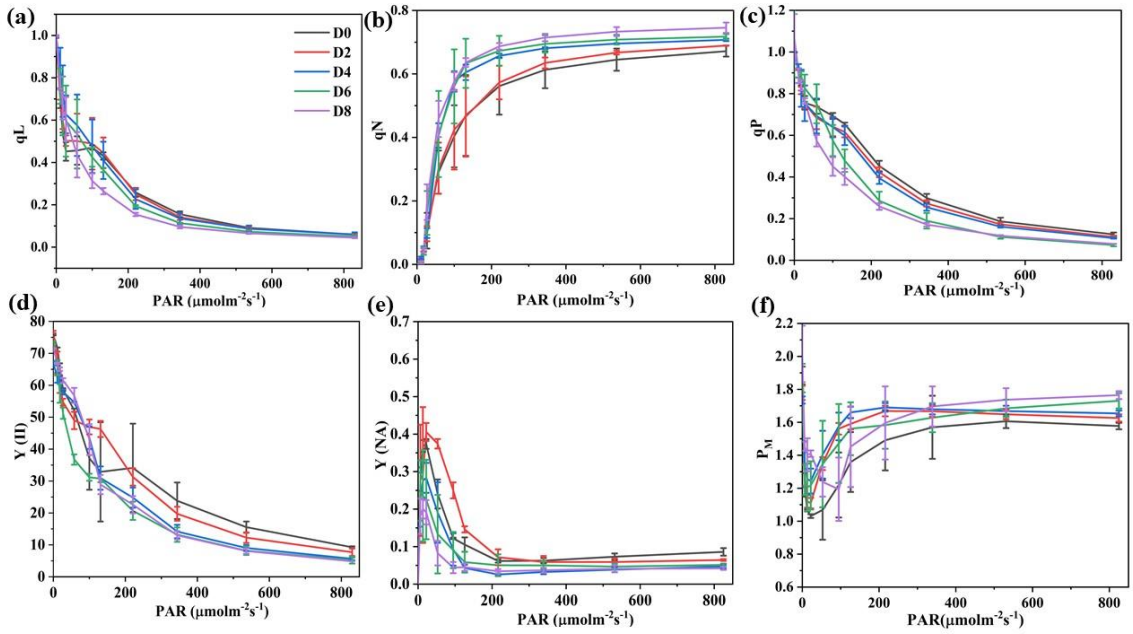

Figure 3.12 *Effect of drought stress on steady-state photosynthetic parameters. The light-intensity dependence of chlorophyll fluorescence parameters of PSII (a-d) and absorbance transients of PSI (e-f) as indicated, determined in control and progressive drought stress conditions (D0, D2, D4, D6, and D8), respectively. Photosynthetic parameters (PSII) were (a) qL, (b) qN, (c) qP and (d) Y(II); and PSI in terms of (e) Y(NA) and (f) PM. The data point we took is the average of three replicates, the error bars represent ±SE. PFD = photon flux density.*

The yield of PSI was measured with increasing photosynthetic active radiation (PAR) from 0 to 800 µmol photons m^{-2} s^{-1} (Figure 3.11e-g and Figure 3.12e, f). The yield of photochemical energy conversion of PSI Y(I), the rate of electron transport of PSI ETR(I), and the donor side limitation of PSI Y(ND) responsive curves exhibited a similar trend to that of controls at D2. In contrast, the pattern of Y(I) and ETR(I) responsive curves reduced at D4, 6, and 8, respectively, in drought-treated plants. However, a linear correlation was observed between ETR (I) and ETR (II) levels (R^2=0.73412) in drought-treated leaves of pea. The Y(ND) responsive curve increased between 110 to 800 µmol photons m^{-2} s^{-1} PAR at D4, 6, and 8, respectively (Figure 3.11g). Notably, at D2, Y(NA) responsive curve patterns increased drastically, whereas the curve pattern slowed down between 0 to 200 µmol photons m^{-2} s^{-1} PAR in drought-treated plants at D6 and 8, respectively (Figure 3.12e). The *Pm* values increased with progressive drought stress regarding controls (Figure 3.12f), indicating that light induced P700 oxidation is reduced under drought stress.

3.2.3 Drought-induced changes in supercomplexes of thylakoid membranes

The pattern of PSII-LHCII, PSI-LHCI complexes, and PSII dimerization changed in drought stress. The PSII-RCs were also affected severely under drought stress (Figure 3.13). The PSII-LHCII supercomplexes were significantly reduced in drought stress. However, LHCII monomeric levels increased, possibly due to the dissociation of PSII-LHCII and PSI-LHCI supercomplexes. The dimers of PSII and PSI contents were marginally reduced. Interestingly, the band intensity of Cyt b_6f and PSII monomer was enhanced in drought-treated plants compared to controls. Our results suggest that the organization of PSII and PSI complexes was disturbed under severe drought stress. In the case of recovery, most of the supercomplexes were restored as in control, indicating

that pea plants can sustain and recover from extreme drought stress. This observation reiterates the resilience of photosynthetic machinery.

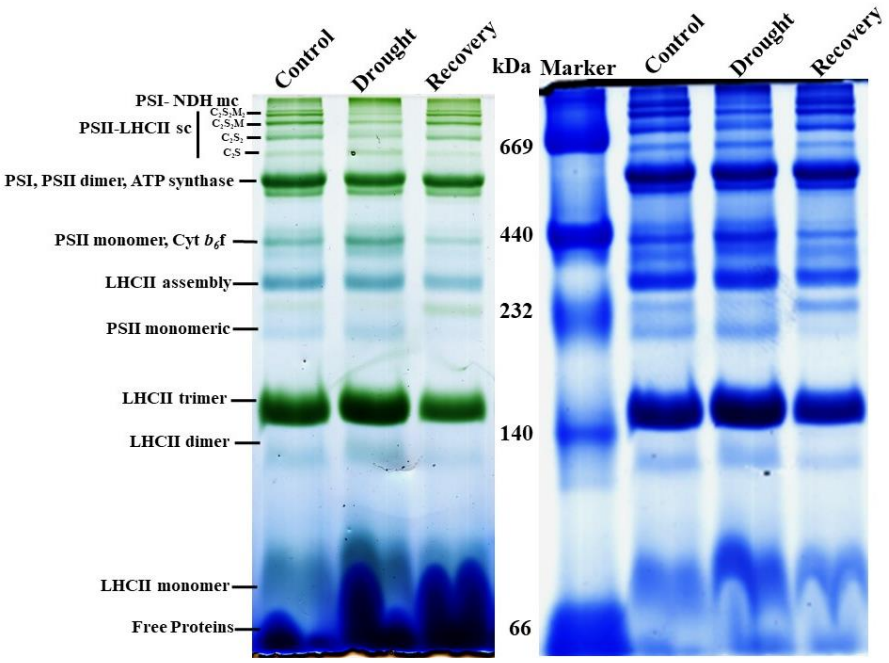

Figure 3.13 *Thylakoid membrane supercomplexes were isolated from control (D0), drought (D8), and recovery (DR) after rewatering on the 22nd day for seven days (10 µg of Chl/lane) and separated through Blue Native-PAGE and they labelled as PSII-LHCII, PSI, PSII dimer, ATP synthase, PSII monomer, Cyt b_6f, LHCII assembly, PSII monomeric, LHCII trimer, LHCII monomer and free protein.*

3.2.4 Analysis of thylakoid proteins of PSII and PSI and disassembled proteins of PSI, PSII, and LHCII

The abundance of PSII proteins D1, D2, CP43, CP47, Cyt *b_6f*, PsbO, and PsbP decreased under drought conditions (Figure 3.14a, b, and Figure 3.15). Interestingly, the levels of D1 and D2 showed no detectable change in drought-treated plants because of continuous turnover. In the LHCII complex, the abundance of Lhcb1, Lhcb2, Lhcb4, Lhcb5, and Lhcb6 were decreased, while the levels of Lhcb3 showed no marked change

in drought-treated plants. Further, the PSBS, a stress-regulated protein that induces NPQ, is marginally increased in drought stress. Surprisingly, the iron-sulfur protein ferredoxin was dramatically reduced (Figure 3.14a). Also, the PSI core proteins abundance of PsaA, PsaB, and PsaH were decreased, while the levels of PsaC, PsaD, PsaE, PsaF, PsaG, and PsaL showed no detectable change in drought-treated plants, respectively (Figure 3.14a, b and Figure 3.15). In the LHCI complex, the abundance of Lhca2, Lhca3, and Lhca4 decreased. However, there was no marked change in Lhca1 in drought-treated plants. Moreover, drought stress-induced proteins such as dehydrin and aquaporin were markedly increased compared to the control.

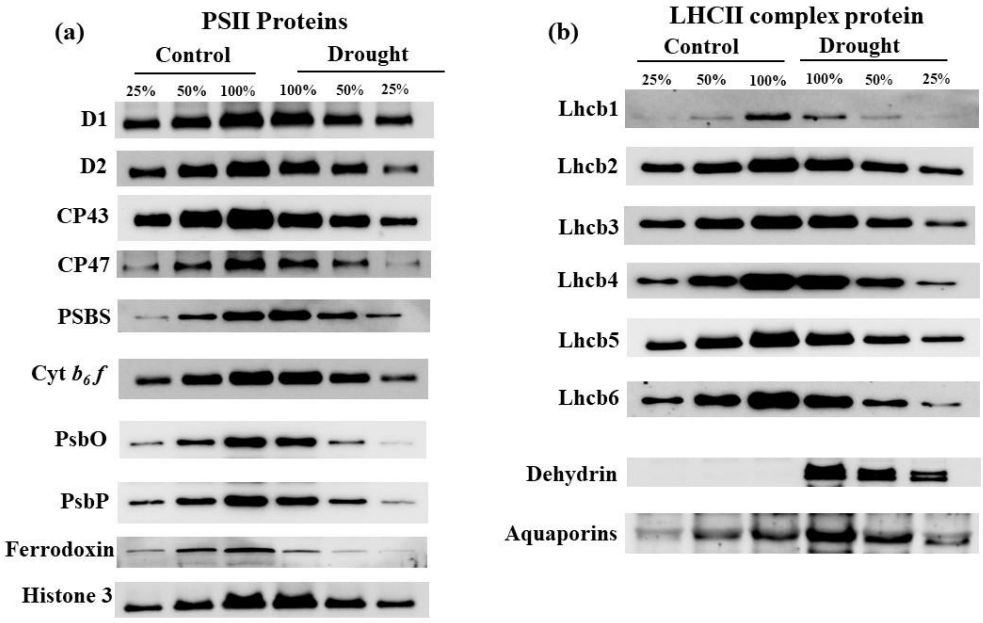

Figure 3.14 *Analysis of protein contents from control (D0) and drought (D8) (a) PSII core protein (D1, D2, CP43, CP47, PSBS, (Cyt) b_6f, OEC (PsbO, PsbP), Ferredoxin and (b) LHCII proteins (Lhcb1, Lhcb2, Lhcb3, Lhcb4, Lhcb5, Lhcb6) from control and drought stress condition. Polypeptides were loaded with equal protein concentration (4 µg) per lane. The dilution was made from control 25, 50, and 100 % as a positive control, and for equal loading was represented with Histone 3 (H3) antibody. The amount of respective protein was quantified by ImageJ 1.53.*

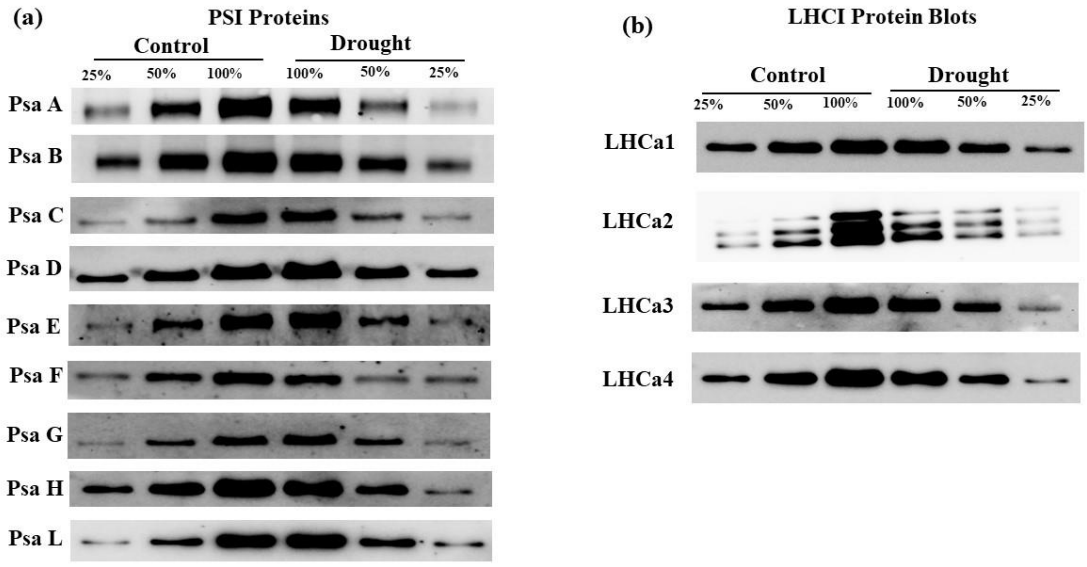

Figure 3.15 *Immunoblot analysis of control (D0) and drought (D8) (a) PSI core proteins (PsaA, PsaB, PsaC, PsaD, PsaE, PsaF, PsaG, PsaH, PsaL) and (b) LHCI protein (LHCa1, LHCa2, LHCa3, and LHCa4). The control and drought proteins were loaded with serial dilution. The different dilutions (25, 50, and 100%) were used for each lane, and Histone 3 (H3) was used as a loading control. The amount of respective protein was quantified by ImageJ 1.53.*

We checked the aggregates-like formation of proteins of the thylakoid membranes using β-DM as detergent and fluorescence and a confocal microscope (Figure 3.16) to investigate further the pelleted proteins after drought stress. No aggregation was observed in control and recovery, but in drought, the association of both PSI, PSII, and LHC proteins occurred, and a significant increase in the size of aggregates like with increased drought stress. Similarly, in temperature stress, there was a considerable increase in LHCII aggregates (Tang et al., 2007). In our case, all the disassembled like aggregated proteins were loosely bound, therefore, they have easily removed and settled in pellets from drought stress samples.

The thylakoids were solubilized in β-DM and centrifuged to obtain the pellet; wherein further analysis of proteins was carried out. In fact, from the leaves obtained from drought (wilted leaves), thylakoids could be isolated from the control. Usually, the disassembled proteins were present in the pellet as they were bound loosely to the proteins (Devadasu et al., 2021, Tang et al., 2007). Therefore, the proteins were probed with antibodies PsaA, PsaB, PsaF, LHCII (Lhcb2, Lhcb5, Lhcb6), D1, D2, CP43, and CP47 in the pellet (Figure 3.16b). Interestingly, the PSI and PSII core proteins, D1, D2, CP43, CP47, PsaA, PsaB, and LHCII protein levels (Lhcb2, Lhcb5, Lhcb6) were increased in pellet, indicating that core and LHCII proteins are in pellet due to their decreased solubility. The levels of PsaF showed no detectable change in drought.

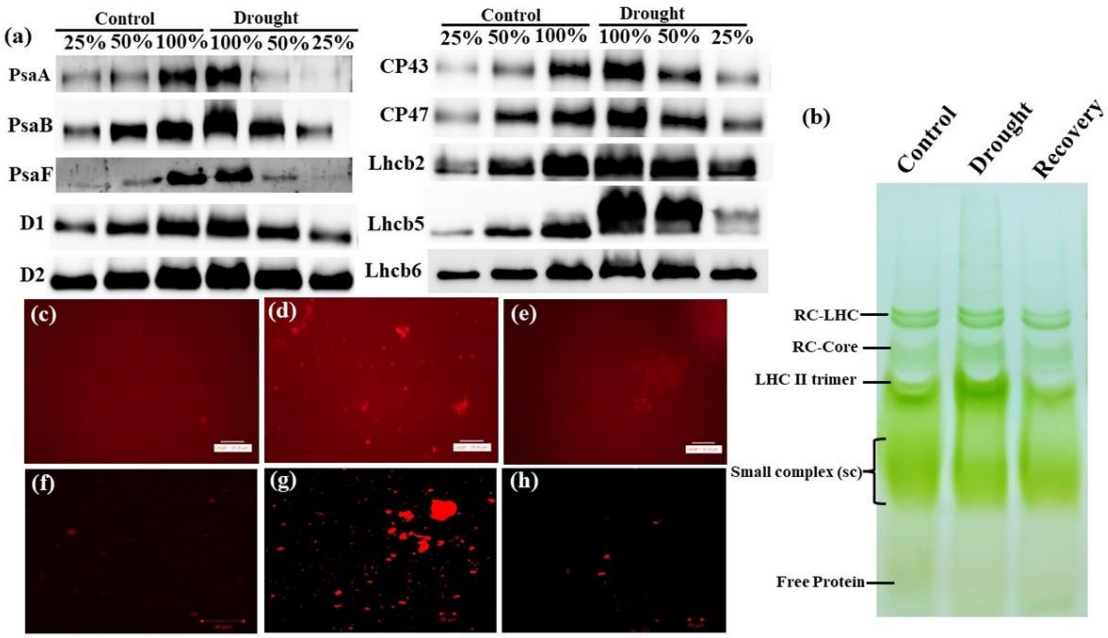

Figure 3.16 *The LHCII disassembled proteins appear during control (D0), drought (D8), and recovery (DR) after rewatering on the 22nd day for seven days in pea plants after incubating with mild detergents. (a) Immunoblot analysis of pellet proteins after solubilization thylakoids with β-DM (1%) and the following proteins were immunoblotted (PsaA, PsaB, PsaF, D1, D2, CP43, CP47) and LHCII (Lhcb2, Lhcb5, Lhcb6). Chlorophyll fluorescence images were determined with the help of fluorescence microscope (b-d) and confocal microscope (e-g). Bars in each plate, 20 µm.*

3.2.5 Macro-organization of thylakoid membranes

Circular dichroism (CD) spectra in the visible region (400-800 nm) carry information about the macro-domain organization of thylakoid membranes and short-range pigment-pigment interactions in the pigment-protein complexes. The CD spectrum obtained from intact granal thylakoids comprises strong psi-type bands at around (+)690 and (-)676 nm and at (+)506 nm (Figure 3.17). These bands have been shown to originate from LHCII-containing chiral macrodomains, macroarrays of PSII, and LHCII (Cseh et al., 2000). We observed a marked reduction in these bands upon drought stress, as reflected by the decreased $CD_{506\text{-}550}$ and $CD_{690\text{-}676}$ amplitudes (Figure 3.17b), indicating reorganizations in the chiral macrodomains of thylakoid membranes. Further changes were observed between about 460 and 480 nm, which appear to reflect alterations in the excitonic interactions involving chlorophyll-b and carotenoid molecules (Garab and van Amerongen, 2009). At severe drought stress, changes in psi-type CD bands were also accompanied by distortions of some excitonic bands in the Soret region, between 484 and 462 nm, suggesting changes in the composition or molecular architecture of some of the pigment-protein complexes (Figure 3.17b).

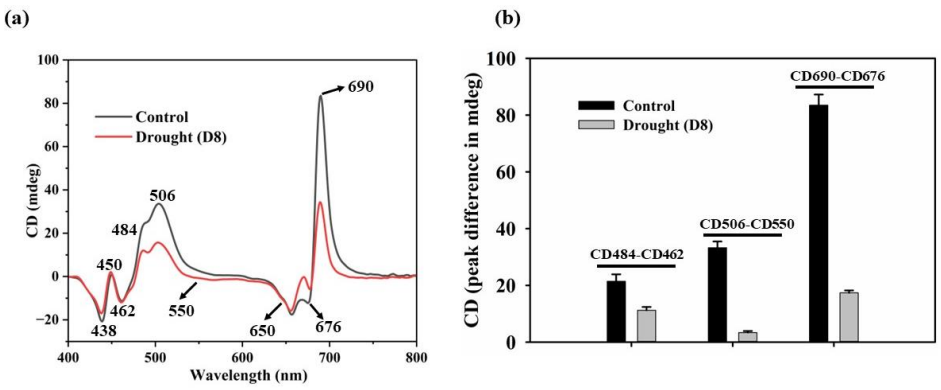

Figure 3.17 *Changes in the chiral organization of the pigment molecules in isolated thylakoid membranes obtained from pea seedlings before (D0, black) and after (D8, red) drought stress, as reflected by (a) circular dichroism spectra and (b) amplitude variations of selected CD bands. Spectra were measured with equal (20 µg/mL) chlorophyll contents.*

3.2.6 Changes in chloroplast ultrastructure

TEM images showed differences in thylakoid architecture in control, drought, and recovered samples. The overall organization of the chloroplasts and the thylakoid membranes in pea leaves followed the regular pattern (Figure 3.18a-c); they contained stacked grana membranes and unstacked stroma lamellae (Daum et al., 2010). After 8 days of drought stress, we could distinctly observe increased repeat distances (average height of thylakoids) in the grana, reflecting loosened or bulged as compared to the control (Figure 3.18d-f). The lamellar structures in drought-stressed samples appeared to be somewhat looser compared to the control and the recovered sample, but thylakoids in all cases were stacked into grana (Figure 3.18g-i). This indicates that thylakoid organization has been modified only moderately under drought conditions. The repeat distances of the granum thylakoid membranes increased by approximately 2.6 nm under long-term drought stress on the 8^{th} day compared with the control (Figure 3.19).

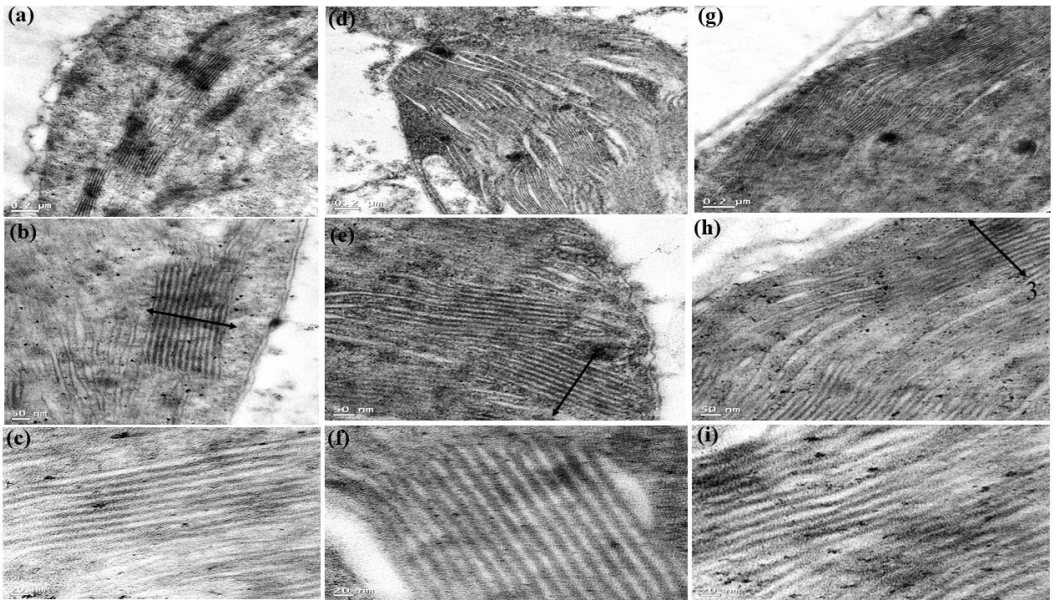

Figure 3.18 *Transmission electron microscope (TEM) images of the control (D0), drought treated (D8), and seven days recovery (DR) after rewatering the plants on the 22nd day. TEM pictures of palisade mesophyll cells with chloroplast in the close-up view. Leaves of control, drought, and recovery were prepared as thin section samples. Bars, 0.2 µm, 50 nm, and 20 nm, respectively, as indicated. The arrows display exemplary grana stacks loosening. Images show different thylakoid arrangements in control (a-c), drought stresses (d-f) and after recovery (g-i).*

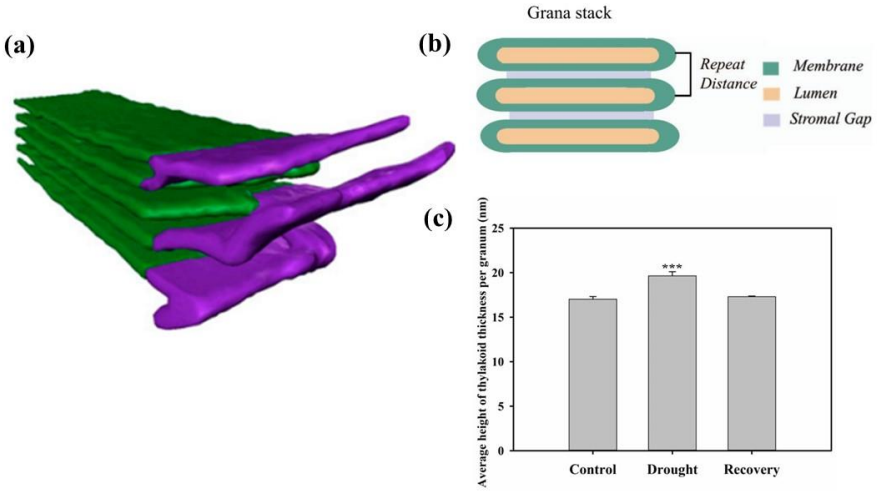

Figure 3.19 *(a) Surface representation of connections between grana (green) and stroma (purple) thylakoids reveals their 3D organization at the grana margin. (b) Model for calculating repeat distance of the grana stacks. (c) Average repeat distance values of granum thylakoid membranes were measured from the control, drought, and recovery samples. Thirty repeat distances were determined and averaged from each group; the error bars represent ±SE. One-way ANOVA (Bonferroni t-test) was performed to measure the P-values; ***, P<0.001.*

3.3 Discussion

3.3.1 Changes in morphology, photosynthesis, and redox status of leaves under drought stress

Plants possess diverse physiological and biochemical strategies to cope with adverse conditions. In our work, pea plants displayed drought stress-induced symptoms such as leaf curling after 4 days of drought stress. As the drought stress progressed, plants showed irreversible stress symptoms such as leaf wilting and scorching. However, drought-induced plants showed recovery signs, with new leaves after 7 days of watering. These symptoms are typical of drought stress, with reduced leaf RWC, which might be responsible for leaf curling and wilting in leaves (Wang et al., 2020). The stomata were closed obviously to avoid water loss, reflected in lowered stomatal conductance with a concomitant decrease in *Pn* and Ci (Henry et al., 2019). The specific leaf area or partial opening of stomata could be responsible for maintaining initial steady values of E, which subsequently decreased (Riboldi et al., 2016). The significant reduction in the chlorophyll content of pea leaves under drought (Figure 3.3a) might be due to impairment in the photosynthetic apparatus or activation of chlorophyll degrading enzymes, or both (Yu et al., 2018; Dalal 2021).

Under water-limited conditions, the absorbed light energy could not be utilized entirely in the metabolic process, leading to the inhibition of photosynthetic activity (Wang et al., 2018). Production of ROS, including H_2O_2, and superoxide radicals, are inevitable under drought stress conditions (Das and Roychoudhury, 2014). We also observed that both H_2O_2 and superoxide radical levels increased with progressive drought stress in pea plants. The increased ROS production results from an imbalance between ROS generation and the antioxidant defense system (Hasanuzzaman et al.,

2020). SOD is one of the essential cellular ROS scavengers that defend against superoxide radicals (Wang et al., 2018). The high levels of superoxide radicals during drought stress would be converted into H_2O_2 (Sharma et al., 2012). Furthermore, the increased APX and catalase levels (Figure 3.5 and Figure 3.6) might protect the cell from H_2O_2 damage by converting it into water (Sofo et al., 2015). The changes in morphological, gas exchange and photosynthesis pigment data demonstrate that pea seedlings have acquired an adaptive mechanism rather than inducing a death signaling process to progressive drought stress.

3.3.2 Modulation and recovery of Chl *a* fluorescence component: focus on PSI and PSII oxidation and their proteins

The rise in initial fluorescence, Fo from **O**JIP curve, with progressive drought stress, indicated the dissociation of antenna complexes from the PSII core. This could limit the energy transfer to the PSII trap, in agreement with earlier reports (Strasser and Srivastava 1995; Kodru et al., 2015). The decrease in J, I, and P indicated the hindrance of electron flow beyond Q_A^- due to the accumulation of inactive reaction centers (Guo et al., 2019). Our results showed a significant positive peak in the L-band in drought stress, which suggests the inefficient operation of both the acceptor and donor sides of PSII. Further, the appearance of the K-band indicated damage to the OEC.

Under progressive drought stress, the significant reduction in qP and qL reflects the fraction of PSII centers closed. As a result, the electron transport chain ETR(II) and, consequently, the yield of PSII Y(II) declined (Figure 3.11). Further, the steady levels of Y(NO) divert the absorbed energy at PSII. The increase in the regulated thermal dissipation components of PSII, such as NPQ, Y(NPQ), and qN, suggested that the excess absorbed light energy was converted into heat, thereby protecting PSII. These

findings are corroborated by an increased abundance of PSBS (stress-related protein) protein under progressive drought stress in pea (Figure 3.14). PSBS is a small subunit of PSII and plays a crucial role in converting excess light energy into thermal dissipation (Johnson and Ruban, 2010).

The PSI acceptor side limitation Y(NA) was lowered in pea under progressive drought stress. This was combined with the decline of Y(I) and the increase of the donor side limitations of PSI (as reflected by Y(ND)), as in tomato leaves under high light (Lu et al., 2017). These authors suggested the reduced proportion of electron carriers on the acceptor side of PSI and the excessive amount of light energy to PSI on the donor side as indicators of PSI photoinhibition. The PSI core is a major pigment-protein complex that comprises 11–13 protein subunits, in which the main core proteins PsaA and PsaB have a molecular mass of 83.2 and 83.4 kDa (Fromme et al., 2003). The reduction in two core proteins, PsaA/B content in severe drought conditions, could lead to PSI oxidation changes. Recently we reported that under iron deficiency, the decrease of PSI core proteins could induce changes in the activity of PSI (Devadasu et al., 2021). We, therefore, believe that the degradation of PsaA/B proteins led to the alteration of the photochemical activity of PSI.

The increased Y(ND) and PSI/PSII ratios might favour the cyclic electron flow (CEF)/alternative electron sink to dissipate excess light energy at PSI (Zivcak et al., 2013). The increased levels of PsaC, PsaD, and PsaE in our observations (Figure 3.15) suggested the functional intactness to sustain electron transfer to Ferredoxin (Fd) suggested earlier (Klukas et al., 1999). Further, the lower values of Y(I) and ETR(I) also point out that photosynthetic acclimation (Figure 3.11) could mitigate photo-induced damage. Earlier studies show that tomato leaves photosynthetic drought response

mechanism could enhance NPQ, CEF, and pmf, which is the signature between photoprotection and photochemistry reactions (Yang et al., 2020).

3.3.3 Reversible changes in pigment-protein interactions, supercomplexes ultrastructure

The CD spectral analysis revealed changes mainly in the macro-domain organization of the pigment-protein complexes, as reflected by the decreased amplitude of the main, psi-type bands (Figure 3.17), which originate from chirally ordered macro-assemblies of PSII- and LHCII-containing complexes (Gregory et al., 1982, Toth et al., 2016, Devadasu et al., 2021). Some drought-stress-induced losses were also observed in excitonic bands, indicating deterioration in some of the antenna protein complexes which dominate these spectra (Garab and van Amerongen, 2008; Akhtar et al., 2015).

Results obtained from CD spectroscopy might be explained by alterations in the supercomplexes of PSII-LHCII, as revealed by Blue Native gel data (Figure 3.13). It is important to point out that the pattern of supercomplexes was restored to a normal state after rewatering plants for 7 days. Such restoration of the supercomplex organization in thylakoids could also occur via *de novo* synthesis. The loss of structural integrity in thylakoids could also be seen in TEM images with pronounced looseness under severe drought stress (Figure 3.18 and Figure 3.19). However, the grana stacks were almost similar to those in control, particularly after rewatering, indicating that pea plants could restore the photosynthetic membrane structures. The disturbed thylakoid ultrastructure could be due to a reduction in the content of the major and minor antenna of PSII core proteins, including CP43, CP47, and Lhcb1-6 (Figure 3.17 and Figure 3.18). The lower abundance of these proteins indicates the disassembly of Lhcb proteins from the PSII core preventing the transfer of excess excited light energy to the PSII core complex and damaging PSII from excess light (Chen et al., 2016). This result coincides with the

change in supercomplexes of thylakoids, especially the PSII-LHCII (Figure 3.17). The reduced abundance of PSII-OEC subunits such as PsbO and PsbP might change in thylakoid membrane architecture, as seen in TEM data.

Further, the accumulation of D1 protein might be due to an imbalance between the spatial extent of newly synthesized D1 protein to replace the damaged D1 protein from the functional PSII core complex, similar to an earlier report (Zhang and Aro, 2002). The observed increase in monomeric and dimeric forms of LHCII indicated that drought-stress-induced disassembly of the LHCII trimeric state partly forms LHCII monomer via the LHCII dimer transition state. These changes in the oligomerization state of LHCII might favor the conversion of excess absorbed light into heat to protect the photosynthetic apparatus (Janik et al., 2017).

3.3.4 Drought-induced change in LHCII and PSI, possibly related to ROS levels in leaf

Electron transport in PSII and PSI is often associated with the formation of ROS (Figure 3.5 and Figure 3.6), and these radicals are responsible for oxidative modifications of thylakoid proteins of both photosystems (Kumar et al., 2021). The decreased abundance of Chl *a* binding light-harvesting complex of PSI, i.e., LHCa1, LHCa2, LHCa3, and LHCa4, indicates severe drought stress might cause disconnection or dissociation of LHC from PSI core due to ROS. Possibly, the Chl molecules with an absorption maximum in the red located at a relatively long wavelength in Lhca3 and Lhca4 could be degraded first. Further, other bulk Chl-containing protein complexes of Lhca1 and Lhca2 got affected by severe drought stress (Figure 3.15). The damage to both PSI and PSII proteins under drought stress suggests they keep a balance.

Elevated levels of dehydrins and aquaporins complemented the adaptive adjustability of thylakoids. Dehydrins belong to the late embryogenesis protein family and are enhanced in response to several biotic and abiotic responses (Mota et al., 2019) to protect plants against dehydration. The increased levels of dehydrins provide a protective microenvironment under drought stress. Similarly, the aquaporins offer another protective mechanism to maintain cellular water homeostasis under varying situations (Hachez et al., 2006). The high abundance of PIP2-1 (Figure 3.14) level might help resilience to drought stress by increasing the water channel activity (Pawłowicz et al., 2017). However, the direct or indirect role of aquaporins, dehydrin, and PIP-2-1 in LHCII's accumulation and reversal needs further studies.

When the thylakoids were solubilized with β-DM, the loosely bound LHCII or other proteins could be separated from the original proteins. Therefore, the degraded proteins of LHCs abundance increased in the pellet. The LHCII, PSI, and PSII core protein content increased in the pellet in drought conditions, indicating that all these proteins could have been disassembled due to drought stress and possibly could have aggregated (Figure 3.16). However, further studies are required to understand the nature of photosystem protein aggregation under drought stress.

The earlier studies showed that the aggregation of LHCII induced the NPQ (Shukla et al., 2020). In this study, the results suggested that the disassembly of components along with ROS induction due to drought stress resulted in a significant increase in non-photochemical dissipation of excitation energy. Isolated LHCII and thylakoid organization was initiated by low intra-thylakoid pH and zeaxanthin, increasing NPQ (Horton et al., 1996). Similarly, the PSI core proteins in *C.reinhardtii* could have aggregated due to denatured proteins in the Fe deficiency condition and associated ROS formation (Devadasu et al., 2021). Thus, oxidative stress appears to be

one of the reasons that induce protein disassembly in photosystems. Therefore, our results emphasize that the increase of ROS in drought stress could lead to protein disassembly.

The reversible disassembly of LHCII proteins is normal under natural conditions. We feel that elevated ROS levels could have disturbed the organization and components of PSI (PsaA, PsaB), PSII (D1, D2, CP43, CP47), and LHCII (Lhcb2, Lhcb5, Lhcb6). Ultimately, oxidative stress appeared to be a significant cause of alteration in several proteins and photosynthetic activity during drought stress. Also, ROS could have induced sizeable aggregation of the photosynthetic proteins in drought stress. However, further studies are required to address this in the future. Once wilted, the leaves may have only a limited capacity to recover on rewatering. However, the marked recovery of photochemical activity, protein complex organization, and ultrastructure that could be predominant in new leaves could be due to *de novo* synthesis of photosynthetic complexes (Figures 3.5, 3.12, 3.17 and 3.18). Such recovery was earlier noticed in the fatty acid content of thylakoids during low temperatures (Takami et al., 2010). Under the recovery process, the initiation of the Chl and protein synthesis ensured the restoration of the normal photosynthetic process. Interestingly, the drought-induced plants flowered faster than the control, obviously to complete their life cycle. It is possible that plants kept a memory of abiotic stress.

3.4 Conclusion

This work represents a comparative picture of the physiological, biochemical, biophysical, and molecular level changes caused by drought in 14-day-old *Pisum sativum* seedlings. My data emphasize the marked differences in the organization and components of LHCII-PSI-LHCI complexes on exposure to drought. The levels of NPQ increased and appeared to be correlated with PSBS protein induction. Most of the

structural alterations were restored when plants were rewatered. The structural changes appeared to be related to the rise in ROS levels. My detailed studies could help develop promising traits based on thylakoid components for breeding pea plants against drought stress.

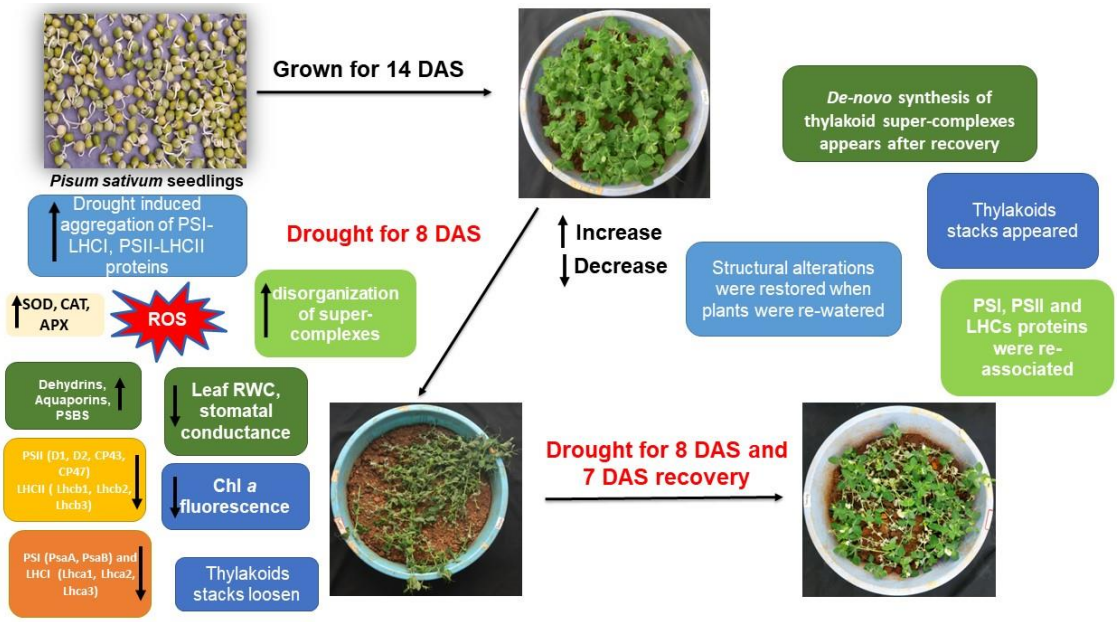

Schematic illustration representing effects of drought stress in P. sativum.

Chapter 4

Macromolecular structural changes of supercomplexes of thylakoids in drought stress

4.1 Introduction

To adapt to unfavourable climatic conditions, plants have evolved a wide range of physiological, biochemical, and molecular mechanisms (Rahman et al., 2019). Dehydration stressors cause plants to perceive and translate stress signals through signalling components, activating stress-related genes and antioxidants in response. In response to drought stress, plants have developed a photoprotective mechanism that involves the utilization of carotenoids. These carotenoids enable the plants to dissipate excess energy as heat, thereby mitigating the detrimental effects of drought stress (Bressan et al., 2001). This photoprotective system plays a crucial role in safeguarding the plants' photosynthetic machinery and overall resilience under challenging environmental conditions. Tightly bound carotenoids, like carotene or lutein, enable the deactivation of excited ^{3}Chl* and $^{1}O_2$ inside the PSI reaction centre (Dall'Osto et al., 2015). Acetyl CoA and geranylgeranyl diphosphate are converted to phytoene by the enzyme phytoene synthase (PSY), which is the first step, to initiate the production of carotenoids.

The reaction can be divided into two cycles: the synthesis of lutein from beta-carotene and the synthesis of violaxanthin from beta-carotene through the action of violaxanthin in the de-epoxidase cycle. These cycles represent the enzymatic processes involved in the conversion of beta-carotene into lutein and violaxanthin, respectively. These transformations are essential steps in the biosynthesis of carotenoids, which play a crucial role in the photoprotective mechanism against drought stress. Phytoene is subsequently transformed into lycopene by phytoene desaturase (Davison et al., 2002). Under drought stress, violaxanthin is converted into zeaxanthin by violaxanthin de-epoxidase (VDE) to dissipate the excess energy from excited chlorophylls (Havaux

and Niyogi, 1999). Carotenoids perform different photoprotection mechanisms, such as reducing ^{3}Chl* yield, scavenging ROS, and dissipating energy from light absorbed more than NPQ (Dall'Osto et al., 2012; Baroli et al., 2004). Xanthophyll protects the chloroplast from photooxidative damage and participates in light harvesting (Jahns et al., 2012). To release the surplus energy from excited chlorophylls during drought stress, violaxanthin is transformed into zeaxanthin by violaxanthin de-epoxidase (VDE) (Havaux and Niyogi, 1999). Xanthophyll participates in light harvesting and is crucial for shielding the chloroplast from photooxidative damage (Jahns et al., 2012). According to various studies (Baroli et al., 2004; Dall'Osto et al., 2012; Kaushik et al., 2014; Ruban et al., 2016), carotenoids perform a variety of photoprotection mechanisms, including reducing ^{3}Chl* yield, scavenging ROS, and dissipating energy from light absorbed more than NPQ.

In higher plants, the photoprotective mechanism known as "non-photochemical quenching" (NPQ) is mediated by PSBS protein (a 22 kDa protein associated with PSII). NPQ is a procedure that aids in releasing extra energy produced by the photosynthetic apparatus, which could otherwise result in photodamage. By attaching to the (LHCs) connected to (PSII), PSBS promotes NPQ by causing conformational changes that cause the release of extra energy as heat (Li et al., 2000; Demmig-Adams, 2006). The protonation state of the thylakoid lumen, which is governed by the pH gradient across the thylakoid membrane, controls the binding of PSBS to LHCs. With the help of this mechanism, plants can modify their NPQ response in accordance with the environmental conditions (Niyogi, 1999; Li et al., 2000). By aiding the disposal of extra energy produced by the photosynthetic system, PSBS plays a critical role in defending plants against oxidative stress and other types of photodamage. Low luminal pH triggers chlorophyll-binding protein, which in turn causes quenching events. As

they attach to pigment-protein complexes like photosynthetic reaction centres, light-harvesting complexes, and Cyt b6/f complexes, carotenoids are crucial for plant photoprotection. Through primary carotenoids, they transmit absorbed energy to chlorophylls, and their positioning in the light-harvesting complex enables singlet and triplet energy transfer amongst these pigments (Takaichi et al., 2011). In order to control their light-harvesting and photoprotective activities and assure their survival and fitness under various lighting and environmental circumstances, plants have evolved sophisticated mechanisms.

A crucial mechanism for photoprotection in plants is the cyclic electron transport pathway, which aids in preventing photo-inhibition of PSI (Munekage et al., 2002). The PSI and PSII complexes contain carotenoids, notably lutein and violaxanthin, which combine to form supercomplexes that make up the core and outer antenna (Takaichi et al., 2011). Other carotenoids including Chl *a* and Chl *b* are also present in these complexes. These pigments in the light LHC enable effective energy transfer between (Müller et al., 2001; Foyer et al., 2018) them and guard against oxidative stress and other types of photodamage. Drought-stressed plants might encounter limitations on the acceptor side of PSI, potentially resulting in the generation of stromal redox poise and ROS (Chouhan et al., 2022). Carotenoids have an important part in the macromolecular structuring of supercomplexes in *P.sativum* during drought circumstances, but their exact function is still not understood. To understand this, I isolated supercomplexes from control, drought-stressed, and recovery-grown *P.sativum* leaves and used sucrose density gradient to separate the supercomplexes. Along with the examination of carotenoid profile from the fractions of sucrose density, I also looked at the expression of particular genes involved in the production of carotenoids. My research attempts to clarify the function of carotenoids-induced

organization of the photosynthetic complexes in drought.

4.2 Results

4.2.1 Characterization of the supercomplexes obtained from sucrose density gradient

Sucrose density gradient centrifugation was used to separate the major pigment-protein complexes from the *P. sativum* thylakoid membranes. The solubilized thylakoid membranes were loaded onto the sucrose density gradient and centrifuged. After centrifugation, four bands (F1, F2, F3, and F4 were designated as LHCII, PSII-LHCII, PSI-PSII-LHCII and PSI-LHC, respectively based on the literature (Yadavalli et al., 2012) from control, drought and recovery conditions were discernible in each tube (Figure 4.1). SDS-PAGE was used to analyse the protein content of all the samples of the F1, F2, F3, and F4 (Figure 4.1c). Three bands of LHCII trimers were present in the F1. In F3, high molecular weight bands about 60–70 kDa were observed to be PsaA and PsaB, and below 30 kDa was observed to be LHCs and other PSI core subunits. The PSII core proteins CP43, CP46, D1, and D2 were present in F2 fractions. As shown by the decrease in the strength of bands corresponding to the drought stress condition in the F2, F3, and F4, it was discovered that the PSI-LHCI supercomplexes were more damaged under drought stress conditions. In comparison to the control, the F3 of the drought stress was substantially impacted. Similar outcomes were found for the stress conditions of salt and Fe deprivation, which resulted in the total loss of PSI-LHCI supercomplexes. These results show that PSI-LHCI supercomplexes are sensitive to the majority of stress situations (Ozawa et al., 2010; Yadavalli et al., 2012).

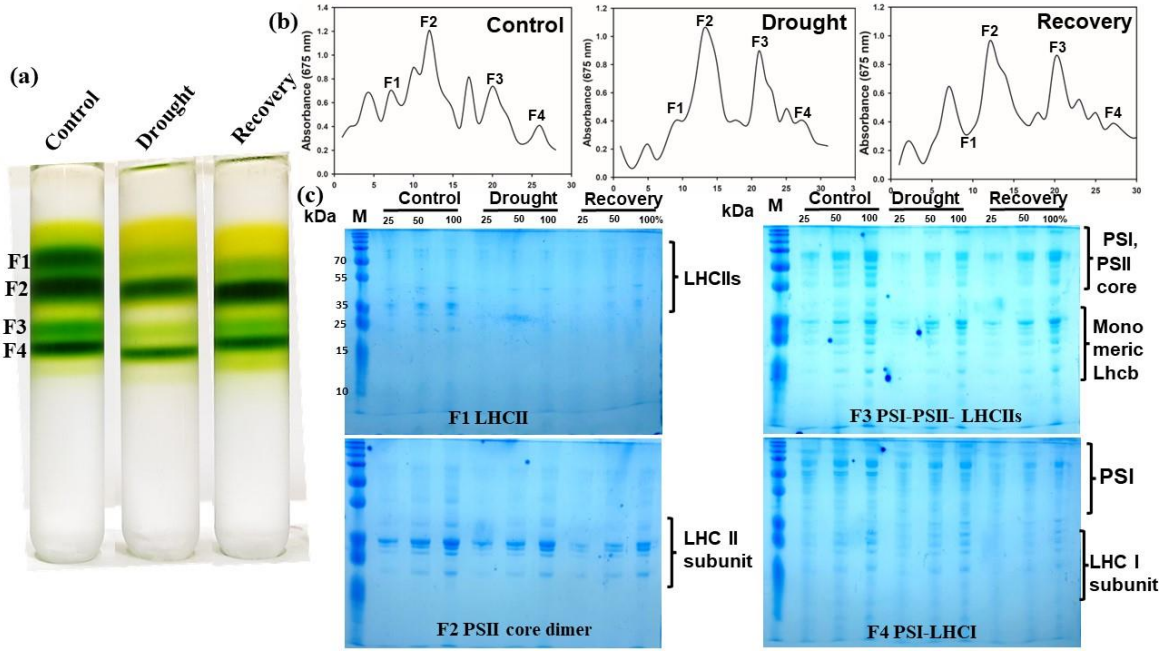

Figure 4.1 *Fractionation of major thylakoid membrane complexes of control, drought, and recovery of P. sativum (a) Isolated thylakoid membranes (0.8 mg/mL of chlorophyll) were* solubilized with 0.8 % (w/v) β-DM, and equal chlorophyll was loaded on sucrose density *gradient (1.3–0.1 M) of control, drought and recovery from P. sativum. (b) Absorbance of fractionated complexes following sucrose density centrifugation at 675 nm recorded from plate reader. (c) Gel electrophoresis of sucrose gradient fractions.*

4.2.2 Analysis of the absorption spectra for sucrose density fractions

To investigate the impact of drought conditions on the absorption cross-section of various complexes, the absorption spectra of four distinct bands were analyzed. These bands corresponded to LHCII, PSII, PSI-PSII-LHCIIs, and PSI-LHCI supercomplexes. When examining the absorption spectra of the F1 fraction, it was observed that the LHCII peaks appeared at 439 nm and 472 nm in the blue region, and at 675 nm and 652 nm in the red region. Under drought conditions, these peaks, which are attributed to Chl *a* and Chl *b*, were only slightly diminished (Figure 4.2). The F2 showed PSII-LHCII by having strong peaks at 675 nm and 439 nm and a small peak at 472 nm. The F2 nearly total lack of the 652 nm signal indicated the presence of the PSII core (Sugimoto et al., 2003). When compared to the Chl *b* derived F1, the absorbance at 470 nm was lower. The Qy region at 677 nm and 439 nm had the highest

absorbance in the F3, which revealed mostly Chl *a*. However, Chl *b* contributions at 470 nm were still present, albeit in a lesser degree. It is most likely that the PSI-PSII-LHCII supercomplex made up the F3 portion (Subramanyam et al., 2006). Variations in the spectra revealed modifications in the pigment concentration and interactions between the pigments. Under drought conditions, the F2, F3 and F4 fractions were more impacted than the F1 fraction. According to my findings, the PSI-LHCI supercomplex is more susceptible to drought stress.

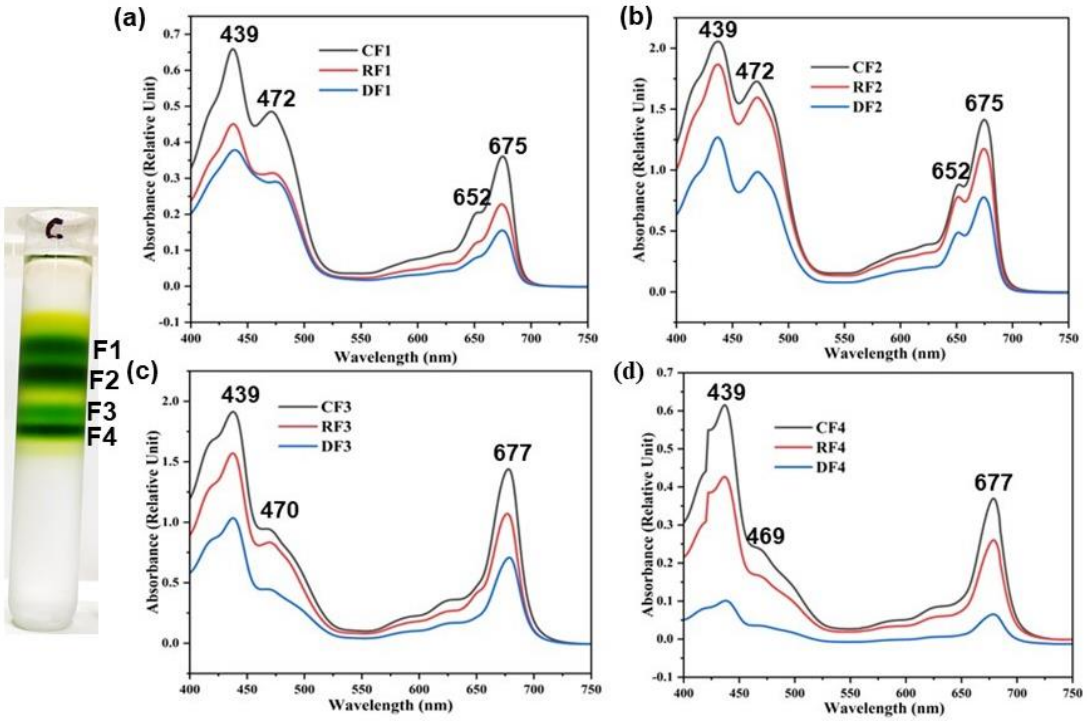

Figure 4.2 *Absorbance spectra of pigment binding complexes isolated from thylakoids of P. sativum. Absorption spectra of F1(a) LHCII F2(b) PSII-LHCII, F3(c) PSI-PSII-LHCII and F4(d) PSI-LHCIfractions of control, drought and recovery of P. sativum. Each data point represents the mean of the three individual preparations (n = 3).*

4.2.3 Analysis of circular dichroism spectra to study the interaction between pigments and proteins

The investigation of pigment-pigment and pigment-protein coupling uses the sensitive visible CD spectrum, which sheds light on the macromolecular structure of the

complexes. In this study, the sucrose density gradient derived F1 green band correlates to LHCII complexes. The red regions spectra of F1 display peaks at (-) 655, (+) 673, and (-) 688 nm linked to the Qy exciton states of Chl *b* and *a* (Akhtar et al., 2015). The PSII-LHCII band (F1) peaks in the Soret region are (+) 446, (-) 474, (+) 480and (-) 493. In contrast, the blue region's structure is more complex due to the abundance of Chl and carotenoid transitions (Figure 4.3). When compared to the control, the LHCII trimer's spectra under drought stress exhibit a drop in peak intensity. The F2 fraction originates from PSII-LHCII, the blue region has prominent peaks at (-) 474 and (+) 446 and the CD bands at Qy exciton states of Chl *a* and *b* (-) 688, (+) 673, and (-) 655. (Figure 4.3). Soret peak intensity of F2 originates from PSII-LHCII decreased in drought and recovery, however, this loss is much more pronounced than in control. The prominent peaks in the blue region of the F3, which is attributed to PSI-LHCI-LHCII supercomplexes, are (-) 460, (+) 480 (+) 446 which is attributely decreased in drought stress in all fractions and in the red region show the excitation states of Chl *a* and *b* (-) 688, (+) 673, and (-) 655, were peak abundancy is decreased. All peaks intensity has been reduced significantly expect 460 nm, however, in recovery they have almost reached to control level. In F4, the prominent peaks at (+) 673, (-) 688, (+) 446 nm were marginally reduced in drought. The negative peak at 655 nm under drought stress demonstrated a reduction in amplitude in drought and a modest reduction in recovery, showing major alterations in pigment interactions in PSI-LHCI complexes (Akhtar et al., 2015). In general, the variation in peak intensity denotes modifications to the excitonic pigment contents in all complexes, which are brought about by modifications to the interactions between pigment molecules.

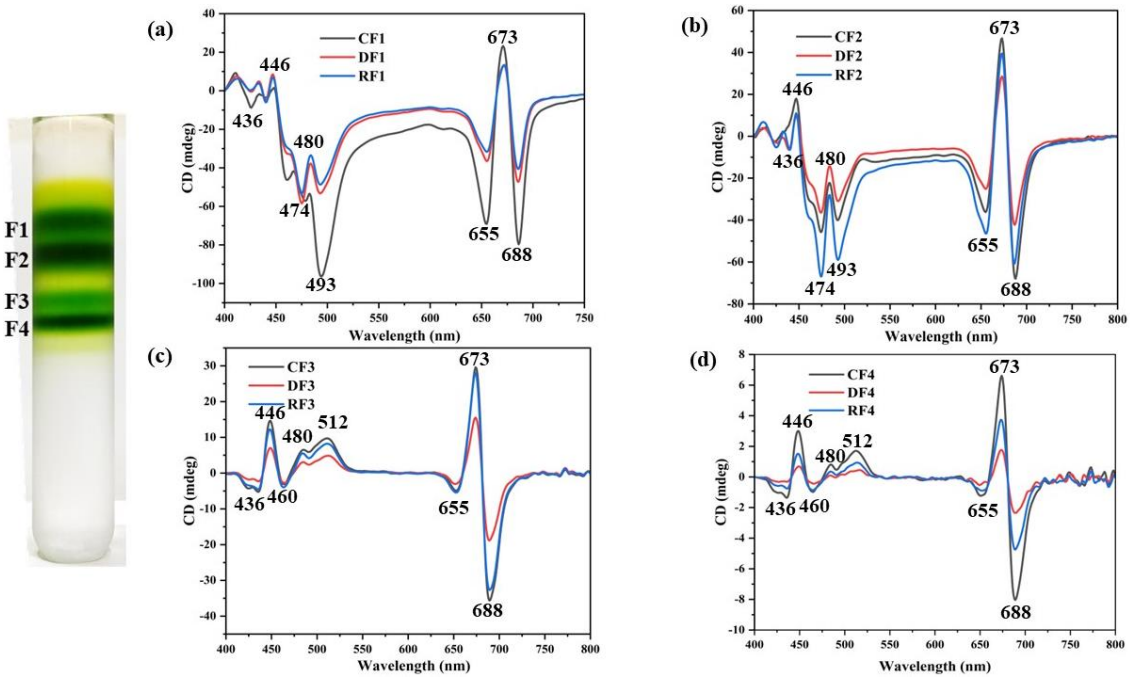

Figure 4.3 *Visible circular dichroism spectra of pigment binding complexes isolated from P. sativum. Visible CD of isolated F1(a) LHCII, F2(b) PSII-LHCII), F3(c) PSI-PSII-LHCII and F4(d) PSI-LHCI) fractions of control, drought, and recovery of P. sativum. CD was measured in absorbance units; each data point represents the mean of the three individual experiments.*

4.2.4 Thermal stability of the thylakoids with temperature

A progressive disintegration of these highly ordered structures may be seen in the thermogram derived from thylakoid membranes, which displays many endothermic transitions between 25 and 80 °C (Figure 4.4). CD spectroscopy was used to provide more light on the thermally induced transitions of the pigmented thylakoids (Figure 4.4). Strong psi-type bands have been identified in the CD spectra of intact granal thylakoids at (+) 690, (-) 676, and (+) 506 nm. These bands have been linked to chiral macrodomains of LHCII, macroarrays of PSII, and LHCII (Cseh et al., 2005). The bands significantly decreased in size in response to the drought stress, and even though they recovered more quickly, they were still below the levels of the control. The psi-type CD bands and some excitonic bands in the Soret region, between 484 and 462 nm, changed in response to severe drought stress, indicating changes in the molecular

structure or makeup of some pigment-protein complexes (Figure 4.4). Interestingly, the drought-stressed thylakoids are more thermally unstable than control and recovery. The 80 °C thermal transition is caused by non-pigmented proteins that are present during drought stress, which has already lost all of its excitonic characteristics and these results are in line with earlier work (Cseh et al., 2005).

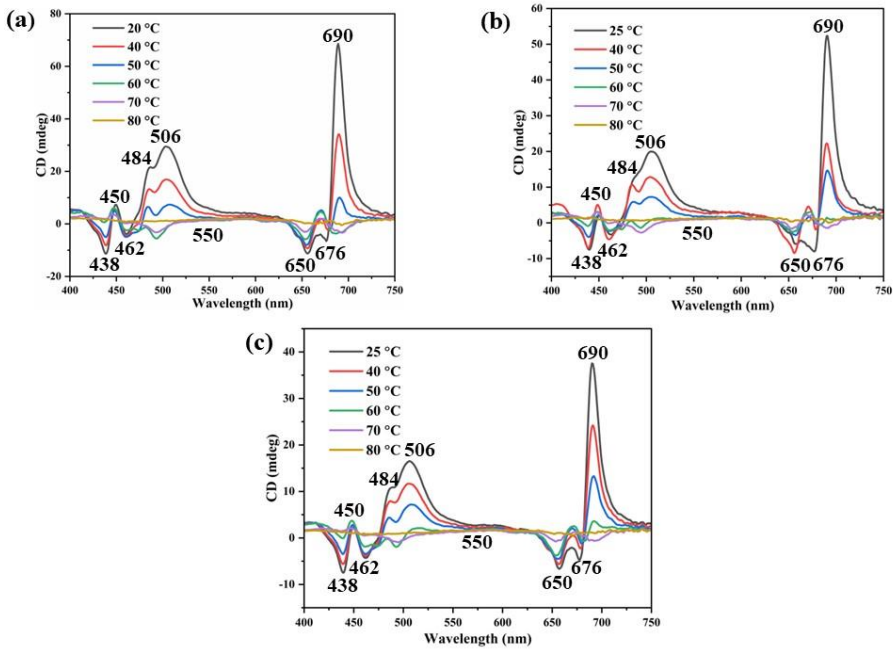

Figure 4.4 *Thermal destabilization of the pigment–protein complexes in shortly heated stroma thylakoid membrane vesicles with CD spectra after 2 min incubation at the indicated temperatures from (25 °C - 80 °C) from (a) control (b) drought and (c) recovery samples. The Chl content of the samples was 20 µg/mL in the CD measurements.*

4.2.5 77 K fluorescence emission spectra

Fluorescence emission spectra of the thylakoid membrane were measured for both control and drought conditions. A standard 77 K fluorescence emission spectrum was obtained, revealing distinct peaks at 685 nm (F680) and 730 nm (F730), attributed to LHCII-PSII and PSI, respectively (Koskela et al., 2018). Our findings indicate that under drought stress, the fluorescence of PSI and PSII was significantly impaired, as illustrated in Figure 4.5. This trend was further confirmed by the corresponding peaks

observed in the fractions, as depicted in Figure 4.6.

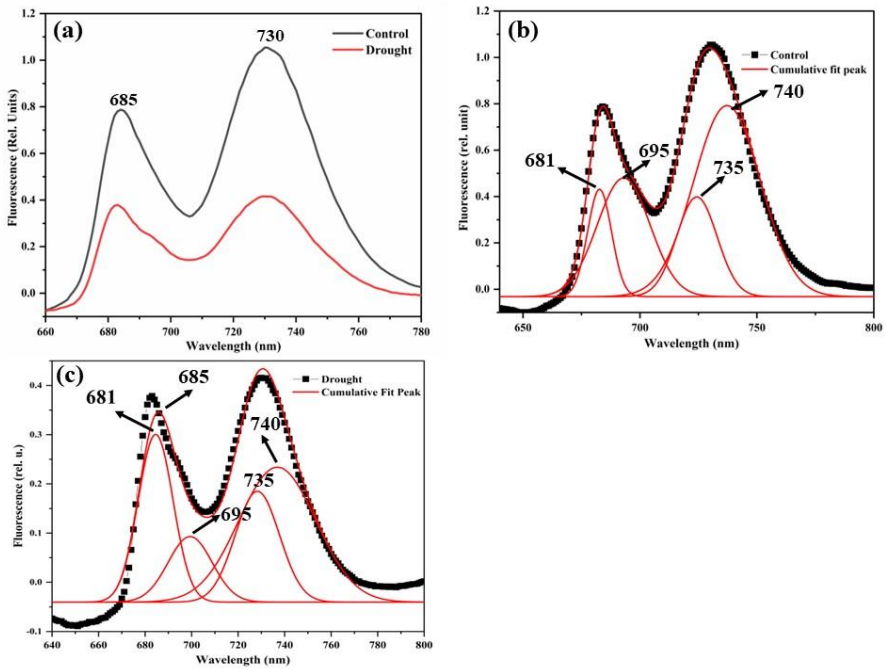

Figure 4.5 *77 K fluorescence emission spectra. 77 K fluorescence emission spectra of thylakoids (a-c) of control and drought conditions. Gaussian component decomposition of the 77 K. The values shown are the means of three independent experiments.*

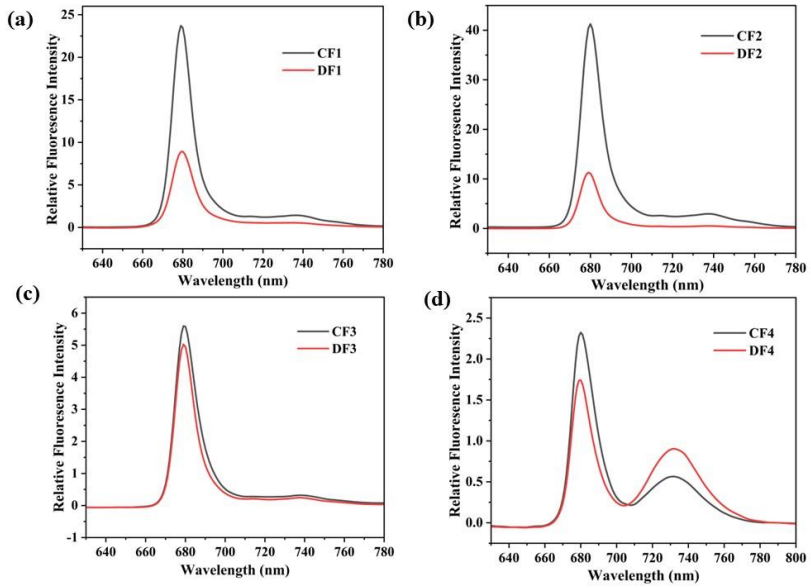

Figure 4.6 *77 K fluorescence emission spectra of the isolated fractions. 77 K fluorescence emission spectra of fractions F1(LHCII), F2(PSII), F3(PSI-PSII-LHCII) and F4(PSI-LHCI) (a-d) of control and drought conditions. The values shown are the means of three independent experiments.*

4.2.6 The impact of drought stress on carotenoid derivatives in *P. sativum*

According to earlier studies, the defensive response to photooxidative stress brought on by nutrient deficit, salt stress, and drought can lead to an increase in carotenoid levels (Birben et al., 2012). By acting as a photoprotectant through triplet Chl quenching and singlet oxygen scavenging processes, xanthophyll plays a significant part in the photosynthetic organism. The xanthophyll cycle is present in all plants and microalgae. During drought stress circumstances to expend extra energy and change violaxanthin to zeaxanthin was observed. Under drought stress, it has been noted that zeaxanthin and violaxanthin levels increased in drought stress from the leaves (Figure 4.7). Additionally, under both drought and recovery conditions, there was a slight shift in the concentration of Chl *a*, but there was a general increase in Chl *b*, whereas in control conditions, Chl *b* was decreased compared to Chl *a*. This indicate that LHCII complexes has been affected. In contrast to control and recovery circumstances, it was discovered that the Chl *a*/*b* ratio decreased during drought stress. Additionally, in both drought and recovery situations, lutein and carotene concentration rose, whereas in control, no discernible changes were seen. The lack of photoprotection and alterations in pigment-protein interactions could be explained by the fact that the levels of carotenoids were steady under control. The protection provided by supercomplexes during drought stress is indicated by a rise in carotene and lutein concentration, and a decrease in Chl a/b ratio indicated that PSII was more negatively impacted. A similar trend of pigment changes were observed from the thylakoids (Figure 4.7).

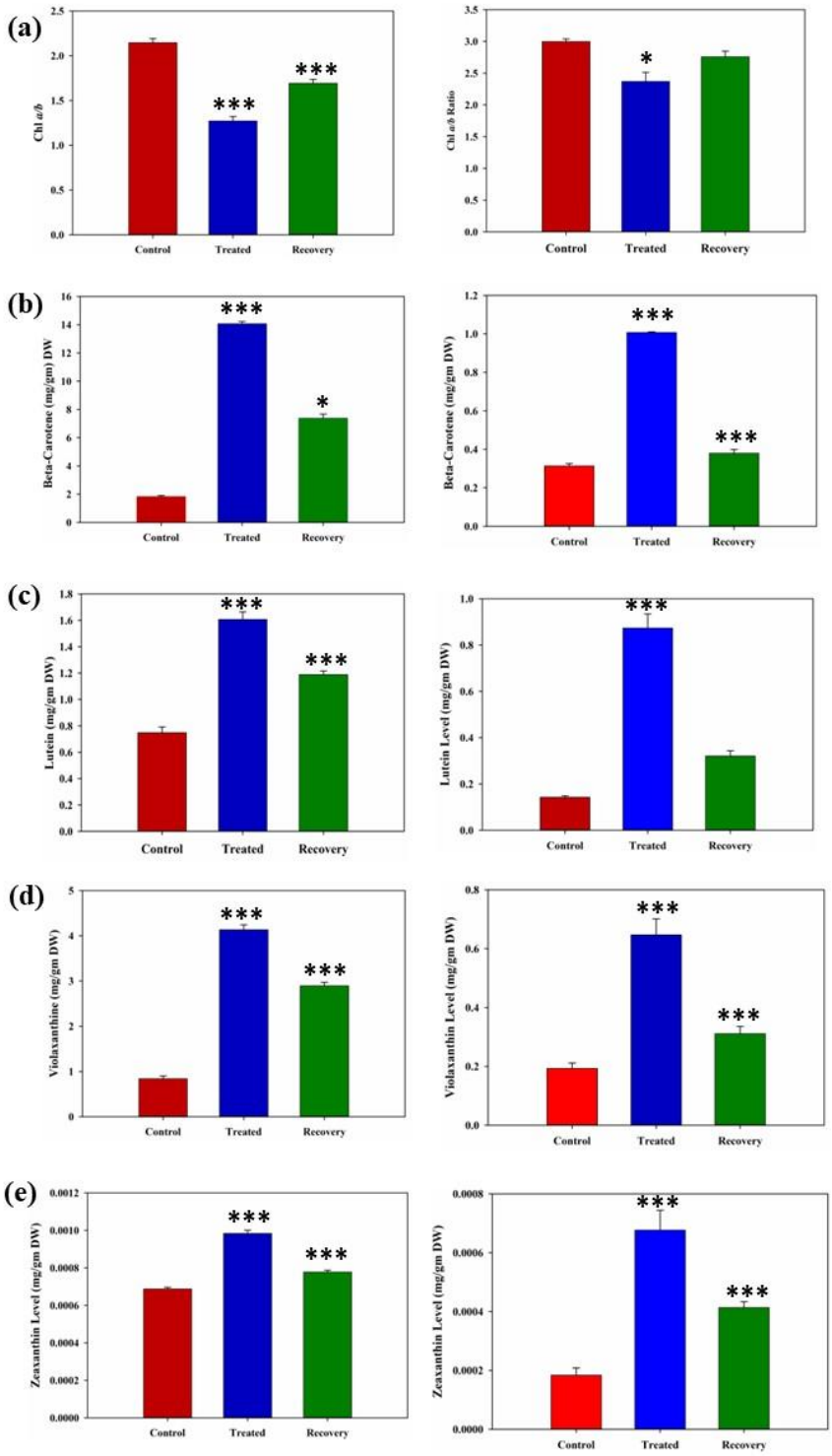

Figure 4.7 *Pigment composition of leaf and thylakoid from control, drought and recovery quantified with HPLC. Data are represented as mean ± standard deviation of triplicates. (a) panel reflects the Chl a/b ratio (b) Beta-carotene levels (c) Lutein content levels (d) Violaxanthin levels (e) Zeaxanthin levels from leaf and thylakoid.*

4.2.7 Carotenoids are pigment molecules that are associated with the F1 fractions (LHCII trimers)

The above data shows the composition of the protective pigments from the leaves and thylakoids under drought stress. To understand the role of photoprotective pigments in the supercomplexes, I have purified the supercomplexes from control, drought, and recovery. Further, using HPLC, the pigments were quantified into four fractions (F1-LHCII, F2-PSII-LHCII, F3-PSI-LHCI, and F4-PSI-LHCI) Figure 4.8. With the exception of F1 and F2, rest fractions had a drop in the Chl *a*/*b* ratio under drought and recovery stress. Under both control and drought circumstances, the carotenoids from F1 (LHCII) were significantly increased. Lutein content was also enhanced in all fractions under drought stress. The xanthophyll pigment binding required by the LHCII complex in the F1 fraction was enhanced and transformed into zeaxanthin during drought stress. This shows that under drought stress, the xanthophyll cycle is active, enabling zeaxanthin and violaxanthin to interconvert and reduce ROS while balancing photosynthesis. These results confirm earlier findings that carotenoids serve as quenchers to dissipate excess light energy (Niyogi et al., 1997).

4.2.8 Carotenoids are pigment molecules that are associated with the F2 fractions (PSII core dimer)

Fraction 2 comprises PSII and a tiny amount of LHCII, and the main carotenoid detected in this fraction is carotene, according to my analysis of the pigments collected from the SDG fractions. It is possible that carotene can operate as a defense mechanism against ROS formation in the PSII complex because its content dramatically increased under drought conditions (Figure 4.8). Additionally, in response to drought stress, the concentration of lutein and zeaxanthin were enhanced in the proportion containing

PSII core complexes. These results imply that lutein might be associated with the PSII core complex. These findings align with earlier research showing that lutein and violaxanthin can interact with PSII core complexes via the antenna or other pigmented subunits (Bassi et al., 1993).

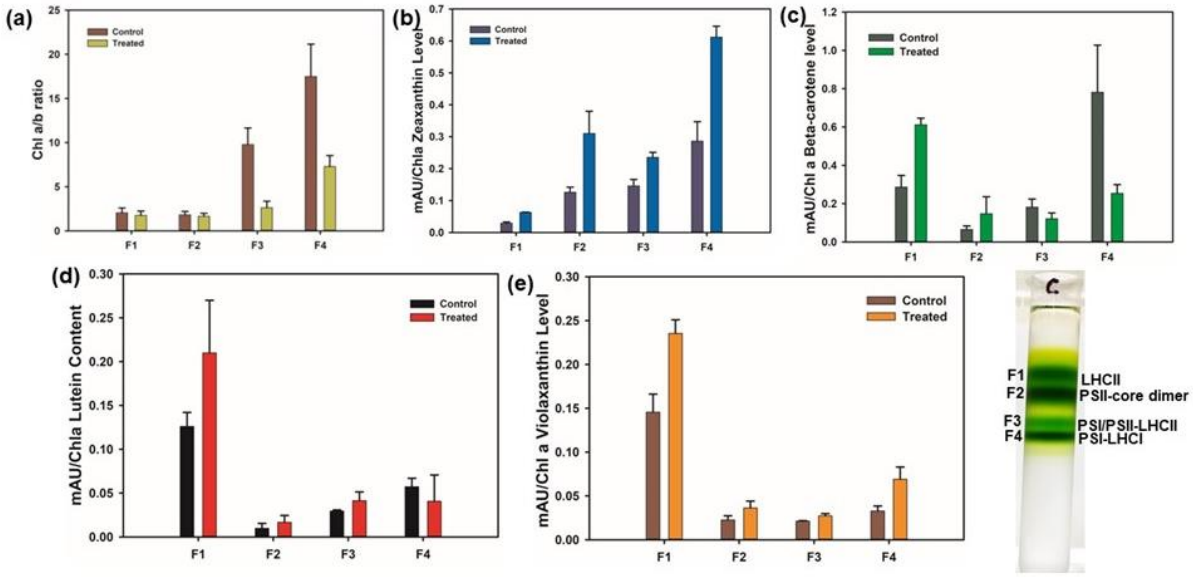

Figure 4.8 *Pigment composition of SDG fractions of control and drought (a) The relative content of Chl a/b ratio of isolated F1, F2, F3 and F4 fractions of control and drought of P. sativum. Xanthophyll content of the SDG fractions F1(b), F2 (c), F3 (d) and F4 (e) fractions of control and drought were analyzed by HPLC. Each data point represents the mean of the three individual experiments (n = 3). The error bars represent standard deviations.*

4.2.9 Carotenoids are pigment molecules that are associated with the F3 fractions (PSI-PSII-LHCII)

Lutein and violaxanthin are the main carotenoids bound to the PSI of *P. sativum* (Havaux et al., 1999). My results suggest that the violaxanthin and zeaxanthin content of the PSI-LHCII supercomplexes in the F3 fraction was lower than that of the F1 and F2 fractions (Figure 4.8). These results show that the F3 fractions carotenoid concentration falls considerably under drought stress than the control. This is in line with earlier studies that indicated that drought stress increased the amount of violaxanthin in PSI-LHCI complexes (Du et al., 2010). However, under drought stress

conditions, an increase in zeaxanthin levels has been linked to oxidative damage and photoinhibition (Du et al., 2010).

4.2.10 Carotenoids are pigment molecules that are associated with the F4 fractions (PSI-LHCI super-complex)

From the lowest layer of sucrose gradients of control, drought, and recovery samples, the PSI-LHCI and LHCII fractions were separated. Zeaxanthin and violaxanthin levels significantly increased under drought, demonstrating their function in releasing extra energy received by Chls through Chl-Car interactions (Figure 4.8). This shows that the non-photochemical quenching (NPQ) mechanism, which is triggered by low lumen pH and induces xanthophyll content, allows plants to adapt to drought stress (Li et al., 2000; Demmig-Adams and Adams, 2006). These results are in line with other studies that found NPQ to be a crucial regulatory mechanism for preventing oxidative damage to the photosynthetic machinery in stressful environments (Müller et al., 2001; Niyogi, 1999).

4.2.11 Drought stress influences the expression of important genes involved in the carotenoid biosynthesis

In order to investigate more about the effects of drought stress on carotenoid production, the key carotenoid pathway gene expression was analyzed by RT-PCR. Those genes are the earliest stages of PSY and PDS, lycopene cyclization LCYE and LCYB, xanthophyll synthesis CHYB, CHYBP, and CHYEP, and violaxanthin synthesis ZEP (Figure 4.9). Each gene's transcript level was standardised to the housekeeping gene CBLP and expressed in relation to the normalised level of the corresponding gene (Figure 4.9). The transcript levels of each gene were normalized using the housekeeping gene CBLP and expressed relative to the baseline level of the

corresponding gene at time zero (Figure 4.9). According to our findings, the expression levels of the genes PSY and PDS increased by 2 and 4-fold during drought. While LCYB was upregulated during a drought, LCYE was dramatically upregulated during the drought. The fact that ZEP was activated by drought stress is consistent with its direct participation in the xanthophyll cycle. Under drought stress, CHYB, which is in charge of converting carotene to zeaxanthin, was gradually stimulated. Also, the protein data show that the ZEP and VDE are significantly increased in drought stress (Figure 4.9c). In line with the transcript data, my HPLC study revealed a modest decline in the expression of these genes. Interestingly, most of the above-said genes were overexpressed during the drought, and the transcript data agrees with the pigment analyses (Figure 4.9).

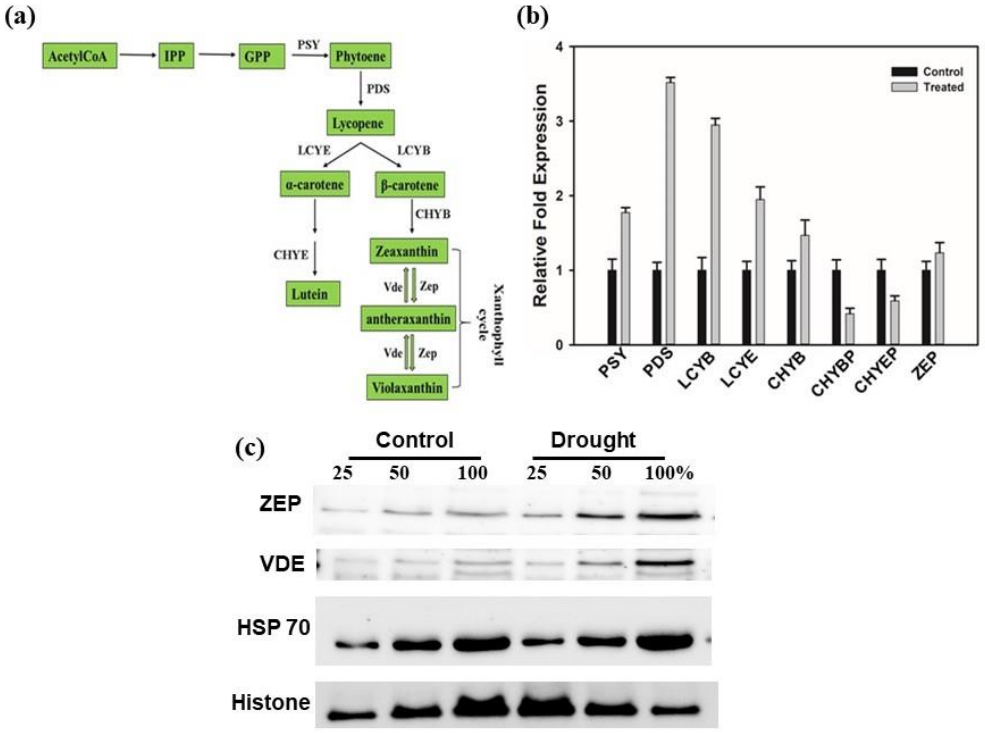

Figure 4.9 *Real-time PCR of control and drought of Pisum sativum (a) Xanthophyll biosynthetic pathways of P.sativum. Abbreviations of carotenoid-biosynthetic enzymes: PSY, phytoene synthase; PDS, phytoene desaturase; LCYE, lycopene epsilon-cyclase; LCYB, lycopene beta-cyclase, CHYB, carotenoid β-hydroxylase; CHYBP, beta-carotene 3-hydroxylase; CHYE, carotenoid ε-hydroxylase; ZEP, zeaxanthin epoxidase; VDE, violaxanthin de-epoxidase. (b) The relative content of xanthophyll cycle pigment of control and drought. The values shown are the means of three independent experiments. The error bars represent standard deviations. (c) Immunoblot analysis of total leaf proteins (ZEP, VDE, HSP70) were performed and Histone 3 as a loading control for control and drought.*

4.3 Discussion

In the first objective, I have discussed that drought affects the photosynthetic complexes by comprising the yield of photosynthesis. Significant ROS was observed in drought stress; however, it is reduced in recovery plants. Also, noticed that NPQ has been increased significantly in drought, however, the recovery reduced the NPQ along with regular photosynthesis. However, the role of protecting pigments in various supercomplexes under drought stress has not been well understood.

(Gonzalez et al., 2021) provided evidence for the activation of energy dissipation mechanisms such as non-photochemical quenching (NPQ) and the xanthophyll cycle by variations in lumen acidification. Low luminal pH triggers the activation of two carotenoid types, namely energy quenching (qE) and zeaxanthin quenching (qZ), which are part of the xanthophyll cycle. These carotenoids play a crucial role in photoprotection and are found in algae and plants. Additionally, carotenoids are antioxidants and reactive oxygen species scavengers (ROS). For effective energy transfer, these pigments are joined with complexes of proteins and pigments that capture light and are linked to the photosynthetic core. The xanthophyll cycle accumulates zeaxanthin in high light, frequently transforming it into violaxanthin, a stable form of carotenoid (Latowski et al., 2011). Additionally, NPQ induction is said to be higher, particularly during drought, and it is known that this factor is important for photoacclimation and photoprotection. For effective energy transfer and photoprotection in plants, the xanthophyll cycle and NPQ must be activated.

The primary LHCII (a trimer) molecule includes 42 chlorophylls (Chls), of which 24 are Chl a, 3 violaxanthin, and 6 lutein, according to earlier studies (Caffarri et al., 2011). These fundamental pigments are in charge of supplying PSII with excitation energy. According to studies conducted by (Caffarri et al., 2011; Morosinotto et al., 2011), the composition of photosystems PSI and PSII, as well as the associated LHCI (lhca1-4), can be characterized by their pigment content. PSI consists of 155 Chl *a*, 18 Chl *b*, and a total of 34 carotenoids, including 3 violaxanthin, 9 lutein, and 22 other carotenoids. In contrast, PSII contains 35 Chl *a* and 12 carotenoid molecules. The PSI-associated LHCI (lhca1-4) consists of 33 Chl *a*, 11 Chl *b*, and 10 carotenoids, including 5 violaxanthin, 7 lutein, and 1 other carotenoid. The

macromolecular alterations in the supercomplexes (LHCII, PSII, PSI-PSII-LHCII, and PSI-LHCI) and carotenoid concentration under drought stress conditions in *P. sativum*, however, have not been previously investigated. Additionally, little is known about how these macromolecular complexes function under drought stress and how many photoprotective pigments are present in them. The connection of photoprotective pigments (carotene and xanthophylls) in macromolecular complexes (LHCII, PSII, PSI-PSII-LHCII, and PSI-LHCI) isolated from thylakoids of *P. sativum* growing under drought stress was not examined, the study showed that during extreme drought stress, ROS is accumulated in *P.sativum* (Pandey et al., 2023). However, it's photoprotective, and acclimation is still not deciphered. It was shown that many photosynthetic species accumulate carotene, lutein, and zeaxanthin in drought and upregulate photoprotective mechanisms, such as NPQ. These pigments boosted resilience to drought stress conditions by assisting in removal of ROS and inducing changes in the structure of thylakoid membrane (Dall'Osto et al., 2012; Kaushik et al., 2014; Nama et al., 2019).

Most algae and higher plants have light-harvesting antenna complexes, and xanthophyll plays a significant role in photoprotection of these complexes (Jahns et al., 2012). Zeaxanthin replaces violaxanthin and binds to LHCII, causing NPQ to perform photoprotective functions under extremely dry conditions (Goss et al., 2015). The PSI-LHCI supercomplexes were less stable than other super complexes under drought (Figure 4.2 and 4.3). Since, PSI-LHCI does not have much vialoxanthin and zeathanthin, the excess energy could quench, therefore, PSI-LHCI is more sensitive than other complexs. As shown by 77 K, PSI-LHCI acclimation causes the interface between peripheral antenna complexes and the PSI core to become unstable under drought stress (Figure 4.6). Interesting evidence of supercomplex interaction and proper energy transfer between the core and LHCII was provided by the Qy peak of

Chls in fraction 2. Due to the unstable supercomplex, which caused the majority of the LHCII trimer and monomer to separate from the supercomplex, redshift was slightly seen under drought stress confirming that there is energy transfer between core and LHCII. In this study, I demonstrated that the instability of both PSI-LHCI and PSII-LHCII is caused by drought stress conditions, which may be caused by the loss of loosely bound LHCs and carotenoid molecules from the complexes (Figure 4.3). According to our group findings, the complexes may become unstable as a result of ROS generation. The whole leaf and thylakoids data (Figure 4.7) of Chl a/b ratio dropped throughout times of drought. According to earlier research, the amount of carotene, lutein, and zeaxanthin increased under drought stress, The NPQ has been increased significantly in drought stress due to acidification of luminal pH. This could be due to the elevated levels of carotene, lutein, and zeaxanthin in drought stress.

The carotenoids and xanthophyll pigment compositions expressed similarly in the *P. sativum* and thylakoids HPLC results (Figures 4.7). Carotenoids were abundant during drought stress, but only slight modifications were seen as levels returned to those of the control. Additionally, under drought stress, the genes CHYB and CHYE and CHYB, which convert carotene to lutein and carotene to zeaxanthin, respectively, were elevated. Zeaxanthin was increased in the transcript data and are also alignment to the western blot data (VDE and ZDE) and also which is consistent with the HPLC pigment results (Figure 4.9). Xanthophyll and lutein concentration in thylakoids increased. Although increasing the accumulation of one of the carotenoids offers some protection against drought stress, this may be one of the reasons drought plants are more vulnerable. As zeaxanthin was previously reported to be present in LHC proteins, the pigment binding characteristics of several isolated fractions (F1–F4) revealed that it was present in all of the fractions (Bassi et al., 1993). Zeaxanthin was noticeably

enriched in the F1 (LHCII) and PSII-LHCII fractions (Figures 4.8). Zeaxanthin enrichment levels are higher in F1 than in the other fractions because it is anticipated that LHCII complexes will include more pigments. Differential expression of the pigment composition under drought stress was seen in LHCII, PSII, PSI-PSII-LHCII, and PSI-LHCI (Figure 4.9). To provide photoprotection, the total pigments in the leaf and thylakoids were divided into four fractions (F1–F4): LHCII, PSII, PSI–PSI–LHCI, and PSI–LHCI.

Increased lutein content may be the reason that drought stress protects LHCII from photodamage. Carotenoids are essential for the deactivation of ^{3}Chl* and $^{1}O_2$ in PSII as well as the reduction of ROS production brought on by thermal dissipation in response to drought stress. Oxidative stress and the buildup of ROS (Figure 3.4 and 3.5) in the chloroplast, followed by export into the cytosol, drive the activation of carotene. This implies that PSII or PSI is more vulnerable to harm under drought like conditions, presumably as a result of an increase in reactive oxygen species during drought, as previously reported (first objective), which affects total photochemical yield. Because carotene is located close to the PSII core complex and is essential for quenching of ^{3}Chl* and $^{1}O_2$, a decline in carotene levels may result in photooxidation of PSII and PSI core complexes (Pineau et al., 2001).

Circular dichroism (CD) data under drought stress (Figure 4.3) showed a significant reduction in intensity in the 400–500 nm region, indicating a change in pigment-protein interaction. The emission spectra at 77 K gave further evidence of damage to PSI and PSII under drought stress conditions. Additionally, the (PSI-LHCI) level decreased significantly in the SDG fractions (Figure 4.6) under drought stress, indicating that this complex is particularly susceptible to drought. This result is in line with earlier studies showing that PSI-LHCI is more vulnerable to drought stress than

PSII (Jansson et al., 1999; Munekage et al., 2004). Decreased levels of carotenoid and proton motive force (pmf) during drought may be a factor in the ineffective quenching of chlorophyll triplet states, which could further harm the PSI-LHCI complex.

ROS have been found to be the cause of PS II photoinactivation, according to (Nishiyama et al., 2006). The first objective show that ROS accumulation was detected during drought stress, which may result in the aggregation of both PSII and PSI proteins. Higher plants PSII proteins have been reported to aggregate as a result of ROS, especially the PSII-LHCII complexes, which are more vulnerable to drought stress due to the buildup of ROS (Yamamoto et al., 2008). Because of this, the majority of the aggregated proteins were not connected to the supercomplexes, which may have contributed to the decreased accumulation of supercomplexes isolated SDG under drought. Protein aggregation is a crucial mechanism involved in photochemical reactions, as reported by our previous findings. Changes in energy pathways and reconfiguration of thylakoid macromolecules have been seen in response to drought stress. The supercomplex may become unstable under drought circumstances due to increased protein aggregation and decreased pigment concentration as a result of this. Therefore, under drought stress photosynthetic efficiency, and macromolecular structure of photosynthetic complexes has been affected.

4.4 Conclusion

This objective aims to examine the variations in carotenoid and xanthophyll composition within thylakoid supercomplexes of *P. sativum* under control and drought conditions. Carotenes, such as β-carotene, and xanthophylls, including violaxanthin and lutein, are essential components of the photosynthetic apparatus. They contribute to enhancing light absorption in both photosystems while providing protection to the

photosystems. β-Carotene is found in the core complexes (LHCII and LHCI), whereas xanthophylls, like lutein and violaxanthin, exclusively bind to the antenna complexes. Zeaxanthin, another xanthophyll, plays a vital role in protecting chloroplasts against photooxidative damage. My results demonstrate an increase in β-carotene, lutein, and zeaxanthin levels under drought stress. The elevated zeaxanthin content corresponds to the dissipation of excess energy absorbed by chlorophylls through Chl-Car interactions, which are responsible for high non-photochemical quenching. As expected, zeaxanthin was more abundant in LHCII complexes compared to the PSII-LHCII and PSI-LHCI supercomplexes under drought conditions. Additionally, β-carotene significantly increased in drought stress, predominantly observed in PSI-LHCI complexes. Conversely, a higher accumulation of lutein was observed in PSII-LHCII complexes. The differential expression of genes involved in carotenoid biosynthesis aligns with the observed pigment content. The changes in pigment composition within the supercomplexes resulted in alterations in pigment-pigment and pigment-protein interactions. The lack of zeaxanthin content and differential expressions of lutein and violaxanthin likely induced modifications in the macromolecular organization of thylakoid supercomplexes, particularly under drought stress.

Chapter 5

Decipher the role of lipids and osmo-protectants in organization of photosynthetic complexes

5.1 Introduction

Enzymatic complexes that are largely present in biological membranes are involved in cell bioenergetics. The plasma membrane of prokaryotic cells, the inner membrane of mitochondria, and the thylakoid membranes of plants, algae, and cyanobacteria are among the cellular structures that contain these membranes, also known as "energy-transducing membranes" (Mitchell, 1961). All energy-transducing membranes contain the ATP synthase complex, which produces ATP by using the proton-motive force produced by other membrane protein complexes (Junge et al., 2015). The protein complexes that produce the proton-motive force can differ depending on the main energy source. The respiratory chain for instance produces the proton-motive force in aerobic bacteria or mitochondria. Contrarily, in chloroplasts or cyanobacteria, a light-driven electron transport pathway that takes place in two photosystems coupled by Cyt b_6f produces the proton-motive force (Rutherford and Faller, 2003).

Energy-transducing membranes need a bilayer architecture in addition to protein complexes to carry out a variety of structural tasks, such as the impermeabilization of ions. The development of an electrochemical proton gradient, which is crucial for ATP synthesis, depends on this arrangement. Membrane lipids are extremely important for the function of photosynthetic complexes.

Acetyl-CoA is converted into malonyl-CoA during the first stage of fatty acid production by the enzyme acetyl-CoA carboxylase. The condensation of another molecule of acetyl-CoA is then catalyzed by the enzyme fatty acid synthase using malonyl-CoA, resulting in palmitic acid, the most basic saturated fatty acid. Through a series of enzymatic processes, palmitic acid can be transformed into various fatty acids with different chain lengths and saturation levels, such as stearic acid, oleic acid, and linoleic acid. DHAP and G3P, both of which can be obtained from the intermediate

product of glycolysis, G3P, formed during the Calvin cycle, are the sources of the glycerol component of triacylglycerols, essential energy storage molecules in plant cells. Triacylglycerols are created by combining glycerol with any three of the fatty acids made from palmitic acid. In addition to being essential for storing energy, these triacylglycerols can act as precursors in the manufacture of membrane lipids, which are essential for maintaining the structure and functionality of plant cells.

Membrane lipids play a critical part in controlling the movement of substances into and out of cells as they are essential parts of cell membranes. Membrane lipids, including phospholipids, galactolipids, sulfolipids, and phosphatidylglycerol, are present in plants. The most prevalent lipids in chloroplast thylakoid membranes and key players in photosynthesis are galactolipids, primarily MGDG and DGDG. It has been established that the SQDG, which is present in photosynthetic membranes, is crucial for photosynthetic activity and for controlling membrane shape and function. In addition, PG, particularly in thylakoid membranes, is an essential membrane lipid in plant cells. It is crucial for the control of protein function, membrane integrity, and photosynthesis. Additionally, PUFAs like omega-3 and omega-6, which are produced in plastids by fatty acid, are crucial for maintaining membrane fluidity and stability (Thibault et al., 2021). The current chapter describes about the roles of lipids and fatty acids, the components of cellular membranes, play in the process of photosynthesis. It focuses on how this will affect the photosynthetic apparatus to adjust to drought stress circumstances.

5.2 Results

5.2.1 Analysis of total biomass, leaf area, carbohydrate, starch, reducing sugar and proline

Plants respond to reactive oxygen species (ROS) by synthesizing osmoprotectants, which serve as protective mechanisms. These osmoprotectants include sugar alcohols, as well as specific amino acids such as proline and glycine betaine and secondary metabolites that cooperate to start crosstalk and keep ROS concentrations constant (Li et al., 2020). The creation of ROS as well as the necrosis, burning of the leaf edges, and chlorosis that are seen in severely drought-stressed plants could be the cause of the decrease in plant growth and leaf area during drought stress (Kosma et al., 2019). The glucose and starch content considerably increased during drought stress, as compared with control acting as an osmoprotectant (Figure 5.1). Additionally, osmotic adjustments brought on by desiccation in leaf tissues or accelerated starch degradation also contributed to an increase in reducing sugars (Gong et al., 2021). An essential amino acid called proline controls cellular redox state and functions as a ROS scavenger (Wahab et al., 2022). Proline, which facilitates storage protein production and functions as an osmoprotectant to prevent desiccation, was found in higher concentrations in the leaves (Figure 5.1e).

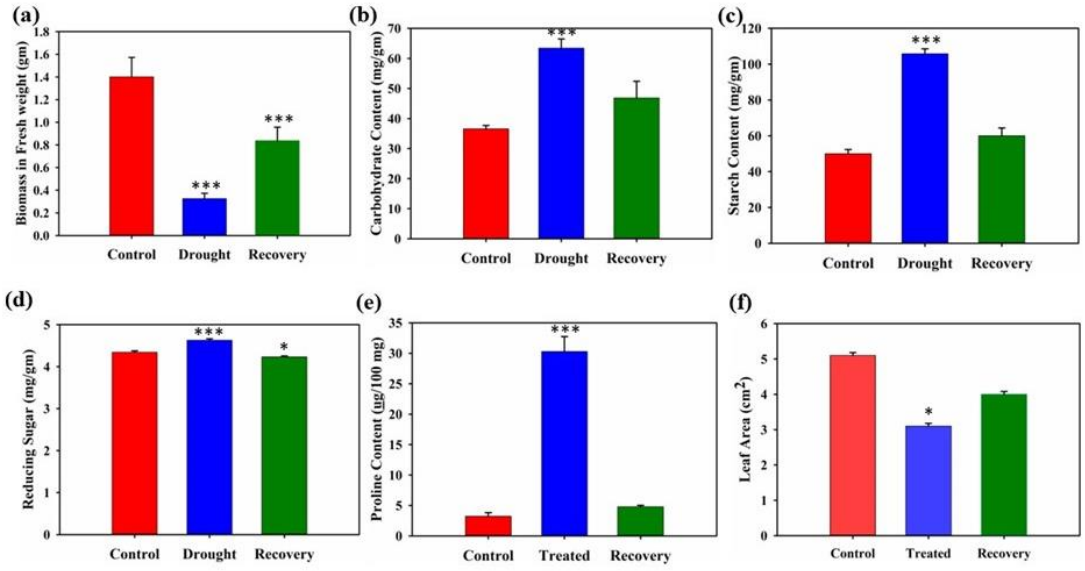

Figure 5.1 *Quantitative analysis of leaf tissues from the control, drought, and recovery from P.sativum (a) Total Biomass obtained from dry weight of lyophilized tissues from leaf (b) Total carbohydrate obtained from the fresh leaf tissues (c) Total starch content from the fresh leaf tissues (d) Total reducing sugar obtained from fresh leaf tissues (e) Total proline content obtained from the leaf tissues (f) Leaf area from the fresh weight of the leaf tissues. The data point I took is the average of three replicates, and the error bars represent the ±SE. One-way ANOVA (Bonferroni t test) was performed to measure the P-values.*

5.2.2 Separation of Neutral and membrane lipids by TLC

In the present study, the focus was on assessing the alterations in neutral lipid content, specifically triglycerides (TAG), as well as the composition and content of membrane lipids and to investigate the effects of drought stress on the synthesis of fatty acids. Neutral lipid extracts were made using equal dry weights of the control, drought, and recovery samples. These extracts were then separated on TLC plates and stained with iodine. The findings demonstrated that drought stress caused a considerable increase of TAG, suggesting that membrane lipids may be involved in TAG formation (Figure 5.2a). Additionally, TLC was performed to evaluate the content of all membrane lipids in *P. sativum*, and the results showed that under drought stress conditions, MGDG and DGDG levels were drastically decreased (Figure 5.2b). According to these results, which are in line with other investigations, the lower levels of MGDG and DGDG could

be translated to TAG synthesis under drought and other abiotic stress (Devadasu and Subramanyam, 2021; Chouhan et al., 2022). Furthermore, the TLC and TEM results to the idea that alterations in membrane lipid composition caused the disruption of the stacks of thylakoids. Based on the findings, it can be inferred that the synthesis of triglycerides (TAG) likely utilized fatty acids derived from both chloroplasts and other internal membrane systems within the plant.

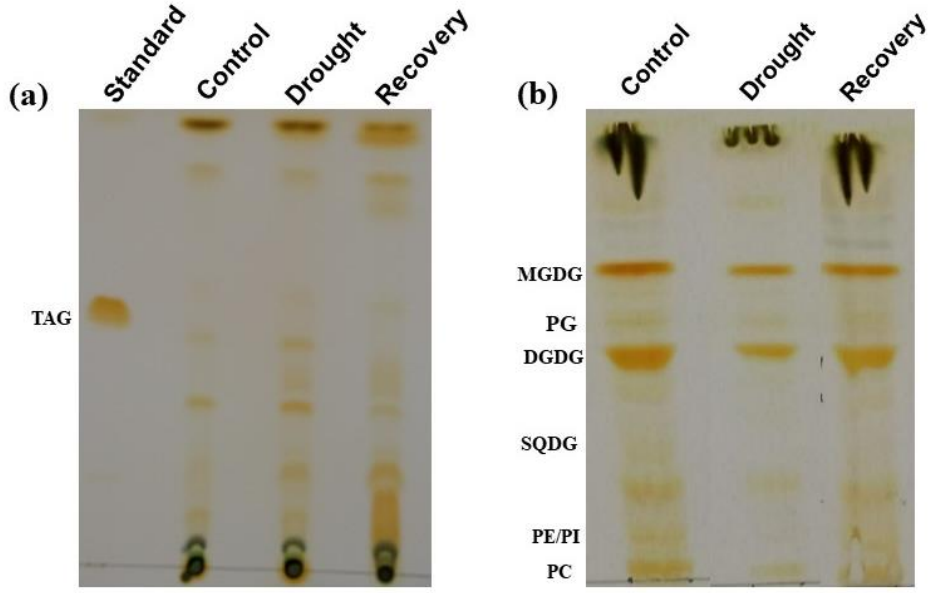

Figure 5.2 *Alteration of membrane lipid and TAG in P.sativum under control, drought and recovery. (a) TLC analysis showing TAG accumulation of P.sativum leaf tissues. Three independent experiments were conducted for all samples (n=3). (b) Separation of polar lipids by TLC from P.sativum. Polar lipids and TAG was visualized by iodine staining. Three independent experiments were conducted for all the samples (n=3) from the control, drought and recovery samples.*

5.2.3 Characterization of membrane lipids from *P.sativum*

The results of our drought investigation reveal that TAG accumulation in *P. sativum* is influenced by the recycling of the individual fatty acids that are formed upon dissociation of the glycolipids MGDG and DGDG, in comparison to the control. In other report, the nitrogen-starved *C. reinhardtii* has been seen to accumulate TAG from

chloroplast membrane lipids. It is conceivable that FAs that have been released from glycolipids enter the Kennedy pathway to create TAGs. Polar lipids, particularly MGDG and DGDG, break down more quickly under drought (Figure 5.3). In order to participate in the creation of TAGs, these two primary classes of lipids and FAs are likely redirected.

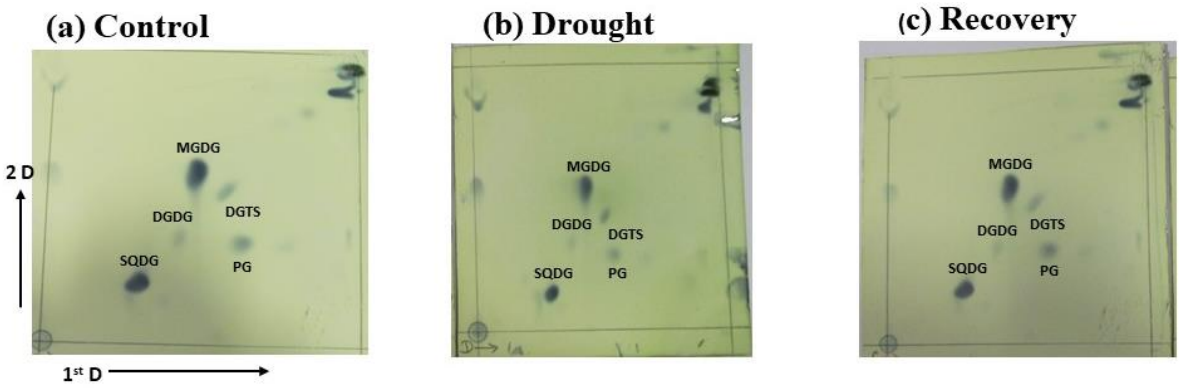

Figure 5.3 *2D TLC analysis of polar lipids extracted from leaf tissues grown under control, drought, and recovery conditions. Degraded lipids MGDG, DGDG, PG, SQDG, and PI were detected in leaf tissues subjected to severe drought. The chromatography run was repeated three times, and representative results were shown.*

5.2.4 Drought alters the fatty acid composition in *P.sativum*

LC/MS was used to assess the FAMEs produced by fatty acid transesterification in order to examine changes in fatty acid composition in response to drought stress in *P. sativum* (Figure 5.4). According to the findings, drought stress increased the content of several fatty acids, such as C12:0, C14:0, C16:O2OH, C17:0, C18:3, and C20:0, when compared to control and recovery samples. Other environmental stresses, such as temperature, and nitrogen deprivation in Chlamydomonas, have also been linked to similar changes in fatty acid composition (Poerschmann et al., 2004). It's interesting to note that under drought stress, total PUFAs increased significantly while they decreased under control and recovery conditions (Figure 5.4). Previous investigations have also

showed alterations in the total fatty acid content of *C. reinhardtii* under Fe deprivation (Devadasu and Subramanyam, 2021). These findings imply that changes in a fatty acid composition may be a typical response of photosynthetic organisms to environmental stresses. Additionally, the observed abundance of TAGs in extreme drought stress shows that this could be a successful tactic to boost biofuel generation from algae and plants.

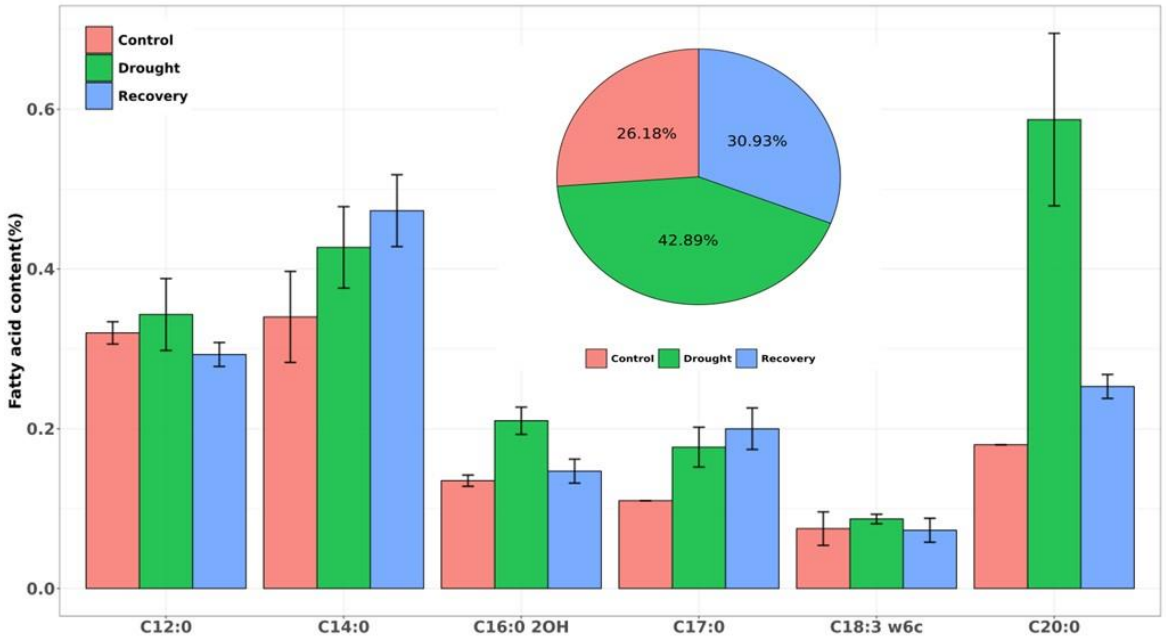

Figure 5.4 *Fatty acid content of leaf tissues from P.sativum under control, drought, and recovery conditions. Averages from three replicate experiments and their standard deviations are shown.*

5.2.5 Relative expression of genes and immunoblots analysis of lipid biosynthesis

In our work, I noticed a considerable accumulation of TAG under drought stress circumstances that were more prominent than under control (Figure 5.5). In line with observations in *C.reinhardtii* and *A. thaliana,* TAG production in my investigation might have been mediated by various acyltransferases. DGAT and PDAT, which are both involved in seed oil accumulation in plants, catalyze the final stage of TAG

production (Zhang et al., 2009). In my research, I looked at how PDAT and DGAT were regulated at both the protein and at mRNA levels, and then I deciphered that both genes accumulated in response to drought stress (Figure 5.5c). According to these results, the accumulation of TAG in my study may have taken place via either the DGAT or PDAT routes, which also corroborates these genes' participation in TAG synthesis under drought stress. Overall, my results show that, in response to drought stress, the PDAT and DGAT proteins/genes increased, which probably played a role in the observed accumulation of TAG.

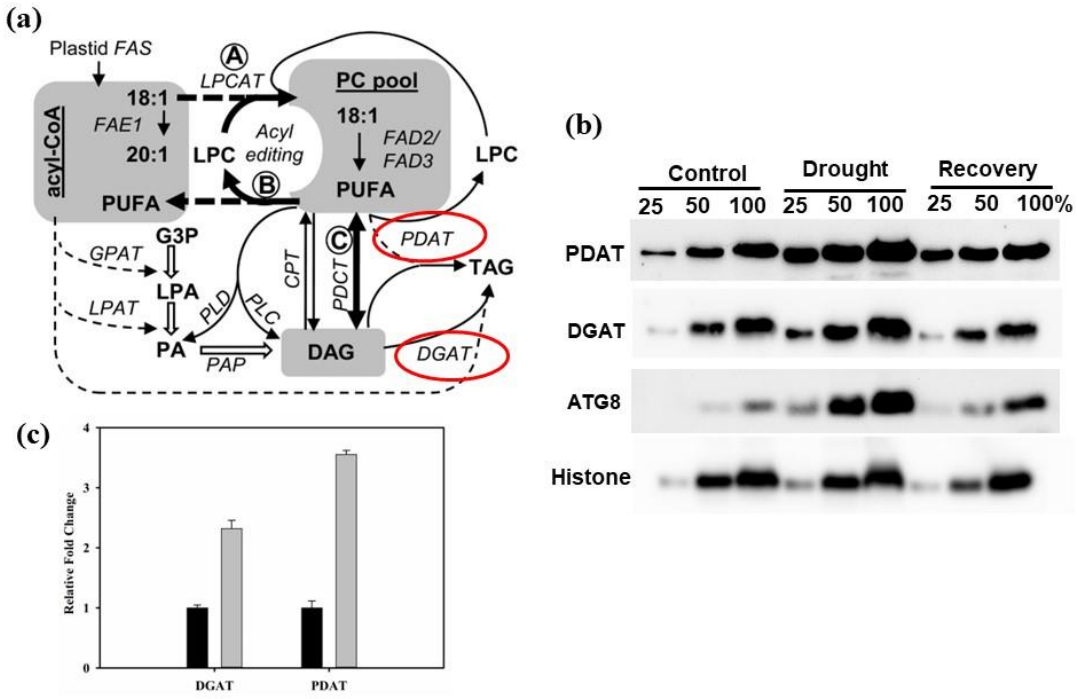

Figure 5.5 *(a) Flow chart to shows the synthesis of TAG from two main enzymes PDAT and DGAT. Protein identification from western blotting (b) The proteins were separated by denaturing gel electrophoresis, transferred to nitrocellulose membranes, and probed for the indicated proteins. Western blot analysis of Acyl-CoA: DGAT2A, PDAT1, and ATG8 evaluated from control, drought and recovery, and each lane (5 µg) protein was loaded onto 10% Bis-Tris gel in denaturing condition. (%) indicates the dilutions of the samples. Histone (H3) was used as a loading control. All the blots were in three independent times (n = 3) and obtained similar results. (c) RT-PCR analysis of the two important genes PDAT and DGAT. Data are expressed as mean ± SD of three replicates.*

5.3 Discussion

Plants that are under drought stress may have substantial damage to their PSII, which will cause the photosynthetic electron transport chain to produce ROS (Li et al., 2009). As noted by (Perez-Martin et al., 2014), plants typically store antioxidants like carotenoids in their leaves to repair the harm caused by ROS. The first objective shows that the total carotenoid content significantly increaseunder drought stress. It's interesting to note that under drought stress, the ROS generation was substantially higher. As reported by one would anticipate increased ROS formation at the PSI acceptor side as a result of this acceptor side limitation (Tiwari et al., 2016).

Carbohydrates and lipids are the main sources of energy storage in plants and algae, and they both share a carbon precursor that is used in biosynthesis. In order to produce biofuels and chemicals, the carbon partitioning process is essential. The majority of plants and microalgae store carbohydrates as starch and sugar, and a subsequent rise in TAG, suggests that lipids may be produced from carbohydrate breakdown. Proline increased during the reproductive phase, showing that proline only did so once the drought was recognised. One of the osmoprotectants that scavenges ROS under drought stress is proline. Proline upregulation increased during the duration of the stress under extreme drought stress and interestingly the key genes (P5CS and P5CR) which is involved in the biosynthesis of proline also increase in drought stress demonstrating the devastating impacts of drought (Liang et al., 2019).

Some species of algae and plants display an increase in both lipid and carbohydrate content under drought stress. Drought stress caused an increase in carbohydrate and starch levels (Figure 5.1). I found that lipid accumulation happens before carbohydrate accumulation. The buildup of lipid droplets in leaves may be

regulated by intricate metabolic processes. Under drought stress, proton gradient prevents, moreover the PSI-dependent CET alters the NADPH and ATP ratio and may cause a change in the metabolic pathways involved in photosynthesis. Some of these metabolic adjustments could lead to lipid conversion, which is essential for adapting to drought stress.

Previous studies have demonstrated the expression of the ATG8 gene in *C. reinhardtii* during various stress conditions, including oxidative stress, rapamycin stress, and ER stress. This observation was made in investigations conducted by (Perez-Martin et al., 2014; Chouhan et al., 2022). The expression of the ATG8 protein significantly increased in drought stress. This finding suggests that ATG8 is essential for triggering autophagy in *P. sativum*. ATG8 protein was also abundant under drought stress circumstances, which might be related to a rise in stromal redox equilibrium, which then caused autophagy to be induced and TAG to accumulate. The ROS that is produced as a result of drought stress can activate the autophagy system. Even though increased ROS levels were seen more in drought stress, the prevalence of ROS generation was significantly higher in the latter. This finding suggests that drought stress causes both oxidative stress and autophagy, both of which are accompanied by an increase in leaf lipid content.

According to earlier research in *A. thaliana* and *C. reinhardtii*, which showed that TAG biosynthesis involved multiple acyltransferases DGAT and PDAT catalysing the final step, my study showed a significant accumulation of TAG in drought stress (Zhang et al., 2009). Further demonstrated that PDAT and DGAT were upregulated under drought stress at both the mRNA and protein levels, confirming their participation in TAG synthesis (Figure 5.5). Therefore, the DGAT or PDAT pathways are most likely involved in the buildup of TAG in *P. sativum*.

Fatty acid concentration and composition play key roles in the synthesis of biofuels. In our investigation, I discovered that the control, drought, and recovery conditions had varied total fatty acid profiles. In particular, I found that the percentage of lauric acid (C12:0), myristic acid (C14:0), palmitic acid (C16:02OH), margaric acid (C17:0), stearic acid (C18:3), and archidic acid (C20:0) significantly increased under drought stress compared to control conditions (Figure 5.4). This shows the plant may benefit from an energy sink by producing more surplus fatty acids under drought stress conditions. Additionally, I discovered that drought had a larger total fatty acid content than control or recovery conditions.

It is interesting to know that the membrane lipids had been decreased, indicating that their breakdown may have been diverted toward TAG synthesis (Figure 5.2a). The decline may also influence TAG buildup in fatty acids generated from MGDG and DGDG (Figure 5.2b). Similar findings have been made in earlier research, which suggests that TAG buildup in *C. reinhardtii* is caused by the recycling of glycolipids and membrane lipids (Devadasu and Subramanyam, 2021). These results imply that fatty acids may be liberated from glycolipids and used by the DGAT enzyme in the Kennedy route to produce TAGs (Yoon et al., 2012).

5.4 Conclusion

My research findings suggest that biomass declines as a result of drought. It's interesting to note that the proline, starch, reducing sugar and carbohydrate enhanced under drought stress. These substances act as osmoprotectants and offer non-enzymatic ROS scavenging protection. The study also discovered that increased autophagy and fatty acid are connected to drought. It has also been established that TAG buildup in plant photosynthesis and drought stress are related. The increased lipid content can result

from the leaf tissues' imbalanced redox state, which produces ROS. Elevated levels of ROS during drought conditions can serve as signals to initiate lipid biosynthesis and activate autophagy inducers, thereby facilitating the recycling of cellular components for lipid formation. As a result, *P. sativum* plants under drought stress can yield high levels of lipids. The study contends that significant chloroplast membrane breakdown occurs in drought along with the rise in TAG accumulation. Fatty acids are separated from membrane lipids to participate in the recycling of TAG. Under drought conditions, these fatty acid compositions can be crucial for biotechnological applications.

Chapter 6

Investigation of the drought-induced changes in transcriptome, proteome, and metabolome from leaf tissues

6.1 Introduction

The pea is a cool-season grain legume that is a member of the Papilionoideae subfamily of the Fabaceae family. It is farmed on over 6.4 million hectares per year for human consumption and stock feed throughout the world (Bouton et al., 2016). The diploid genome of the pea is 4,300 Mb, which is 10 times larger than the genome of the model legume species that is most closely related to it, *M. truncatula* (c. 500 Mb). The high proportion of repetitive DNA, which makes up between 50 and 70 percent of the nuclear genome complement and is made up of different families of mobile genetic elements, is the main cause of this genome (Macas et al., 2007). The exomic component of the pea genome makes up less of the total genomic DNA than in other legume species as *M. truncatula*, (c. 472 Mb) (Sato et al., 2008), and *C. arietinum* (c. 740 Mb) (Varshney et al., 2013). In order to provide effective tools for molecular breeding, which can result in enhanced productivity, crop quality, and sustainable farming techniques, it is urgently necessary to enrich the genetic resources for field pea.

Transcriptome analysis has been transformed by the low cost and high throughput of second-generation DNA sequencing, which has made it possible to directly evaluate transcripts sequences, identify gene transcriptional structures, find alternate splicing patterns, and measure expression levels. In contrast to prior techniques like microarrays, RNA-Seq has shown to be more effective in detecting low abundance transcripts, identifying genetic polymorphisms like alternative alleles, and differentiating biologically important isoforms. Model plant species like *A. thaliana* have been the subject of transcript expression profiling in the past to learn more about the functional developmental modules. Comparably, research on legumes has also revealed specific gene transcriptional activity across tissues and developmental stages. RNA-Seq has recently been utilised to characterise the genome-wide transcriptomes of

model and non-model plant species and to comprehend the dynamics of transcriptomic expression during plant responses to various abiotic stressors. With the development of genomic technology, it is now possible to provide richer genetic resources for field pea that will make it easier to create superior cultivars.

Significant alterations in biological processes were discovered by (Gao et al., 2021) in their recent global transcriptome analysis on *P. sativum*. Improvements in photosynthesis, ROS levels, antioxidant enzyme, protein turnover, and carbon fixation were among these modifications. A novel and highly efficient tool for examining an organism's transcriptome is RNA-seq, because it has given scientists a thorough understanding of the RNA level's functional facets and molecular constituents, it has revolutionised the field of molecular biology. Researchers have been able to use RNA-seq to discover and quantify genes that are differently expressed under a variety of circumstances, including biotic and abiotic stressors, and to investigate the underlying molecular mechanisms involved.

Recent comparative transcriptomic research on *P. sativum* revealed both specific pathways and rare pathways shared by drought stress. Using high throughput RNA-seq data, the study analysed DEGs to better understand how *P. sativum* responds to drought stress and how it adapts. Since chloroplasts are the main environmental sensors, the study focused on chloroplast transcripts and how they relate to physiological studies. Crosstalk between redox, photosynthetic genes/stress indicators, and transporter genes was deciphered in the chloroplast of *P. sativum* using gene expression profiling, and its significance in long-term acclimation under drought was highlighted. The results of this work offer a significant resource for creating tools for molecular breeding of this significant species of grain legume. This work has uncovered

numerous important pathways that might have gone overlooked in the presence of drought stress.

Due to the rich genetic variety of the plants and the spatiotemporal heterogeneity of soil drought, crop productivity in drought marginal areas has proven to be a difficult challenge (Tsai et al., 2018). Due to their genetic and physiological robustness, economically or ecologically significant plant species have not been widely cultivated. Therefore, in order to maintain and encourage economic gain in marginal drought-prone lands, it is crucial to comprehend the physiological as well as the proteomic analysis of crop species (Samuel et al., 2013).

When a plant is under drought stress, its root system usually sense and reacts to the stress first, then the leaf. Plants activate a number of adaptive mechanisms in response to environmental stress, such as the production of secondary metabolites like flavonoids and anthocyanins to fend off oxidative damage brought on by ROS (Chen et al., 2019). Additionally, in order to combat the oxidative stress brought on by dehydration, plants engage their antioxidant defence mechanisms (Al-Kharusi et al., 2019).

Most chloroplast proteins are translated in the cytosol after being transcribed by the nuclear genome and then transferred to the chloroplasts. There are just 120–130 genes in the chloroplast genome, the majority of which are involved in photosynthesis (Jansen et al., 2008). Since the genomes of the chloroplast and the nucleus both encode subunits for multi-subunit protein complexes like PSI, PSII, RuBisCo, and Cyto b6f, precise coordination of gene expression within the organelle is necessary (Bose et al., 2017; Pottier et al., 2018).

The nucleus and chloroplast communicate, with the nucleus controlling chloroplast gene expression, biosynthesis, and development (anterograde

communication) (Vigani et al., 2013). However, recent research suggests that nuclear-encoded genes involved in photosynthesis may also be regulated by chloroplasts. Retrograde signalling is the suppression of gene expression of nuclear-encoded chloroplast proteins by damaged or developmental-arrested chloroplasts (Nott et al., 2006). These retrograde signals might modify the redox status of the photosystems of tetrapyrrole depending on the organelle's maturation stage or how external environmental stimuli are perceived (Kleine et al., 2016).

Plants are frequently subjected to a variety of environmental conditions that might have an impact on their survival and growth. Plants use a range of tactics to overcome these obstacles. Understanding the physicochemical changes to the cellular environment that take place when plants are subjected to adverse conditions is crucial. Proteins are more responsive to stress than other biological molecules because they regulate nearly all metabolic pathways that are otherwise susceptible to changes in the environment. Particularly, chloroplasts are essential for plants to adapt and acclimate to changing environmental conditions (Nomura et al., 2012).

It should be emphasised that due to the variation in stress tolerance not just between different species but also between various varieties, studies on stress adaptation in model plants do not necessarily translate to crops. Dehydration tolerance in plants involves numerous processes and is a complicated genetic characteristic, making it a problem that affects all plants. The current work intends to evaluate the modifications in the proteome of chloroplasts in response to dehydration in a leguminous crop, pea, in order to address this problem.

Since oxidative stress is a fundamental aspect of these difficulties, plants respond to abiotic stress conditions in a similar molecular and physiological manner (Apel and Hirt, 2004). These reactions frequently result in metabolic changes, which

may also be a sign of oxidative stress (Baxter et al., 2007). Amino acids, carbohydrates, and their derivatives undergo unique alterations as a result of oxidative stress conditions. Understanding the changes brought on by stress is challenging given these dynamic changes in metabolites. Identification of the specific metabolic markers of oxidative stress in plants is therefore vital (Obata and Fernie, 2012).

Changes in metabolites are another sign of oxidative stress in addition to ROS levels (Noctor et al., 2015). These metabolite alterations can be measured using the "metabolomics" method (Fernie et al., 2004). Analyzing the fingerprints of metabolites can be used for the severity of oxidative stress in plants. Under stress, proline and GABA levels rise to maintain redox balance (Liu et al., 2020). Similarly, during cold stress, sugars such as sucrose, galactose, and raffinose accumulate to provide protection (Morsy et al., 2007).

A typical reaction to oxidative stress is the buildup of suitable solutes (Hare et al., 1998; Yancey, 2005). These solutes, which include amino acids, raffinose family oligosaccharides, soluble sugars, and polyamines, are created in greater amounts to support cellular metabolism (Jorge et al., 2016). These osmolytes are crucial for maintaining osmotic balance, stabilising proteins and enzymes, and keeping the turgor of plant cells. These solutes build up over time, protecting plants from oxidative stress and ensuring their survival in harsh environments.

6.2 Results

6.2.1 Sequencing and *de novo* assembly of *P.sativum* transcriptome

A total of 37,985,457 paired end reads made up the dataset. These readings ranged in length from 30 to 140 base pairs on average (bp). A total of 3.7 gigabytes (GB) of fastQ-format sequencing data made up the dataset. The dataset consists about 37 million very good quality reads were annotated using *de novo* transcriptome assembly with help of

Fabaceae data base. Trinity version 2.1.1 tool was used to process all reads into contigs without any reference genome using default parameters. The raw reads of control and treated samples were filtered, and the sequences has phred value <20 were considered for this study Figure 6.1. The *de novo* assembly was performed on the final data set, which consisted of approximately 22 million high-quality reads. Without using a reference sequence, a contig was created from the processed reads. *De novo* assembly was carried out based just on the data present in the processed readings themselves.

Different hash lengths (K-mers) were tested during the assembly process, and 40 was determined to be the optimal hash length. The number of contigs created, the total number of reads, the cumulative length of the contigs, and the occurrence of non-ATGC characters in the assembled sequences were only a few of the variables that helped determine the ideal K-mer size. These factors aided in choosing the best K-mer size for the assembly procedure. A total of 152,265 trinity genes were identified and among them, 213025 trinity transcript, GC percentage of ~39.01, median contig length of 64 bp and an average contig length of 1075 bp. Following RSEM normalisation, contigs were converted into transcripts, and each contig's abundance was determined. A total of 81,270 transcripts were identified which are commonly expressed in both control and drought treated samples and a total of 28,385 transcripts were uniquely expressed in control and drought samples respectively. To investigate the relationship between replicates of control and drought-treated samples (Figure 6.1c), a correlation analysis using Pearson correlation was conducted. A correlation coefficient (r) greater than 0.5 was considered indicative of a positive correlation, while a correlation coefficient less than -0.5 indicated a strong negative correlation. The control duplicates are strongly associated within them, and the correlation between the samples that had

been subjected to drought was equally high. it is evident that no significant correlation between the control and drought samples.

(a)

Sample	Raw Reads	Q20 %	Q30 %	Clean Reads
C1	34212856	98.08	94.13	33855054
C2	36912854	98.11	94.18	36529238
D1	41776082	98.01	93.89	41308422
D2	40687714	97.96	93.77	40249116

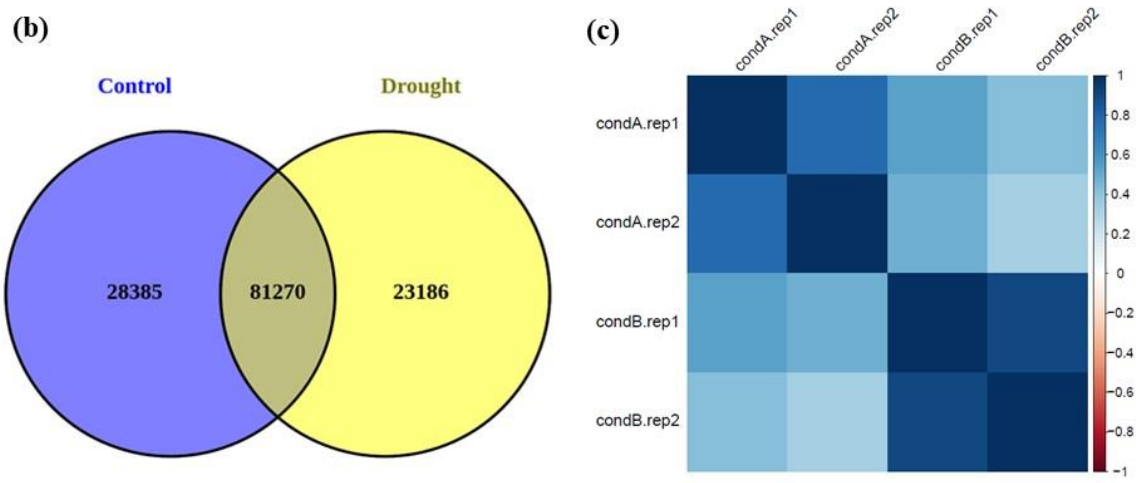

Figure 6.1 *Sequenced reads statistics summary (a) De novo assembly statistics of P. sativum contig. (b) Gene level transcript statistics (c) Pearson correlation analysis between replicates.*

6.2.2 Identification of Differentially expressed genes (DEGs) of *P. sativum*

We used the Trinity suite's "run DE analysis.pl" software to identifying differentially expressed gene-level transcripts. A total of 1719 transcripts up-regulated in the drought-treated samples and 1344 transcripts were up-regulated transcripts in the control samples. The number of differentially expressed transcripts was greater in the drought condition when compared to the control condition. Volcano plots and MA plots are both valuable tools in transcriptomics to visualizing and identifying differentially expressed genes. volcano plots show the statistical significance and fold change, while MA plots

focus on the average expression and log-ratio or log-fold change. Both plots aid researchers in understanding gene expression differences and selecting genes for further analysis and interpretation. (Figure 6.2) Volcano and MA plots showed the differential expressed genes (DEGs) represented withred dots and unchanged expressed genes were represented in black dots. (Figure 6.2). Most of the heat shock genes (HSP70, HSP20), stress marker genes (DHN2, PIP2) and calcium binding genes (CDPK3, CDPK13 and CDPK32) were highly expressed in drought-treated samples. The differentially expressed gene level trinity IDs identified cluster, and among them subclusters 3 (Figure 6.3) associated transcript were majority of the genes (DHN2, PIP2, PSBS) and further we carried out the KEGG pathways interestingly many genes involved in metabolic process, ATP binding, and oxidoreductase activity are highly represented and interestingly the majority of the genes included in KEGG pathways were those involved in protein synthesis, inositol phosphate metabolism, and amino acid biosynthesis, which made up the bulk of the genes impacted by drought stress and further in GO analysis mainly genes which encodes for biosynthesis of amino acids, secondary metabolites and arginine and proline metabolism shows there representation and are highly represented in these process (Figure 6.3 b,c).

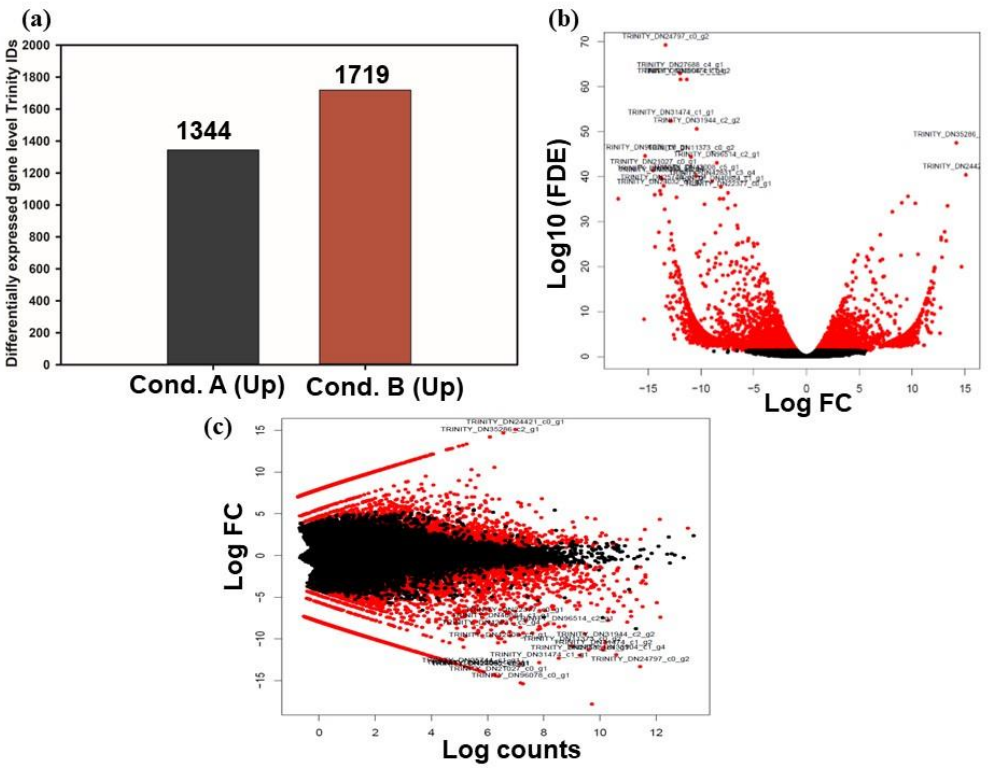

Figure 6.2 *(a) The number of DEGs in the control and drought treated (b) Volcano plots of differentially expressed transcripts (c) MA Plots of differentially expressed transcripts.*

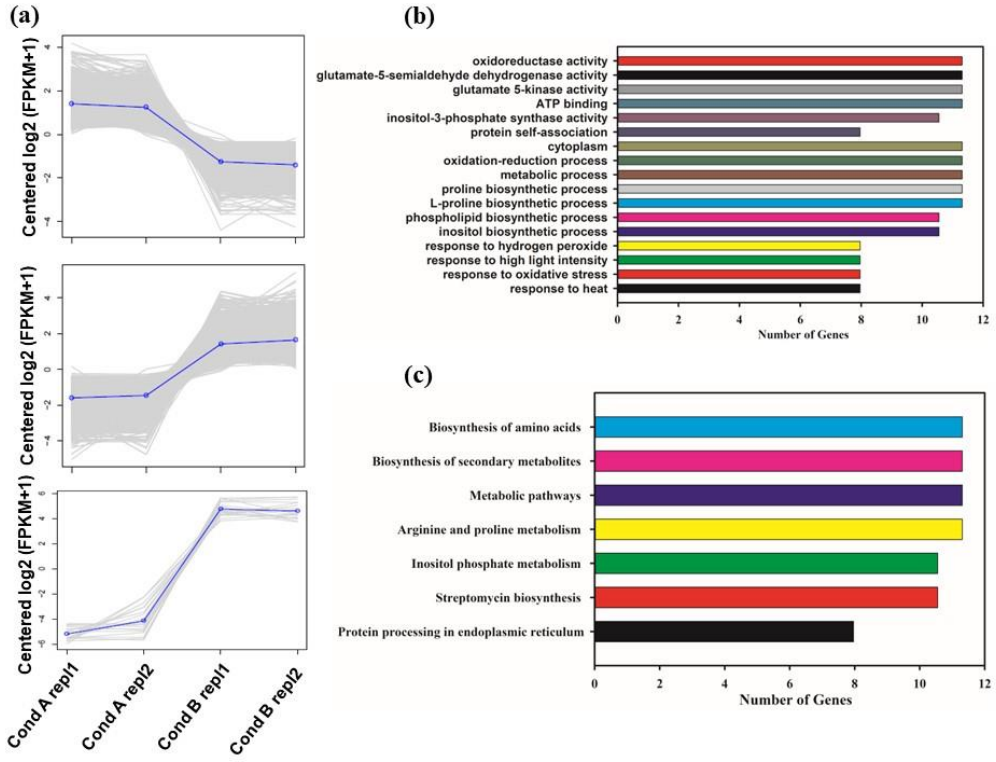

Figure 6.3 *(a) Control vs drought differentially expressed gene level trinity IDs identified clusters (b) Sub cluster3 associated IDs KEGG pathways (c) Sub cluster3 Gene Ontology pathways.*

6.2.3 Differentially expressed gene level of *P.sativum* under drought

In this study, a total of 200 transcripts were identified representing the elongation, fatty acid degradation, fatty acid biosynthesis, phospholipid and glycerolipids metabolism, photosynthesis, and stress marker genes. It is also evident that 48 genes have mapped for photosynthesis Figure 6.4. Transcripts were visualised as heatmap with rows denoting genes with notable expression difference between the two groups and columns denoting specific samples from the two groups (Condition A and Condition B with replicates). Transcripts related to photosynthesis including PSI and PSII complexes genes showed a moderate downregulation (Figure 6.4). Further, Transcripts such as PIP2, PIP27, PSBS, DHN2 and ATG16 showed significant upregulation, whereas PSBO, Cyto b6f complex, PsaC, LHCa2, PsaA, PsaA and PsaB showed down regulation in drought treated plants with respect to controls (Figure 6.4c). Also, most of the PSI light-harvesting proteins showed a moderate up-regulation which is further validated with western and RT-PCR data. In the treated condition, the expression of DHN2 and PSBS genes rise, while the expression of PSII and PSI core complex genes were markedly reduced under drought stress in pea, the expression levels of LHCII major and minor components were reduced. These results corroborated withour earlier immunoblot and transcript (qPCR) results (Figure 6.5).

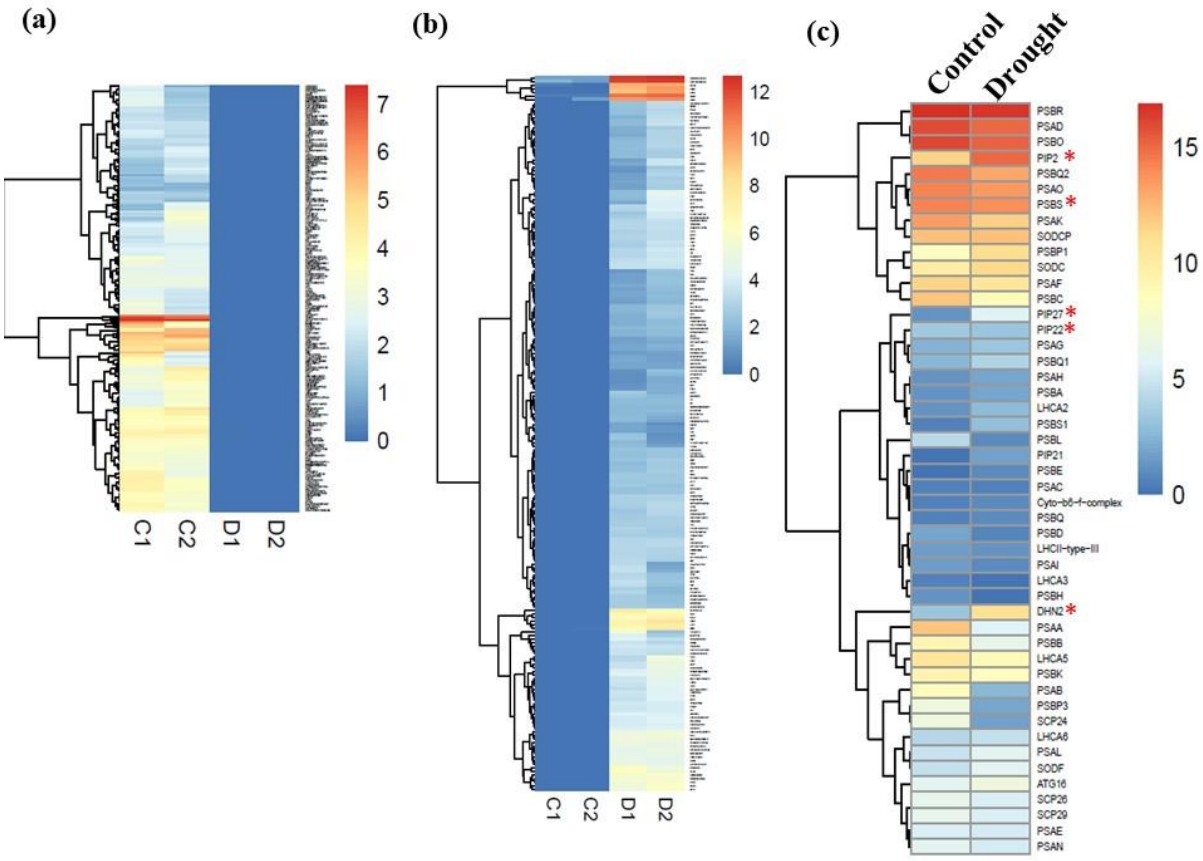

Figure 6.4 *(a) Heat Map representing expression of top 200 condition A upregulated and (b) Top 200 condition B upregulated and (c) Photosynthetic genes of control and drought treated condition in P.sativum. Heat map was constructed using gplot in R package.*

6.2.4 Differential expression of genes associated with photosynthesis, ROS and transporter

We monitored gene expression levels drought responsive genes using RT-PCR including the photosynthesis genes (PSI and PSII), ROS and calcium dependent protein kinase (Figure 6.5). Genes such as dehydrins, aquaporins, PSBS was showed significant upregulation ~2.5 fold in drought treated leaves after 8 days of drought treatment, whereas the photosynthetic genes (D1, D2, CP43, CP47, PsaA, PsaB, PsbO, PsbP) were downregulated in drought treated plants.

and interestingly some genes (CP43, Lhca3, PsbO, PetC, PsbP and Fed1) were also recovered but not to the levels of the control (Figure 6.5). The expression levels of ROS

and antioxidant genes were induced significantly increased ~6 fold (MnSOD, CAT4, FeSOD), ~4-fold APX, ~3 fold (Cu-ZnSOD, Cu-ZnSOD1). However, we did not observe many changes in the levels of transporter genes, however, the levels of vacuolar proton transporter genes as (V-H^+ATPaseB, V-H^+ATPaseE) subunit expression were decreased in drought plants. We also monitored the expression levels of plasma membrane proton ATPase (PM-H^+ATPase) isoforms PM-H^+ATPase1, PM-H^+ATPase4.1-like, PM-H^+ATPase4.1 in leaves of drought treated plants. The Calcium-Dependent Protein Kinase 32 (CDPK32) and CDPK13 levels were increased in leaves of drought treated plants.

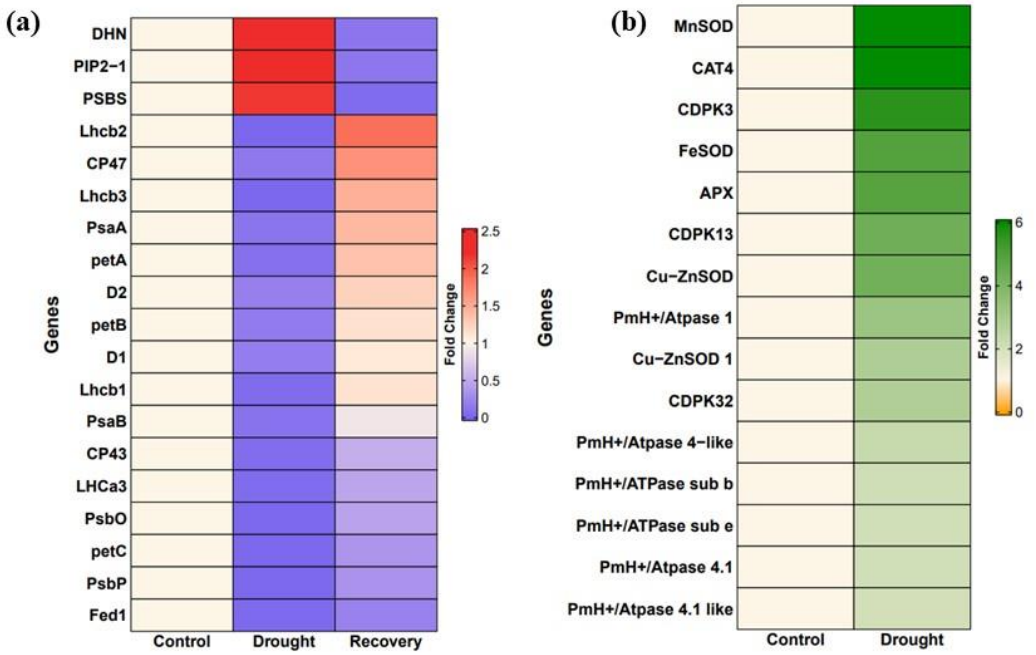

Figure 6.5 *(a)RT-PCR analysis of photosynthetic genes of control, drought and recovery leaf tissues samples (b) RT-PCR analysis of ROS, calcium modulation and transporter genes.*

6.2.5 Comparison of differentially expressed gene transcript levels from KEGG pathways

The KEGG automatic annotation server (KAAS) was used to map the ortholog contigs to biological pathways. This involved utilising the BLASTX programme to compare each contig to the KEGG database. The orthologs and associated biological pathways were identified by matching the contigs with recognised sequences in the KEGG database and they were mapped to respective pathways (Figure 6.6). The transcriptome represents enzymes which are involved in carbon metabolism, fatty acid metabolism, biosynthesis of amino acids. Further, we also observed genes related to genetic information, which include translation, folding, degradation, replication and repair process. Numerous biological activities, including cell communication, proliferation, and environmental processing such membrane transport and signalling molecules, were discovered in the KEGG annotation of the Pisum transcriptome. Minor groups are represented by these processes in the annotation. The KAAS study also demonstrated the participation of many genes in metabolic processes connected to nitrogen metabolism, carbon fixation, and fatty acid metabolism. In addition, genes related to glucose metabolism and protein synthesis and modification were found in the control condition. These discoveries shed light on the metabolic processes in the Pisum transcriptome's molecular activity and pathways (Figure 6.6a). We also identified genes involved in sugar production, fatty acid degradation, and ubiquitin-mediated proteolysis, were more prominent seen in the drought situation (Figure 6.6b). Additionally, the drought stress also contain pathways for autophagy, protein breakdown, and sugar production were present and were increased subsequently as the severity of the drought increased. In addition, our study focused on identifying the genes

that are predominantly involved in the observed events, as they play a significant role in enhancing both the yield and quality of Pisum.

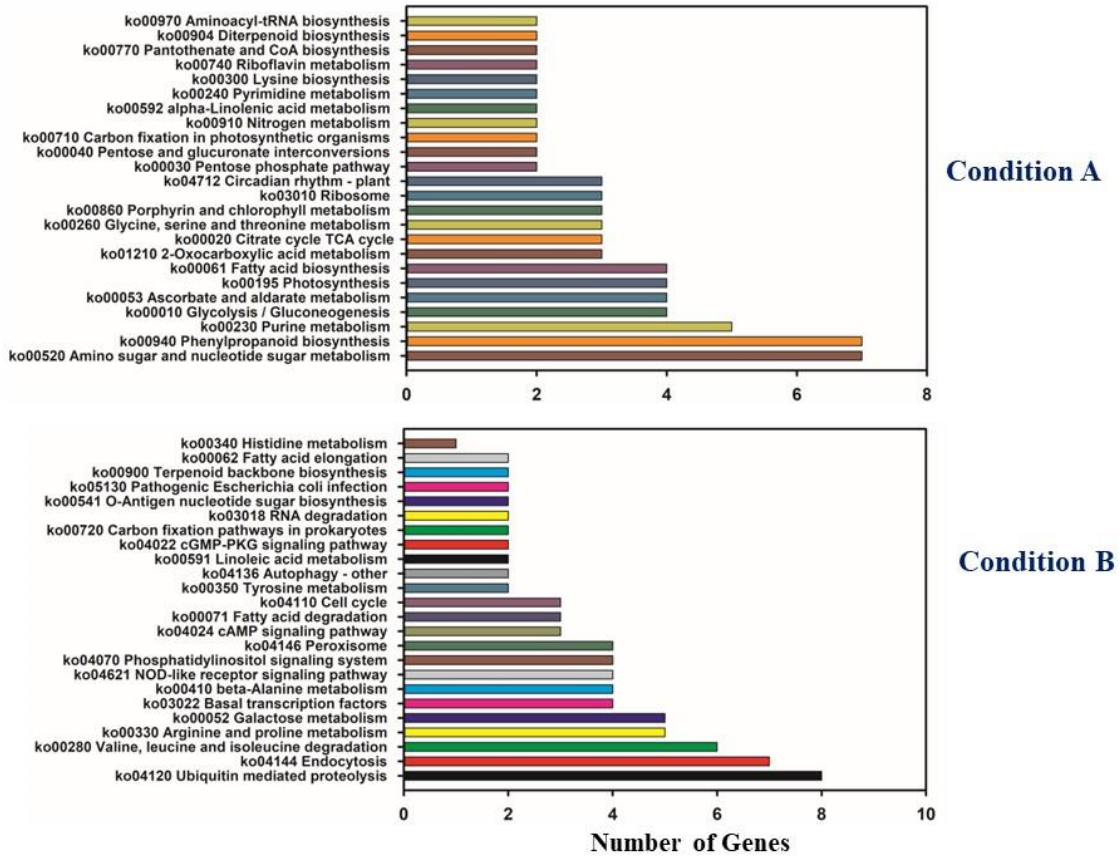

Figure 6.6 *Comparison of differentially expressed transcript level KEGG pathway (a) pathways in condition A (b) pathways in condition B.*

6.2.6 GO analysis of differentially expressed gene

The GO analysis of control and drought-treated samples showed that genes involved in many biological, cellular, and molecular processes (Figure 6.7 and 6.8). At the biological process level, drought stressed samples was found to increase the activity of transcripts related to defence response process, the metabolite biosynthesis response, and the ubiquitin-dependent protein catabolic process. The identified genes in our investigation were shown to be involved in a variety of biological processes. Zinc ion binding, DNA binding, oxidoreductase activity, hydrolase activity, and metal ion

binding were all included in these processes. Additionally, several of the genes were linked to transcription control, generally falling under the heading of molecular function. These findings illustrate the functional diversity of the discovered genes and the diverse biological and molecular processes in which they participate. Furthermore, these genes were found to be predominantly located in the cytoplasm and membranes.

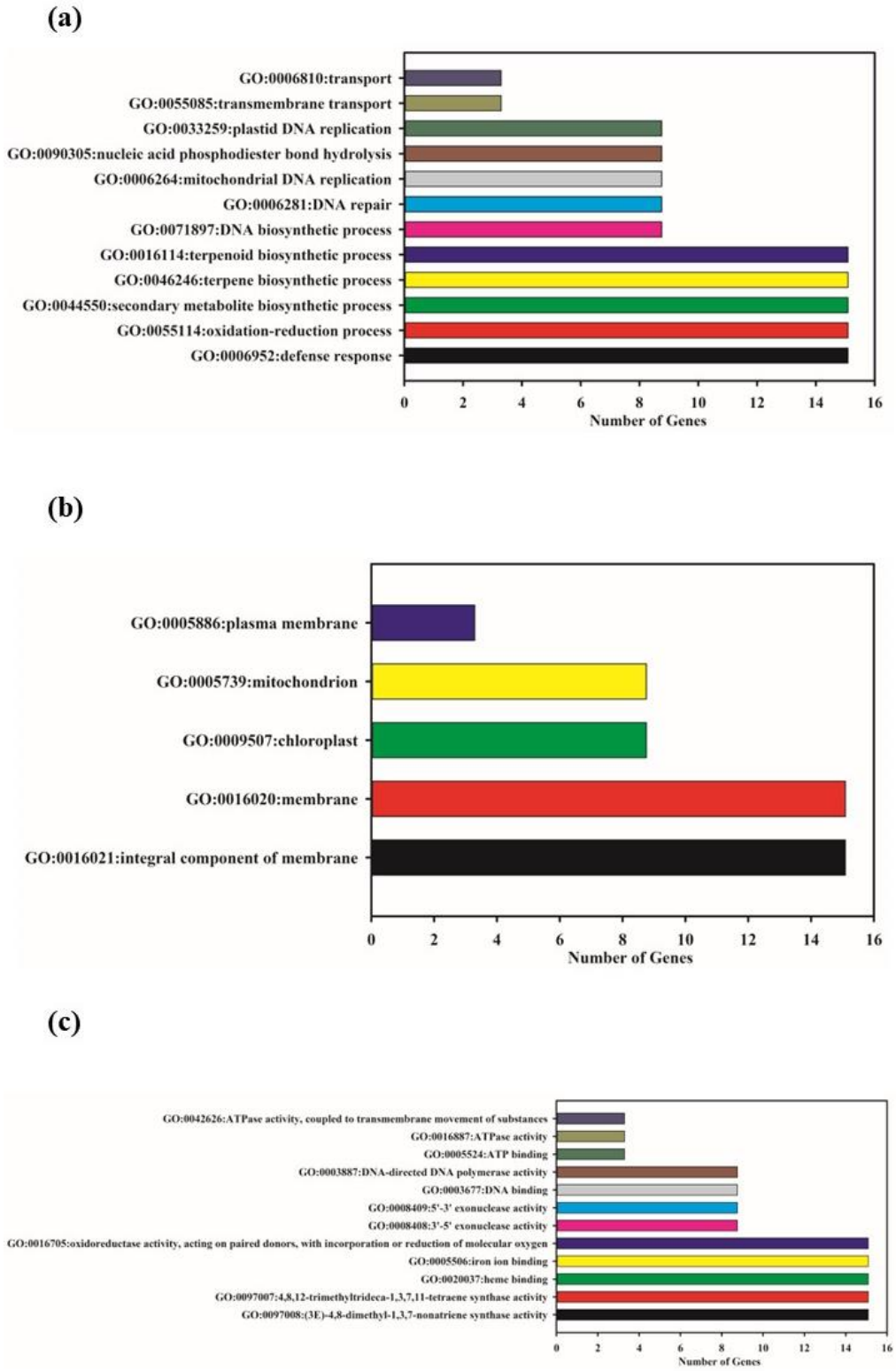

Figure 6.7 *GO analysis of DEGs between control (a) Gene ontology distribution of condition A (Biological process) (b) Cellular process and (c) Molecular process.*

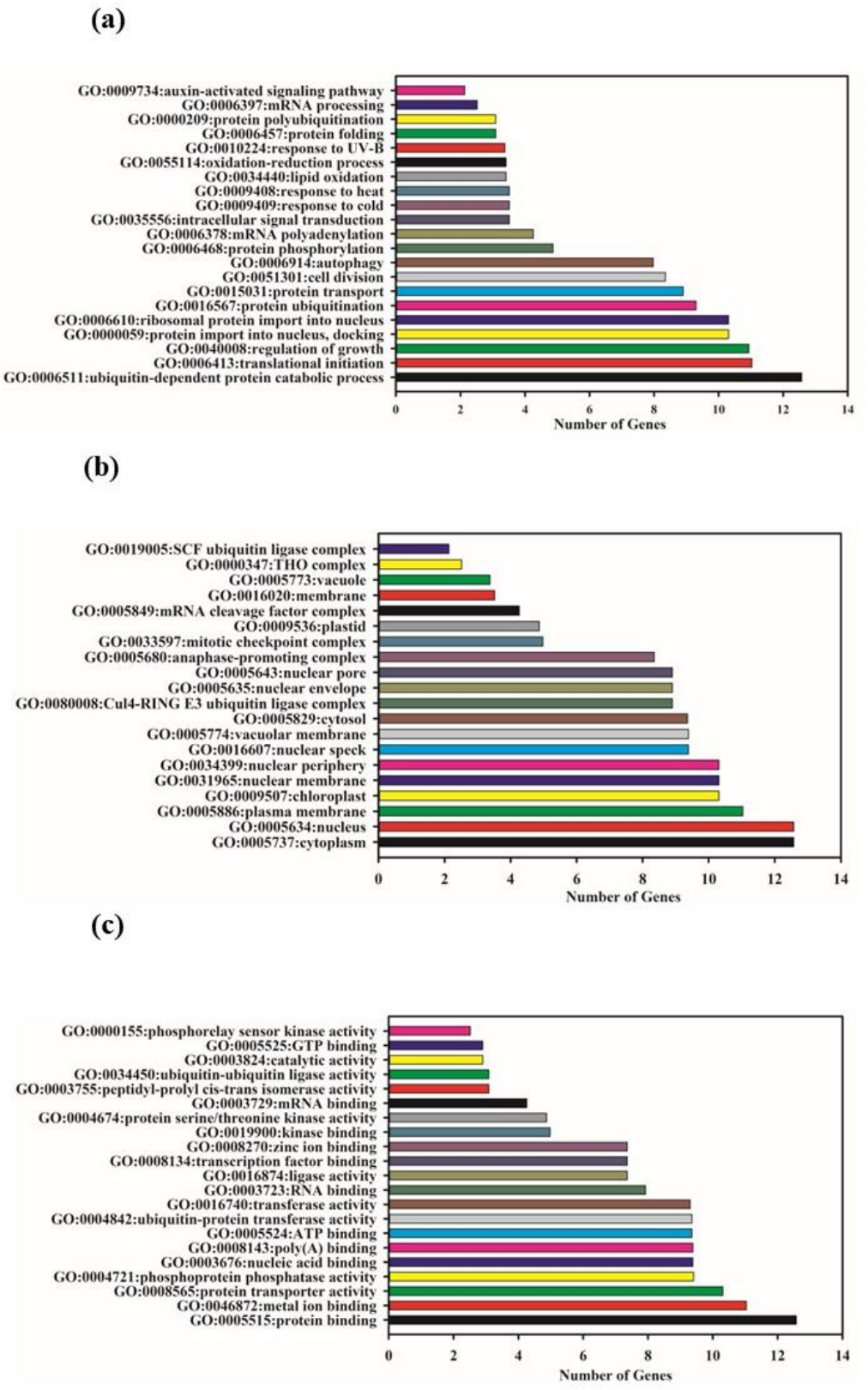

Figure 6.8 *GO analysis of DEGs between drought (a) Gene ontology distribution of condition B (Biological process) (b) Cellular process (c) Molecular process.*

6.2.7 Identification of transcription factor families

A total of 15 families were identified in the transcriptome of drought-treated and control samples. Transcription factor family genes such as ABF, HSFF, and ERF1 were highly expressed, while less transcripts were observed in GBF, MADS, TBP, NFYA, HD-ZIP, MYBP, and ERBP family transcripts (Figure 6.9). Further, we analysed transcription factors that were only specific to heat shock, nuclear transcription factor, and ethylene transcription factor, which led to the identification of genes from the groups under drought stress.

(a)

KEGG I.D	Transcription Factor	Description
ko: ko:K14431	TGA	transcription factor TGA
ko: K09338	HD-ZIP	homeobox-leucine zipper protein
ko: K09422	MYBP	transcription factor MYB, plant
ko: K09286	EREBP	EREBP-like factor

(b)

KEGG I.D	Transcription Factor	Description
ko:K09060	GBF	plant G-box-binding factor
ko:K09264	MADS	MADS-box transcription factor
ko:K03120	TBP	transcription initiation factor TFIID TATA-box-binding protein
ko:K08064	NFYA	nuclear transcription factor Y, alpha
ko:K14432	ABF	ABA responsive element binding factor
ko:K09338	HD-ZIP	homeobox-leucine zipper protein
ko:K09419	HSFF	heat shock transcription factor, other eukaryote
ko:K09422	MYBP	transcription factor MYB, plant
ko:K09286	EREBP	EREBP-like factor
ko:K14516	ERF1	ethylene-responsive transcription factor 1

Figure 6.9 *Identification of transcription factors (a) condition a upregulated transcription factors (b) Condition b Upregulated transcription factors.*

6.2.8 Proteome analysis of Pea proteins in leaves under drought stress by iTRAQ

Isobaric tag for relative and absolute quantification, (iTRAQ) the technique is based upon chemically tagging the N-terminus of peptides generated from protein digests that have been isolated from leaf tissues. The two labelled samples were fractionated by nanoLC and analysed using tandem mass spectrometry. Fragmentation of the tag attached to the peptides generate a low molecular mass reporter ion, that is unique to the tag used to label each of the digests. Measurement of the intensity of these reporter ions, enables relative quantification of the peptides in each digest and hence the proteins from where they originate study of *P. sativum* leaf proteome revealed a total of 4,021 proteins, among these proteins 972 proteins are upregulated, 1244 are downregulated, and 1805 proteins are unchanged, and proteins with an expression ratio or fold change 0.83 were taken as considerably downregulated and those with 1.2 as highly upregulated. Based on their functions, the proteins were divided into different classes, including those involved in glucose metabolism, kinase activity, GTP-binding activity, ABC-ATP transport, translation, carotenoid activity, PSII-LHCII, photosynthetic activity, and heat shock activity (Figure 6.10).

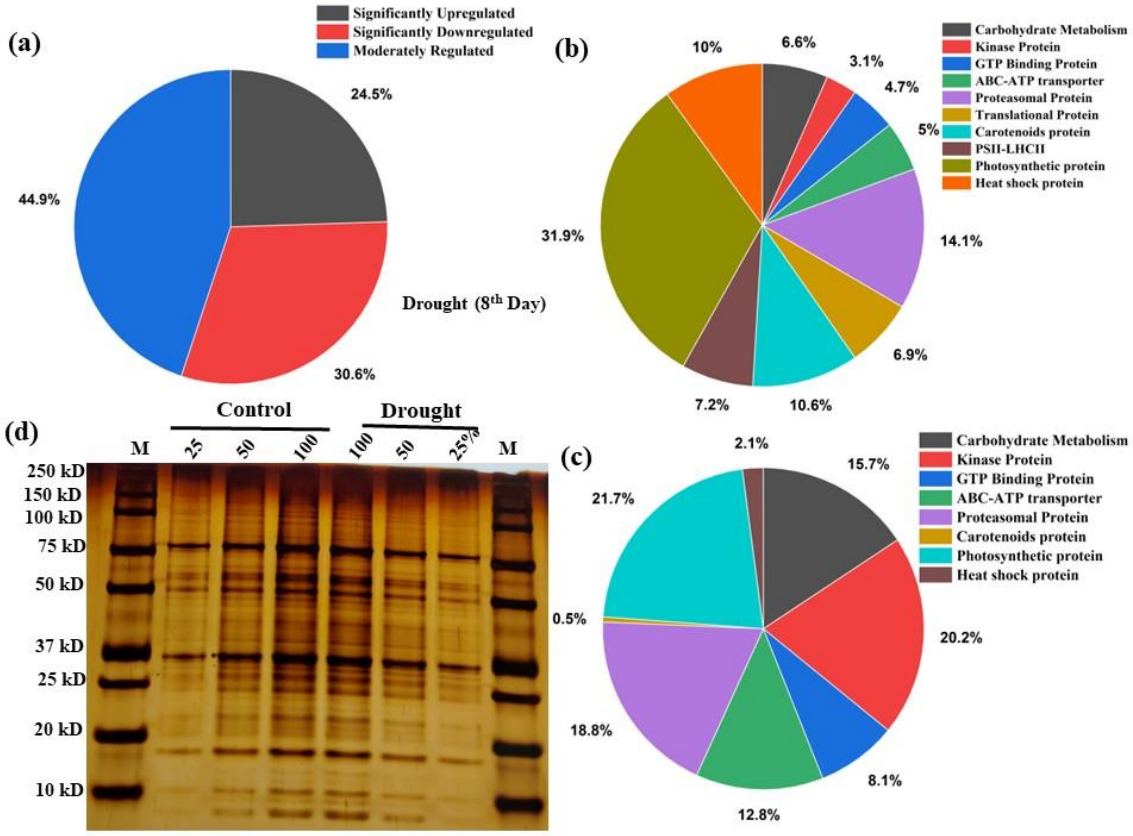

Figure 6.10 *(a) Characterization of the proteome of P.sativum plant based on significance (b) downregulated proteins in P.sativum under drought stress (c) upregulated proteins in P.sativum under drought stress based on their functionality (d) Silver staining of the proteins isolated from the leaf tissues, and to check the purity of the proteins for iTRAQ.*

6.2.9 Correlation-based clustering among proteins in leaves of *P. sativum* under drought

In order to explore the relationship among the proteins a HAC (hierarchical cluster) analysis was performed. Different class of proteins i.e ABC-ATP transporter, ATP binding protein, carotenoids-transporter proteins, GTP binding protein, heat shock proteins, kinase protein, PSI-LHCI, and PSII-LHCII were divided into two clusters. To enhance the clarity of the graphics, only proteins with strong correlations ($r \geq 0.6$) were presented, thereby simplifying the visual representation. Positive interaction among FDX_2 and LHCA3, PsaB_1 and PsaE, PSAG and PSAL and the correlation between proteins FDX and PETB, PETA and PSAF, PSAF and LHCA3 showed negative correlation with each other (Figure 6.11). Similarly, we observed high positive

correlations within the PSII-LHCII proteins. A significant positive interaction was observed, including PSBO_1, LEA, PIP2_4, LEA_5, PSBS_1 and PSBS_1, LEA_5, however, PSBP_1, DHN_2, PSBS, PIP2 and LHCB3, DHN3 shows negative correlation (Figure 6.12).

Proteins related to ROS and antioxidants showed a strong positive association with each another (Figure 6.13). Notably, photosynthetic, antioxidant, and ROS proteins showed a strong positive correlation these results are corroborated withour previous western and RT-PCR analysis (Chapter 3). Additionally, ABC-ATP transporter showed a strong positive interaction with each other and FTSH_2 (ATP dependent zinc metalloprotease) ATPase, ABC, CUPA (laminin binding proteins), FTSH, CLBP, FTSH_1, AWA (cell wall proteins), FTSH_2, HIPP_2 (heavy metal transporter proteins) showed positive correlation. Conversely, ABC, AWA and ATPase, HIPP_3 showed a negative correlation with each other proteins Figure 6.14 and a similar trend was seen with carotenoids transporter proteins. In addition, DEAD (RNA helicases proteins), CLPA_4 (ATP dependent clp protease ATP binding proteins), H_ATPASE, V-ATPase showed a significant positive interaction (Figure 6.15). Positive interaction was also observed between GTP binding proteins, namely GTP, RBP1, RBM30, ARF3_1, RNPS1, RAN3 (GTP binding proteins), whereas negative correlation ARF3, RAN3, Lys-Trna, GTP_1, RPL (Ribosomal protein), RABG (RAB GTPase proteins) shows negative correlation with each other (Figure 6.16). As the drought stress progressed from day 1 to day 8, a strong positive interaction was noticed between HSP70_6, HSP70_3, HSP70_7, HSP70_2, HSP70_2, HSP70_5 (Heat shock proteins) showed a strong positive interaction with each other (Figure 6.17).

We also recorded a significant positive correlation with PTDSS_3 (phosphatidylserine synthase), PRMT, TP, ANK, PTDSS1, APK1A_5 (protein kinase)

showed a positive correlation with each other, while, ANK, APK1A_4, ANK_1, APK1A_5 showed negative correlation with each other. Figure 6.18 RBG (glycine rich binding proteins), ACT_1, RBG_1, GS2, ABC_1, FTSH showed highly positive correlation with each other (Figure 6.19). In treated plants, proteins levels (Figure 6.20) of PSI, PSII such as PsaA, PsaB, PsaE, PsaF, PsaG, PsaH, PsaL, FDX, LHCA3 were significantly decreased and PSII proteins PSBO, PSBP and LHCB3 were also in agreement with our western and RT-PCR data. Some of the stress marker proteins which are crucial in drought stress were upregulated DHN3, DHN2, PIP2, LEA and PSBS also corroborated with our western and RT-PCR results. However, some stable proteins COX, TP, TRX, NOD, dnaJ, MFS, iscU, Cyto5, GRPE, VHA, PER, RDX, TCP, FeS and CytoP450 were increased in severe drought stress suggests that these proteins play their key role in stress adaptation (Figure 6.21).

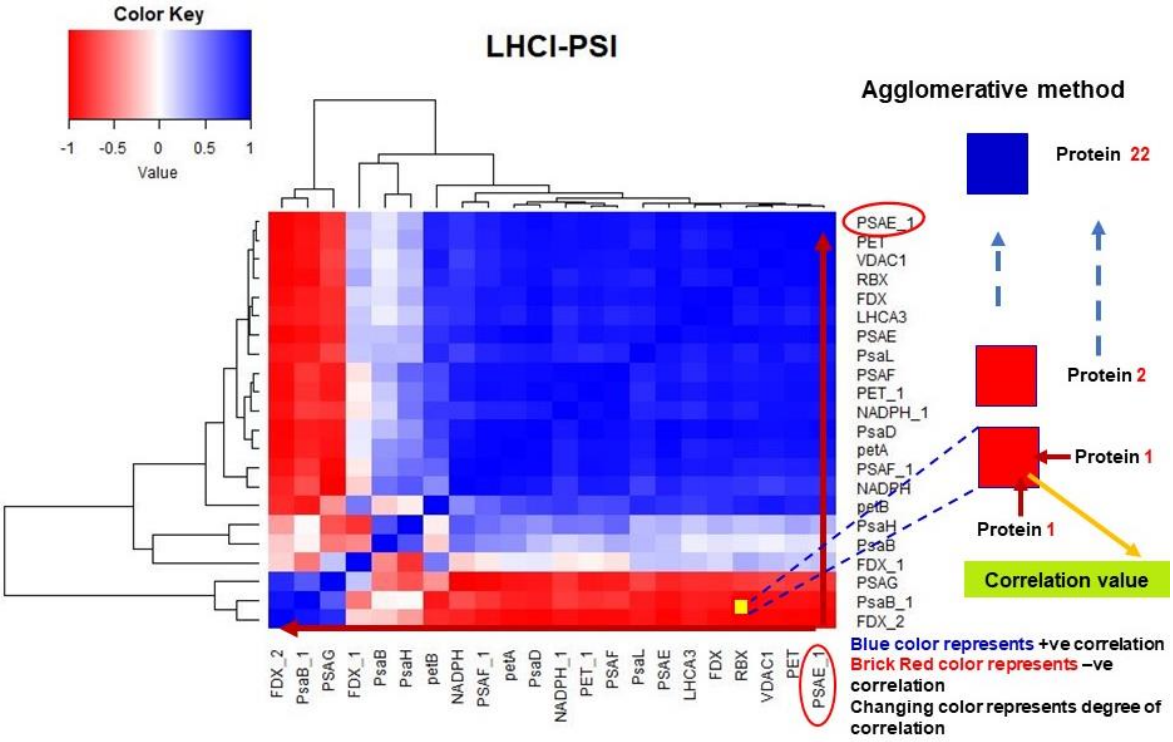

Figure 6.11 *Hierarchical cluster heat maps of down and up regulated proteins and protein-protein correlations in leaf of P.sativum at drought stress in PSI-LHCI proteins. Each correlation value (based on Pearson correlation coefficient) corresponds to average of three biological replicates. Boxes were drawn to represent individual groups of DEPs. The colour key and histogram show degree of correlation.*

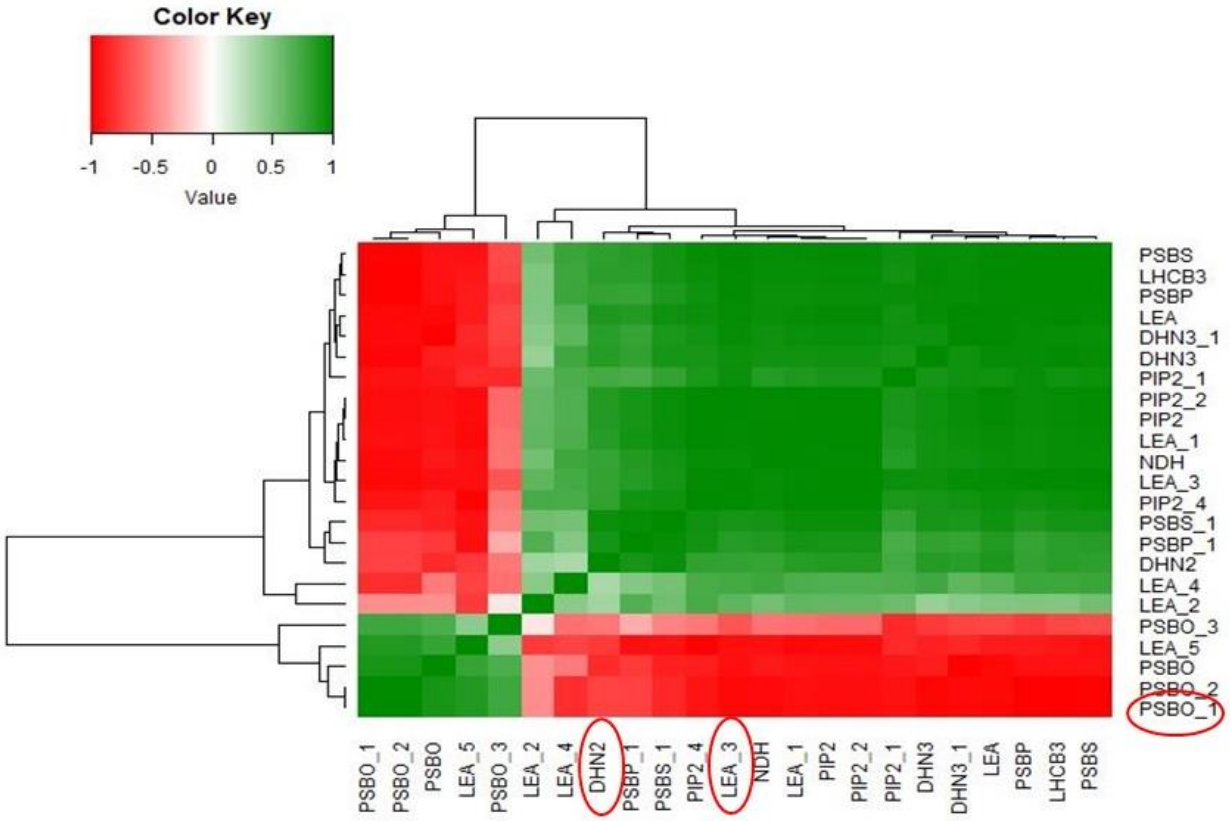

Figure 6.12 *Hierarchical cluster heat maps of down and up regulated proteins and protein-protein correlations in leaf of P.sativum at drought stress in PSII-LHCII proteins. Each correlation value (based on Pearson correlation coefficient) corresponds to average of three biological replicates. Boxes were drawn to represent individual groups of DEPs. The colour key and histogram show degree of correlation.*

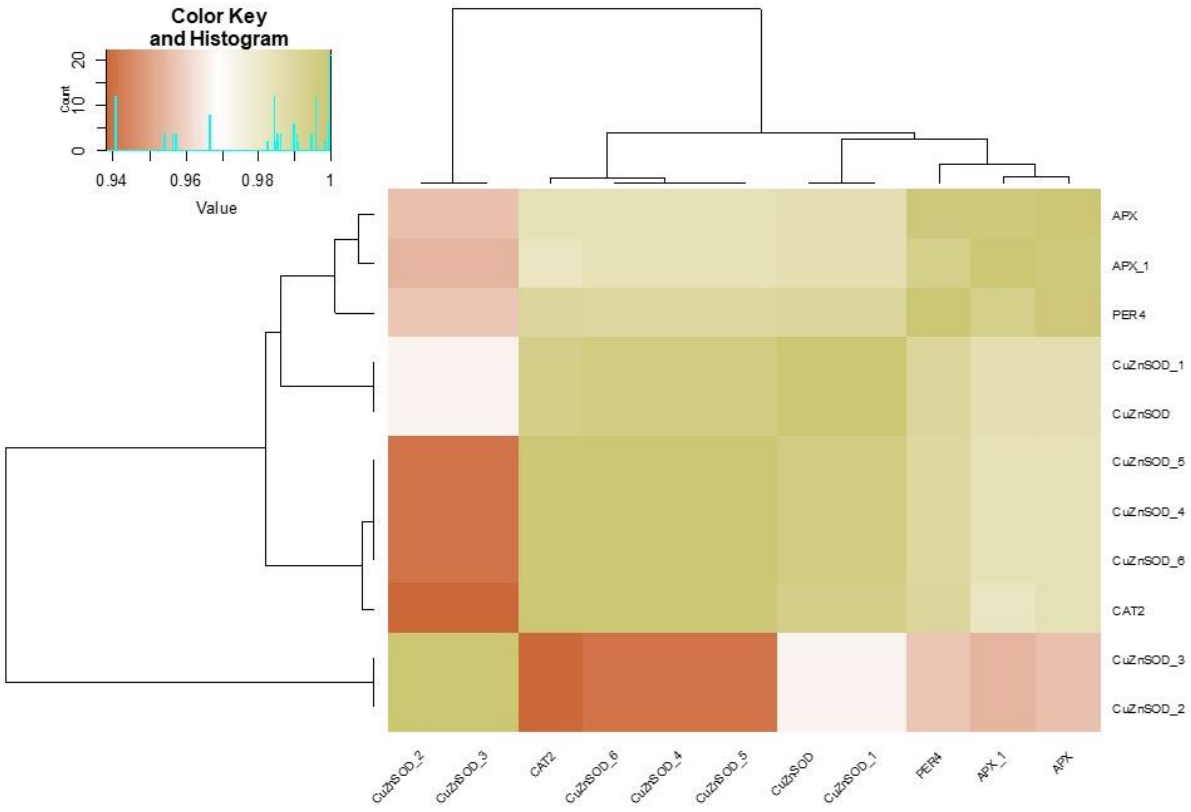

Figure 6.13 *Hierarchical cluster heat maps of down and up regulated proteins and protein-protein correlations in leaf of P.sativum at drought stress in ROS proteins. Each correlation value (based on Pearson correlation coefficient) corresponds to average of three biological replicates. Boxes were drawn to represent individual groups of DEPs. The colour key and histogram show degree of correlation.*

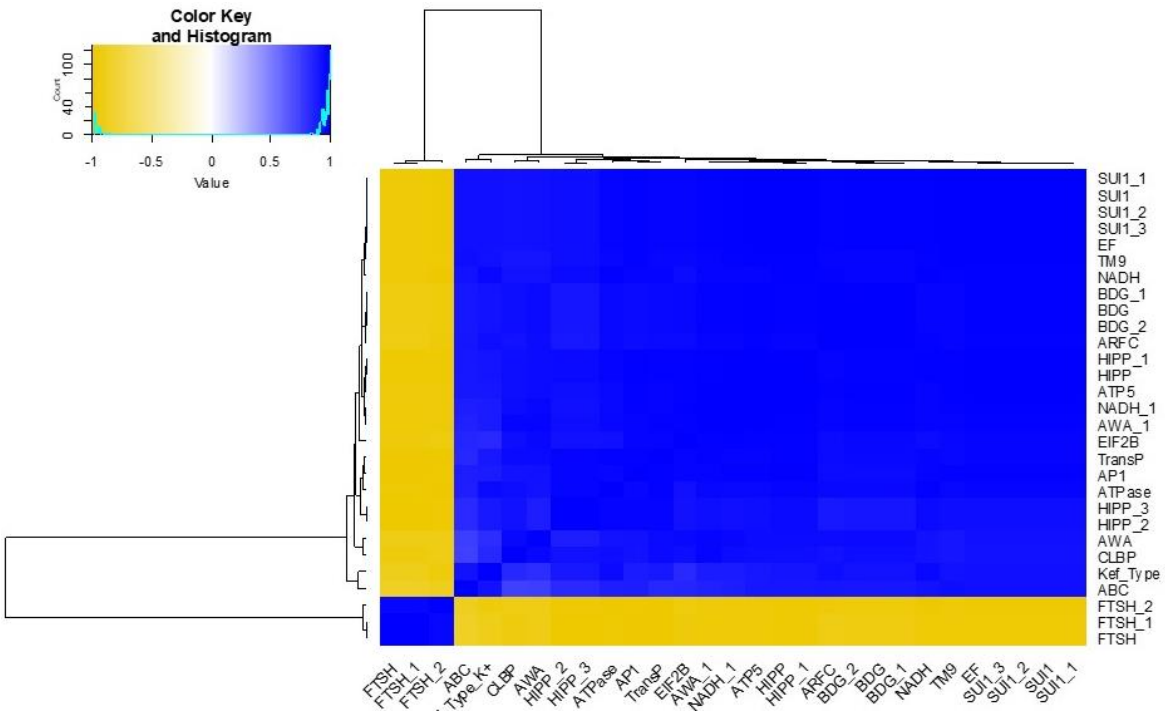

Figure 6.14 *Hierarchical cluster heat maps of down and up regulated proteins and protein-protein correlations in leaf of P.sativum at drought stress in ABC_ATP transporter proteins. Each correlation value (based on Pearson correlation coefficient) corresponds to average of three biological replicates. Boxes were drawn to represent individual groups of DEPs. The colour key and histogram show degree of correlation.*

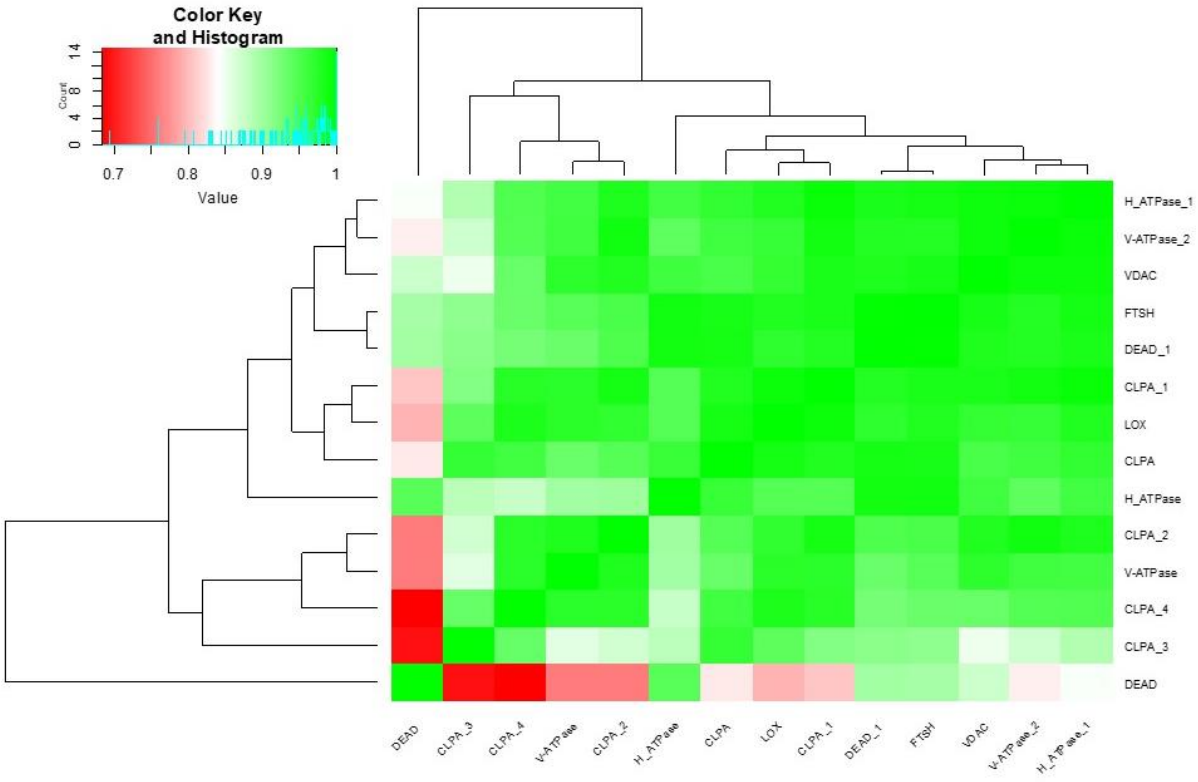

Figure 6.15 *Hierarchical cluster heat maps of down and up regulated proteins and protein-protein correlations in leaf of P.sativum at drought stress in carotenoids transporter proteins. Each correlation value (based on Pearson correlation coefficient) corresponds to average of three biological replicates. Boxes were drawn to represent individual groups of DEPs. The colour key and histogram show degree of correlation.*

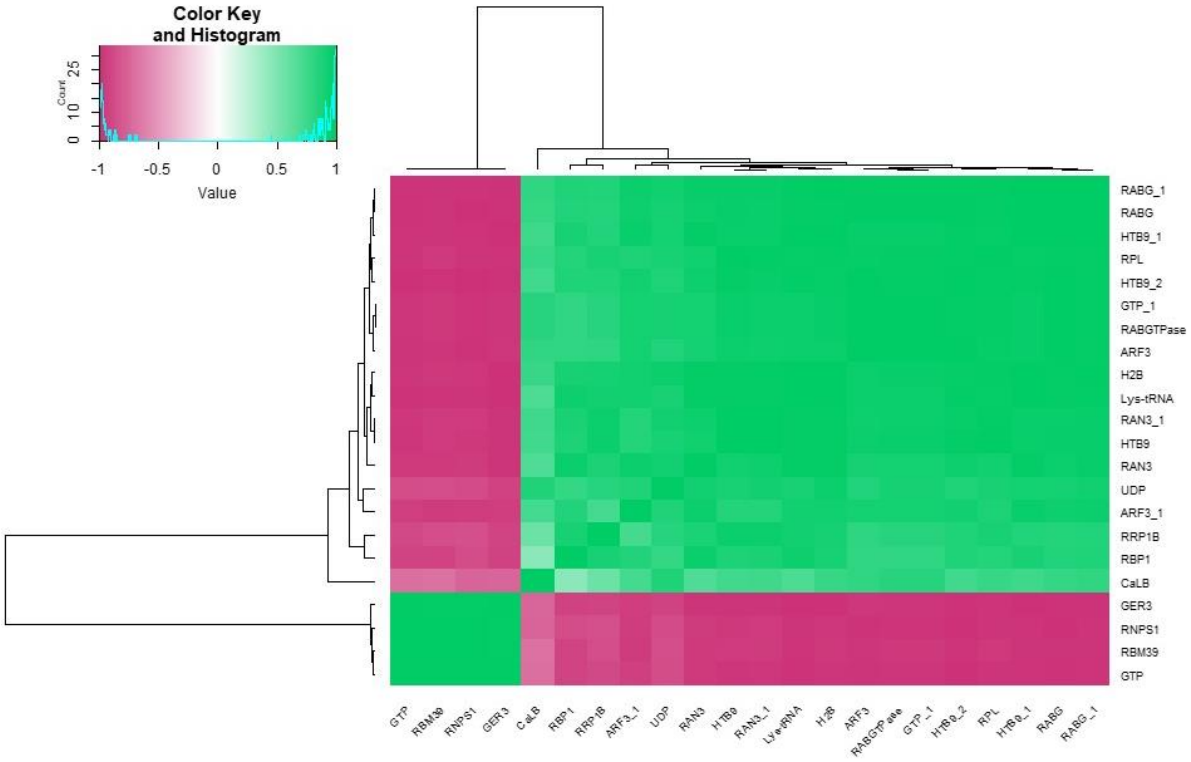

Figure 6.16 *Hierarchical cluster heat maps of down and up regulated proteins and protein-protein correlations in leaf of P.sativum at drought stress in GTP binding proteins. Each correlation value (based on Pearson correlation coefficient) corresponds to average of three biological replicates. Boxes were drawn to represent individual groups of DEPs. The colour key and histogram show degree of correlation.*

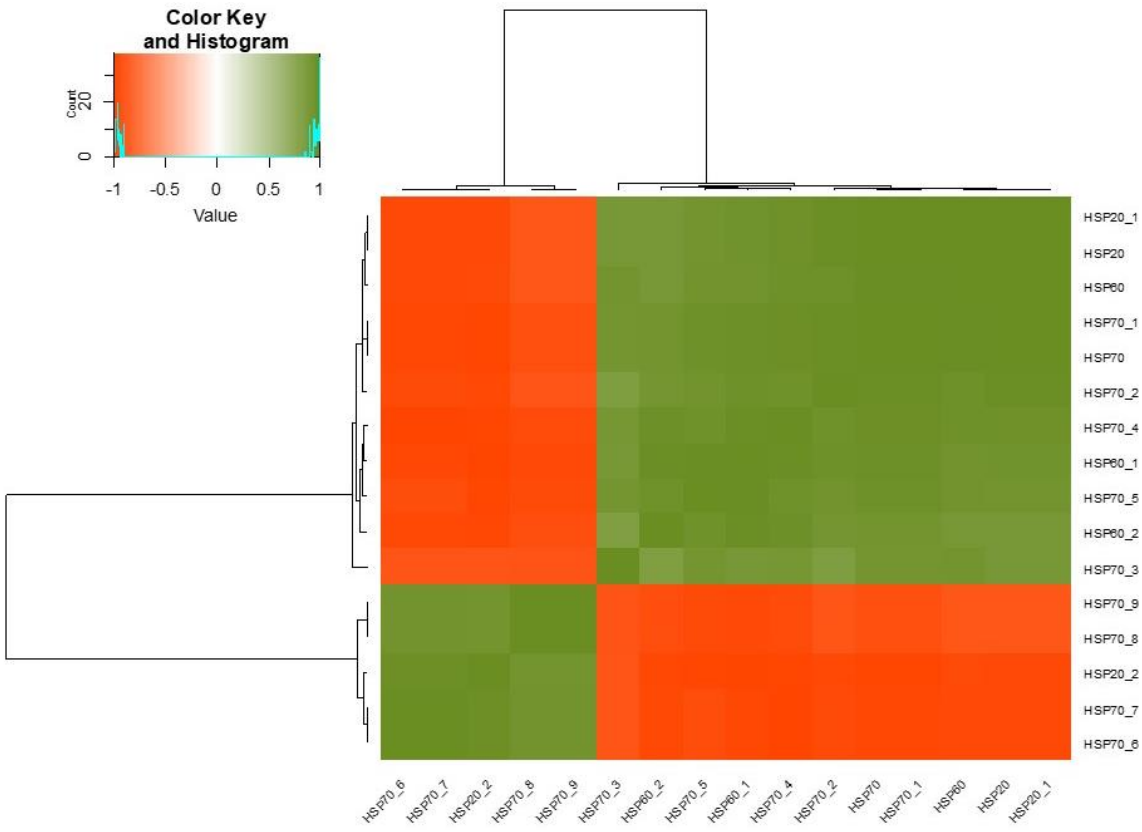

Figure 6.17 *Hierarchical cluster heat maps of down and up regulated proteins and protein-protein correlations in leaf of P.sativum at drought stress in heat shock proteins. Each correlation value (based on Pearson correlation coefficient) corresponds to average of three biological replicates. Boxes were drawn to represent individual groups of DEPs. The colour key and histogram show degree of correlation.*

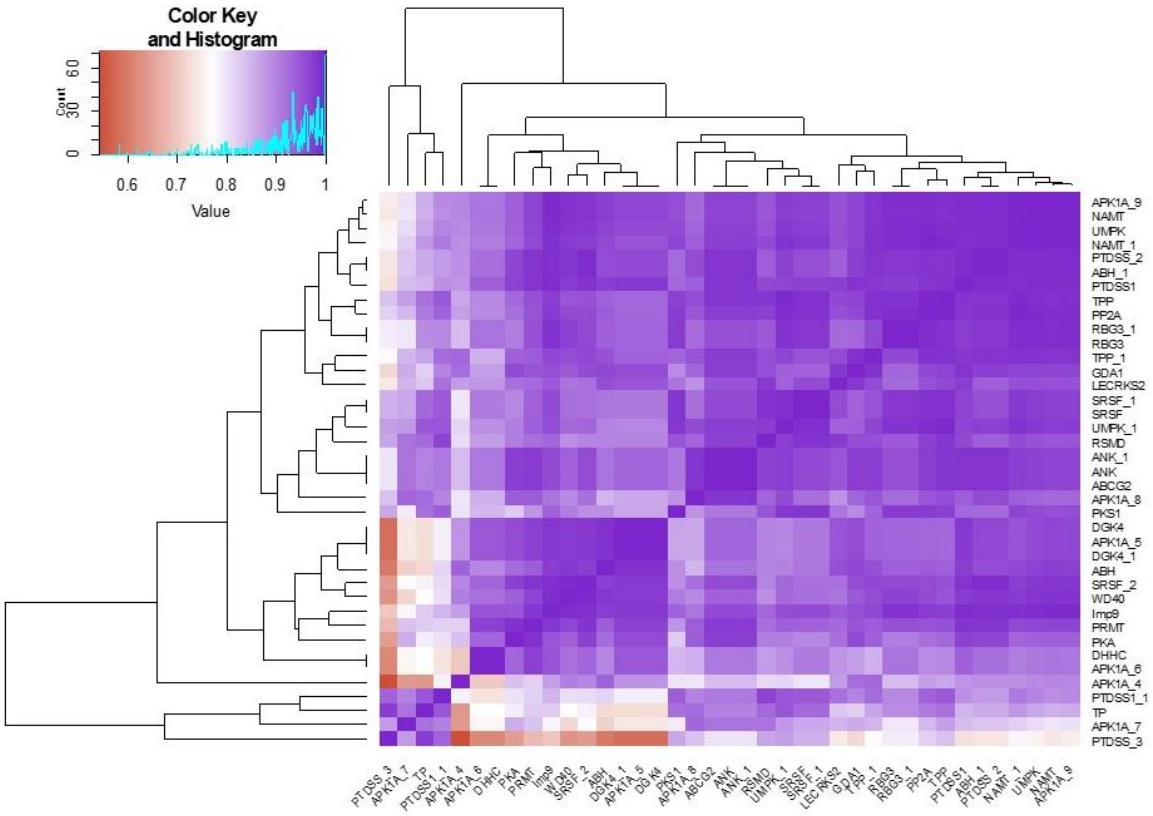

Figure 6.18 *Hierarchical cluster heat maps of down and up regulated proteins and protein-protein correlations in leaf of P.sativum at drought stress in Kinase proteins. Each correlation value (based on Pearson correlation coefficient) corresponds to average of three biological replicates. Boxes were drawn to represent individual groups of DEPs. The colour key and histogram show degree of correlation.*

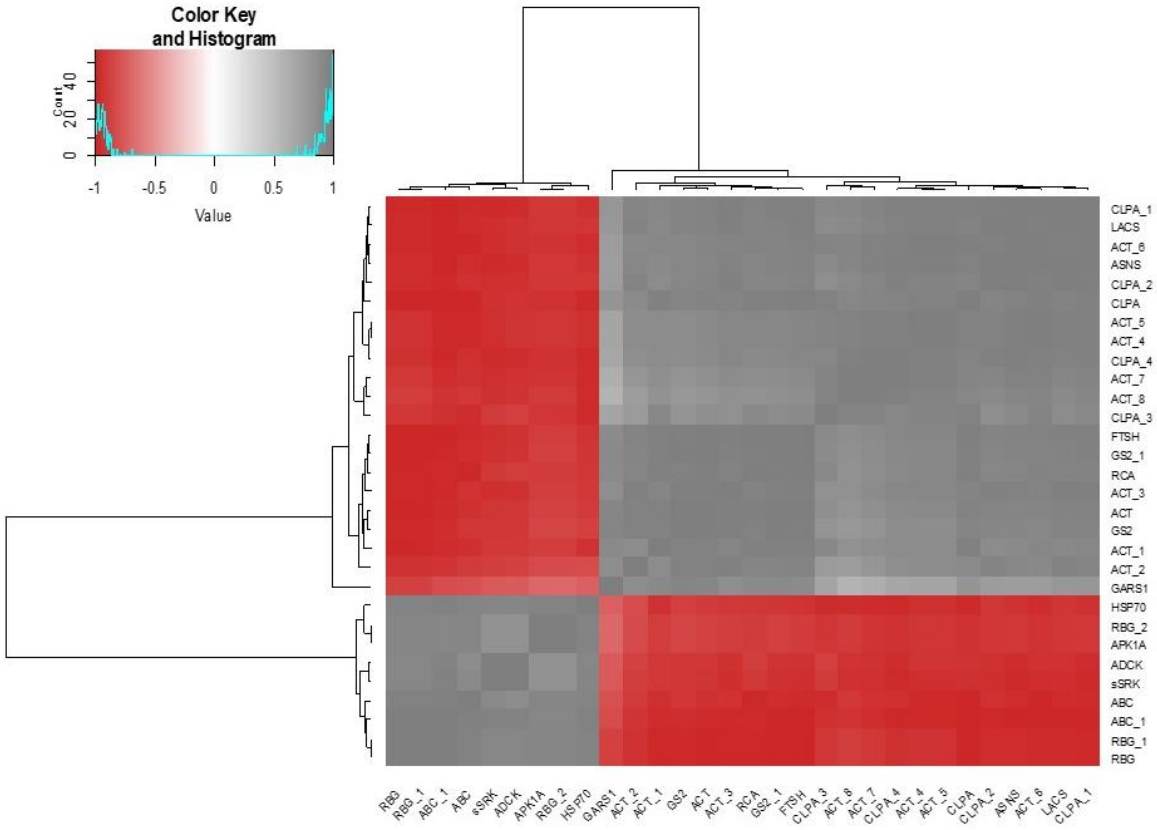

Figure 6.19 *Hierarchical cluster heat maps of down and up regulated proteins and protein-protein correlations in leaf of P.sativum at drought stress in ATP_binding proteins. Each correlation value (based on Pearson correlation coefficient) corresponds to average of three biological replicates. Boxes were drawn to represent individual groups of DEPs. The colour key and histogram show degree of correlation.*

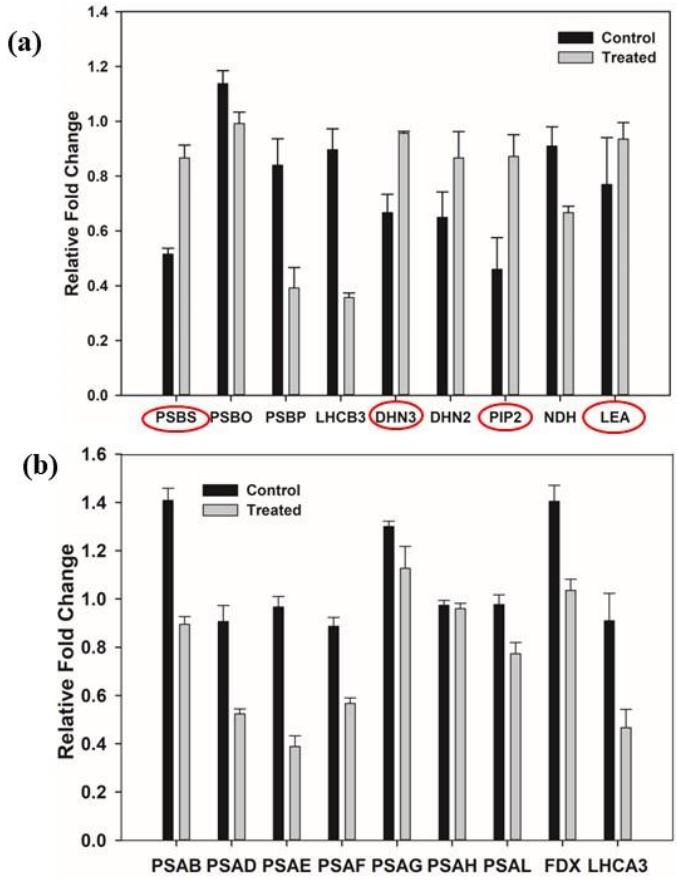

Figure 6.20 *Photosynthetic proteins obtained from iTRAQ analysis from drought stress leaf tissues from PSI, PSII and stress marker proteins.*

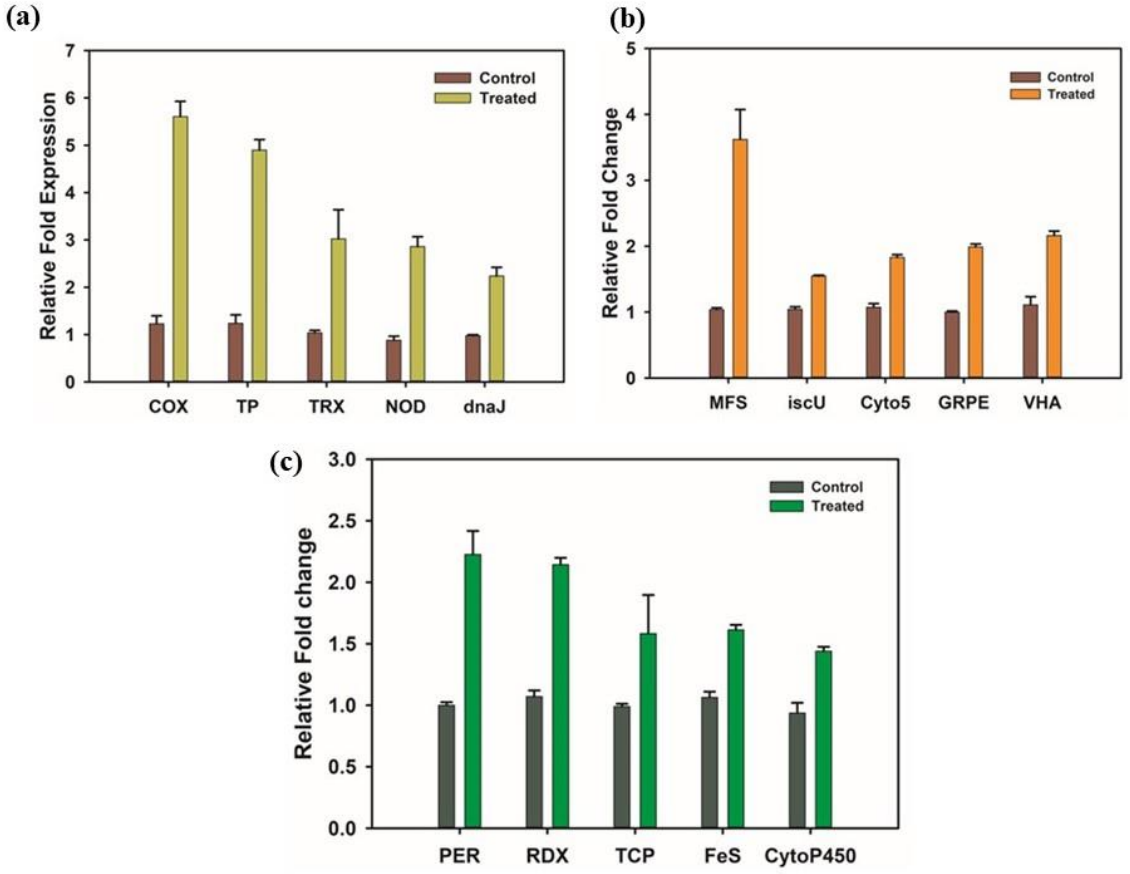

Figure 6.21 *iTRAQ proteins quantification obtained from leaf tissues of P.sativum. Most of the proteins are upregulated in drought stress (TP, TRX, dnaJ, PER, RDX).*

6.2.10 Correlation network analysis of the proteins in leaves of *P.sativum*

To explore the protein-protein interaction network, we utilized Pearson's correlation coefficient (r) with a chosen fold value of $p > 0.05$. Each data point in the correlation network was represented as a node, with circles symbolizing these nodes as individual proteins. On average, a total of 350 edges, representing neighboring interactions, were formed among the nodes. In total, six distinct networks were constructed through correlation-based network modeling, focusing on both the control and severe drought stress conditions. These networks provide insights into the interconnectedness and relationships among the proteins under different stress levels. They are classified as (ABC-ATP binding), carotenoids transporter, GTP binding, Heat shock, Kinase proteins, ROS proteins, photosynthesis and stress marker proteins. Interestingly, we observed a high degree of correlation to ascertain the level of interaction between the different proteins. Almost all the proteins showed a huge network with the neighbouring nodes.

High positive associations between the ABC-ATP transporter proteins FTSH, HIPP_3, Kef_Type_K+ are showing positive interaction with FTSH, FTSH_2, FTSH_1 and HIPP Figure 6.22. In carotenoids transporter protein specifically Figure 6.23, the DEAD_1 is showing positive interaction with VDAC, V-ATPase, CLPA_3, LOX and FTSH, but showed negative interaction with DEAD. In the leaf proteins, the correlations among the proteins in GTP binding (Figure 6.24) most of the proteins showed positive correlation (e.g GTP is showing positive interactions with RABG, RPL, RAN3, GER3 but negative interactions with RRP1B. Interestingly the heat shock proteins Figure 6.25 shows all the proteins are significant positive correlation within the proteins, e.g HSP_70 is showing positive correlation with HSP60_1, HSP20_1, HSP70_6. Kinase binding proteins (Figure 6.26) SRSF_1 is showing positive interactions and

interestingly SRSF_1 is showing positive interactions with ABCG2, ANK_1, ANK, PTDSS_1 and negative interactions with APK1A_7, PTDSS1_1, TP with PTDSS_3. In ROS proteins (Figure 6.27) significant positive interactions between the proteins were observed including Cu-ZnSOD is showing positive interactions with other antioxidants proteins like CAT2, APX, Cu-ZnSOD_6, PER4 and Cu-ZnSOD_5 and interestingly photosynthetic proteins and stress marker proteins, we monitored a significant positive correlation between the photosynthetic proteins (e.g FDX_2 is showing positive interaction with PsaD, PsaF, VDAC1 and PsaL and negative interactions with PetB, NADPH and PsaB_1. Similarly, the stress marker proteins which are drought-responsive proteins showed high positive correlation with each other (e.g PSBO is positive correlated with DHN3, PIP2 and LEA5 and negatively correlated with the DHN2, LEA_4 and PSBP_1.

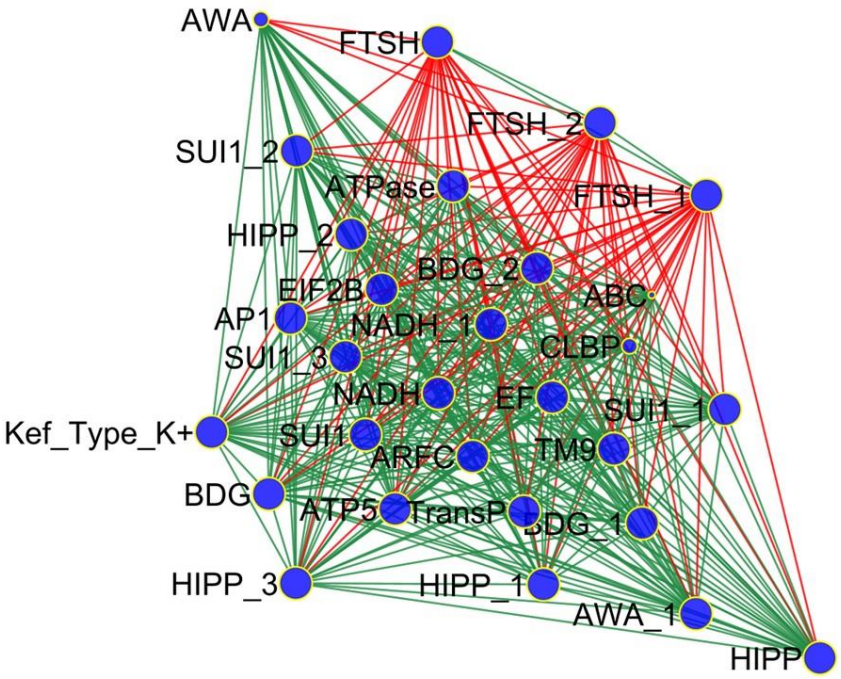

Figure 6.22 *Correlation network analysis to illustrate relationships among the ABC_ATP binding proteins with control and drought treated leaf tissues of P.sativum.*

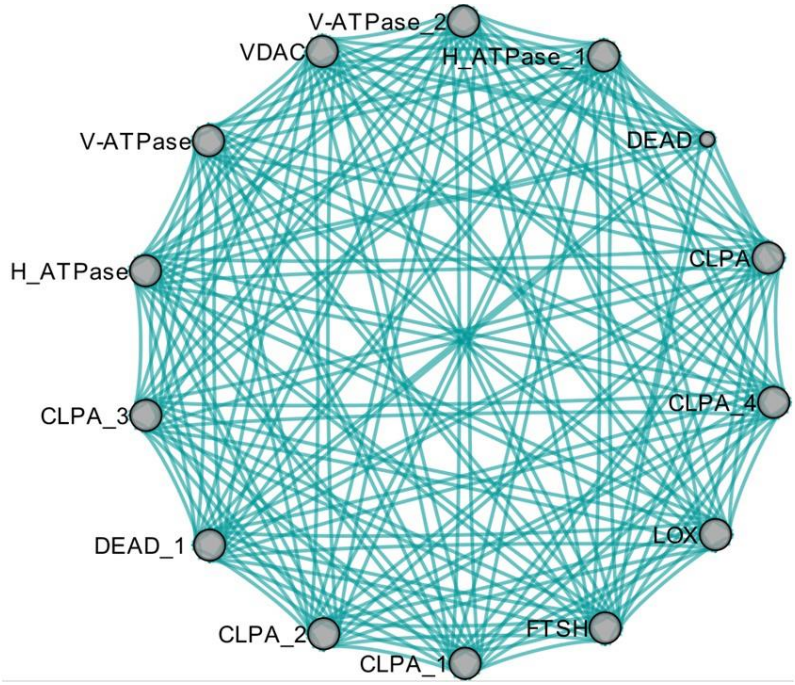

Figure 6.23 *Correlation network analysis to illustrate relationships among the carotenoids transporter proteins with control and drought treated leaf tissues of P.sativum.*

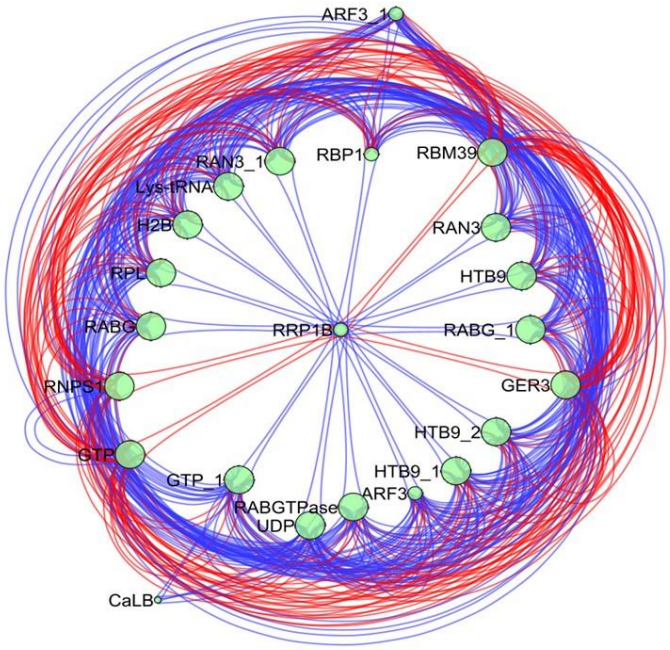

Figure 6.24 *Correlation network analysis to illustrate relationships among the GTP binding proteins with control and drought treated leaf tissues of P.sativum.*

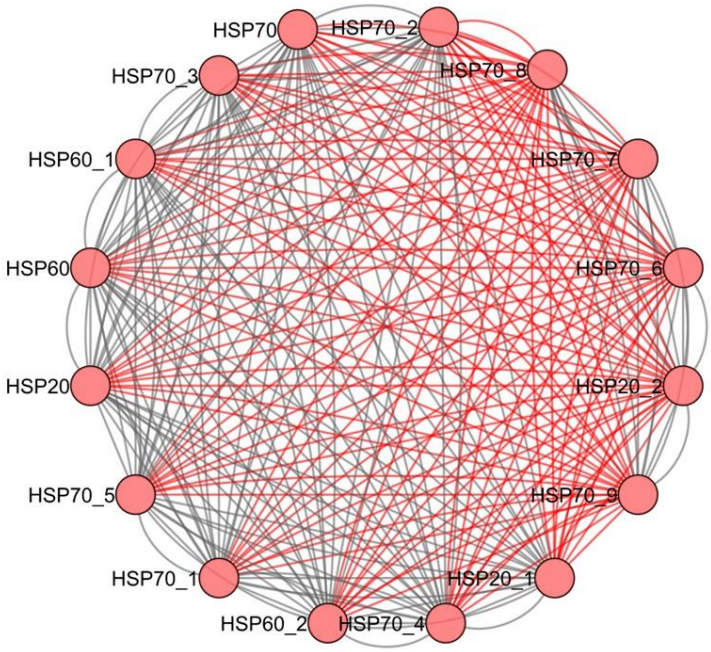

Figure 6.25 *Correlation network analysis to illustrate relationships among the Heat shock proteins with control and drought treated leaf tissues of P.sativum.*

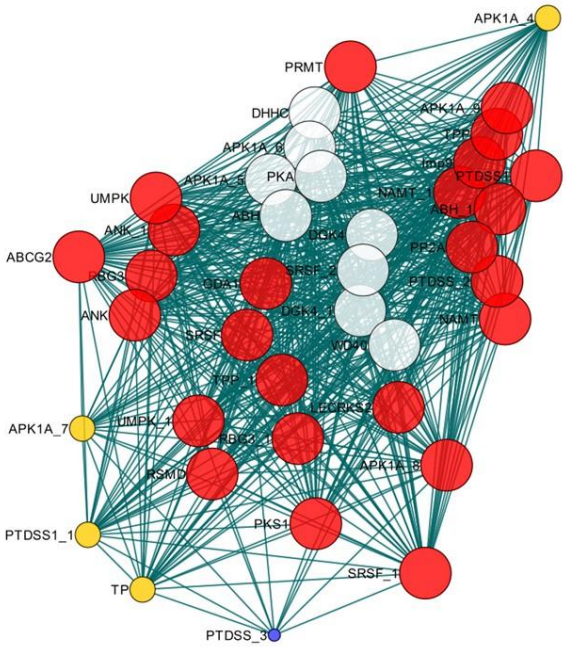

Figure 6.26 *Correlation network analysis to illustrate relationships among the Kinase binding proteins with control and drought treated leaf tissues of P.sativum.*

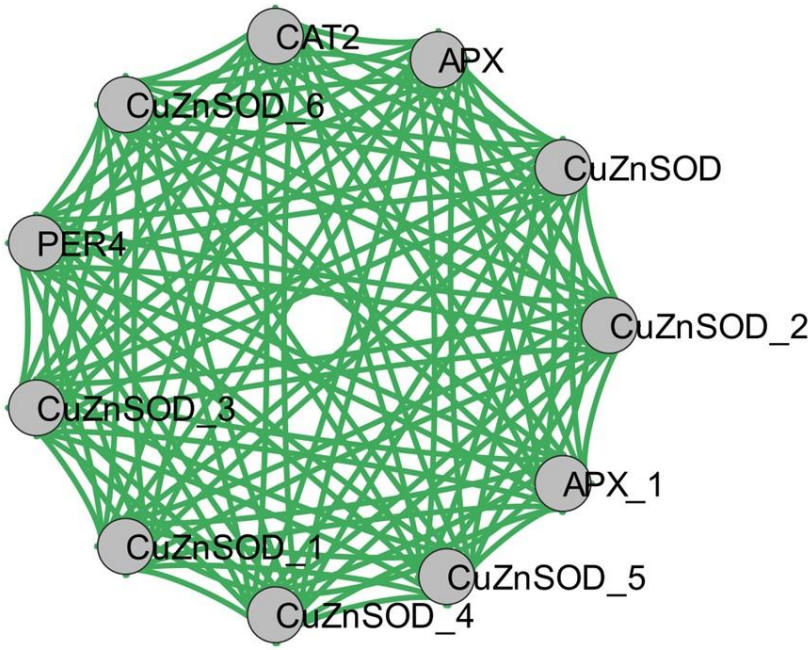

Figure 6.27 *Correlation network analysis to illustrate relationships among the ROS proteins with control and drought treated leaf tissues of P.sativum.*

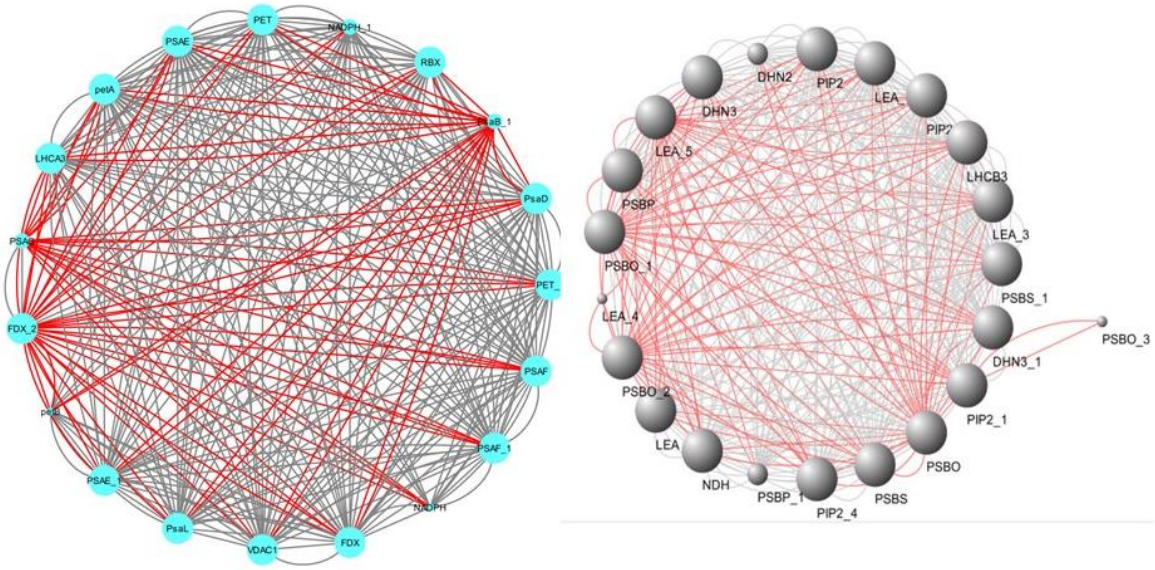

Figure 6.28 *Network analysis among the photosynthetic and stress marker proteins with the control and treated leaf tissues of P.sativum.*

6.2.11 Metabolite analysis of *P.sativum* leaf under drought stress

GC-MS was used to examine the metabolite differential expression in the leaves of control, drought, and recoveryplants. A total of 25 metabolites were found and divided into three groups: carbohydrate (15), polyols (4) and other metabolites (6). (Figure 6.29). Polyols and sugars such as trehalose, erythritol, sucrose, pinitol, galactose, glucose, mannoic acid, fructose, galactose, arabitol, and mannobiose were shown to be upregulated plants grown under drought stress, (Figure 6.30).

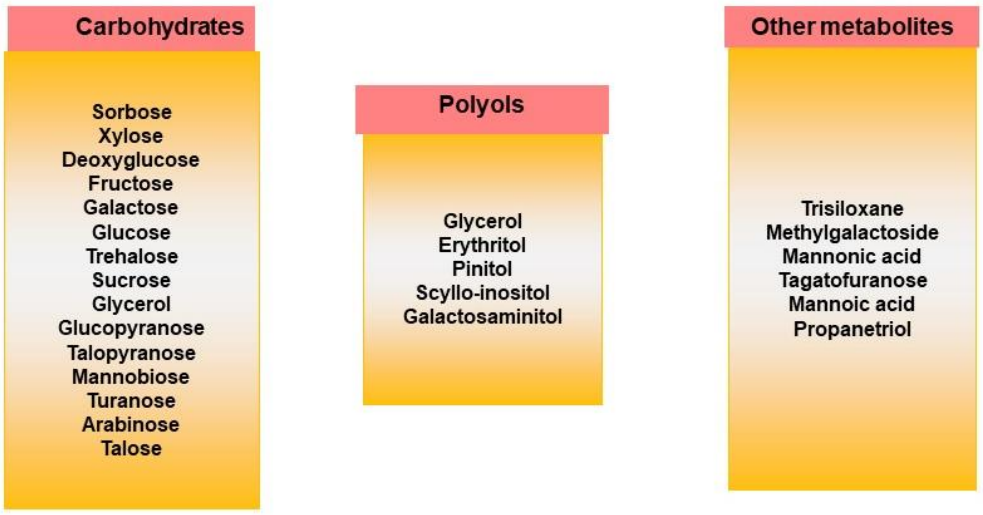

Figure 6.29 *Metabolites changes in leaves were measured by using GC-MS analysis. Among all 25 metabolites were identified and classified into three types. These are carbohydrate, polyols and other metabolites.*

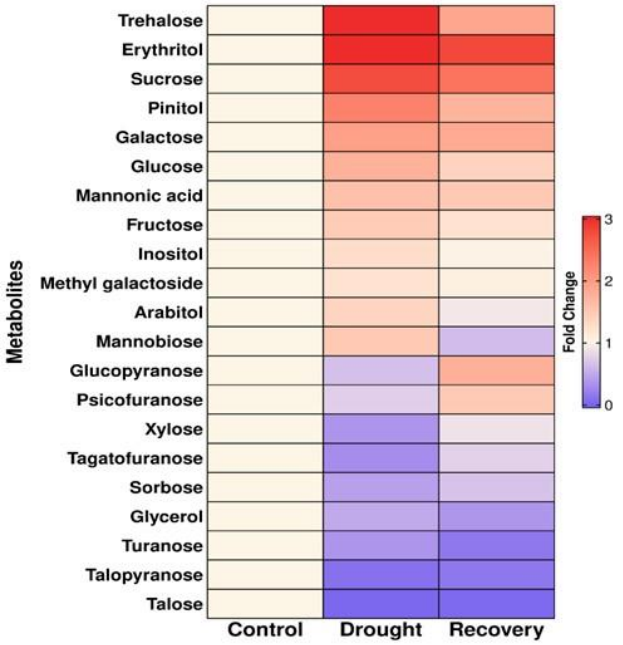

Figure 6.30 *Heat map of hierarchical clustering of metabolite-metabolite correlations in leaves of P.sativum under drought stress. Each correlation value (based on Pearson correlation coefficient) corresponds to average of three biological replicates.*

To evaluate the variation between and among the samples, a PCA analysis was used. The PCA score plot demonstrated how the drought and recovery samples were different from one another due to their geographic distribution in various quadrants. However, the replications of control, drought and recovery were grouped together closely, The results suggest that drought stress had a significant impact on the composition of the samples (Figure 6.31).

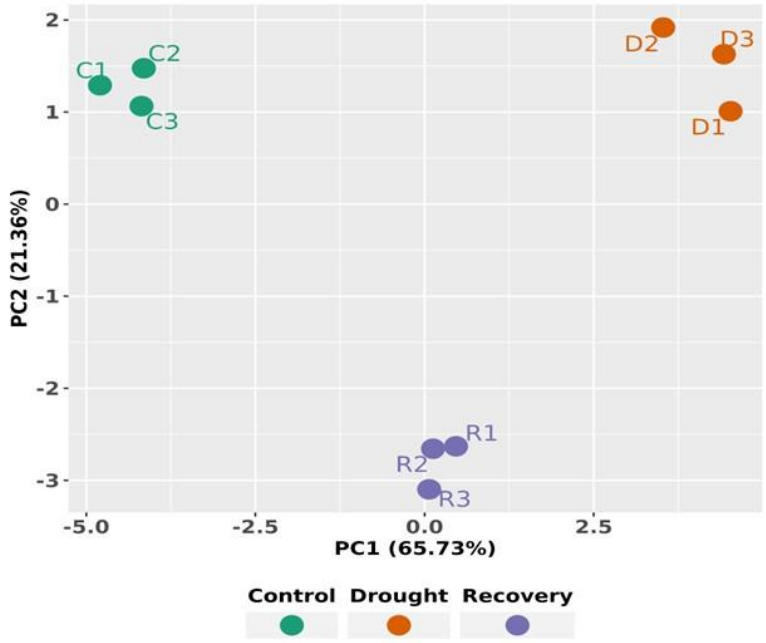

Figure 6.31 *PCA analysis of metabolites in control, drought and recovery grown P.sativum.*

6.2.12 Differential expression of genes associated with TCA cycle under drought

To evaluate, I looked at a few important TCA cycle genes to determine how our metabolomic data and experimental correlated with each other. Further, the relative mRNA expression of TCA cycle genes (FUM1, OGD2, DLA2, MDH1, MDH5, IDH3, OGD3, DLD1, DLD2, MDH3, ACH1, ACS1, CIS2, SDH2, IDH2, SDH3, SDH1, MDH2, PDC3, SCLB1, and ACS3) and found that FUM1, OGD2, and MDH1 were significantly upregulated (2-fold) under drought stress conditions. These TCA cycle genes are upregulated in drought-treated plants, which suggests a compensatory mechanism to maintain energy output. Fascinatingly, recovery observed a 6-fold rise in FUM1 expression, showing a proactive reaction to stress and to re-establish normal metabolic function (Figure 6.32). However, certain TCA cycle genes remained downregulated in recovery plants, indicating a limited response to dryness.

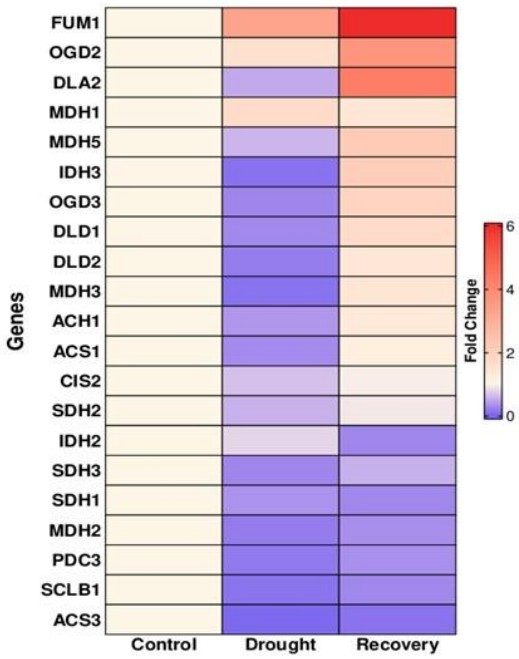

Figure 6.32 *The relative content of the TCA cycle intermediate of control, drought and recovery. The values shown are the means of three independent experiments. The genes consists of, Citrate synthase (CIS2), aconitase (ACS1 and ACS3), 2-oxoglutarate (OGD2 and OGD3) acetyl-CoA hydrolase (ACH1) fumarate (FUM1), malate dehydrogenase (MDH1), isocitrate dehydrogenase (IDH3), isocitrate dehydrogenase (IDH2), SCLB1 pyruvate dehydrogenase complexes (PDC3), D-lactate dehydrogenase (DLD1).*

6.3 Discussion

In this study, *P. sativum*, a non-model legume crop with sequencing data not readily available in public databases, had its entire transcriptome characterised using the Illumina NextSeq platform (Figure 6.1). To examine the temporal expression patterns in *P. sativum*, we concentrated on genes associated with the photosynthesis, ROS, antioxidant, and sugar biosynthesis pathways. We are able to characterize the unique transcripts and abundant transcripts by synthesising normalized cDNA from leaf total RNA. 92 percent of the sequenced raw data annotated into functional transcripts associated with critical metabolic pathways in leaves. *P. sativum* transcripts were found to have a GC content of 50%, which was higher than that of J. curcas (43%) and only marginally lower than that of C. sativa transcripts (49 %). The complexity and diversity

of the *P. sativum* transcriptome sequence in comparison to other species can be seen in the differential in GC content. Furthermore, many proteins connected to various metabolic pathways were discovered through the annotation of transcripts to UniProt. This annotation technique aided in revealing the transcripts' functional information and provided information on the roles played by these proteins in various *P. sativum* metabolic processes. Additionally, number of transcription factors that are crucial in the control of gene expression in diverse metabolic pathways, including ABA responsive element binding factor and heat shock transcription factor, actually these transcripts are important in abiotic stress which acts as a protection mechanisms for plants during the drought stress.

GO enrichment analysis was conducted on DEGs with a fold change over 1.5. Cellular component, molecular function, and biological process were the three functional categories used to categorise the upregulated and downregulated transcripts. Specifically, parts of the photosystem and proteins found in the thylakoid membrane were localised in the chloroplast, were more than 50% of the transcripts categorised as cellular components were also found. Another major percentage of the transcriptome displayed an increase in nucleus and nucleolus localization, pointing to cellular rearrangement.

Transmembrane transport is critical during drought, and the activity of the transporter and symporter genes is particularly significant. Utilizing KOBAS software's pathway enrichment analysis, it was possible to pinpoint particular pathways that show notable alterations in both upregulated and downregulated transcripts. Carbon fixation, secondary metabolite production, carotenoid biosynthesis, and fatty acid metabolism showed the most significant modifications of these pathways (Figures 6.3). Additionally, pathway enrichment and gene ontology (GO) analysis revealed an

effective chloroplast signalling system in response to drought, operating as an important environmental sensor. The GO analysis also revealed modifications in the amounts of the photosystem subunits, which are probably crucial in drought acclimation. Furthermore, the acclimatisation and repair processes are aided by the increased levels of carotenoid biosynthesis and secondary metabolite synthesis, which is compatible with the RT-PCR gene results.

Analysis of DEGs reveals that the transcript levels of genes related to PSI and PSII generally trend toward mild downregulation, with the thylakoid transcript exhibiting a considerable rise (Figure 6.4). Variable photosynthetic organisms exhibit different transcriptional control of photosystem-related proteins for ecological and evolutionary reasons. For instance, it has been observed that salt stress reduces the transcriptional expression of PSI light-harvesting proteins in the model organism *C. reinhardtii* (Wang et al., 2018).

Dehydrins, Aquaporins, and PSBS were found to be the most elevated transcripts after the photosynthetic transcripts in PSI and II from the DEGs were analysed. The majority of PSI light-harvesting proteins, however, displayed a moderate downregulation. The functional implication of their absence in the current study could be for reducing association in certain conditions or for promoting specific remodelling and distinct interactions under certain conditions. In other organisms, missing subunits function in associating additional Lhc proteins under certain physiological conditions (Figure 6.4).

Immunoblotting was used to analyse the PS I and PS II subunits, and the results showed that PsaA degrades more quickly than PsaB while PsaF is unaffected. Furthermore, the LHCs' expression levels of Lhca2 and Lhca1 were lowered, which

may be related to oxidative damage (Figure 3.12 and 3.13). These outcomes agree with the findings of our RT-PCR and western blotting experiments (Figure 6.5).

One vital element of PSII that is crucial to the photolysis of water is the oxygen evolving complex (OEC). Both PSBO and PSBP displayed a moderate downregulation in our study (Figure 6.4c), which is in line with the western blot findings and RT-PCR. Two extrinsic OEC subunits called PSBO and PSBP are important in binding cofactors like calcium (Ca^-) and chloride (Cl^-) ions (Mayfield et al., 1989).

Studies have shown that abiotic and biotic stress conditions can cause crosstalk between ROS and calcium signalling pathways in cells (Jalmi et al., 2018; Wei et al., 2019). Observing the raised antioxidant enzymes, both the organelles' mitochondria and chloroplast accommodate an efficient antioxidant network to minimize the deleterious effect of excess accumulated ROS and to rebalance the redox state of the internal environment (cite). In plants, the intracellular calcium level-activated antioxidant system has been studied in several plants. Increased calmodulin calcium-dependent kinase (CDK), calcium load activated calcium channel, calcium-sensing protein transcript accumulation brings the idea of intracellular elevated calcium level in Pisum under drought (Dubrovina et al., 2017; Zhu et al., 2020). It is widely known that calcium has a role in plants in the activation of antioxidant enzymes (Zhang et al., 2015). We found that during drought stress, calmodulin and calcium-dependent kinase transcript levels (CDPK3, CDPK13 and CDPK32) increased in *P. sativum* shwing upregulation of 6-fold change in RT-PCR data and the same results are in agreement with salt stress (Marriboina et al., 2021) suggesting that raised calcium levels may be involved in the activation of the antioxidant system in this species (Figure 6.5b).

The calcium-sensing protein calmodulin is extensively distributed and functions as a signalling molecule in a number of physiological processes, including plant

responses to abiotic stress. A important component of calcium-mediated signalling systems that control a variety of downstream activities, CDPKs exhibit a mild increase in response to drought stress. ROS molecule equilibrium is essential for preserving cellular health. Role in controlling ROS levels of calcium-calmodulin signalling. Studies shows that the activation of enzymatic and non-enzymatic ROS scavenging mechanisms that regulate H_2O_2 levels is mediated by peroxisomal Ca^{2+} (Costa et al., 2010). Additionally, under drought and salinity stress conditions in *A. thaliana*, the rise of calcium levels and associated signalling processes are essential (Knight et al., 1997). Using isobaric tags for relative and absolute quantification (iTRAQ), the proteome of entire leaf samples from control and drought-treated *P. sativum* plants was examined. The leaf sample proteins had 4020 different protein species, according to the iTRAQ analysis. 1244 proteins out of these were downregulated, 972 were upregulated, and 1804 were unaltered. The proteins were divided into many functional groups, such as those involved in glucose metabolism, kinase activity, GTP binding, ABC-ATP transport, proteasomal activity, translation, carotenoid activity, PSII-LHCII, photosynthetic activity, and heat shock activity.

Additionally, we used GO-based study of the global proteome modifications in *P. sativum* using computational tools from the R programme, which facilitated its representation in network and visual graphical representations and allowed for a more thorough comprehension of the complicated dataset. Notably, the data showed that most protein species remained unaltered (about 85%) in response to drought stress, highlighting the dynamic character of the leaf proteome and its crucial function in maintaining cellular processes in the face of altering environmental cues.

The downregulation of PSII and PSI regulatory subunits as well as proteins involved in photosynthetic electron transport may be the cause of this decline in

photosynthesis. For instance, the iron-sulfur subunit of the cyto b6f complex and cytochrome b559 of PSII were both downregulated. However, stress signal proteins such DHN3, PIP2, LEA, and PSBS were more prevalent and immunoblot analysis of all PSII, PSI, and associated light-harvesting complex proteins to further corroborate to my findings, with our western blot and RT-PCR data. Additionally, these results were supported by our network analysis of genes involved in photosynthesis (Figure 6.28).

In support to dehydration stress, a substantial rise in carbohydrate, especially fructose and glucose. Dehydration may have enhanced proteolysis in addition to inducing autophagy, which speeds up the breakdown of subcellular structures when the availability of carbohydrates is compromised. The majority of the proteins involved in photosynthesis, metabolic pathways, glycolysis, protein synthesis, cytoskeleton assembly, were downregulated. In response to drought stress, the majority of the proteins (COX, TP, TRX, dnaJ, RDX, and TCP) displayed steady or notable overexpression (Figure 6.21). Trehalose is a sugar that can function as an osmoprotectant in cells, and TP is an enzyme that is involved in its manufacture. some plant species' TP expression and activity can rise in response to drought stress, offering defence against drought stress. Protein called TRX can serve as a redox regulator (Lee et al., 2013) ensuring that other proteins continue to operate as intended. TRX expression and activity may be increased in response to drought stress, shielding proteins from oxidative stress-related protein degradation. A particular class of molecular chaperone called DnaJ aids in the stability and proper folding of other proteins. Some plant species have demonstrated increased DnaJ expression in response to drought stress, which might aid in preventing denaturation or unfolding of other proteins. The protein RDX is essential for the growth and development of plants. Studies have revealed that RDX expression may be elevated in response to drought

stress in some plant species, even if the precise role of RDX in the drought stress response is not fully characterised (Figures 6.21).

Our iTRAQ data revealed that *P. sativum* demonstrated an elevation of different secondary metabolism-related proteins in response to drought, which may aid in protecting against ROS and preserving cell wall turgidity. During drought, the activation of proteins involved in the carbohydrate metabolism, which may replace the fast energy supplies needed to maintain essential metabolic function in the leaves. Additionally, overexpression of GTP-binding and phytohormone-related leaf proteins, both of have been linked to active long-distance signalling.

Previous studies have indicated that dehydrins, which are extremely hydrophilic proteins and belong to the group II LEA proteins, have a protective role in the plant stress response (Liu et al., 2017). In the present work, a 20 kDa dehydrin that is found in the thylakoid membrane was found to have both phosphorylated (DHN1) and non-phosphorylated (DHN2) isoforms (Figure 6.20).

Under unfavourable environmental conditions, increased production of the chloroplast proteins may aid to maintain cellular redox status and shield cellular organelles from oxidative stress damage. It is believed that *P. sativum* chloroplast viability may be essential for preserving the leaf in drought-like conditions. *P. sativum* promotes the expression of a large number of the chaperone proteins (HSP20, HSP70, and HSP40) in the leaf under drought stress to stop the misfolding of proteins by drought stress. Furthermore, during drought stress (Sofo et al., 2015) revealed a significant up-regulation of antioxidant enzymes in *P. sativum* leaf, including APX1, CAT4, and MDAR, to lessen ROS formation inside the cell. In addition, *P. sativum* produced a large number of minor G family proteins, including GAP, RABG, GTP, and ARF3 (Figure 6.16). Under drought stress, the altered expression of these proteins may

promote cell wall reinforcement, cell, and tissue morphogenesis, which may aid in plant development (Cheval et al., 2013; Zeng et al., 2015). In conclusion, this work examined alterations in the leaf proteome that are essential for preserving long-term leaf physiology.

The study investigated the regulation of 25 primary metabolites, including sugars, polyols, and other metabolites, under drought stress conditions. The investigation revealed that alterations in metabolite levels accurately mirrored the redox status of the cell, indicating that the plant was experiencing stress. Oxidative stress was frequently assessed and linked to changes in metabolites as part of the plant's response to stress (Noctor et al., 2015). Additionally, amino acids, compatible solutes and TCA cycle intermediates were among the metabolites which shows more effects during drought stress (Baxter et al., 2007).

As depicted in (Figure 6.30) carbohydrates are the main by-products of photosynthesis (Blechschmidt-Schneider et al., 1989). According to the study, compared to the control condition, the fructose availability increased more noticeably under the drought treatment. According to prior research, this fructose buildup during drought stress may be directed toward the production of fatty acids. However, during the period of recovery, fructose levels did not significantly change. The rise in fructose during drought conditions may make it possible to use renewable biomass as an alternate source of carbon for cellular metabolism.

The majority of studies on drought stress in plants have revealed, according to (Farooq et al., 2009), that sugars, particularly sucrose, are increased in response to drought conditions as part of the defence mechanism and also serve as osmoprotectant. Soluble sugars like sucrose, glucose, and fructose were shown to be increased in the leaves of rice varieties (Xu et al., 2015) that are susceptible to drought, as opposed to

being decreased in the leaves of resistant or tolerant types. Specifically, during the vegetative stages of growth (Silvente et al., 2012) no appreciable differences levels of sucrose between drought and control plants in soybean, suggesting that sugars may not be a significant factor in a plant's osmoprotection under drought stress. However, the present study found that during extreme drought stress, sucrose levels increased, suggesting that sucrose may be crucial for osmoprotection. Additionally, in response to water stress and decreased photosynthesis, metabolites such trehalose, erythritol, inositol, sucrose, fructose, and glucose are increased during drought stress. This suggests that they are acting as an energy source and osmoprotectant. Sugars were elevated in drought-treated plants continued to be upregulated during the recovery period, whereas other metabolites tried to revert to control levels. In contrast to the control plants, sugars were still downregulated in the recovery plants.

The manufacture of glucose, amino acids, and fatty acids involve the usage of TCA intermediates, which is a critical component of the plant metabolic process. In response to drought stress, a rise in TCA cycle intermediates (TCA, FA, MA, and CA) was seen. This supports real-time PCR results that the genes FUM1, OGD2, and MHD1 were also upregulated (Figure 6.32). In addition, it was noted that under drought stress, DLA2, was enhanced. A rise in the carbon flow from glycolysis into the TCA cycle, which increases the generation of reducing powers like NADH and ATP, may be the cause of the rise in TCA cycle intermediates. Furthermore, acetyl-CoA serves multiple purposes in the cell. It can be utilized for gluconeogenesis, supporting various anabolic activities, generating NADH for the respiratory chain, and producing ATP in the Krebs cycle through the glyoxylate cycle (Plancke et al., 2014). This shows that the TCA cycle genes is essential for generating the energy needed to produce defence chemicals to combat the oxidative stress during drought stress. Our research findings indicate that

the TCA cycle serves a dual role. It not only helps maintain stable oxidative levels within the cells but also releases precursors necessary for amino acid synthesis by enabling the opening of the malate, fumarate, and citrate channels. This highlights the significance of the TCA cycle in supporting cellular metabolism and the biosynthesis of essential molecules (such as amino acids).

The findings of the study imply that to deal with drought effects of stress, it could be required to maintain carbohydrates during the process. The persistent overexpression of sugars in recovery plants may be a sign that the plant is still making physiological and metabolic adaptations to go back to normal development and growth. A constant osmoticum may be provided at the cellular level by higher quantities of polyols such erythritol and pinitol in addition to carbohydrates to maintain the osmotic imbalance brought on by drought stress. Under drought stress, this is essential to keep *P. sativum* pH balance, cell wall integrity, and osmotic balance in check.

6.4 Conclusion

The majority of photosynthetic genes are downregulated, according to my transcriptome data, whereas stress signal genes, such as dehydrins, PSBS, heat shock, LEA, ROS, and aquaporins, are upregulated. The direct and indirect effect of hypersaline conditions imposes a robust retrograde signaling mechanism by a possible crosstalk between the ROS and calcium signaling mechanism The majority of transcription factors, including ABA responsive element, heat shock transcription factor were upregulated in drought stress, which can cause plants to activate a photoprotection mechanism and aid in the photoacclimation process. According to iTRAQ proteome analysis, some photosynthesis-related proteins (PSI-LHCI, PSII-LHCII), ROS proteins, and heat shock proteins were induced to improve leaf performance under extreme drought circumstances, and some of the proteins (TP, TRX, dnaJ, and VHA) remain stable. In

P. sativum under drought stress, increased levels of carbohydrates such as trehalose, sucrose, galactose, and polyols (erythritol, pinitol) may provide a osmoticum at the cellular level and to mitigate the osmotic imbalance raised by the drought stress. This is crucial for maintaining pH balance, cell wall integrity, and osmotic balance. All these combined approach (transcriptomics, proteomics and metabolomics) mechanisms play synergistically to rebalance the photosynthetic apparatus's redox state and help cope with the drought stress in Pisum. We hope that the genes, protein and metabolite expressed in Pisum to the drought condition could be transferred to the other plants to withstand the high drought conditions and improve crop yield.

Chapter 7

Summary and Conclusions

7. Summary and Conclusion

The thesis has emphasized the effect of drought stress on plant growth, photosynthetic performance, redox status, biochemical characterization of photosynthetic supercomplexes and its macromolecular structure, lipid content, carotenoid content, composition of fatty acid, membrane lipids and changes in proteome, transcriptome and metabolome content from leaf tissues of *P.sativum* plant.

The first objective represents a comparative picture of the physiological, biochemical, biophysical, and molecular level changes caused by drought in 14-day-old *P. sativum* seedlings. The work focused on the drought in the photosynthesis of (*P.sativum*). The progressive drought is deleterious to the plants, and the yield of biomass and production of seeds reduces significantly. I understood that the Pea plants keep the memory of drought stress and flowers faster to finish the life cycle. In this study, the protection mechanism was identified against drought, i.e., one of the crucial mechanisms called NPQ, and specifically, a PSBS subunit of photosystem (PS) II was increased. Further, specific drought markers were identified like dehydrins, aquaporins and some of the PSI, PSII and light-harvesting complex proteins were stable during the drought stress. Moreover, the light-harvesting complexes (LHCs), and some of the PSI and PSII core proteins were disassembled in drought conditions, whereas these complexes were reassociated during recovery. My detailed studies show that drought-induced dissociation of thylakoid supercomplexes and these changes were reversible by the *de novo* synthesis.

The second objective was to investigate the pigment-pigment and pigment-protein interactions and were changed due to the differential expression of pigments with supercomplexes. Since an increase in zeaxanthin could lead to a change in protein

conformation, it is evident that LHCII trimer conformation is significantly modified than other supercomplexes. Therefore, the lack of zeaxanthin and differential expressions of other pigments (lutein and violaxanthin) induced change in the macromolecular organization of thylakoid supercomplexes, which ultimately involved photoprotection.

The third objective describes that biomass is decrease in drought, and interestingly carbohydrate, starch, reducing sugar, and proline content is increased, which serve as osmoprotectant but also provide nonenzymatic ROS scavenging protection under drought stress. My results suggest that an increase in TAG accumulation is accompanied by substantial chloroplast membrane degradation in drought. Membrane lipids were dissociated into individual fatty acids, and they are involved in the recycling of TAG. In drought conditions, the elevated levels of ROS can serve a dual role. Firstly, they can function as signals to activate lipid biosynthesis, triggering the production of lipids. Secondly, ROS can act as inducers of autophagy, a process that facilitates the recycling of cellular components, ultimately contributing to lipid production.

The fourth objective describes about the transcriptomics data revealed that most of the photosynthetic genes are downregulated, and stress marker genes, especially (dehydrins, PSBS, heat shock, and aquaporins) are increased and the majority of the photosynthetic genes are downregulated. My transcriptome data showed a relationship between the ROS and calcium signalling pathways and the overexpression of signalling molecules in higher plants. iTRAQ proteome analysis revealed the induction of several proteins related to photosynthesis (PSI-LHCI, PSII-LHCII), ROS protein, and heat shock protein enhance the performance of leaf under drought conditions. Increased levels of carbohydrates and polyols (erythritol, pinitol) may provide a continuous

osmoticum at the cellular level to mitigate the osmotic imbalance raised by the drought stress, which plays an important role in maintaining pH balance cell wall integrity and osmotic balance in *P.sativum* under drought stress. This study could be important in that under minimal water conditions, and the plants were acclimated to drought stress by overproduction of several biomolecules. Further, I identified several marker proteins, transcripts and metabolites differentially expressed in drought stress, giving clues to developing drought-tolerant Pea plants.

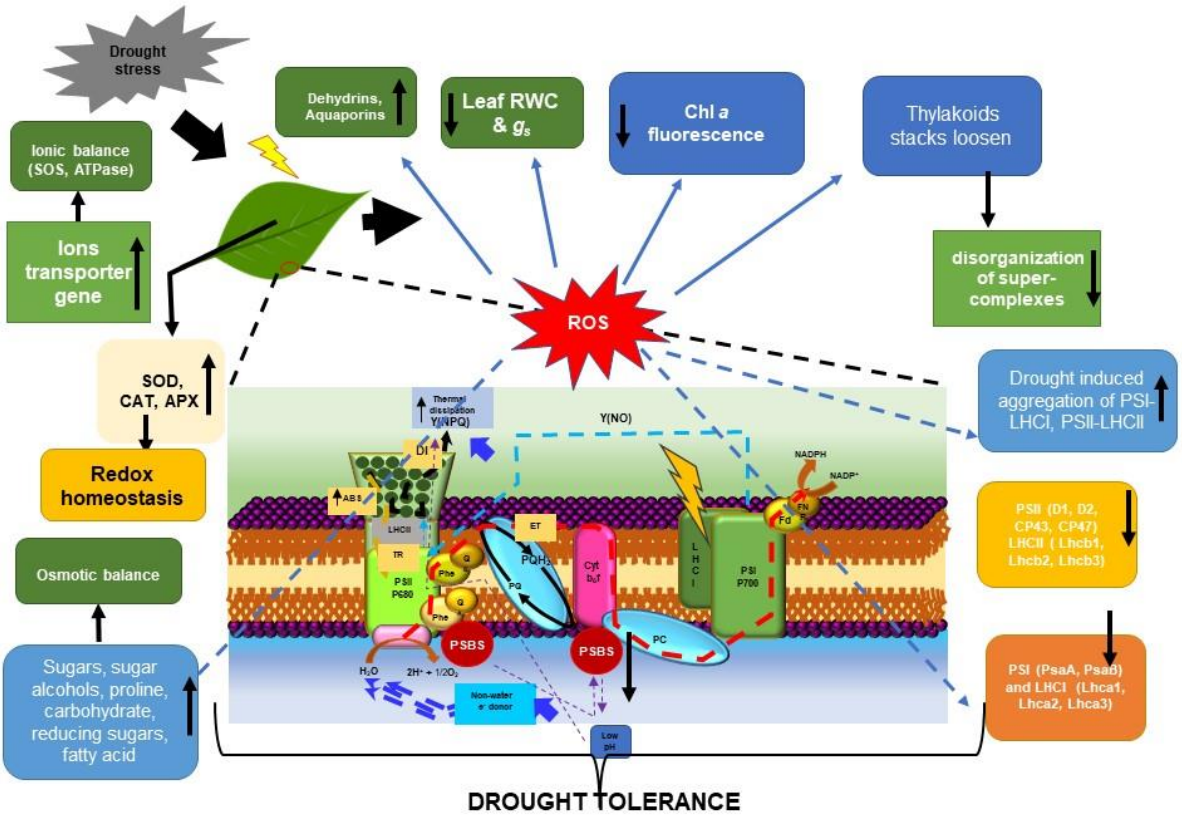

Schematic representation show the mechanism of drought tolerance in *P.sativum*

Chapter 8

Literature cited

Literature Cited

Abida, H., Dolch, L. J., Meï, C., Villanova, V., Conte, M., Block, M. A., ... & Maréchal, E. (2015). Membrane glycerolipid remodeling triggered by nitrogen and phosphorus starvation in *Phaeodactylum tricornutum*. *Plant Physiology*, *167*, 118-136.

Akhtar, P., Dorogi, M., Pawlak, K., Kovacs, L., Bota, A., Kiss, T., Garab, G., Lambrev, P. H. (2015). Pigment interactions in light-harvesting complex II in different molecular environments. *The Journal of Biological Chemistry*, *290*, 4877-4886.

Al Kharusi, L., Al Yahyai, R., & Yaish, M. W. (2019). Antioxidant response to salinity in salt-tolerant and salt-susceptible cultivars of date palm. *Agriculture*, *9*, 8.

Alados, I., Foyo-Moreno, I. Y., & Alados-Arboledas, L. (1996). Photosynthetically active radiation: measurements and modelling. *Agricultural and Forest Meteorology*, *78*, 121-131.

Amunts, A., Drory, O., & Nelson, N. (2007). The structure of a plant photosystem I supercomplex at 3.4 Å resolution. *Nature*, *447*, 58-63.

Apel, K., & Hirt, H. (2004). Reactive oxygen species: metabolism, oxidative stress, and signal transduction. *Annual Review of Plant Biology*, *55*, 373-399.

Arnon, D.I. (1949). Copper enzymes in isolated chloroplasts polyphenoloxidase in *Beta vulgaris*. *Plant Physiology, 24*, 1-15.

Ashraf, M. H. P. J. C., & Harris, P. J. (2013). Photosynthesis under stressful environments: an overview. *Photosynthetica*, *51*, 163-190.

Baniulis, D., Yamashita, E., Whitelegge, J. P., Zatsman, A. I., Hendrich, M. P., Hasan, S. S., ... & Cramer, W. A. (2009). Structure-function, stability, and chemical modification of the cyanobacterial cytochrome b_6f complex from Nostoc sp. PCC 7120. *Journal of Biological Chemistry*, *284*, 9861-9869.

Bapatla, R. B., Saini, D., Aswani, V., Rajsheel, P., Sunil, B., Timm, S., Raghavendra, A. S. (2021). Modulation of photorespiratory enzymes by oxidative and photo-oxidative stress induced by menadione in leaves of pea *Pisum sativum*. *Plants*, *10*, 987.

Baroli, I., Gutman, B. L., Ledford, H. K., Shin, J. W., Chin, B. L., Havaux, M., & Niyogi, K. K. (2004). Photo-oxidative stress in a xanthophyll-deficient mutant of Chlamydomonas. *Journal of Biological Chemistry*, *279*, 6337-6344.

Bassi, R., Pineau, B., Dainese, P., & Marquardt, J. (1993). Carotenoid-binding proteins of photosystem II. *European Journal of Biochemistry*, *212*, 297-303.

Bates, L. S., Waldren, R. A., & Teare, I. D. (1973). Rapid determination of free proline for water-stress studies. *Plant and soil*, *39*, 205-207.

Baxter, C. J., Redestig, H., Schauer, N., Repsilber, D., Patil, K. R., Nielsen, J., ... & Sweetlove, L. J. (2007). The metabolic response of heterotrophic Arabidopsis cells to oxidative stress. *Plant Physiology*, *143*, 312-325.

Ben-Shem, A., Frolow, F., & Nelson, N. (2003). Crystal structure of plant photosystem I. *Nature*, *426*, 630-635.

Birben, E., Sahiner, U. M., Sackesen, C., Erzurum, S., & Kalayci, O. (2012). Oxidative stress and antioxidant defense. *World Allergy Organization Journal*, *5*, 9-19.

Blechschmidt-Schneider, S., Ferrar, P., & Osmond, C. B. (1989). Control of photosynthesis by the carbohydrate level in leaves of the C4 plant *Amaranthus edulis* L. *Planta*, *177*, 515-525.

Bligh, E. G., & Dyer, W. J. (1959). A rapid method of total lipid extraction and purification. *Canadian Journal of Biochemistry and Physiology*, *37*, 911-917.

Busch, A., Hippler, M. (2011). The structure and function of eukaryotic photosystem I. *Biochimica et Biophysica Acta*, *1807*, 864-877.

Caffarri, S., Broess, K., Croce, R., & van Amerongen, H. (2011). Excitation energy transfer and trapping in higher plant photosystem II complexes with different antenna sizes. *Biophysical Journal*, *100*, 2094-2103.

Caspy, I., & Nelson, N. (2018). Structure of the plant photosystem I. *Biochemical Society Transactions*, *46*, 285-294.

Cazzaniga, Stefano, Zhirong Li, Krishna K. Niyogi, Roberto Bassi, and Luca Dall'Osto. (2012) "The Arabidopsis szl1 mutant reveals a critical role of β-carotene in photosystem I photoprotection." *Plant Physiology* 159, 745-1758.

Chen, J. Q., Meng, X. P., Zhang, Y., Xia, M., & Wang, X. P. (2008). Over-expression of OsDREB genes lead to enhanced drought tolerance in rice. *Biotechnology Letters*, *30*, 2191-2198.

Chen, Y. E., Liu, W. J., Su, Y. Q., Cui, J. M., Zhang, Z.W., Yuan, M., Zhang, H. Y., Yuan, S. (2016). Different response of photosystem II to short and long-term drought stress in *Arabidopsis*. *Physiologia Plantarum*, *158*, 225-235.

Cheval, C., Aldon, D., Galaud, J. P., & Ranty, B. (2013). Calcium/calmodulin-mediated regulation of plant immunity. *Biochimica et Biophysica Acta (BBA)-Molecular Cell Research*, *1833*, 1766-1771.

Chouhan, N., Devadasu, E., Yadav, R. M., & Subramanyam, R. (2022). Autophagy induced accumulation of lipids in pgrl1 and pgr5 of *Chlamydomonas reinhardtii* under high light. *Frontiers in Plant Science*, *12*, 3308.

Corpas, F. J., González-Gordo, S., & Palma, J. M. (2021). Protein nitration: a connecting bridge between nitric oxide (NO) and plant stress. *Plant Stress*, *2*, 100026.

Costa, A., Drago, I., Behera, S., Zottini, M., Pizzo, P., Schroeder, J. I., ... & Schiavo, F. L. (2010). H_2O_2 in plant peroxisomes: an in vivo analysis uncovers a Ca^{2+}dependent scavenging system. *The Plant Journal*, *62*, 760-772.

Cseh, Z., Vianelli, A., Rajagopal, S., Krumova, S., Kovacs, L., Papp, E., ... & Garab, G. (2005). Thermo-optically induced reorganizations in the main light harvesting antenna of plants. I. Non-Arrhenius type of temperature dependence and linear light-intensity dependencies. *Photosynthesis Research*, *86*, 263-273.

Dalal, V. K. (2021). Modulation of photosynthesis and other proteins during water-stress. *Molecular Biology Reports*, *48*, 3681-3693.

Dall'Osto, L., Holt, N. E., Kaligotla, S., Fuciman, M., Cazzaniga, S., Carbonera, D., ... & Bassi, R. (2012). Zeaxanthin protects plant photosynthesis by modulating chlorophyll triplet yield in specific light-harvesting antenna subunits. *Journal of Biological Chemistry*, *287*, 41820-41834.

Das, K., & Roychoudhury, A. (2014). Reactive oxygen species (ROS) and response of antioxidants as ROS-scavengers during environmental stress in plants. *Frontiers in Environmental Science*, *2*, 53.

Daum, B., Nicastro, D., Austin, J., McIntosh, J. R., Kühlbrandt, W. (2010). Arrangement of photosystem II and ATP synthase in chloroplast membranes of spinach and pea. *The Plant Cell*, *22*, 1299-1312.

De la Coba, F., Aguilera, J., Figueroa, F. L., De Gálvez, M. V., & Herrera, E. (2009). Antioxidant activity of mycosporine-like amino acids isolated from three red macroalgae and one marine lichen. *Journal of Applied Phycology*, *21*, 161-169.

Debus, R. J., Barry, B. A., Sithole, I., Babcock, G. T., & McIntosh, L. (1988). Directed mutagenesis indicates that the donor to P 680^{+} in photosystem II is tyrosine-161 of the D1 polypeptide. *Biochemistry*, *27*, 9071-9074.

Demmig Adams, B. (1990). Carotenoids and photoprotection in plants: a role for the xanthophyll zeaxanthin. *Biochimica et Biophysica Acta*, *1020*, 1-24.

Demmig-Adams, B., & Adams III, W. W. (2006). Photoprotection in an ecological context: the remarkable complexity of thermal energy dissipation. *New Phytologist*, *172*, 11-21.

Devadasu, E., & Subramanyam, R. (2021). Enhanced lipid production in *Chlamydomonas reinhardtii* caused by severe Iron Deficiency. *Frontiers in Plant Science*, 12, 615577.

Devadasu, E., Chinthapalli, D. K., Chouhan, N., Madireddi, S. K., Rasineni, G. K., Sripadi, P., & Subramanyam, R. (2019). Changes in the photosynthetic apparatus and lipid droplet formation in *Chlamydomonas reinhardtii* under iron deficiency. *Photosynthesis Research*, 139, 253-266.

Devadasu, E., Pandey, J., Dhokne, K., Subramanyam, R. (2021). Restoration of photosynthetic activity and supercomplexes from severe iron starvation in *Chlamydomonas reinhardtii Biochimica et Biophysica Acta*, *1862*, 148331.

Du, H., Wang, N., Cui, F., Li, X., Xiao, J., & Xiong, L. (2010). Characterization of the β-carotene hydroxylase gene DSM2 conferring drought and oxidative stress resistance by increasing xanthophylls and abscisic acid synthesis in rice. *Plant Physiology*, *154*, 1304-1318.

Dubrovina, A. S., Kiselev, K. V., Khristenko, V. S., & Aleynova, O. A. (2017). The calcium-dependent protein kinase gene VaCPK29 is involved in grapevine responses to heat and osmotic stresses. *Plant Growth Regulation*, *82*, 79-89.

Fang, Y., & Xiong, L. (2015). General mechanisms of drought response and their application in drought resistance improvement in plants. *Cellular and Molecular Life Sciences*, *72*, 673-689.

Farooq, M., Wahid, A., Kobayashi, N. S. M. A., Fujita, D. B. S. M. A., & Basra, S. M. A. (2009). Plant drought stress: effects, mechanisms and management. *Sustainable agriculture*, 153-188.

Fernie, A. R., Carrari, F., & Sweetlove, L. J. (2004). Respiratory metabolism: glycolysis, the TCA cycle and mitochondrial electron transport. *Current Opinion in Plant Biology*, *7*, 254-261.

Ferreira, K. N., Iverson, T. M., Maghlaoui, K., Barber, J., & Iwata, S. (2004). Architecture of the photosynthetic oxygen-evolving center. *Science*, *303*, 1831-1838.

Foyer, C. H., & Noctor, G. (2000). Tansley Review No. 112 Oxygen processing in photosynthesis: regulation and signalling. *The New Phytologist*, *146*, 359-388.

Foyer, C. H., & Noctor, G. (2005). Oxidant and antioxidant signalling in plants: a re-evaluation of the concept of oxidative stress in a physiological context. *Plant, Cell & Environment*, *28*, 1056-1071.

Foyer, C. H., Lelandais, M., & Kunert, K. J. (1994). Photooxidative stress in plants.

Fromme, P., Melkozernov, A., Jordan, P., Krauss, N. (2003). Structure and function of photosystem I interaction with its soluble electron carriers and external antenna systems. *FEBS letters*, *555*, 40-44.

Frugoli, J. A., Zhong, H. H., Nuccio, M. L., McCourt, P., McPeek, M. A., Thomas, T. L., & McClung, C. R. (1996). Catalase is encoded by a multigene family in *Arabidopsis thaliana* (L.) Heynh. *Plant Physiology*, *112*, 327-336.

Furlan, A. L., Bianucci, E., Giordano, W., Castro, S., & Becker, D. F. (2020). Proline metabolic dynamics and implications in drought tolerance of peanut plants. *Plant Physiology and Biochemistry, 151,* 566-578.

Gao, C. (2021). Genome engineering for crop improvement and future agriculture. *Cell*, *184*, 1621-1635.

Garab, G., van Amerongen, H. (2009). Linear dichroism and circular dichroism in photosynthesis research. *Photosynthesis Research*, *101*, 135-146.

Garstka, M., Drożak, A., Rosiak, M., Venema, J. H., Kierdaszuk, B., Simeonova, E., ... & Mostowska, A. (2005). Light-dependent reversal of dark-chilling induced changes in chloroplast structure and arrangement of chlorophyll–protein complexes in bean thylakoid membranes. *Biochimica et Biophysica Acta (BBA)-Bioenergetics*, *1710*, 13-23.

Giannoccaro, E., Wang, Y. J., & Chen, P. (2006). Effects of solvent, temperature, time, solvent-to-sample ratio, sample size, and defatting on the extraction of soluble sugars in soybean. *Journal of Food Science, 71*, 59-64.

Giardi, M. T., Cona, A., Geiken, B., Kucera, T., Masojidek, J., Mattoo, A. K. (1996). Long-term drought stress induces structural and functional reorganization of photosystem II. *Planta*, *199*, 118-125.

González, M. C., Cejudo, F. J., Sahrawy, M., & Serrato, A. J. (2021). Current knowledge on mechanisms preventing photosynthesis redox imbalance in plants. *Antioxidants*, *10*, 1789.

Guo, Y., Cheng, J., Lu, Y., Wang, H., Gao, Y., Shi, J., Qiang, S. (2020). Novel action targets of natural product gliotoxin in photosynthetic apparatus. *Frontiers in Plant Science, 10*, 1688.

Hanin, M., Ebel, C., Ngom, M., Laplaze, L., & Masmoudi, K. (2016). New insights on plant salt tolerance mechanisms and their potential use for breeding. *Frontiers in Plant Science, 7*, 1787.

Hare, P. D., Cress, W. A., & Van Staden, J. (1998). Dissecting the roles of osmolyte accumulation during stress. *Plant, Cell & Environment*, *21*, 535-553.

Hasan, S. S., & Cramer, W. A. (2014). Internal lipid architecture of the hetero-oligomeric cytochrome b_6f complex. *Structure*, *22*, 1008-1015.

Hasanuzzaman, M., Bhuyan, M. B., Anee, T. I., Parvin, K., Nahar, K., Mahmud, J. A., & Fujita, M. (2019). Regulation of ascorbate-glutathione pathway in mitigating oxidative damage in plants under abiotic stress. *Antioxidants*, *8*, 384.

Hasanuzzaman, M., Bhuyan, M. B., Zulfiqar, F., Raza, A., Mohsin, S. M., Mahmud, J. A., ... & Fotopoulos, V. (2020). Reactive oxygen species and antioxidant defense in plants under abiotic stress: Revisiting the crucial role of a universal defense regulator. *Antioxidants*, *9*, 681.

Havaux, M., & Niyogi, K. K. (1999). The violaxanthin cycle protects plants from photooxidative damage by more than one mechanism. *Proceedings of the National Academy of Sciences*, *96*, 8762-8767.

Henry, C., John, G. P., Pan, R., Bartlett, M. K., Fletcher, L. R., Scoffoni, C., Sack, L. (2019). A stomatal safety efficiency trade off constrains responses to leaf dehydration. *Nature Communications*, *10*, 1-9.

Hill, R. (1937). Oxygen evolved by isolated chloroplasts. *Nature*, *139*, 881-882.

Horton, P., Ruban, A. V., Walters, R. G. (1996). Regulation of light harvesting in green plants. *Annual Review of Plant Biology*, *47*, 655-684.

Hu, H., Dai, M., Yao, J., Xiao, B., Li, X., Zhang, Q., & Xiong, L. (2006). Overexpressing a NAM, ATAF, and CUC (NAC) transcription factor enhances drought resistance and salt tolerance in rice. *Proceedings of the National Academy of Sciences*, *103*, 12987-12992.

Huang, T., & Jander, G. (2017). Abscisic acid-regulated protein degradation causes osmotic stress-induced accumulation of branched-chain amino acids in *Arabidopsis thaliana*. *Planta*, *246*, 737-747.

Iqbal, N., Hussain, S., Raza, M. A., Yang, C. Q., Safdar, M. E., Brestic, M., Liu, J. (2019). Drought Tolerance of Soybean *Glycine max* L. Merr. by improved photosynthetic characteristics and an efficient antioxidant enzyme activity under a split-root system. *Frontiers in Physiology*, *10*, 786.

Jackowski, G., Kacprzak, K., & Jansson, S. (2001). Identification of Lhcb1/Lhcb2/Lhcb3 heterotrimers of the main light-harvesting chlorophyll a/b–protein complex of Photosystem II (LHC II). *Biochimica et Biophysica Acta (BBA)-Bioenergetics*, *1504*, 340-345.

Jahns, P., & Holzwarth, A. R. (2012). The role of the xanthophyll cycle and of lutein in photoprotection of photosystem II. *Biochimica et Biophysica Acta (BBA)-Bioenergetics*, *1817*, 182-193.

Jalmi, S. K., Bhagat, P. K., Verma, D., Noryang, S., Tayyeba, S., Singh, K., ... & Sinha, A. K. (2018). Traversing the links between heavy metal stress and plant signaling. *Frontiers in Plant Science*, *9*, 12.

James, G. O., Hocart, C. H., Hillier, W., Chen, H., Kordbacheh, F., Price, G. D., & Djordjevic, M. A. (2011). Fatty acid profiling of *Chlamydomonas reinhardtii* under nitrogen deprivation. *Bioresource Technology*, *102*, 3343-3351.

Janik, E., Bednarska, J., Sowinski, K., Luchowski, R., Zubik, M., Grudzinski, W., Gruszecki, W. I. (2017). Light-induced formation of dimeric LHCII. *Photosynthesis Research*, *132*, 265-276.

Johnson, M. P., Ruban, A. V. (2010). Arabidopsis plants lacking PsbS protein possess photoprotective energy dissipation. *The Plant Journal*, *61*, 283-289.

Jordan, P., Fromme, P., Witt, H. T., Klukas, O., Saenger, W., & Krauß, N. (2001). Three-dimensional structure of cyanobacterial photosystem I at 2.5 Å resolution. *Nature*, *411*, 909-917.

Jorge, T. F., Rodrigues, J. A., Caldana, C., Schmidt, R., van Dongen, J. T., Thomas-Oates, J., & António, C. (2016). Mass spectrometry-based plant metabolomics: Metabolite responses to abiotic stress. *Mass Spectrometry Reviews*, *35*, 620-649.

Junge, W., & Nelson, N. (2015). ATP synthase. *Annual review of biochemistry*, *84*, 631-657.

Kaur, G., & Asthir, B. (2017). Molecular responses to drought stress in plants. *Biologia Plantarum*, *61*, 201-209.

Kelly, J. W., Duursma, R. A., Atwell, B. J., Tissue, D. T., Medlyn, B. E. (2016). Drought CO_2 interactions in trees a test of the low-intercellular CO_2 concentration (Ci) mechanism. *New Phytologist*, *209*, 1600-1612.

Klughammer, C., Schreiber, U. (1994). Saturation pulse method for assessment of energy conversion in PSI. *Planta*, *1992*, 261-268.

Klukas, O., Schubert, W. D., Jordan, P., Krauss, N., Fromme, P., Witt, H. T., Saenger, W. (1999). Photosystem I, an improved model of the stromal subunits PsaC, PsaD, and PsaE. *The Journal of Biological Chemistry*, *274*, 7351-7360.

Knight, H., Trewavas, A. J., & Knight, M. R. (1997). Calcium signalling in *Arabidopsis thaliana* responding to drought and salinity. *The Plant Journal*, *12*, 1067-1078.

Kodru, S., Malavath, T., Devadasu, E., Nellaepalli, S., Stirbet, A., Subramanyam, R., Govindjee. (2015). The slow S to M rise of chlorophyll a fluorescence reflects transition from state 2 to state 1 in the green alga *Chlamydomonas reinhardtii*. *Photosynthesis Research*, *125*, 219-231.

Koskela, M. M., Brünje, A., Ivanauskaite, A., Grabsztunowicz, M., Lassowskat, I., Neumann, U., ... & Mulo, P. (2018). Chloroplast acetyltransferase NSI is required for state transitions in *Arabidopsis thaliana*. *The Plant Cell*, *30*, 1695-1709.

Kramer, D. M., Johnson, G., Kiirats, O., Edwards, G. E. (2004). New fluorescence parameters for the determination of Q_A redox state and excitation energy fluxes. *Photosynthesis Research*, *79*, 209-218.

Krasensky, J., & Jonak, C. (2012). Drought, salt, and temperature stress-induced metabolic rearrangements and regulatory networks. *Journal of Experimental Botany*, *63*, 1593-1608.

Kubota-Kawai, H., Mutoh, R., Shinmura, K., Sétif, P., Nowaczyk, M. M., Rögner, M., ... & Kurisu, G. (2018). X-ray structure of an asymmetrical trimeric ferredoxin–photosystem I complex. *Nature Plants*, *4*, 218-224.

Kumar, A., Prasad, A., Sedlářová, M., Kale, R., Frankel, L. K., Sallans, L., Pospíšil, P. (2021). Tocopherol controls D1 amino acid oxidation by oxygen radicals in Photosystem II. *Proceedings of the National Academy of Sciences 118,* e2019246118.

Kuromori, T., Fujita, M., Takahashi, F., Yamaguchi-Shinozaki, K., & Shinozaki, K. (2022). Inter-tissue and inter-organ signaling in drought stress response and phenotyping of drought tolerance. *The Plant Journal*, *109*, 342-358.

Kwon, K. C., Verma, D., Jin, S., Kwon, K. C., Verma, D., Jin, S., Singh, N. D., Daniell, H. (2013). Release of proteins from intact chloroplasts induced by reactive oxygen species during biotic and abiotic stress. *PloS One*, *8*, e67106.

Latowski, D., Kuczyńska, P., & Strzałka, K. (2011). Xanthophyll cycle–a mechanism protecting plants against oxidative stress. *Redox Report*, *16*, 78-90.

Lehmann, M., Laxa, M., Sweetlove, L. J., Fernie, A. R., & Obata, T. (2012). Metabolic recovery of *Arabidopsis thaliana* roots following cessation of oxidative stress. *Metabolomics*, *8*, 143-153.

Li, M., Mukhopadhyay, R., Svoboda, V., Oung, H. M. O., Mullendore, D. L., Kirchhoff, H. (2020). Measuring the dynamic response of the thylakoid architecture in plant leaves by electron microscopy. *Plant Direct*, *4*, e00280.

Li, Y., Li, H., Li, Y., Zhang, S. (2017). Improving water-use efficiency by decreasing stomatal conductance and transpiration rate to maintain higher ear photosynthetic rate in drought-resistant wheat. *The Crop Journal*, *5*, 231-239.

Liu, T., Jiao, X., Yang, S., Zhang, Z., Ye, X., Li, J., ... & Hu, X. (2020). Crosstalk between GABA and ALA to improve antioxidation and cell expansion of tomato seedling under cold stress. *Environmental and Experimental Botany*, *180*, 104228.

Liu, Y., Song, Q., Li, D., Yang, X., & Li, D. (2017). Multifunctional roles of plant dehydrins in response to environmental stresses. *Frontiers in Plant Science*, *8*, 1018.

Livak, K. J., & Schmittgen, T. D. (2001). Analysis of relative gene expression data using real-time quantitative PCR and the $2^{-\Delta\Delta CT}$ method. *Methods*, *25*, 402-408.

Lu, T., Meng, Z., Zhang, G., Qi, M., Sun, Z., Liu, Y., Li, T. (2017). Sub-high temperature and high light intensity induced irreversible inhibition on photosynthesis system of tomato plant *Solanum lycopersicum* L. *Frontiers in Plant Science*, *8*, 365.

Macas, J., Neumann, P., & Navrátilová, A. (2007). Repetitive DNA in the pea (*Pisum sativum L.*) genome: comprehensive characterization using 454 sequencing and comparison to soybean and *Medicago truncatula*. *BMC genomics*, *8*, 1-16.

Madireddi, S. K., Nama, S., Devadasu, E. R., Subramanyam, R. (2014). Photosynthetic membrane organization and role of state transition in cyt, cpII, stt7 and npq mutants of *Chlamydomonas reinhardtii*. *Journal of Photochemistry and Photobiology B: Biology*, *137*, 77-83.

Mansoor, S., Ali Wani, O., Lone, J. K., Manhas, S., Kour, N., Alam, P., ... & Ahmad, P. (2022). Reactive oxygen species in plants: from source to sink. *Antioxidants*, *11*, 225.

Maroc, J., Trémolières, A., Garnier, J., & Guyon, D. (1987). Oligomeric form of the light-harvesting chlorophyll a+ b-protein complex CP II, phosphatidyldiacylglycerol, Δ3-trans-hexadecenoic acid and energy transfer in *Chlamydomonas reinhardtii*, wild type and mutants. *Biochimica et Biophysica Acta (BBA)-Bioenergetics*, *893*, 91-99.

Marriboina, S., Attipalli, R. R. (2020). Hydrophobic cell-wall barriers and vacuolar sequestration of Na^+ ions are among the key mechanisms conferring high salinity tolerance in a biofuel tree species, *Pongamia pinnata* L. pierre. *Environmental and Experimental Botany*, *171*, 103949.

Marriboina, S., Sengupta, D., Kumar, S., Reddy, A. R. (2017). Physiological and molecular insights into the high salinity tolerance of *Pongamia pinnata* L. pierre, a potential biofuel tree species. *Plant Science*, *258*, 102-111.

Mayfield, S. P., Schirmer-Rahire, M., Frank, G., Zuber, H., & Rochaix, J. D. (1989). Analysis of the genes of the OEE1 and OEE3 proteins of the photosystem II complex from *Chlamydomonas reinhardtii*. *Plant Molecular Biology*, *12*, 683-693.

Mazor, Y., Borovikova, A., Caspy, I., & Nelson, N. (2017). Structure of the plant photosystem I supercomplex at 2.6 Å resolution. *Nature plants*, *3*, 1-9.

Mazor, Y., Borovikova, A., Nelson, N. (2015). The structure of plant photosystem I super-complex at 2.8 Å resolution. *elife*, *4*, e07433.

Mehler, A. H. (1951). Studies on reactions of illuminated chloroplasts. II. Stimulation and inhibition of the reaction with molecular oxygen. *Archives of Biochemistry and Biophysics*, *34*, 339-351.

Mhamdi, A., Noctor, G., & Baker, A. (2012). Plant catalases: peroxisomal redox guardians. *Archives of Biochemistry and Biophysics*, *525*, 181-194.

Mhamdi, Amna, Guillaume Queval, Sejir Chaouch, Sandy Vanderauwera, Frank Van Breusegem, and Graham Noctor. (2010) "Catalase function in plants: a focus on Arabidopsis mutants as stress-mimic models." *Journal of Experimental Botany* 61, 4197-4220.

Mittler, R. (2002). Oxidative stress, antioxidants and stress tolerance. *Trends in Plant Science*, *7*, 405-410.

Moran, J. F., Becana, M., Iturbe-Ormaetxe, I., Frechilla, S., Klucas, R. V., & Aparicio-Tejo, P. (1994). Drought induces oxidative stress in pea plants. *Planta*, *194*, 346-352.

Morosinotto, T., Breton, J., Bassi, R., & Croce, R. (2003). The nature of a chlorophyll ligand in Lhca proteins determines the far-red fluorescence emission typical of photosystem I. *Journal of Biological Chemistry*, *278*, 49223-49229.

Morsy, M. R., Jouve, L., Hausman, J. F., Hoffmann, L., & Stewart, J. M. (2007). Alteration of oxidative and carbohydrate metabolism under abiotic stress in two rice *Oryza sativa L*. genotypes contrasting in chilling tolerance. *Journal of Plant Physiology*, *164*, 157-167.

Mota, A., Oliveira, T. N., Vinson, C. C., Williams, T., Costa, M., Araujo, A., Danchin, E., Grossi-de-Sa, M. F., Guimaraes, P. M., Brasileiro, A. (2019). Contrasting effects of wild Arachis dehydrin under abiotic and biotic stresses. *Frontiers in Plant Science*, *10*, 497.

Mukarram, M., Choudhary, S., Kurjak, D., Petek, A., & Khan, M. M. A. (2021). Drought: Sensing, signalling, effects and tolerance in higher plants. *Physiologia Plantarum*, *172*, 1291-1300.

Muller, P., Li, X. P., & Niyogi, K. K. (2001). Non-photochemical quenching. A response to excess light energy. *Plant Physiology*, *125*, 1558-1566.

Munekage, Y., Hashimoto, M., Miyake, C., Tomizawa, K. I., Endo, T., Tasaka, M., & Shikanai, T. (2004). Cyclic electron flow around photosystem I is essential for photosynthesis. *Nature*, *429*, 579-582.

Munekage, Y., Hojo, M., Meurer, J., Endo, T., Tasaka, M., & Shikanai, T. (2002). PGR5 is involved in cyclic electron flow around photosystem I and is essential for photoprotection in Arabidopsis. *Cell*, *110*, 361-371.

Murchie, E. H., Lawson, T. (2013). Chlorophyll fluorescence analysis: a guide to good practice and understanding some new applications. *Journal of Experimental Botany*, *64*, 3983-3998.

Nakabayashi, R., Yonekura-Sakakibara, K., Urano, K., Suzuki, M., Yamada, Y., Nishizawa, T., ... & Saito, K. (2014). Enhancement of oxidative and drought tolerance in Arabidopsis by overaccumulation of antioxidant flavonoids. *The Plant Journal*, *77*, 367-379.

Nakano, Y., Asada, K. (1981). Hydrogen peroxide is scavenged by ascorbate-specific peroxidase in spinach chloroplasts. *Plant and Cell Physiology*, *22*, 867-880.

Nama, S., Madireddi, S. K., Yadav, R. M., Subramanyam, R. (2019). Non-photochemical quenching-dependent acclimation and thylakoid organization of *Chlamydomonas reinhardtii* to high light stress. *Photosynthesis Research*, *139*, 387-400.

Natarajan, P., & Parani, M. (2011). De novo assembly and transcriptome analysis of five major tissues of Jatropha curcas L. using GS FLX titanium platform of 454 pyrosequencing. *BMC genomics*, *12*, 1-12.

Neill, S., Desikan, R., & Hancock, J. (2002). Hydrogen peroxide signalling. *Current Opinion in Plant Biology*, *5*, 388-395.

Nelson, N., & Yocum, C. F. (2006). Structure and function of photosystems I and II. *Annual Review Plant Biology*, *57*, 521-565.

Nishiyama, Y., Allakhverdiev, S. I., & Murata, N. (2006). A new paradigm for the action of reactive oxygen species in the photoinhibition of photosystem II. *Biochimica et Biophysica Acta (BBA)-Bioenergetics*, *1757*, 742-749.

Niyogi, K. K., Björkman, O., & Grossman, A. R. (1997). The roles of specific xanthophylls in photoprotection. *Proceedings of the National Academy of Sciences*, *94*, 14162-14167.

Niyogi, K. K., Shih, C., Soon Chow, W., Pogson, B. J., DellaPenna, D., & Björkman, O. (2001). Photoprotection in a zeaxanthin-and lutein-deficient double mutant of Arabidopsis. *Photosynthesis Research*, *67*, 139-145.

Noctor, G., & Foyer, C. H. (1998). Ascorbate and glutathione: keeping active oxygen under control. *Annual Review of Plant Biology*, *49*, 249-279.

Noctor, G., Gomez, L., Vanacker, H., & Foyer, C. H. (2002). Interactions between biosynthesis, compartmentation and transport in the control of glutathione homeostasis and signalling. *Journal of Experimental Botany*, *53*, 1283-1304.

Noctor, G., Lelarge-Trouverie, C., & Mhamdi, A. (2015). The metabolomics of oxidative stress. *Phytochemistry*, *112*, 33-53.

Nomura, H., Komori, T., Uemura, S., Kanda, Y., Shimotani, K., Nakai, K., ... & Shiina, T. (2012). Chloroplast-mediated activation of plant immune signalling in Arabidopsis. *Nature Communications*, *3*, 926.

Nott, A., Jung, H. S., Koussevitzky, S., & Chory, J. (2006). Plastid-to-nucleus retrograde signaling. *Annual Review Plant Biology*, *57*, 739-759.

Obata, T., & Fernie, A. R. (2012). The use of metabolomics to dissect plant responses to abiotic stresses. *Cellular and Molecular Life Sciences*, *69*, 3225-3243.

Pandey, J., Devadasu, E., Saini, D., Dhokne, K., Marriboina, S., Raghavendra, A. S., & Subramanyam, R. (2023). Reversible changes in structure and function of photosynthetic apparatus of pea (*Pisum sativum*) leaves under drought stress. *The Plant Journal*, *113*, 60-74.

Patterson, B. D., Payne, L. A., Chen, Y. Z., Graham, D. (1984). An inhibitor of catalase induced by cold in chilling-sensitive plants. *Plant Physiology*, *76*, 1014-1018.

Pawłowicz, I., Rapacz, M., Perlikowski, D., Gondek, K., Kosmala, A. (2017). Abiotic stresses influence the transcript abundance of PIP and TIP aquaporins in Festuca species. *Journal of Applied Genetics*, *58*, 421-435.

Perez-Martin, A., Michelazzo, C., Torres-Ruiz, J. M., Flexas, J., Fernández, J. E., Sebastiani, L., & Diaz-Espejo, A. (2014). Regulation of photosynthesis and stomatal and mesophyll conductance under water stress and recovery in olive trees: correlation with gene expression of carbonic anhydrase and aquaporins. *Journal of Experimental Botany*, *65*, 3143-3156.

Pilon, M., Ravet, K., & Tapken, W. (2011). The biogenesis and physiological function of chloroplast superoxide dismutases. *Biochimica et Biophysica Acta (BBA)-Bioenergetics*, *1807*, 989-998.

Pineau, B., Gérard-Hirne, C., & Selve, C. (2001). Carotenoid binding to photosystems I and II of *Chlamydomonas reinhardtii* cells grown under weak light or exposed to intense light. *Plant Physiology and Biochemistry*, *39*, 73-85.

Pinto, E., Sigaud-kutner, T. C., Leitao, M. A., Okamoto, O. K., Morse, D., & Colepicolo, P. (2003). Heavy metal–induced oxidative stress in algae 1. *Journal of Phycology*, *39*, 1008-1018.

Plancke, C., Vigeolas, H., Höhner, R., Roberty, S., Emonds-Alt, B., Larosa, V., ... & Remacle, C. (2014). Lack of isocitrate lyase in Chlamydomonas leads to changes in carbon metabolism and in the response to oxidative stress under mixotrophic growth. *The Plant Journal*, *77*, 404-417.

Poerschmann, J., Spijkerman, E., & Langer, U. (2004). Fatty acid patterns in Chlamydomonas sp. as a marker for nutritional regimes and temperature under extremely acidic conditions. *Microbial Ecology*, 48, 78-89.

Raven, J. A., & Falkowski, P. G. (1999). Oceanic sinks for atmospheric CO_2. *Plant, Cell & Environment*, *22*, 741-755.

Reddy, A. R., Chaitanya, K. V., & Vivekanandan, M. (2004). Drought-induced responses of photosynthesis and antioxidant metabolism in higher plants. *Journal of Plant Physiology*, *161*, 1189-1202.

Reddy, A. R., Chaitanya, K. V., Jutur, P. P., & Sumithra, K. (2004). Differential antioxidative responses to water stress among five mulberry (*Morus alba* L.) cultivars. *Environmental and Experimental Botany*, *52*, 33-42.

Riboldi, L. B., Oliveira, R. F., Angelocci, L. R. (2016). Leaf turgor pressure in maize plants under water stress. *Australian Journal of Crop Science, 10*, 878-886.

Ruban, A. V. (2016). Nonphotochemical chlorophyll fluorescence quenching: mechanism and effectiveness in protecting plants from photodamage. *Plant Physiology*, *170*, 1903-1916.

Rutherford, A. W., & Faller, P. (2003). Photosystem II: evolutionary perspectives. *Philosophical Transactions of the Royal Society of London. Series B: Biological Sciences*, *358*, 245-253.

Sánchez-Reinoso, A. D., Ligarreto-Moreno, G. A., Restrepo-Díaz, H. (2019). Chlorophyll a fluorescence parameter as an indicator to identify drought susceptibility in common bush bean. *Agronomy, 9*, 526.

Sasi, S., Venkatesh, J., Daneshi, R. F., Gururani, M. A. (2018). Photosystem II extrinsic proteins and their putative role in abiotic stress tolerance in higher plants. *Plants, 7*, 100.

Sato, S., Isobe, S., & Tabata, S. (2010). Structural analyses of the genomes in legumes. *Current Opinion in Plant Biology*, *13*, 146-152.

Schagger, H., Von, J. G. (1991). Blue native electrophoresis for isolation of membrane protein complexes in enzymatically active form. *Analytical Biochemistry*, *199*, 223-231.

Schauer, N., Steinhauser, D., Strelkov, S., Schomburg, D., Allison, G., Moritz, T., ... & Kopka, J. (2005). GC–MS libraries for the rapid identification of metabolites in complex biological samples. *FEBS letters*, *579*, 1332-1337.

Schreiber, U. (1986). Detection of rapid induction kinetics with a new type of high frequency modulated chlorophyll fluorometer. *Photosynthesis Research*, *9*, 261-272.

Schreiber, U., Klughammer, C. (2008). New accessory for the DUAL-PAM-100: The P515/535 module and examples of its application. *PAM Application Notes*, *1*, 1-10.

Seleiman, M. F., Al-Suhaibani, N., Ali, N., Akmal, M., Alotaibi, M., Refay, Y., Battaglia, M. L. (2021). Drought stress impacts on plants and different approaches to alleviate its adverse effects. *Plants, 10*, 259.

Senge, M. O., Ryan, A. A., Letchford, K. A., MacGowan, S. A., & Mielke, T. (2014). Chlorophylls, symmetry, chirality, and photosynthesis. *Symmetry*, *6*, 781-843.

Shahid, M., Pourrut, B., Dumat, C., Nadeem, M., Aslam, M., & Pinelli, E. (2014). Heavy-metal-induced reactive oxygen species: phytotoxicity and physicochemical

changes in plants. *Reviews of Environmental Contamination and Toxicology Volume 232*, 1-44.

Sharma, P., Jha, A. B., Dubey, R. S., & Pessarakli, M. (2012). Reactive oxygen species, oxidative damage, and antioxidative defense mechanism in plants under stressful conditions. *Journal of Botany*, *2012*.

Shukla, M. K., Watanabe, A., Wilson, S., Giovagnetti, V., Moustafa, E. I., Minagawa, J., Ruban, A. V. (2020). A novel method produces native light-harvesting complex II aggregates from the photosynthetic membrane revealing their role in non-photochemical quenching. *The Journal of Biological Chemistry*, *295*, 17816-17826.

Silvente, S., Sobolev, A. P., & Lara, M. (2012). Metabolite adjustments in drought tolerant and sensitive soybean genotypes in response to water stress. *Plos One*, *7*, e38554.

Sipka, G. B., Magyar, M., Mezzetti, A., Akhtar, P., Zhu, Q., Xiao, Y., Han, G., Santabarbara, S., Shen, J. R., Lambrev, P. H., Garab, G. (2021). Light-adapted charge-separated state of photosystem II: structural and functional dynamics of the closed reaction center. *The Plant Cell*, *33*, 1286-1302.

Sofo, A., Scopa, A., Nuzzaci, M., & Vitti, A. (2015). Ascorbate peroxidase and catalase activities and their genetic regulation in plants subjected to drought and salinity stresses. *International Journal of Molecular Sciences*, *16*, 13561-13578.

Spicher, L., Almeida, J., Gutbrod, K., Pipitone, R., Dörmann, P., Glauser, G., ... & Kessler, F. (2017). Essential role for phytol kinase and tocopherol in tolerance to combined light and temperature stress in tomato. *Journal of Experimental Botany*, *68*, 5845-5856.

Stirbet, A., Govindjee. (2011). On the relation between the Kautsky effect (chlorophyll *a* fluorescence induction) and photosystem II: basics and applications of the OJIP fluorescence transient. *Journal of Photochemistry and Photobiology B: Biology*, *104*, 236-257.

Strasser, R. J., Srivastava, A., Govindjee. (1995). Polyphasic chlorophyll a fluorescence transient in plants and cyanobacteria. *Photochemistry and Photobiology*, *61*, 32-42.

Stroebel, D., Choquet, Y., Popot, J. L., & Picot, D. (2003). An atypical haem in the cytochrome b 6 f complex. *Nature*, *426*, 413-418.

Styring, S., Sjöholm, J., & Mamedov, F. (2012). Two tyrosines that changed the world: Interfacing the oxidizing power of photochemistry to water splitting in photosystem II. *Biochimica et Biophysica Acta (BBA)-Bioenergetics*, *1817*, 76-87.

Subramanyam, R., Jolley, C., Brune, D. C., Fromme, P., & Webber, A. N. (2006). Characterization of a novel Photosystem I–LHCI supercomplex isolated from *Chlamydomonas reinhardtii* under anaerobic (State II) conditions. *FEBS letters*, *580*, 233-238.

Sugimoto, I., & Takahashi, Y. (2003). Evidence that the PsbK polypeptide is associated with the photosystem II core antenna complex CP43. *Journal of Biological Chemistry*, *278*, 45004-45010.

Szarka, A., Tomasskovics, B., & Bánhegyi, G. (2012). The ascorbate-glutathione-α-tocopherol triad in abiotic stress response. *International Journal of Molecular Sciences*, *13*, 4458-4483.

Takaichi, S. (2011). Carotenoids in algae: distributions, biosyntheses and functions. *Marine Drugs*, *9*, 1101-1118.

Takami, T., Shibata, M., Kobayashi, Y., Shikanai, T. (2010). De novo biosynthesis of fatty acids plays critical roles in the response of the photosynthetic machinery to low temperature in Arabidopsis. *Plant and Cell Physiology*, *51*, 1265-1275.

Tang, Y., Wen, X., Lu, Q., Yang, Z., Cheng, Z., Lu, C. (2007). Heat stress induces an aggregation of the light-harvesting complex of photosystem II in spinach plants. *Plant Physiology*, *143*, 629-638.

Thakur, M., Anand, A. (2021). Hydrogen sulfide: An emerging signaling molecule regulating drought stress response in plants. *Physiologia Plantarum*, *172*, 1227-1243.

Tikhonov, A. N. (2014). The cytochrome b6f complex at the crossroad of photosynthetic electron transport pathways. *Plant Physiology and Biochemistry*, *81*, 163-183.

Tiwari, A., Mamedov, F., Grieco, M., Suorsa, M., Jajoo, A., Styring, S., ... & Aro, E. M. (2016). Photodamage of iron–sulphur clusters in photosystem I induces non-photochemical energy dissipation. *Nature Plants*, *2*, 1-9.

ul Haq, S., Khan, A., Ali, M., Khattak, A. M., Gai, W. X., Zhang, H. X., ... & Gong, Z. H. (2019). Heat shock proteins: dynamic biomolecules to counter plant biotic and abiotic stresses. *International Journal of Molecular Sciences*, *20*, 5321.

Umena, Y., Kawakami, K., Shen, J. R., & Kamiya, N. (2011). Crystal structure of oxygen-evolving photosystem II at a resolution of 1.9 Å. *Nature*, *473*, 55-60.

Varshney, R. K., Song, C., Saxena, R. K., Azam, S., Yu, S., Sharpe, A. G., ... & Cook, D. R. (2013). Draft genome sequence of chickpea (*Cicer arietinum*) provides a resource for trait improvement. *Nature Biotechnology*, *31*, 240-246.

Vigani, G., Zocchi, G., Bashir, K., Philippar, K., & Briat, J. F. (2013). Signals from chloroplasts and mitochondria for iron homeostasis regulation. *Trends in Plant Science*, *18*, 305-311.

Vredenberg, W. J., & Duysens, L. N. (1963). Transfer of energy from bacteriochlorophyll to a reaction centre during bacterial photosynthesis. *Nature*, *197*, 355-357.

Wahab, A., Abdi, G., Saleem, M. H., Ali, B., Ullah, S., Shah, W., ... & Marc, R. A. (2022). Plants' physio-biochemical and phyto-hormonal responses to alleviate the adverse effects of drought stress: A comprehensive review. *Plants*, *11*, 1620.

Wang, N., Qian, Z., Luo, M., Fan, S., Zhang, X., & Zhang, L. (2018). Identification of salt stress responding genes using transcriptome analysis in green alga *Chlamydomonas reinhardtii*. *International Journal of Molecular Sciences*, *19*, 3359.

Wang, W. H., Chen, J., Liu, T. W., Chen, J., Han, A. D., Simon, M., ... & Zheng, H. L. (2014). Regulation of the calcium-sensing receptor in both stomatal movement and

photosynthetic electron transport is crucial for water use efficiency and drought tolerance in Arabidopsis. *Journal of Experimental Botany, 65*, 223-234.

Wang, Y., Huang, Y., Fu, W., Guo, W., Ren, N., Zhao, Y., Ye, Y. (2020). Efficient physiological and nutrient use efficiency responses of maize leaves to drought stress under different field nitrogen conditions. *Agronomy*, *10*, 523.

Wang, Z., Li, G., Sun, H., Ma, L., Guo, Y., Zhao, Z., Gao, H., Mei, L. (2018). Effects of drought stress on photosynthesis and photosynthetic electron transport chain in young apple tree leaves. *Biology Open, 7*, bio035279.

Watanabe, M., Kubota, H., Wada, H., Narikawa, R., & Ikeuchi, M. (2011). Novel supercomplex organization of photosystem I in Anabaena and *Cyanophora paradoxa*. *Plant and Cell Physiology*, *52*, 162-168.

Whitelegge, J. P., Zhang, H., Aguilera, R., Taylor, R. M., & Cramer, W. A. (2002). Full Subunit Coverage Liquid Chromatography Electrospray Ionization Mass Spectrometry ($LCMS^+$) of an Oligomeric Membrane Protein: Cytochrome b_6f Complex From Spinach and the Cyanobacterium *Mastigocladus Laminosus* S. *Molecular & Cellular Proteomics*, *1*, 816-827.

Xu, X. H., Wang, C., Li, S. X., Su, Z. Z., Zhou, H. N., Mao, L. J., ... & Lin, F. C. (2015). Friend or foe: differential responses of rice to invasion by mutualistic or pathogenic fungi revealed by RNAseq and metabolite profiling. *Scientific Reports*, *5*, 1-14.

Yadav, S., Modi, P., Dave, A., Vijapura, A., Patel, D., & Patel, M. (2020). Effect of abiotic stress on crops. *Sustainable Crop Production*, *3*.

Yadavalli, V., Jolley, C. C., Malleda, C., Thangaraj, B., Fromme, P., & Subramanyam, R. (2012). Alteration of proteins and pigments influence the function of photosystem I under iron deficiency from *Chlamydomonas reinhardtii*. *PLoS One*, *7*, e35084.

Yadavalli, V., Malleda, C., & Subramanyam, R. (2011). Protein–protein interactions by molecular modeling and biochemical characterization of PSI-LHCI supercomplexes from *Chlamydomonas reinhardtii*. *Molecular BioSystems*, *7*, 3143-3151.

Yamamoto, Y., Kai, S., Ohnishi, A., Tsumura, N., Ishikawa, T., Hori, H., Morita, N., Ishikawa, Y. (2014). Quality control of PSII: behavior of PSII in the highly crowded grana thylakoids under excessive light. *Plant and Cell Physiology*, *55*, 1206-1215.

Yang, M., Meng, Y., Chu, Y., Fan, Y., Cao, X., Xue, S., & Chi, Z. (2018). Triacylglycerol accumulates exclusively outside the chloroplast in short-term nitrogen deprived *Chlamydomonas reinhardtii*. *Biochimica et Biophysica Acta (BBA)-Molecular and Cell Biology of Lipids*, 1863, 1478-1487.

Yang, X., Li, Y., Chen, H., Huang, J., Zhang, Y., Qi, M., Liu, Y., Li, T. (2020). Photosynthetic response mechanism of soil salinity-induced cross-tolerance to subsequent drought stress in tomato plants. *Plants*, *9*, 363.

Yoon, K., Han, D., Li, Y., Sommerfeld, M., & Hu, Q. (2012). Phospholipid: diacylglycerol acyltransferase is a multifunctional enzyme involved in membrane lipid turnover and degradation while synthesizing triacylglycerol in the unicellular green microalga *Chlamydomonas reinhardtii*. *The Plant Cell*, *24*, 3708-3724.

Yu, Z, Wang, X., Zhang, L. (2018). Structural and functional dynamics of dehydrins: a plant protector protein under abiotic stress. *International Journal of Molecular Sciences*, *19*, 3420.

Zhang, L., Aro, E. M. (2002). Synthesis, membrane insertion and assembly of the chloroplast encoded D1 protein into photosystem II. *FEBS Letters*, *512*, 13-18.

Zhang, M., Fan, J., Taylor, D. C., & Ohlrogge, J. B. (2009). DGAT1 and PDAT1 acyltransferases have overlapping functions in Arabidopsis triacylglycerol biosynthesis and are essential for normal pollen and seed development. *The Plant Cell, 21, 3885-3901*.

Zhang, Y., Li, Z., Peng, Y., Wang, X., Peng, D., Li, Y., ... & Yan, Y. (2015). Clones of FeSOD, MDHAR, DHAR genes from white clover and gene expression analysis of ROS-scavenging enzymes during abiotic stress and hormone treatments. *Molecules*, *20*, 20939-20954.

Zheng, L., Li, Y., Li, X., Zhong, Q., Li, N., Zhang, K., ... & Gao, N. (2019). Structural and functional insights into the tetrameric photosystem I from heterocyst-forming cyanobacteria. *Nature Plants*, *5*, 1087-1097.

Zhu, J. K. (2002). Salt and drought stress signal transduction in plants. *Annual Review of Plant Biology*, *53*, 247-273.

Appendix

Research Articles Published and Papers Presented

at Conferences by Jayendra Pandey

(First pages of the articles are attached)

LIST OF PUBLICATIONS/ PRESENTATIONS

PUBLICATIONS IN REFEREED JOURNALS

1. **Pandey, J**., Devadasu, E., Saini, D., Dhokne, K., Marriboina, S., Raghavendra, A. S., & Subramanyam, R. (2023). Reversible changes in structure and function of photosynthetic apparatus of pea (*Pisum sativum*) leaves under drought stress. *The Plant Journal*, *113*, 60-74.
2. Rath, J. R[#.], **Pandey, J[#]**., Yadav, R. M[#]., Zamal, M. Y., Ramachandran, P., Mekala, N. R., ... & Subramanyam, R. (2022). Temperature-induced reversible changes in photosynthesis efficiency and organization of thylakoid membranes from pea (*Pisum sativum*). *Plant Physiology and Biochemistry*, *185*, 144-154. (#) These authors contributed equally to the work.
3. Dhokne, K., **Pandey, J**., Yadav, R. M., Ramachandran, P., Rath, J. R., & Subramanyam, R. (2022). Change in the photochemical and structural organization of thylakoids from pea (*Pisum sativum*) under salt stress. *Plant Physiology and Biochemistry*, *177*, 46-60.
4. Devadasu, E., **Pandey, J**., Dhokne, K., & Subramanyam, R. (2021). Restoration of photosynthetic activity and supercomplexes from severe iron starvation in *Chlamydomonas reinhardtii*. *Biochimica et Biophysica Acta (BBA)-Bioenergetics*, *1862*, 148331.
5. Chouhan, N., Yadav, R. M., **Pandey, J**., & Subramanyam, R. (2023). High light-induced changes in thylakoid supercomplexes organization from cyclic electron transport mutants of *Chlamydomonas reinhardtii*. *Biochimica et Biophysica Acta (BBA)-Bioenergetics*, *1864*, 148917.
6. Saini, D., Baptala, R. B., **Pandey, J**., Aswani, V., Sunil, B., Gahir, S., ... & Raghavendra, A. S. (2023). Modulation by S-nitrosoglutathione (a natural

nitric oxide donor) of photosystem in *Pisum sativum* leaves, as revealed by chlorophyll fluorescence: Light-dependent aggravation of nitric oxide effects. *Plant Science Today, 10,* 393-398.

7. Yadav RM, Marriboina S, Zamal MY, **Pandey J** and Subramanyam R (2023) High light-induced changes in whole-cell proteomic profile and its correlation with the organization of thylakoid super-complex in cyclic electron transport mutants of *Chlamydomonas reinhardtii*. *Frontiers in Plant Science, 14,* 1198474.

PRESENTATIONS AT SCIENTIFIC MEETINGS

1. **Pandey Jayendra** and Prof S. Rajagopal (2022) "Reversible changes in structure and function of photosynthetic apparatus of pea (*Pisum sativum*) under drought stress*"* orally presented at '*International Conference on Physiological and Molecular Mechanisms for Abiotic Stress Tolerance in Plants*' held at Department of Botany, University of Calicut, Kerala on 26th October-28th October 2022.
2. Highest Impact factor (Mahesh award) for publishing my work with the below citation **Pandey J**, Devadasu E, Saini D, Dhokne K, Marriboina S, Raghavendra AS, Rajagopal S (2023) Reversible changes in structure and function of photosynthetic apparatus of pea (*Pisum sativum*) leaves under drought stress. *The Plant Journal* 113: 60-74 in a Journal having the highest impact factor (JCR 2021) of 7.091 organized by the Department of Plant Sciences, School of Life Sciences, University of Hyderabad, Telangana (February 23-25, 2023).
3. International Seminar, joint seminar between University of Okayama and University of Hyderabad, presentation entitled as Reversible changes in

photosynthetic apparatus of pea (*Pisum sativum*) leaves under drought stress: Aggregation of LHCII and PSI core complexes on November 18, 2021, jointly organized by University of Hyderabad and Okayama University.

4. Poster presentation on Reversible changes in structure and function of photosynthetic apparatus of pea (*Pisum sativum*) leaves under drought stress in the International conference on "Current Trends and Future Prospects of Plant Biology (CTFPPB-2023) organized by the Department of Plant Sciences, School of Life Sciences, University of Hyderabad, Telangana (February 23-25, 2023).
5. Oral presentation on Reversible changes in photosynthetic apparatus of pea (*Pisum sativum*) leaves under drought stress: Aggregation of LHCII and PSI core complexes on October 29, 2021, in the Plant science colloquium organized by University of Hyderabad.
6. MHRD, Government of India, GIAN Workshop on Chloroplast structure and function participated in the course entitled Chloroplast structure and function from August 26- September 6, 2019, organized by University of Hyderabad.
7. MHRD, Government of India, GIAN Workshop on applied Photosynthesis: Putting nature to work participated and obtained A in the course titled Applied Photosynthesis Putting nature to work during the period of September 16-20, 2019, University of Hyderabad.

the plant journal

SEB SOCIETY FOR EXPERIMENTAL BIOLOGY

The Plant Journal (2023) **113,** 60–74 doi: 10.1111/tpj.16034

Reversible changes in structure and function of photosynthetic apparatus of pea (*Pisum sativum*) leaves under drought stress

Jayendra Pandey, Elsinraju Devadasu[†], Deepak Saini, Kunal Dhokne, Sureshbabu Marriboina, Agepati S. Raghavendra and Rajagopal Subramanyam[*]

Department of Plant Sciences, School of Life Sciences, University of Hyderabad, Hyderabad 500046, India

Received 15 March 2022; accepted 8 November 2022; published online 14 November 2022.

*For correspondence (e-mail srgsl@uohyd.ac.in)

[†]Present address: Department of Biochemistry and Molecular Biology, Michigan State University, East Lansing, MI, 48824, USA

SUMMARY

The effects of drought on photosynthesis have been extensively studied, whereas those on thylakoid organization are limited. We observed a significant decline in gas exchange parameters of pea (*Pisum sativum*) leaves under progressive drought stress. Chl *a* fluorescence kinetics revealed the reduction of photochemical efficiency of photosystem (PS)II and PSI. The non-photochemical quenching (NPQ) and the levels of PSII subunit PSBS increased. Furthermore, the light-harvesting complexes (LHCs) and some of the PSI and PSII core proteins were disassembled in drought conditions, whereas these complexes were reassociated during recovery. By contrast, the abundance of supercomplexes of PSII-LHCII and PSII dimer were reduced, whereas LHCII monomers increased following the change in the macro-organization of thylakoids. The stacks of thylakoids were loosely arranged in drought-affected plants, which could be attributed to changes in the supercomplexes of thylakoids. Severe drought stress caused a reduction of both LHCI and LHCII and a few reaction center proteins of PSI and PSII, indicating significant disorganization of the photosynthetic machinery. After 7 days of rewatering, plants recovered well, with restored chloroplast thylakoid structure and photosynthetic efficiency. The correlation of structural changes with leaf reactive oxygen species levels indicated that these changes were associated with the production of reactive oxygen species.

Keywords: disassembly of LHCII and PSI core, drought stress, non-photochemical quenching, pigment–protein complexes, photosystem, *Pisum sativum*, thylakoid organization.

INTRODUCTION

Drought stress is a significant environmental constraint that hampers crop yield, particularly in arid and semi-arid regions. There is an urgent need to develop varieties that can grow under limited water conditions without compromising yields. In this direction, it is crucial to understand the physiological, molecular, and photosynthetic responses of crop species under drought. Upon exposure to drought stress, plants displayed various morphological symptoms such as wilting, desiccation of leaves, chlorosis, leaf curling, burning of leaf edges, and necrosis (Seleiman et al., 2021). Parallelly, the stomatal conductance decreased to reduce the water evaporation through leaves (Li et al., 2017). Low stomatal conductance decreases intercellular CO_2, minimizing the supply for photosynthesis (Kelly et al., 2016). As a result, plants water use efficiency (WUE) decreased. Similarly, the leaf relative water content (RWC), an indicator of stress intensity, was also lowered.

The drought-induced imbalance between light capture and its utilization leads to the accumulation of reactive oxygen species (ROS) in the chloroplast and, subsequently, the disorganization of thylakoid membranes (Das & Roychoudhury, 2014). To combat ROS, plants utilize several antioxidant enzymes, such as ascorbate peroxidase (APX), catalase (CAT), and superoxide dismutase (SOD) during drought stress (Thakur & Anand, 2021). The net photosynthetic rate, chlorophyll (Chl) fluorescence, and antioxidant activities were significantly altered under water deficit conditions (Iqbal et al., 2019). The fast Chl *a* fluorescence is an efficient parameter to monitor the photosystem (PS)II and PSI photochemistry (Sánchez-Reinoso et al., 2019; Sipka et al., 2021). However, drought stress can limit the availability of water molecules for the photolysis of water, affecting the efficiency of the PSII oxygen-evolving complex (OEC), particularly D1 activity of PSII (Sasi et al., 2018).

Plant Physiology and Biochemistry 185 (2022) 144–154

Contents lists available at ScienceDirect

Plant Physiology and Biochemistry

journal homepage: www.elsevier.com/locate/plaphy

Temperature-induced reversible changes in photosynthesis efficiency and organization of thylakoid membranes from pea (*Pisum sativum*)

Jyoti Ranjan Rath [a,1], Jayendra Pandey [a,1], Ranay Mohan Yadav [a,1], Mohammad Yusuf Zamal [a], Pavithra Ramachandran [a], Nageswara Rao Mekala [a], Suleyman I. Allakhverdiev [b], Rajagopal Subramanyam [a,*]

[a] Department of Plant Sciences, School of Life Sciences, University of Hyderabad, Hyderabad, 500046, India
[b] K.A. Timiryazev Institute of Plant Physiology, Russian Academy of Sciences, Botanicheskaya St. 35, Moscow, 127276, Russia

A B S T R A C T

High temperature can induce a substantial adverse effect on plant photosynthesis. This study addressed the impact of moderately high temperature (35 °C) on photosynthetic efficiency and thylakoid membrane organization in *Pisum sativum*. The Chl *a* fluorescence curves showed a significant change, indicating a reduction in photosynthetic efficiency when pea plants were exposed to moderate high-temperature stress. The pulse-amplitude modulation measurements showed decreased non-photochemical quenching while the non-regulated energy dissipation increased in treated compared to control and recovery plants. Both parameters indicated that the photosystem (PS)II was prone to temperature stress. The PSI donor side limitation increased in treated and recovery plants compared to control, suggesting the donor side of PSI is hampered in moderate-high temperature. Further, the PSI acceptor side increased in recovery plants compared to control, suggesting that the cyclic electron transport is repressed after temperature treatment but revert back to normal in recovery conditions. Also, the content of photoprotective carotenoid pigments like lutein and xanthophylls increased in temperature-treated leaves. These results indicate the alteration of macro-organization of thylakoid membranes under moderately elevated temperature, whereas supercomplexes restored to the control levels under recovery conditions. Further, the light harvesting complex (LHC)II trimers, and monomers were significantly decreased in temperature-treated plants. Furthermore, the amount of PSII reaction center proteins D1, D2, PsbO, and Cyt *b*6 was reduced under moderate temperature, whereas the content of LHC proteins of PSI was stable. These observations suggest that moderately high temperature can alter supercomplexes, which leads to change in the pigment-protein organization.

1. Introduction

Plants are subjected to various biotic and abiotic stress factors during their growth period. Several abiotic stress factors affect plant growth, yield, and productivity. Among the abiotic stress factors, the role of temperature stress on the plant photosynthetic machinery cannot be overlooked. The remarkable growth, yield, and productivity of a plant depend on proper functioning of its photosynthetic machinery. Plants are exposed to fluctuations in temperatures throughout their growth period. Temperatures above the optimum levels that can induce any morphological, physiological, molecular, or biochemical changes to the exposed plant can be designated as heat stress (Wahid et al., 2007).

Several studies have revealed the physiological mechanisms involved in heat stress responses and their tolerance mechanism developed in plants. Since plants are sessile, they have to endure and develop specific preventive measures that help them adhere to this situation (Sattari et al., 2020). The productivity of a plant is affected in several ways under high-temperature stress (Allakhverdiev et al., 2008). Although several physiological, biochemical, and molecular processes contribute to plant growth and productivity, photosynthesis is the major pathway that affects these processes directly or indirectly (Mathur et al., 2014). Temperature stress primarily inhibits plant photosynthesis before impairing other cell functions (Berry and Bjorkman, 2003). Any form of stress is initially perceived by the plant's photosynthetic machinery that includes both the photosystems (PSII and PSI) along with the oxygen-evolving complex (OEC), ATP synthase, and the enzymes involved in the dark reaction process (Aro et al., 1993; Mohanty et al., 2007).

Plant chloroplast pigments play an essential role in capturing light energy. They are also a constituent of the reaction centers (RC) and light-harvesting complexes (LHCs). The electron excitation from pigments leads to photochemical reactions, including the photolysis of water that mainly drives the photosynthesis process. Temperature stressed plants have reduced chlorophyll biosynthesis (Efeoglu and Terzioglu, 2009). This decrease is correlated with the inactivation of chlorophyll

* Corresponding author. Department of Plant Sciences, School of Life Sciences, University of Hyderabad, Hyderabad, 500046, Telangana, India.
E-mail address: srgsl@uohyd.ac.in (R. Subramanyam).
[1] These authors contributed equally.

https://doi.org/10.1016/j.plaphy.2022.05.036
Received 24 May 2022; Accepted 30 May 2022
Available online 7 June 2022

Plant Physiology and Biochemistry 177 (2022) 46–60

Contents lists available at ScienceDirect

Plant Physiology and Biochemistry

journal homepage: www.elsevier.com/locate/plaphy

Change in the photochemical and structural organization of thylakoids from pea (*Pisum sativum*) under salt stress

Kunal Dhokne [a,b], Jayendra Pandey [a], Ranay Mohan Yadav [a], Pavithra Ramachandran [a], Jyoti Ranjan Rath [a], Rajagopal Subramanyam [a,*]

[a] Department of Plant Sciences, School of Life Sciences, University of Hyderabad, Hyderabad, 500046, India
[b] Department of Botany, Shri Vitthal Rukmini College, Sawana, Yavatmal, 445001, India

ARTICLE INFO

Keywords:
Chl *a* fluorescence
Non-photochemical quenching
Pigment-protein complexes
Photosystem
Pisum sativum
Proton motive force
Salt stress
Thylakoid organization

ABSTRACT

Salt can induce adverse effects, primarily on the photosynthetic process, ultimately influencing plant productivity. Still, the impact of salt on the photosynthesis process in terms of supercomplexes organization of thylakoid structure and function is not understood in Pea (*Pisum sativum*). To understand the structure and function in the leaves and thylakoids under salt (NaCl) treatment, we used various biophysical and biochemical techniques like infrared gas analyzer, chlorophyll *a* fluorescence, circular dichroism, electron microscopy, blue native gels, and western blots. The net photosynthetic rate, transpiration rate, and stomatal conductance were reduced significantly, whereas the water use efficiency was enhanced remarkably under high salt conditions (200 mM NaCl). The photochemical efficiency of both photosystem (PS) I and II was reduced in high salt by inhibiting their donor and acceptor sides. Interestingly the non-photochemical quenching (NPQ) is reduced in high salt; however, the non-regulated energy dissipation (NO) of PSII increased, leading to inactivation of PSII. The obtained results exhibit inhibition of NAD(P)H dehydrogenase (NDH) mediated pathway-dependent cyclic electron transport under salinity caused a decrease in proton motive force of ΔpH and Δψ. Further, the electron micrographs show the disorganization of grana thylakoids under salt stress. Furthermore, the macro-organization and supercomplexes of thylakoids were significantly affected by high salt. Specifically, the mega complexes, PSII-LHCII, PSI-LHCI, and NDH complexes were notably reduced, ultimately altering the electron transport. The reaction center proteins of oxygen-evolving complexes, D1 and D2 proteins were affected to high salt indicating changes in photochemical activities.

1. Introduction

Salinity stress is a major environmental threat to the world by restricting plant growth, leading to ultimately reduced crop yield. Since photosynthesis is one of the most important metabolic processes in plants, the adverse impact of salinity generally caused by developing osmotic stress and ion-specific toxicity (Na^+) limiting the crop productivity (Pandolfi et al., 2012; Roy et al., 2014). This dual stress condition induces significant changes in photosynthetic activities by inhibiting the quantum yield of photosystem (PS)II electron transport and disorganizing the thylakoid membrane.

Photosynthetic efficiency often decreased under the salinity stress (Yuan et al., 2014; Shu et al., 2019). PSII is susceptible to salinity stress causes the photoinhibition of PSII, which leads to the generation of reactive oxygen species (Gururani et al., 2015). Salt stress damages the oxygen evolving complex (OEC), blocks the electron from photo-oxidized water to PSII donor side and acceptor side of PSII and inactive the PSII reaction center (Lu et al., 2020; Demetriou et al., 2007; Goussi et al., 2018). In higher plants, the OEC 23 kDa protein, which is extrinsically bound to PSII, was dissociated under salt stress (Murata et al., 1992). The previous reports exhibit that both PSI and PSII were inactivated by osmotic stress (Allakhverdiev et al., 2000). Other reports

Abbreviations: β-DM, n-dodecyl β-D-maltoside; Chl, chlorophyll; F_O, initial fluorescence; Fm, maximum fluorescence; kDa, kilodaltons; LHCI, light-harvesting chlorophyll-protein of PSI; LHCII, light-harvesting chlorophyll-protein of PSII; PAGE, polyacrylamide gel electrophoresis; PSI, photosystem I; PSII, photosystem II; NPQ, non-photochemical quenching; OEC, oxygen-evolving complex; PPFD, photosynthetic photon flux density; SDS, sodium dodecyl sulfate; WUE, water use efficiency; Y(NA), acceptor side limitation of PSI; Y(ND), donor side regulation of PSI.

* Corresponding author. Department of Plant Sciences, School of Life Sciences, University of Hyderabad, Hyderabad, 500046, Telangana, India.
E-mail address: srgsl@uohyd.ac.in (R. Subramanyam).

https://doi.org/10.1016/j.plaphy.2022.02.004
Received 17 January 2022; Received in revised form 2 February 2022; Accepted 7 February 2022
Available online 12 February 2022

BBA - Bioenergetics 1864 (2023) 148917

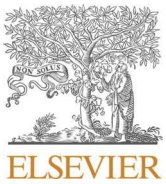

Contents lists available at ScienceDirect

BBA - Bioenergetics

journal homepage: www.elsevier.com/locate/bbabio

High light-induced changes in thylakoid supercomplexes organization from cyclic electron transport mutants of *Chlamydomonas reinhardtii*

Nisha Chouhan, Ranay Mohan Yadav, Jayendra Pandey, Rajagopal Subramanyam *

Department of Plant Sciences, School of Life Sciences, University of Hyderabad, Hyderabad 500046, India

ARTICLE INFO

Keywords:
Aggregation
Carotenoid
Chlamydomonas reinhardtii
Macromolecular structure
Photosystems
Supercomplexes
Xanthophyll cycle

ABSTRACT

The localization of carotenoids and macromolecular organization of thylakoid supercomplexes have not been reported yet in *Chlamydomonas reinhardtii* WT and cyclic electron transport mutants (*pgrl1* and *pgr5*) under high light. Here, the various pigments, protein composition, and pigment-protein interactions were analyzed from the cells, thylakoids, and sucrose density gradient (SDG) fractions. Also, the supercomplexes of thylakoids were separated from BN-PAGE and SDG. The abundance of light-harvesting complex (LHC) II trimer complexes and pigment-pigment interaction were changed slightly under high light, shown by circular dichroism. However, a drastic change was seen in photosystem (PS)I-LHCI complexes than PSII complexes, especially in *pgrl1* and *pgr5*. The lutein and β-carotene increased under high light in LHCII trimers compared to other supercomplexes, indicating that these pigments protected the LHCII trimers against high light. However, the presence of xanthophylls, lutein, and β-carotene was less in PSI-LHCI, indicating that pigment-protein complexes altered in high light. Even the real-time PCR data shows that the *pgr5* mutant does not accumulate zeaxanthin dependent genes under high light, which shows that violaxanthin is not converting into zeaxanthin under high light. Also, the protein data confirms that the LHCSR3 expression is absent in *pgr5*, however *it is presented in LHCII trimer in WT and pgrl1*. Interestingly, some of the core proteins were aggregated in *pgr5,* which led to change in photosynthesis efficiency in high light.

1. Introduction

Light is a critical environmental factor for photosynthesis; however, excessive light damages the photosynthetic apparatus. For example, high-intensity light can trigger the conversion of chlorophyll singlets excited state (^{1}Chl*) into the triplet state, ^{3}Chl*. This results in energy transfer reactions that produce singlet oxygen ($^1O_2$) which causes photodamage and photoinhibition [1]. Plants and algae have evolved photoprotection mechanisms such as the cyclic electron transport (CET) around the photosystem (PS)I. To mitigate light-induced damages, plants have developed a photoprotective mechanism involving carotenoids to dissipate excess energy in the form of heat. Tightly bound carotenoids constitutively provide the deactivation of excited ^{3}Chl* and $^1O_2$ within the PSI reaction center and antenna proteins (e.g., β-carotene or lutein).

The carotenoid synthetic pathway is well established, as shown in SFig. 1. Briefly, acetyl CoA and geranylgeranyl diphosphate is converted by the phytoene synthase enzyme (PSY) into phytoene, the first committed step in the biosynthesis of carotenoids. Next, phytoene is converted to lycopene by phytoene desaturase, a reaction that can be divided into two cycles, namely, (i) the synthesis of lutein from α-carotene and (ii) the synthesis of violaxanthin from β-carotene by violaxanthin in the de-epoxidase cycle. Under strong light intensity, violaxanthin is converted into zeaxanthin by violaxanthin de-epoxidase (Vde) to dissipate the excess energy from excited chlorophylls, as depicted in SFig. 1 [2].

Carotenoids perform different photoprotection mechanisms like the change of ^{3}Chl* yield [3], scavenging of reactive oxygen species (ROS) [4,5], and dissipation of energy from light absorbed more than non-photochemical quenching (NPQ) [6]. Xanthophyll is essential in protecting the chloroplast from photooxidative damage and participates in light harvesting [7]. Algae and plants regulate photosynthetic light-harvesting and use various antioxidant molecules and enzymes to detoxify ROS [8] and free radicals, which form because of stress conditions [9,10].

Most plants and algae receive the optimal amount of sunlight. Still, too much light can lead to over-excitation of the photosystem, which is deexcited by thermal energy dissipation called NPQ [11]. The most

* Corresponding author.
E-mail address: srgsl@uohyd.ernet.in (R. Subramanyam).

https://doi.org/10.1016/j.bbabio.2022.148917
Received 15 February 2022; Received in revised form 3 September 2022; Accepted 8 September 2022
Available online 13 September 2022

PLANT SCIENCE TODAY
ISSN 2348-1900 (online)
Vol x(x): xx–xx
https://doi.org/10.14719/pst.2248

HORIZON
e-Publishing Group
HePG

RESEARCH ARTICLE

Modulation by S-nitrosoglutathione (a natural nitric oxide donor) of photosystem in *Pisum sativum* leaves, as revealed by chlorophyll fluorescence: Light-dependent aggravation of nitric oxide effects

Deepak Saini[1], Ramesh B. Bapatla[1], Jayendra Pandey[1],Vetcha Aswani[1], Bobba Sunil[1],Shashibhushan Gahir[1], Pulimamidi Bharath[1], Rajagopal Subramanyam[1] & Agepati S. Raghavendra[1*]

[1]Department of Plant Sciences, School of Life Sciences, University of Hyderabad, Hyderabad, 500046, India

*Email: asrsls@gmail.com, asrsl@uohyd.ernet.in

OPEN ACCESS

ARTICLE HISTORY

Received: 22 November 2022
Accepted: 01 January 2023

Available online
Version 1.0 : 15 January 2023

Check for updates

Additional information

Peer review: Publisher thanks Sectional Editor and the other anonymous reviewers for their contribution to the peer review of this work.

Reprints & permissions information is available at https://horizonepublishing.com/journals/index.php/PST/open_access_policy

Publisher's Note: Horizon e-Publishing Group remains neutral with regard to jurisdictional claims in published maps and institutional affiliations.

Indexing: Plant Science Today, published by Horizon e-Publishing Group, is covered by Scopus, Web of Science, BIOSIS Previews, Clarivate Analytics, NAAS etc.
See https://horizonepublishing.com/journals/index.php/PST/indexing_abstracting

CITE THIS ARTICLE

Saini D, Bapatla R B, Pandey J, Aswani V, Sunil B, Gahir S, Bharath P, Subramanyam R & Raghavendra A S. Modulation by S-nitrosoglutathione (a natural nitric oxide donor) of photosystem in *Pisum sativum* leaves, as revealed by chlorophyll fluorescence: Light-dependent aggravation of nitric oxide effects. Plant Science Today (Early Access). https://doi.org/10.14719/pst.2248

Abstract

The reported effects of nitric oxide (NO), a signaling molecule, on the photochemical components of leaves are ambiguous. We examined the changes by a natural NO donor, S-nitrosoglutathione (GSNO). The effect of GSNO on *Pisum sativum* leaves was studied after a 3-hour exposure in dark, moderate (ML), or high light (HL). The NO levels in GSNO-treated samples were at their maximum under HL, compared to those under ML or dark. Most of the elevated NO was decreased by 2-4-carboxyphenyl-4,4,5,5-tetramethylimidazoline-1-oxyl-3-oxide (cPTIO), a NO scavenger, confirming the NO increase. Treatment with GSNO caused inhibition of photosynthesis/respiration and restricted electron transport mediated by both photosystem (PS)II and PSI. However, the inhibition by NO-donor of PSII components was stronger than those of PSI. A marked increase in the PSI acceptor side limitation [Y(NA)] and a decrease in PSI donor side limitation [Y(ND)] indicated an upregulation of cyclic electron transport, possibly to balance the damage to PSII by GSNO. We suggest that NO aggravated the HL-induced inhibition of photosynthesis and dark respiration.

Keywords

Chl fluorescence; nitric oxide; photosynthesis; photosystems; respiration; high light.

Introduction

Abiotic stress affects photosynthesis in higher plants by targeting the photosynthetic apparatus, particularly photosystem (PS) II (1, 2). A common consequence of abiotic/biotic stress is the increase in both reactive oxygen species (ROS) and nitric oxide (NO) levels in plant cells (3, 4). ROS and NO could exert multiple effects on photosynthetic and mitochondrial metabolisms (5, 6). The impact of ROS on photosynthesis was studied by several groups (7, 8), while the studies with NO are just catching up (9). Nitric oxide (NO), can modulate various physiological processes in plants (9, 10). There are contrasting claims that NO can be harmful or beneficial for plant cells against stress (4, 11, 12).

In addition to its role as a primary signal, NO may affect respiration and photosynthesis. However, the reports on the modulation by NO of photosynthesis, particularly photosystems (PSI and PSII) are ambiguous. Studies on chlorophyll (Chl) fluorescence indicated that the PSII-related reactions were either decreased (13) or increased on exposure to NO (14). Some studies have suggested that NO may protect PSII components from osmotic or salinity stress (15, 16). Most of these studies were with sodium nitroprusside

BBA - Bioenergetics 1862 (2021) 148331

Contents lists available at ScienceDirect

BBA - Bioenergetics

journal homepage: www.elsevier.com/locate/bbabio

Restoration of photosynthetic activity and supercomplexes from severe iron starvation in *Chlamydomonas reinhardtii*

Elsinraju Devadasu, Jayendra Pandey, Kunal Dhokne, Rajagopal Subramanyam *

Department of Plant Sciences, School of Life Sciences, University of Hyderabad, Hyderabad, Gachibowli, Telangana 500046, India

ARTICLE INFO

Keywords:
Chlamydomonas reinhardtti
Fe deficiency, recovery of photosystems
Pigment-protein complexes, protein aggregation
Super-complexes

ABSTRACT

The eukaryotic alga *Chlamydomonas* (*C.*) *reinhardtii* is used as a model organism to study photosynthetic efficiency. We studied the organization and protein profile of thylakoid membranes under severe iron (Fe^{2+}) deficiency condition and iron supplement for their restoration. Chlorophyll (Chl) *a* fluorescence fast OJIP transients were decreased in the severe Fe^{2+} deficient cells resulting in the reduction of the photochemical efficiency. The circular dichroism (CD) results from Fe^{2+} deficient thylakoid membranes show a significant change in pigment–pigment and pigment-protein excitonic interactions. The organization of super-complexes was also affected significantly. Furthermore, super-complexes of photosystem (PS) II and PSI, along with its dimers, were severely reduced. The complexes separated using sucrose gradient centrifugation shows that loss of super-complexes and excitonic pigment-pigment interactions were restored in the severely Fe^{2+} deficient cells upon Fe supplementation for three generations. Additionally, the immunoblots demonstrated that both PSII, PSI core, and their light-harvesting complex antenna proteins were differentially decreased. However, reduced core proteins were aggregated, which in turn proteins were unfold and destabilized the supercomplexes and its function. Interestingly, the aggregated proteins were insoluble after n-Dodecyl β-D-maltoside solubilization. Further, they were identified in the pellet form. When Fe^{2+} was added to the severely deficient cells, the photosynthetic activity, pigment-proteins complexes, and proteins were restored to the level of control after 3rd generation.

1. Introduction

Iron (Fe^{2+}) is an essential micronutrient required for metabolic processes in all living organisms ranging from cyanobacteria to higher plants. Under aerobic conditions, iron predominantly exists in its insoluble form as Fe(III) oxides in the soil and water compared to the lesser concentration of its soluble form as Fe(II). All organisms have evolved complex mechanisms for Fe acquisition to survive in lower Fe concentrations, as it is an indispensable element. In oxygenic photosynthesis, iron acts as a cofactor in various biochemical pathways. It exists in heme- and iron-sulfur proteins essential for energy transfer mechanisms such as respiration and photosynthesis. The central part of Fe in algae and plants is associated with the chloroplast [1]. Reports have shown that deficiency of optimal iron uptake has led to the reduction of phytoplankton growth by 40% in ocean and 30% in arable lands [2,3]. This highlights the severe effects of the life forms due to the low bioavailability of iron in the food chains and carbon sequestration that affects the photosynthetic complexes of cyanobacteria, algae, and plants.

Fe deficiency can lead to chlorosis in photosynthetic organisms resulting in the inhibition of photosynthetic electron transport, leading to the loss of photosynthetic machinery [4]. Reduced bioavailability of iron decreases the size of chloroplast and the disorganization of thylakoid membranes [5,6]. It is well known that Fe is involved as a co-factor in major protein complexes such as photosystem (PS)II, water-plastoquinone oxidoreductase, cytochrome b_6f complex (Cyt b_6f), plastoquinone- plastocyanin oxidoreductase, PSI, plastocyanin, and ferredoxin oxidoreductase. Several reports show that the PSI complex is a major target of iron starvation because it contains 12 iron molecules present per monomer [7]. In higher plants, iron limitation leads to an alteration of the electron transport chain and decreased abundance of the photosynthetic proteins, reduction of energy transfer between PSII and PSI, and decreased PSII quantum yield [8,9]. In cyanobacteria, light-harvesting phycobilisomes' content is decreased in response to iron deficiency, thereby decreasing the PSI to PSII (PSI/PSII) ratio [7]. As an additional response, the "iron-stress-induced" gene *isiA* is expressed,

* Corresponding author.
E-mail address: srgsl@uohyd.ac.in (R. Subramanyam).

https://doi.org/10.1016/j.bbabio.2020.148331
Received 24 September 2020; Accepted 24 October 2020
Available online 27 October 2020

frontiers | Frontiers in Plant Science

TYPE Original Research
PUBLISHED xx xx 2023
DOI 10.3389/fpls.2023.1198474

OPEN ACCESS

EDITED BY
Bhanu Prakash Petla,
International Crops Research Institute for the Semi-Arid Tropics (ICRISAT), India

REVIEWED BY
Suleyman I. Allakhverdiev,
Russian Academy of Sciences (RAS), Russia
Dinakar Challabathula,
Central University of Tamil Nadu, India

*CORRESPONDENCE
Rajagopal Subramanyam
srgsl@uohyd.ernet.in

†PRESENT ADDRESS
Sureshbabu Marriboina,
Microalgae Biotecnology, Ben-Gurion University of the Negev, Midreshet Ben-Gurion, Israel

RECEIVED 01 April 2023
ACCEPTED 11 May 2023
PUBLISHED xx xx 2023

CITATION
Yadav RM, Marriboina S, Zamal MY, Pandey J and Subramanyam R (2023) High light-induced changes in whole-cell proteomic profile and its correlation with the organization of thylakoid super-complex in cyclic electron transport mutants of *Chlamydomonas reinhardtii*. *Front. Plant Sci.* 14:1198474. doi: 10.3389/fpls.2023.1198474

High light-induced changes in whole-cell proteomic profile and its correlation with the organization of thylakoid super-complex in cyclic electron transport mutants of *Chlamydomonas reinhardtii*

Ranay Mohan Yadav, Sureshbabu Marriboina†, Mohammad Yusuf Zamal, Jayendra Pandey and Rajagopal Subramanyam*

Department of Plant Sciences, School of Life Sciences, University of Hyderabad, Hyderabad, India

Light and nutrients are essential components of photosynthesis. Activating the signaling cascades is critical in starting adaptive processes in response to high light. In this study, we have used wild-type (WT), cyclic electron transport (CET) mutants like Proton Gradient Regulation (PGR) Like 1 (*PGRL1*), and *PGR5* mutants to elucidate the actual role in regulation and assembly of photosynthetic pigment–protein complexes under high light. Here, we have correlated the biophysical, biochemical, and proteomic approaches to understand the targeted proteins and the organization of thylakoid pigment–protein complexes in the photoacclimation. The proteomic analysis showed that 320 proteins were significantly affected under high light compared to the control and are mainly involved in the photosynthetic electron transport chain, protein synthesis, metabolic process, glycolysis, and proteins involved in cytoskeleton assembly. Additionally, we observed that the cytochrome (*Cyt*) b_6 expression is increased in the *pgr5* mutant to regulate proton motive force and ATPase across the thylakoid membrane. The increased Cyt b_6 function in *pgr5* could be due to the compromised function of chloroplast (cp) ATP synthase subunits for energy generation and photoprotection under high light. Moreover, our proteome data show that the photosystem subunit II (PSBS) protein isoforms (PSBS1 and PSBS2) expressed more than the Light-Harvesting Complex Stress-Related (LHCSR) protein in *pgr5* compared to WT and *pgrl1* under high light. In addition, we immunoblotted the photosystems (PS) II and PSI core and associated light-harvesting complex proteins to compare with the total cell proteome. The PSII proteins D1 and D2 accumulated more in *pgrl1* and *pgr5* than WT under high light. In high light, CP43 and CP47 showed a reduced amount in *pgr5* under high light due to changes in chlorophyll and carotenoid content around the PSII protein, which coordinates as a cofactor for efficient energy transfer from the light-harvesting antenna to the photosystem core. BN-PAGE and circular dichroism studies indicate changes in macromolecular assembly and thylakoid

Physiological and Molecular changes of Photosynthetic Apparatus under Drought Stress in Pisum sativum L. (pea)

by Jayendra Pandey

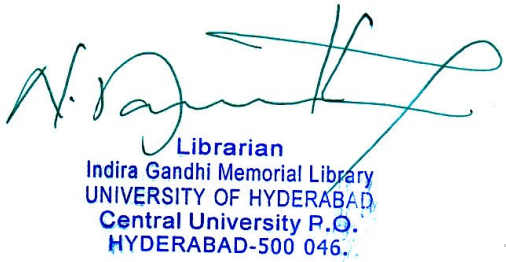

Submission date: 19-Jun-2023 10:40AM (UTC+0530)
Submission ID: 2118803684
File name: Complete_Thesis_17LPPH05_17th_June.pdf (698.17K)
Word count: 34882
Character count: 194355

24% of Similarity is from Mr. Jayendra's Publications

Physiological and Molecular changes of Photosynthetic Apparatus under Drought Stress in Pisum sativum L. (pea)

Prof. S. RAJAGOPAL
Dept. of Plant Sciences
School of Life Sciences
University of Hyderabad
Hyderabad-500 046.

ORIGINALITY REPORT

33%	10%	32%	5%
SIMILARITY INDEX	INTERNET SOURCES	PUBLICATIONS	STUDENT PAPERS

Prof. S. RAJAGOPAL
Dept. of Plant Sciences
School of Life Sciences
University of Hyderabad
Hyderabad-500 046.

PRIMARY SOURCES

1	Jayendra Pandey, Elsinraju Devadasu, Deepak Saini, Kunal Dhokne et al. " Reversible changes in structure and function of photosynthetic apparatus of pea ( ) leaves under drought stress ", The Plant Journal, 2022 Publication	19%
2	Nisha Chouhan, Ranay Mohan Yadav, Jayendra Pandey, Rajagopal Subramanyam. "High light-induced changes in thylakoid supercomplexes organization from cyclic electron transport mutants of Chlamydomonas reinhardtii", Biochimica et Biophysica Acta (BBA) - Bioenergetics, 2022 Publication	2%
3	Submitted to University of Hyderabad, Hyderabad Student Paper	2%
4	Jyoti Ranjan Rath, Jayendra Pandey, Ranay Mohan Yadav, Mohammad Yusuf Zamal et al.	1%

Prof. S. RAJAGOPAL
Dept. of Plant Sciences
School of Life Sciences
University of Hyderabad
Hyderabad-500 046.

	"Temperature-induced reversible changes in photosynthesis efficiency and organization of thylakoid membranes from pea (Pisum sativum)", Plant Physiology and Biochemistry, 2022 Publication	
5	herald.uohyd.ac.in Internet Source	<1 %
6	www.sirsyedcollege.ac.in Internet Source	<1 %
7	"Photosynthesis: Mechanisms and Effects", Springer Science and Business Media LLC, 1998 Publication	<1 %
8	www.frontiersin.org Internet Source	<1 %
9	www.ncbi.nlm.nih.gov Internet Source	<1 %
10	krishikosh.egranth.ac.in Internet Source	<1 %
11	help.igb.illinois.edu Internet Source	<1 %
12	www.science.org Internet Source	<1 %
13	"Photosynthesis: Molecular Approaches to Solar Energy Conversion", Springer Science	<1 %

and Business Media LLC, 2021
Publication

14	Sureshbabu Marriboina, Kapil Sharma, Debashree Sengupta, Anurupa Devi Yadavalli, Rameshwar Prasad Sharma, Ramachandra Attipalli. " Evaluation of high salinity tolerance in (L.) Pierre by a systematic analysis of network ", Physiologia Plantarum, 2021 Publication	<1 %
15	www.mdpi.com Internet Source	<1 %
16	Advances in Photosynthesis and Respiration, 2012. Publication	<1 %
17	www.biorxiv.org Internet Source	<1 %
18	jnanobiotechnology.biomedcentral.com Internet Source	<1 %
19	link.springer.com Internet Source	<1 %
20	www.nature.com Internet Source	<1 %
21	Submitted to CSU, Long Beach Student Paper	<1 %
22	Nisha Chouhan, Ranay Mohan Yadav, Jayendra Pandey, Rajagopal Subramanyam.	<1 %

"High light-induced changes in thylakoid supercomplexes organization from cyclic electron transport mutants of Chlamydomonas reinhardtii", Biochimica et Biophysica Acta (BBA) - Bioenergetics, 2023
Publication

---

23 Y. Liang, Y. Huang, C. Liu, K. Chen, M. Li. "Functions and interaction of plant lipid signalling under abiotic stresses", Plant Biology, 2023 <1 %
Publication

---

24 Jin Koh, Gang Chen, Mi-Jeong Yoo, Ning Zhu, Daniel Dufresne, John E. Erickson, Hongbo Shao, Sixue Chen. " Comparative Proteomic Analysis of in Response to Drought Stress ", Journal of Proteome Research, 2015 <1 %
Publication

---

25 "Photosynthetic Protein Complexes", Wiley, 2008 <1 %
Publication

---

26 dokumen.pub <1 %
Internet Source

---

27 Methods in Molecular Biology, 2014. <1 %
Publication

---

28 Shimna Sudheesh, Timothy I. Sawbridge, Noel OI Cogan, Peter Kennedy, John W. Forster, Sukhjiwan Kaur. "De novo assembly and <1 %

characterisation of the field pea transcriptome using RNA-Seq", BMC Genomics, 2015
Publication

29	Bioenergetic Processes of Cyanobacteria, 2011. Publication	<1 %
30	Sekar Nishanth, Radha Prasanna. "Untargeted GC-MS reveals differential regulation of metabolic pathways in cyanobacterium Anabaena and its biofilms with Trichoderma viride and Providencia sp.", Current Research in Microbial Sciences, 2022 Publication	<1 %
31	Yujie Liu, Kefan Xing, Congcong Yan, Yongzhao Zhou, Xuemei Xu, Yuying Sun, Jiquan Zhang. "Transcriptome analysis of Neocaridina denticulate sinensis challenged by Vibrio parahemolyticus", Fish & Shellfish Immunology, 2022 Publication	<1 %
32	biohpc.cornell.edu Internet Source	<1 %
33	"Cytochrome Complexes: Evolution, Structures, Energy Transduction, and Signaling", Springer Nature, 2016 Publication	<1 %

34	A. Bhattacharya. "Physiological Processes in Plants Under Low Temperature Stress", Springer Science and Business Media LLC, 2022 Publication	<1 %
35	Elsinraju Devadasu, Jayendra Pandey, Kunal Dhokne, Rajagopal Subramanyam. "Restoration of photosynthetic activity and supercomplexes from severe iron starvation in Chlamydomonas reinhardtii", Biochimica et Biophysica Acta (BBA) - Bioenergetics, 2021 Publication	<1 %
36	Sureshbabu Marriboina, Kapil Sharma, Debashree Sengupta, Anurupa Devi Yadavalli et al. " Evaluation of High Salinity Tolerance in (L.) Pierre by a Systematic Analysis of Network ", Physiologia Plantarum, 2021 Publication	<1 %
37	Tatyana Savchenko, Konstantin Tikhonov. "Oxidative Stress-Induced Alteration of Plant Central Metabolism", Life, 2021 Publication	<1 %
38	cyberleninka.org Internet Source	<1 %
39	Chao Yuan, Shaowei Zhang, Ruolin Hu, Dayong Wei, Qinglin Tang, Yongqin Wang, Shibing Tian, Yi Niu, Zhimin Wang.	<1 %

"Comparative transcriptome analysis provides insight into the molecular mechanisms of anther dehiscence in eggplant (Solanum melongena L.)", Genomics, 2021
Publication

40	biotechnologyforbiofuels.biomedcentral.com Internet Source	<1 %
41	ir.lib.uwo.ca Internet Source	<1 %
42	Advances in Photosynthesis and Respiration, 2014. Publication	<1 %
43	Xiaodong Su, Jun Ma, Xuepeng Wei, Peng Cao, Dongjie Zhu, Wenrui Chang, Zhenfeng Liu, Xinzheng Zhang, Mei Li. " Structure and assembly mechanism of plant C S M -type PSII-LHCII supercomplex ", Science, 2017 Publication	<1 %
44	Mayalen Zubia, Yolanda Freile-Pelegrín, Daniel Robledo. "Photosynthesis, pigment composition and antioxidant defences in the red alga Gracilariopsis tenuifrons (Gracilariales, Rhodophyta) under environmental stress", Journal of Applied Phycology, 2014 Publication	<1 %
45	bmcgenomics.biomedcentral.com Internet Source	

		<1 %
46	doktori.bibl.u-szeged.hu Internet Source	<1 %
47	open.library.ubc.ca Internet Source	<1 %
48	Koichi Kobayashi. "Role of membrane glycerolipids in photosynthesis, thylakoid biogenesis and chloroplast development", Journal of Plant Research, 2016 Publication	<1 %
49	Vijaya Pasapula. "Expression of an Arabidopsis vacuolar H+-pyrophosphatase gene (AVP1) in cotton improves drought- and salt tolerance and increases fibre yield in the field conditions : Using AVP1 to improve drought and salt tolerance in cotton", Plant Biotechnology Journal, 05/2010 Publication	<1 %
50	rucore.libraries.rutgers.edu Internet Source	<1 %
51	tailieu.vn Internet Source	<1 %
52	Attipalli Ramachandra Reddy, Kolluru Viswanatha Chaitanya, Munusamy Vivekanandan. "Drought-induced responses	<1 %

of photosynthesis and antioxidant metabolism in higher plants", Journal of Plant Physiology, 2004
Publication

53	doczz.net Internet Source	<1 %
54	Maria Helena Cruz de Carvalho. "Drought stress and reactive oxygen species: production, scavenging and signaling", Plant Signaling & Behavior, 03/01/2008 Publication	<1 %
55	Xiaohong Kou, Cuiyu Mao, Mengshi Wu, Lihua Han, Chen Liu, Bianling Jiang, Zhaohui Xue. " Divergent functions of and possible mechanisms for tomato adaptation to abiotic stresses ", The Journal of Horticultural Science and Biotechnology, 2016 Publication	<1 %
56	hdl.handle.net Internet Source	<1 %
57	academy.ac.il Internet Source	<1 %
58	hal-pasteur.archives-ouvertes.fr Internet Source	<1 %
59	helda.helsinki.fi Internet Source	<1 %

60	kuscholarworks.ku.edu Internet Source	<1 %
61	real-j.mtak.hu Internet Source	<1 %
62	www.researchgate.net Internet Source	<1 %
63	Chunlai Wu, Zehong Ding, Mingjie Chen, Guangxiao Yang, Weiwei Tie, Yan Yan, Jian Zeng, Guangyuan He, Wei Hu. "Identification and functional prediction of lncRNAs in response to PEG and ABA treatment in cassava", Environmental and Experimental Botany, 2019 Publication	<1 %
64	Haichao Hu, Yonghong Liu, Beibei He, Xin Chen, Lei Ma, Yingli Luo, Xitong Fei, Anzhi Wei. "Integrative physiological, transcriptome, and metabolome analysis uncovers the drought responses of two Zanthoxylum bungeanum cultivars", Industrial Crops and Products, 2022 Publication	<1 %
65	Hussan Bano, Habib - ur - Rehman Athar, Zafar Ullah Zafar, Hazem M. Kalaji, Muhammad Ashraf. " Linking changes in chlorophyll fluorescence with drought stress susceptibility in mung bean [(L.) Wilczek] ", Physiologia Plantarum, 2021	<1 %

Publication

66	Submitted to Queen Mary and Westfield College Student Paper	<1 %
67	Tânia Almeida, Glória Pinto, Barbara Correia, Conceição Santos, Sónia Gonçalves. "QsMYB1 expression is modulated in response to heat and drought stresses and during plant recovery in Quercus suber", Plant Physiology and Biochemistry, 2013 Publication	<1 %
68	Xu Lu, Guiping Chen, Lei Ma, Congcong Zhang et al. "Integrated transcriptome and metabolome analysis reveals antioxidant machinery in grapevine exposed to salt and alkali stress", Physiologia Plantarum, 2023 Publication	<1 %
69	amb-express.springeropen.com Internet Source	<1 %
70	etheses.whiterose.ac.uk Internet Source	<1 %
71	www.islandscholar.ca Internet Source	<1 %
72	"Abstract", Photosynthesis Research, 2007 Publication	<1 %

73	(5-24-16) http://14.139.186.108/jspui/bitstream/123456789/2431 Internet Source	<1%
74	Fachao Shi, Yijie Dong, Yi Zhang, Xiufeng Yang, Dewen Qiu. "Overexpression of the PeaT1 Elicitor Gene from Alternaria tenuissima Improves Drought Tolerance in Rice Plants via Interaction with a Myo-Inositol Oxygenase", Frontiers in Plant Science, 2017 Publication	<1%
75	Yuanyuan Xu, Xiaogang Li, Jing Lin, Zhonghua Wang, Qingsong Yang, Youhong Chang. "Transcriptome sequencing and analysis of major genes involved in calcium signaling pathways in pear plants (Pyrus calleryana Decne.)", BMC Genomics, 2015 Publication	<1%
76	eprints.nottingham.ac.uk Internet Source	<1%
77	mdpi-res.com Internet Source	<1%
78	www.science.gov Internet Source	<1%
79	Hongmei, Luo, Zhu Yingjie, Song Jingyuan, Xu Lijia, Sun Chao, Zhang Xin, Xu Yanhong, He Liu, Sun Wei, Xu Haibin, Wang Bo, Li Xian'en, Li Chuyuan, Liu Juyan, and Chen Shilin.	<1%

"Transcriptional data mining of Salvia miltiorrhiza in response to methyl jasmonate to examine the mechanism of bioactive compound biosynthesis and regulation", Physiologia Plantarum, 2014.
Publication

---

80 Submitted to Jawaharlal Nehru University (JNU) <1%
Student Paper

---

81 Li, Huie, Weijie Yao, Yaru Fu, Shaoke Li, and Qiqiang Guo. "De Novo Assembly and Discovery of Genes That Are Involved in Drought Tolerance in Tibetan Sophora moorcroftiana", PLoS ONE, 2015. <1%
Publication

---

82 www.deepdyve.com <1%
Internet Source

Exclude quotes	On	Exclude matches	< 14 words
Exclude bibliography	On		